AD-A084 037 EATON CORP DEER PARK NY AIL DIV F/G 17/7
SIMULATION OF PRECISION AIRCRAFT POSITIONING SYSTEM UTILIZING T--ETC(U)
MAR 78 A CHARYCH N00123-76-C-1322
UNCLASSIFIED NL

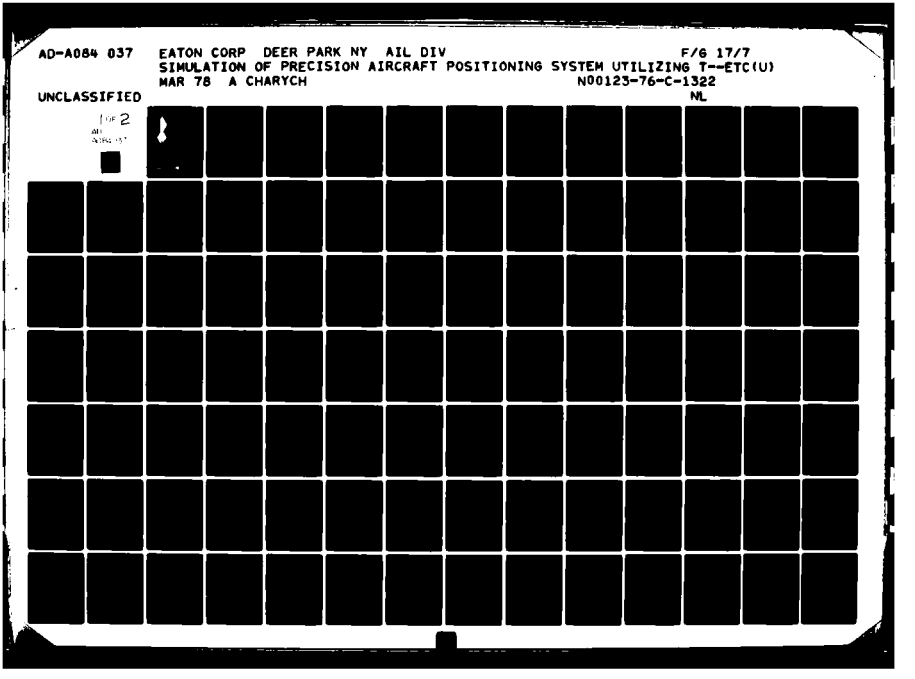

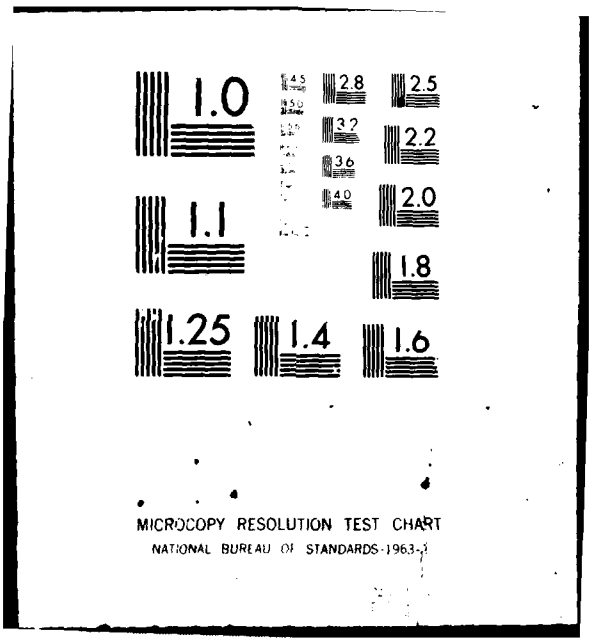
1.0
2.8
2.5
3.2
2.2
3.6
4.0
2.0
1.1
1.8
1.25
1.4
1.6
MICROCOPY RESOLUTION TEST CHART
NATIONAL BUREAU OF STANDARDS-1963-A

LEVEL II

SIMULATION OF PRECISION AIRCRAFT POSITIONING SYSTEM UTILIZING TRIANGULATION, DME AND INERTIAL SMOOTHING TECHNIQUES

A. CHARYCH

FINAL REPORT
MARCH 1978

PREPARED FOR:

NAVAL OCEAN SYSTEMS CENTER
SAN DIEGO, CALIFORNIA 92152

CONTRACT N00123-76-C-1322

AIL a division of CUTLER-HAMMER
DEER PARK, LONG ISLAND, NEW YORK 11729

UNCLASSIFIED
SECURITY CLASSIFICATION OF THIS PAGE (When Data Entered)

REPORT DOCUMENTATION PAGE	READ INSTRUCTIONS BEFORE COMPLETING FORM
1. REPORT NUMBER: none 2. GOVT ACCESSION NO.: AD-A084 037	3. RECIPIENT'S CATALOG NUMBER
4. TITLE (and Subtitle): SIMULATION OF PRECISION AIRCRAFT POSITIONING SYSTEM UTILIZING TRIANGULATION, DME AND INERTIAL SMOOTHING TECHNIQUES	5. TYPE OF REPORT & PERIOD COVERED: final 6. PERFORMING ORG. REPORT NUMBER
7. AUTHOR(s): A. Charych	8. CONTRACT OR GRANT NUMBER(s): N00123-76-C-1322
9. PERFORMING ORGANIZATION NAME AND ADDRESS: Airborne Instrument Laboratory (AIL), a division of Cutler-Hammer, Deer Park, Long Island, NY 11729	10. PROGRAM ELEMENT, PROJECT, TASK AREA & WORK UNIT NUMBERS
11. CONTROLLING OFFICE NAME AND ADDRESS: Naval Ocean Systems Center, San Diego, CA 92152	12. REPORT DATE: Mar[illegible]78 13. NUMBER OF PAGES: 139
14. MONITORING AGENCY NAME & ADDRESS (if different from Controlling Office)	15. SECURITY CLASS. (of this report): Unclassified 15a. DECLASSIFICATION/DOWNGRADING SCHEDULE

16. DISTRIBUTION STATEMENT (of this Report)

Approved for public release; distribution unlimited

17. DISTRIBUTION STATEMENT (of the abstract entered in Block 20, if different from Report)

18. SUPPLEMENTARY NOTES

19. KEY WORDS (Continue on reverse side if necessary and identify by block number)

20. ABSTRACT (Continue on reverse side if necessary and identify by block number)

The purpose of this simulation is to determine the accuracy performance capability of an aircraft positioning system based on the triangulation principle when combined with distance measuring equipment (DME), inertial elements and filtering (blending) of data from the various sensors. The simulation also determines how sensitive the overall system accuracy is to changes in certain key sensor parameters.

DD FORM 1 JAN 73 1473 EDITION OF 1 NOV 65 IS OBSOLETE
S/N 0102-LF-014-6601

UNCLASSIFIED
SECURITY CLASSIFICATION OF THIS PAGE (When Data Entered)

TABLE OF CONTENTS

I. PURPOSE OF SIMULATION

The purpose of this simulation is to determine the accuracy performance capability of an aircraft positioning system based on the triangulation principle when combined with distance measuring equipment (DME), inertial elements and filtering (blending) of data from the various sensors.

The simulation also determines how sensitive the overall system accuracy is to changes in certain key sensor parameters.

II. DESCRIPTION OF SIMULATION

A. GENERAL

The simulation generates position and position rate accuracy data for an aircraft approach and landing on a small aviation ship.

Since only the accuracy of the positioning system is of interest here, aircraft dynamics and closed loop responses have not been implemented. The simulation does, however, generate a nominal aircraft trajectory as well as positional disturbances along that trajectory so as to provide a realistic exercise for the positioning system.

Each simulation consists of 20 individual approaches from 3,000 feet range to touchdown. Accuracy statistics are compiled during three short segments (2.5 seconds long) along the trajectory. The segments start at 1,000 feet, 300 feet, and 40 feet from touchdown.

Trajectory and ship motion parameters were chosen as "typical" for a VSTOL approach and landing on a small aviation ship.

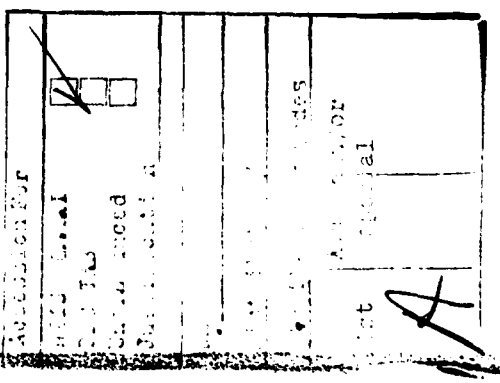

Nominal sensor parameters were chosen to reflect the capability of todays technology as well as to minimize as much as possible the expected size, weight, and cost of the overall system.

The nominal sensor parameter simulation is used as a reference point for simulations in which key sensor parameters are varied, one at a time. The resultant output forms a basis for analyzing the sensitivity of the systems position and rate accuracy to changes in these parameters.

The sensitivity analysis evaluates system performance under varying conditions as well as point out which sensor parameters must be tightly controlled and which parameters can be relaxed with minimal effect on the overall system accuracy.

B. AIRCRAFT TRAJECTORY

Aircraft trajectory starts at 3,000 feet from ship, 150 ft/sec ground speed, at an altitude of 160 feet. A fixed average horizontal deceleration of 3.75 ft/sec^2 is used so that ground speed becomes zero at touchdown (X=0). Altitude is made to decrease linearly with time to yield an exponential-like decay of height versus X distance as shown in Figure 1.

Figure 1 also shows perturbation in the horizontal velocity and the vertical trajectory. These perturbations were programmed by adding random acceleration fluctuations to the nominal trajectory. This simulates aircraft movements due to air disturbances and flight control corrections.

The acceleration fluctuations were simulated as gaussian distributed, zero mean and .1G standard deviation pseudorandom variable in each of the coordinate axes.

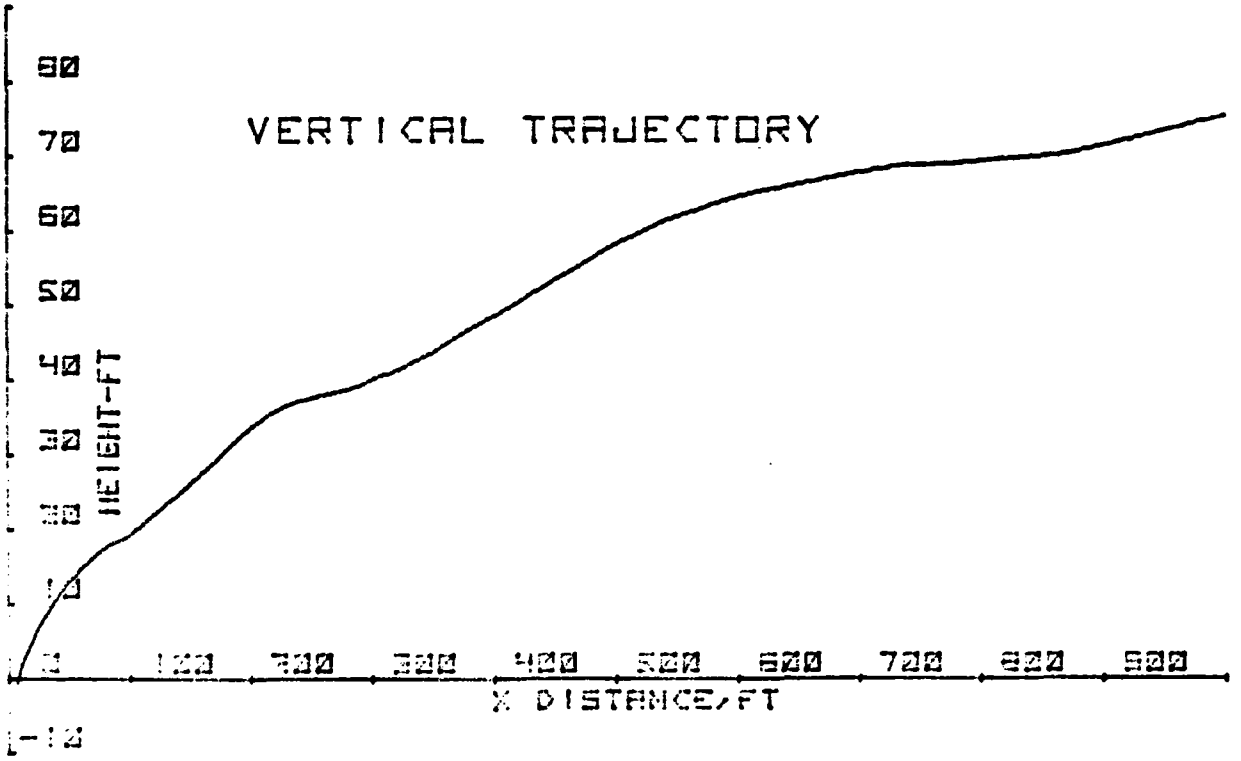
VERTICAL TRAJECTORY
80
70
60
50
40
30
20
10
HEIGHT-FT
0
100
200
300
400
500
600
700
800
900
X DISTANCE-FT
-10

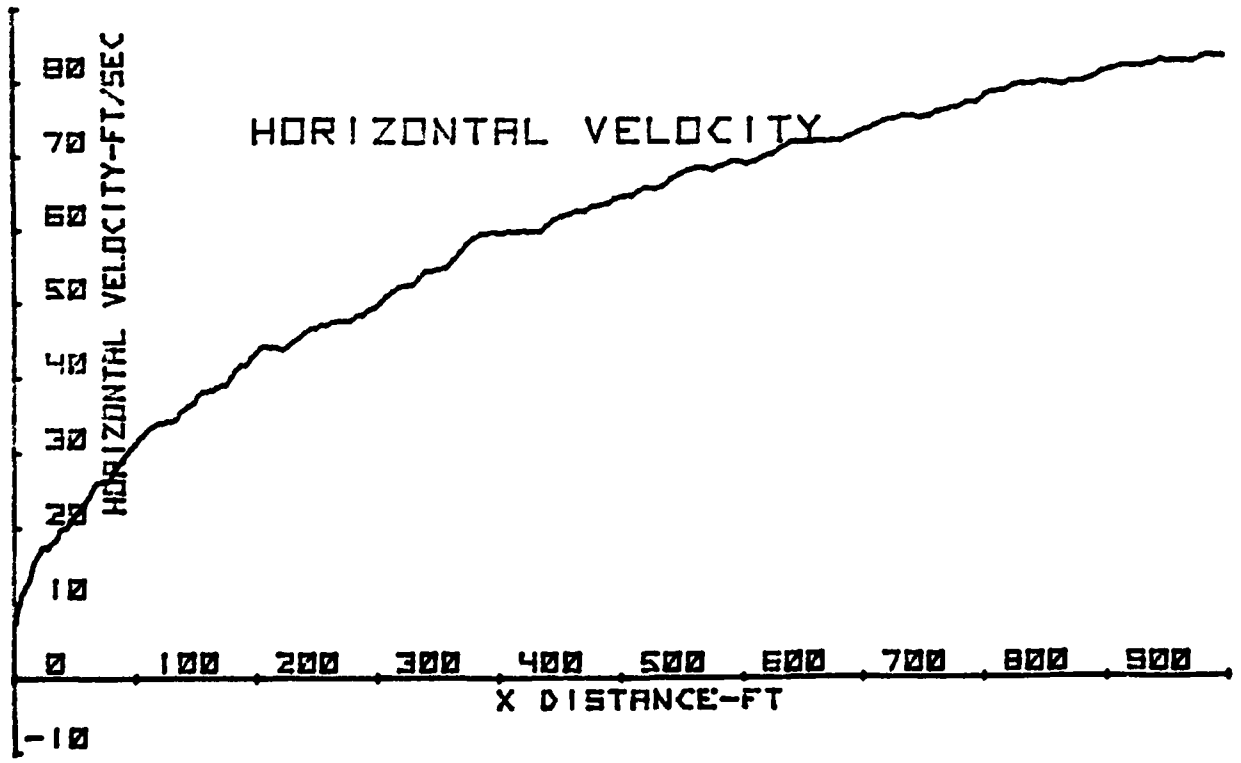
HORIZONTAL VELOCITY
80
70
60
50
40
30
20
10
HORIZONTAL VELOCITY-FT/SEC
0
100
200
300
400
500
600
700
800
900
X DISTANCE-FT
-10

FIGURE 1

C. SHIP MOTION SIMULATION

The ships pitch, roll and heave is simulated by doubly integrating a time correlated pseudorandom process. This results in smooth slowly changing fluctuations as shown in Figures 2 and 3.

Constants were chosen to obtain a cyclic period of approximately 6 seconds. The pitch/roll amplitude is approximately 5 degrees (1 sigma). Vertical acceleration is set at .2 G's (1 sigma).

D. SENSORS AND SENSOR ERROR MODELS

The shipboard equipment consists of two azimuth scanners separated by a distance of 40 feet as depicted in Figure 4. The azimuth 2 scanner is colocated with an elevation scanner and a distance measuring beacon (DME).

Azimuth decoding equipment receives guidance signals from the scanners and measures the two azimuth angles θ_1 and θ_2, the elevation angle ϕ and the DME range R_{DME}.

These four basic measurements are made at an update rate of 10 per second. At distances within a few hundred feet of the touchdown point, triangulation utilizing the θ_1, θ_2, and ϕ measurement is primarily used for precision position. At longer distances, geometric dilution renders the triangulation measurement of the X coordinate useless, so the DME measurement together with θ_1 and ϕ provides primary guidance.

In addition to the guidance signals, ship motion at the origin of the coordinate frame is sensed and made available to the airborne system. The pitch, roll and vertical acceleration is sensed and transmitted to the aircraft for pocessing.

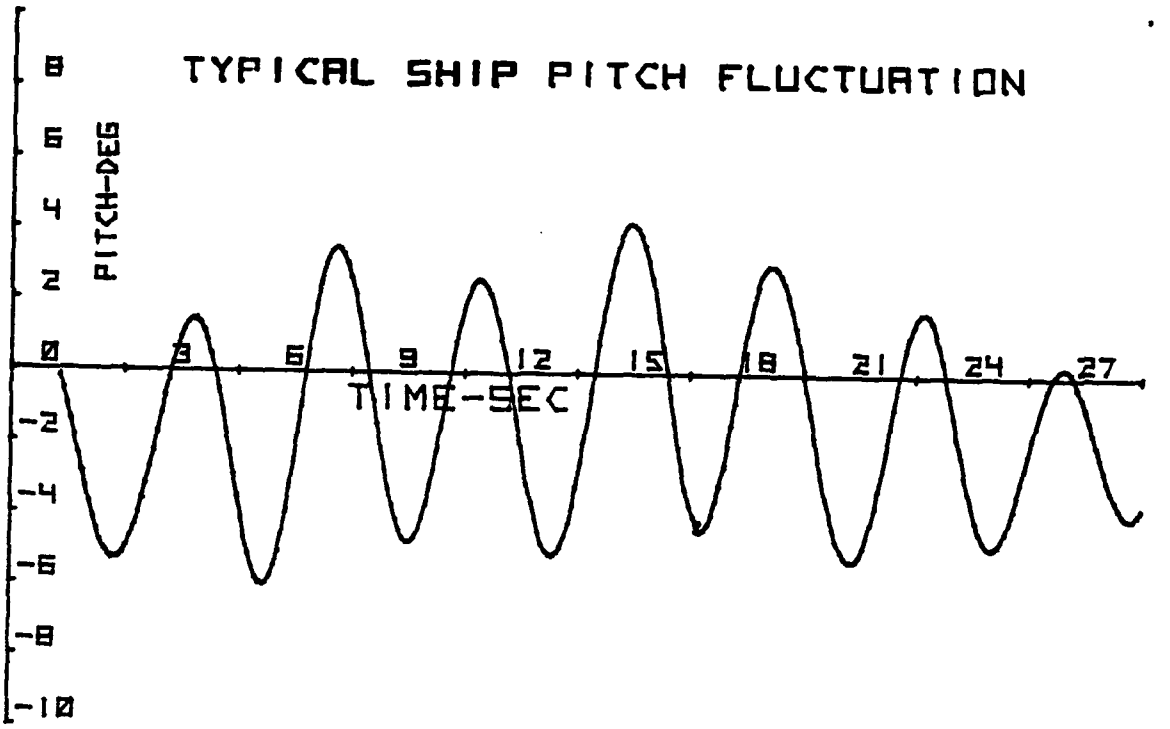
TYPICAL SHIP PITCH FLUCTUATION
PITCH-DEG
8
6
4
2
0
-2
-4
-6
-8
-10
3
6
9
12
15
18
21
24
27
TIME-SEC

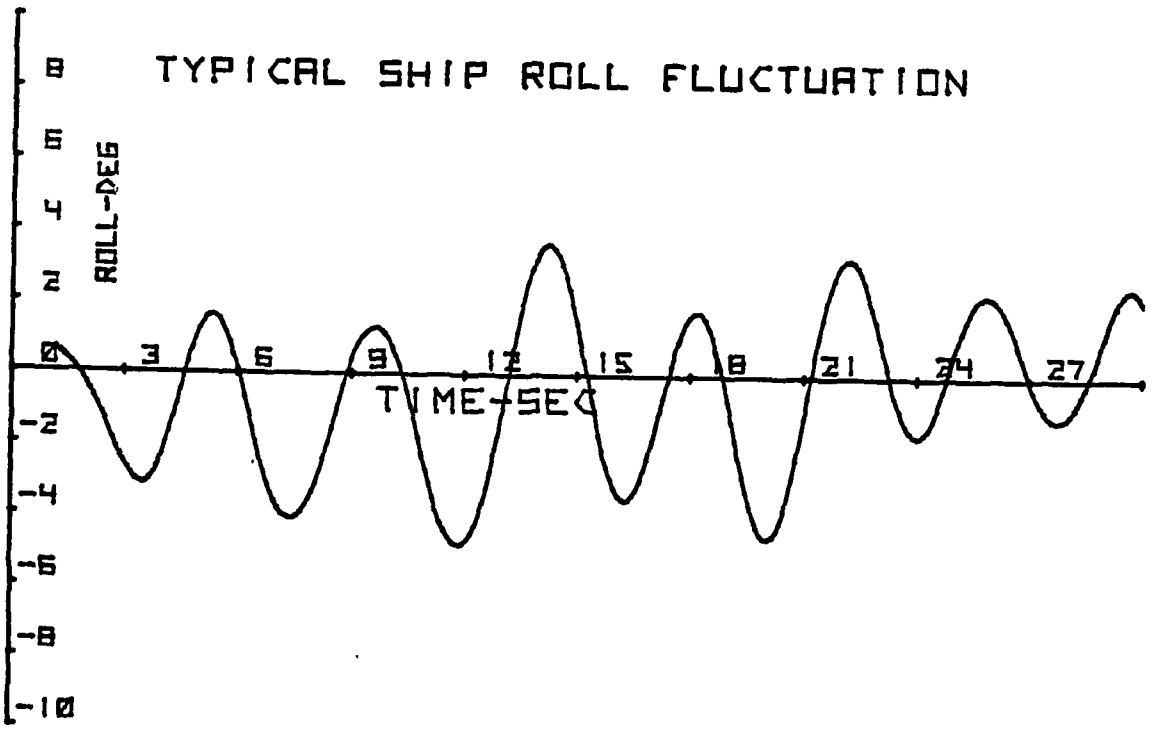
TYPICAL SHIP ROLL FLUCTUATION
ROLL-DEG
8
6
4
2
0
-2
-4
-6
-8
-10
3
6
9
12
15
18
21
24
27
TIME-SEC

FIGURE 2

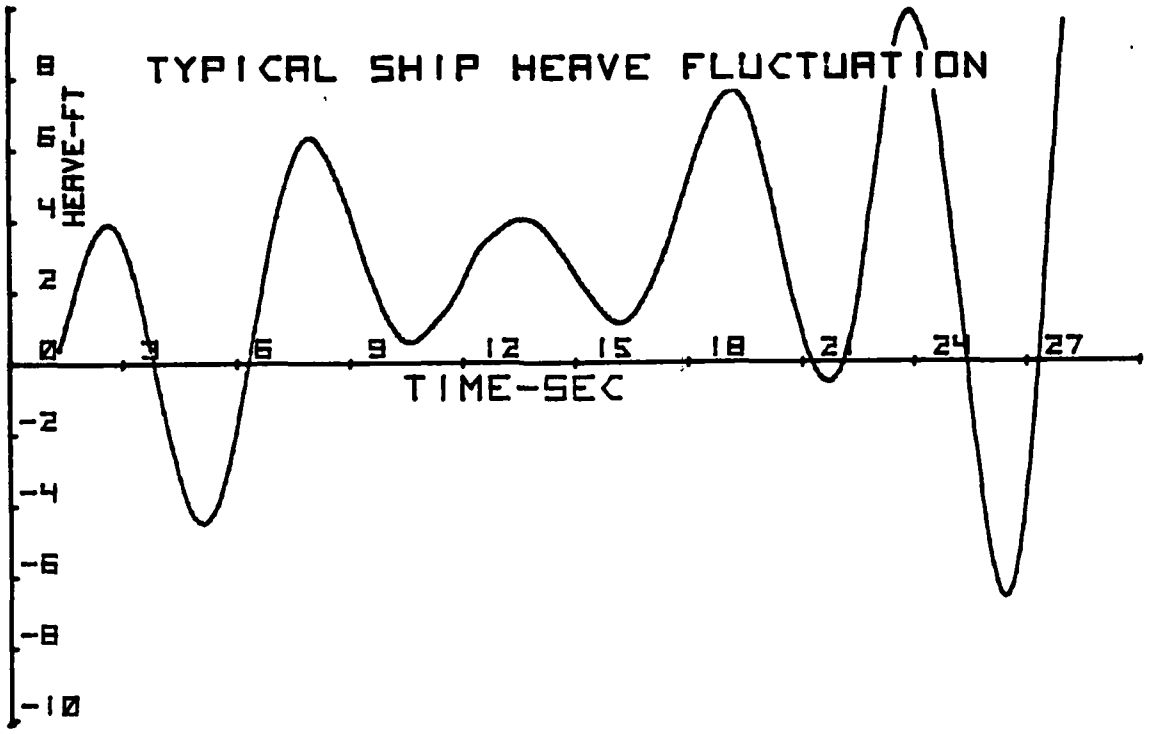
TYPICAL SHIP HEAVE FLUCTUATION
HEAVE-FT
8
6
4
2
0
-2
-4
-6
-8
-10
0
3
6
9
12
15
18
21
24
27
TIME-SEC

FIGURE 3

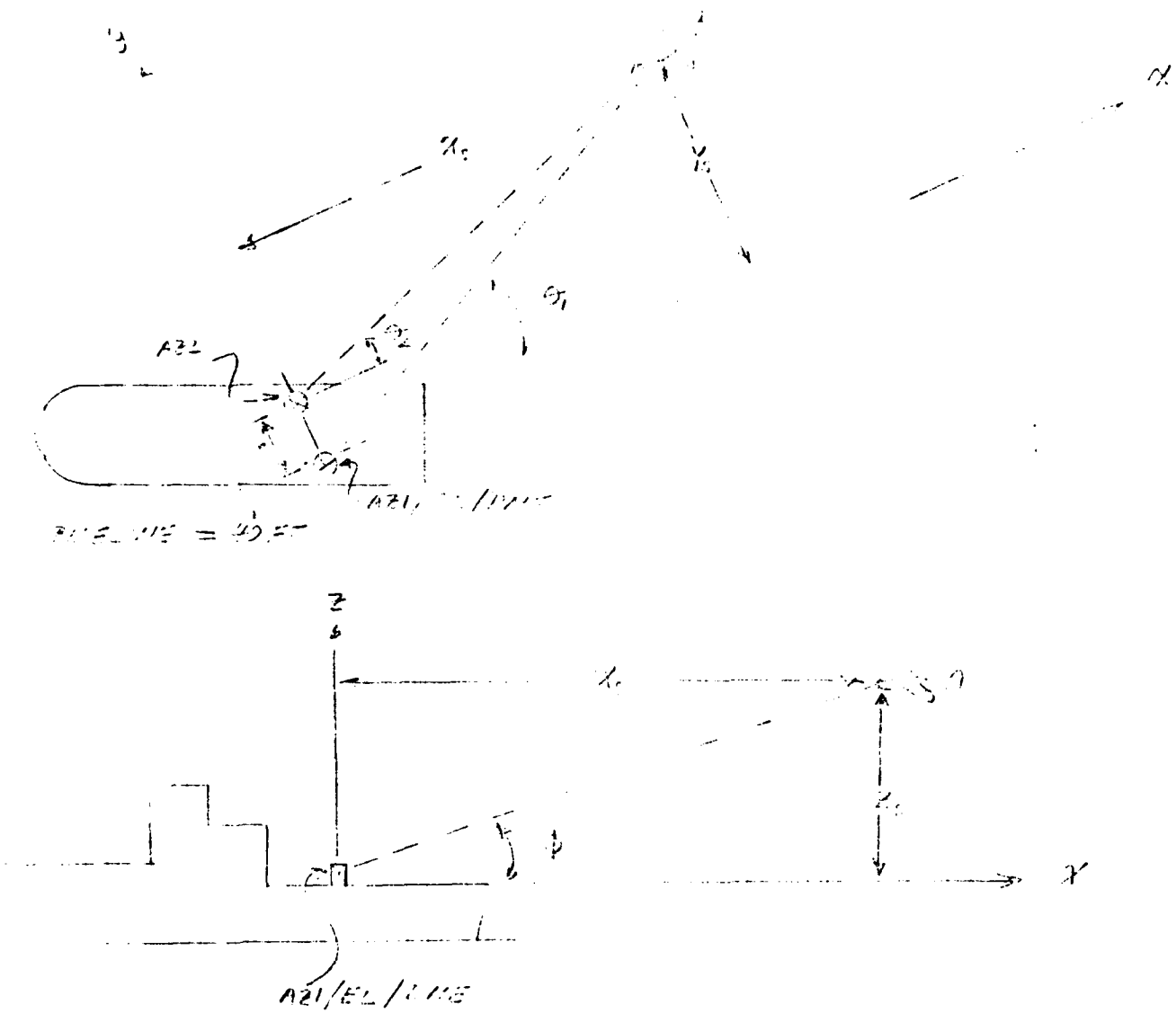

FIGURE 4. SHIP REFERENCED COORDINATE SYSTEM

The airborne system also has access to data derived from accelerometers mounted on a stable platform. The inertial data is used to essentially smooth out the angle and DME data in order to provide precision rates required for VSTOL autoland flight controls.

AZIMUTH AND ELEVATION SENSOR ERROR MODEL

The azimuth and elevation sensors are modeled as a pseudorandom gauss markoff process. A fixed .1 degree bias (held constant in all simulations) is utilized. Standard deviation is fixed at .07 degrees and the correlation time constant of the process is nominally .5 sec.

Correlation time constant of the pseudorandom process determines the spectum of the resultant noise. A time constant of .5 seconds is roughly equivalent to a cyclic noise fluctuation with a periodicity of 2 seconds. Figure 5 shows the angle noise characteristics as a function of time.

The azimuth and elevation sensor occurances can be realized with a scanning antenna beamwidth at approximately 3 degrees. Since the slow cyclic error fluctuations are multipath related, the period of the fluctuations is dependent on the systems operating frequency. The nominal .5 second correlation time constant is empirically chosen for a system operating at Ku-Band.

DME ERROR MODEL

Two distance measuring elements are considered. The first is a DME operated at Ku-Band. Its error is modeled as a nominal 30 foot bias and a 10 foot 1 sigma noise component. Correlation time constant is nominally set at .5 sec.

The second DME is a precision L-band unit (similar to TACAN). Its error is modeled as a nominal 80 foot bias, 70 foot 1 sigma noise component, and because of the lower operationg frequency, the time constant is nominally set at 5 seconds.

AIRBORNE INERTIAL SENSORS

The inertial sensors are assumed to be high quality instruments normally used for inertial navigation. Acceleration data is derived from three orthogonal accelerometers mounted on a stable platform. Nominal accelerometer bias is set at 60 micro G's. A scale factor error (error linearly increasing with increasing acceleration) of 34 parts per million is assumed. The accelerometer mounting axes are assumed milligned from true orthogonal by .01 degrees.

Biases and drifts of the stable platform are not modeled except for the difference in error between the shipboard and the airborne heading reference. A nominal heading error of 1 degree is assumed.

SHIP MOTION SENSORS

The ship motion sensors measure the ships pitch, ships roll and the ships vertical acceleration.

The pitch and roll sensor is assumed to have a nominal .05 degree bias error and a .05 degree 1 sigma random noise error.

Nominal error model for the vertical accelerometer is taken to be identical with the airborne accelerometer model. Nominal parameters being:

bias = 60 micro G's
scale factor = 34 PPM
misalignment = .01 degree

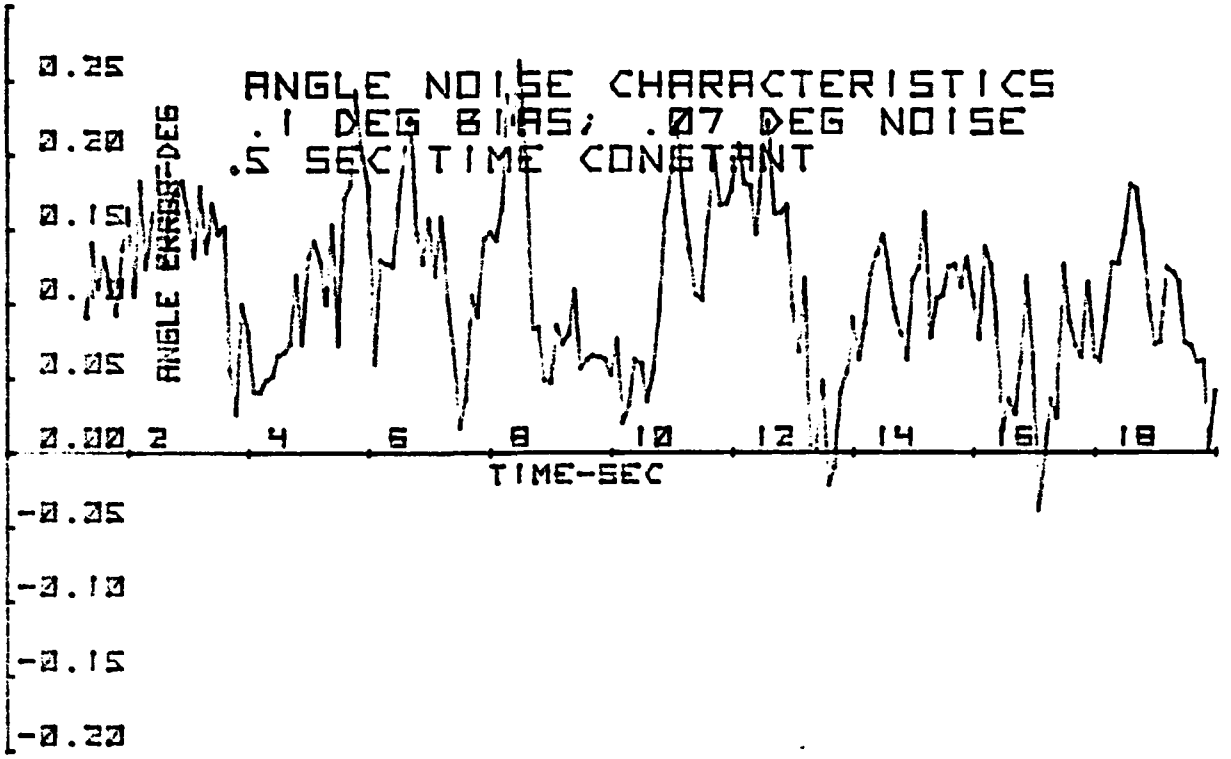
ANGLE NOISE CHARACTERISTICS
.1 DEG BIAS; .07 DEG NOISE
.5 SEC TIME CONSTANT
ANGLE ERROR-DEG
0.25
0.20
0.15
0.05
0.00
-0.05
-0.10
-0.15
-0.20
2
4
6
8
10
12
14
16
18
TIME-SEC

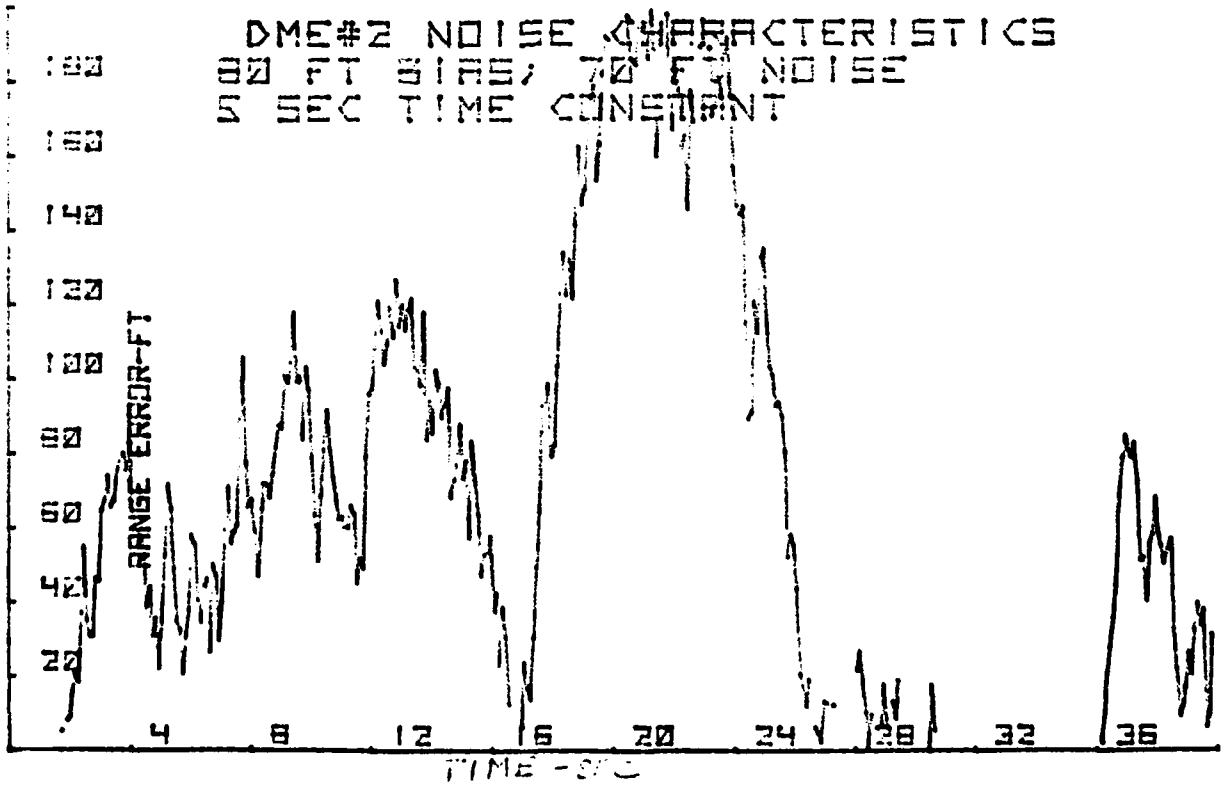
DME#2 NOISE CHARACTERISTICS
80 FT BIAS; 70 FT NOISE
5 SEC TIME CONSTANT
RANGE ERROR-FT
160
140
120
100
80
60
40
20
4
8
12
16
20
24
28
32
36
TIME-SEC

FIGURE 5

A tabulation of nominal parameters for trajectory, ship motion and sensor error model appears in Table I.

E. AIRBORNE SYSTEM MECHANIZATION

Mechanization of the airborne system is shown in block diagram form in Figure 6. The main purpose of the mechanization is to combine angle measurement data, distance measurement data and inertial data to obtain near optimum estimates of aircraft positions and rates relative to ship.

RANGE BLENDING

As shown in Figuire 6, Angle measurement data θ_1, θ_2 and ϕ is triangulated to compute range. The accuracy of this measurement is highly dependent on range from ship because of the limited 40 foot baseline, upon which triangulation is based. The DME measurement accuracy, however, is nearly constant as a function of range.

In order to optimally combine triangulation range and DME range, the expected 1 sigma triangulation accuracy is computed as function of DME range. A sample output of the triangulation range accuracy (1 sigma) as well as raw triangulation range error is given in Figure 7.

A blending coefficient for combining triangulation and DME range is computed next. The coefficient (shown in Figure 8 for DME #1) is based on relative variances of the 2 data sources. At 1,000 feet range for example, the blending coefficient has the value of .86. 86 percent of the DME data sample is, therefore, combined with 14% of the triangulation range sample to produce the optimum range. At distances within 300 feet, most of the range data is taken from triangulation with very little coming from the DME.

TABLE I. NOMINAL PARAMETERS

AIRBORNE TRAJECTORY PARAMETERS

X AXIS ACCELERATION FLUCTUATION (1 SIGMA)	.1G
Y AXIS ACCELERATION FLUCTUATION (1 SIGMA)	.1G
Z AXIS FLUCTUATION (1 SIGMA)	.1

AIRBORNE SENSORS

SENSOR	PARAMETER	NOMINAL VALUE
AZIMUTH 1 AZIMUTH 2 ELEVATION	BIAS NOISE CORRELATION TIME CONST	.1 DEG .07 DEG .5 SEC
DME #1	BIAS NOISE CORRELATION TIME CONST	30 FT 10 FT .5 SEC
DME #2	BIAS NOISE CORRELATION TIME CONST	80 FT 70 FT 5 SEC
ACCELEROMETER	BIAS SCALE FACTOR MISALIGNMENT	60 uG 34 PPM .011 DEG
HEADING SENSOR	SHIP/AIR HEADING MISALIGNMENT	1 DEG

ADDITIONAL PARAMETERS FOR SIMULATION WITH SHIP MOTION

SHIP MOTION PARAMETERS

PITCH FLUCTUATION (1 SIGMA)	5 DEG
ROLL FLUCTUATION (1 SIGMA)	5 DEG
VERTICAL ACCELERATION (1 SIGMA)	.2 G

SHIP SENSORS

SENSOR	PARAMETER	NOMINAL VALUE
PITCH SENSOR	BIAS NOISE	.05 DEG .05 DEG
ROLL SENSOR	BIAS NOISE	.05 DEG .05 DEG
VERTICAL ACCELEROMETER	BIAS NOISE	60 uG 30 uG

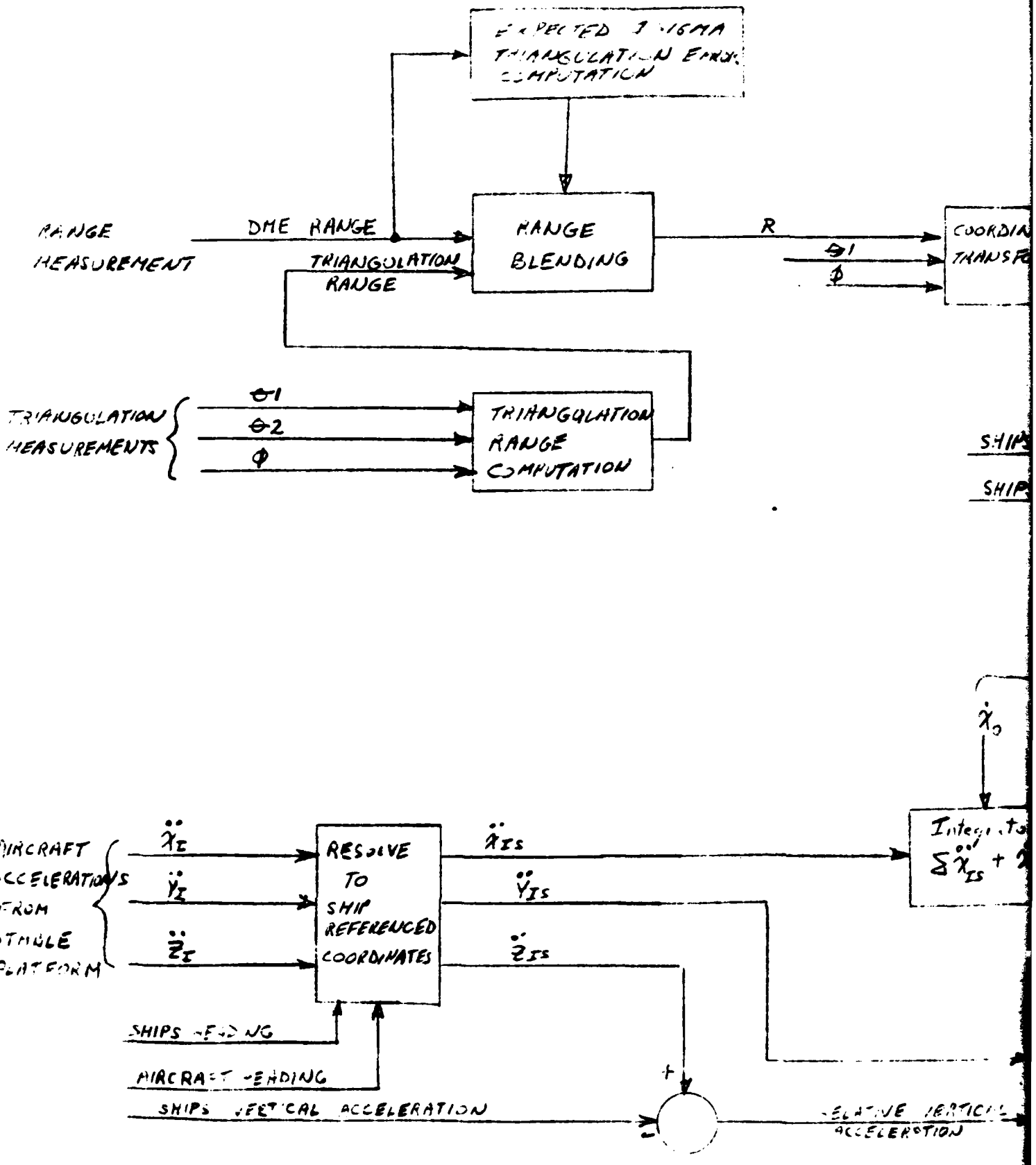
EXPECTED 1 SIGMA TRIANGULATION ERROR COMPUTATION
RANGE MEASUREMENT
DME RANGE
TRIANGULATION RANGE
RANGE BLENDING
R
θ1
Φ
TRIANGULATION MEASUREMENTS
θ1
θ2
Φ
TRIANGULATION RANGE COMPUTATION
SHIP
SHIP
$\dot{\lambda}_0$
AIRCRAFT ACCELERATIONS FROM STABLE PLATFORM
$\ddot{x}_I$
$\ddot{y}_I$
$\ddot{z}_I$
RESOLVE TO SHIP REFERENCED COORDINATES
$\ddot{x}_{IS}$
$\ddot{y}_{IS}$
$\ddot{z}_{IS}$
SHIPS HEADING
AIRCRAFT HEADING
SHIPS VERTICAL ACCELERATION
+
−
RELATIVE VERTICAL ACCELERATION

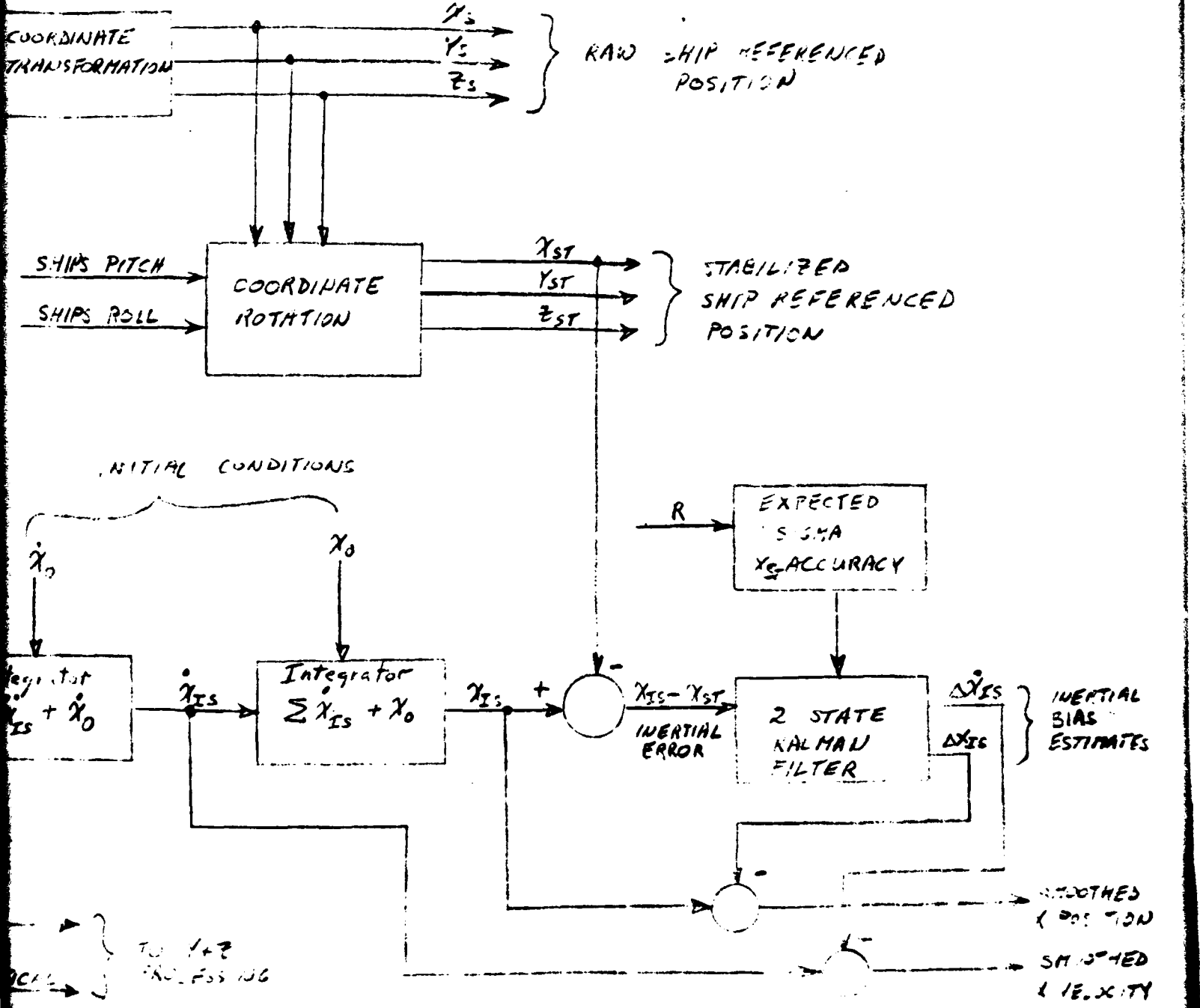

FIGURE 6. AIRBORNE SYSTEM MECHANIZATION

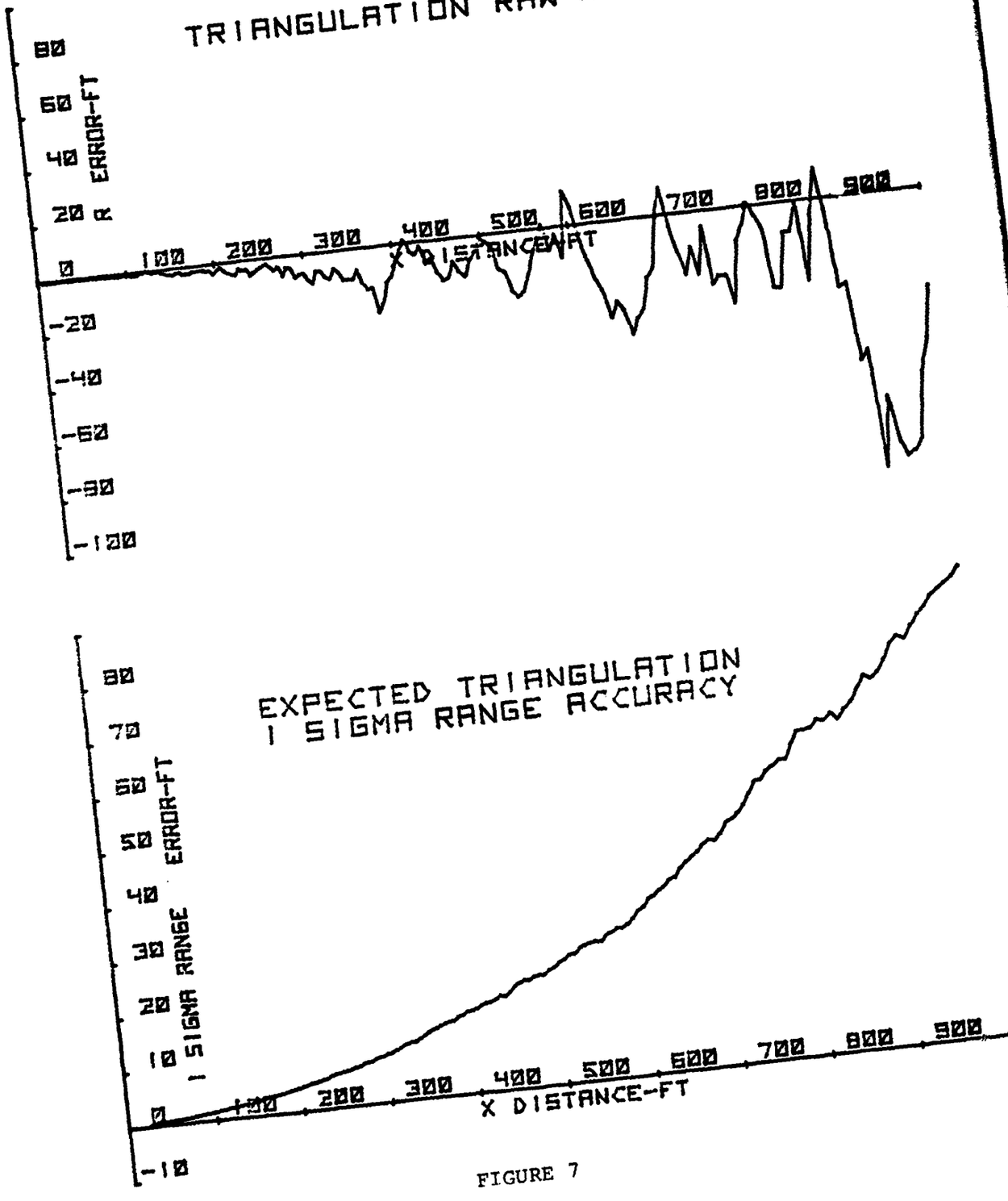
TRIANGULATION RAW RANGE ERROR
80
60
40
20
0
-20
-40
-60
-80
-100
R ERROR-FT
100
200
300
400
500
600
700
800
900
X DISTANCE-FT
EXPECTED TRIANGULATION
1 SIGMA RANGE ACCURACY
80
70
60
50
40
30
20
10
0
-10
1 SIGMA RANGE ERROR-FT
100
200
300
400
500
600
700
800
900
X DISTANCE-FT

FIGURE 7

COORDINATE TRANSFORMATION

Once an optimum range, R, is computed, a coordinate transformation utilizing the θ_1 and ϕ angle measurements is performed to obtain X_s, Y_s, Z_s position referenced to the ship (see Figure 6). The X_s, Y_s, and Z_s measurements are referenced to the ships landing platform and, therefore, pitch, roll and heave with the movements of the platform. The pitch and roll fluctuations are taken out by a coordainte rotation utilizing data from the ships pitch and roll sensors. Aircraft postion X_{ST}, Y_{ST}, Z_{ST} is, therefore, relative to the touchdown point, but stabilized with reference to the horizon.

The 1 sigma accuracy in the X_{ST} parameter is given in Figure 8 as a function of range. At ranges around 1,000 feet, the X_{ST} accuracy is very nearly determined by the accuray of the DME. The expected accuracy improves with decreasing range until it very nearly becomes triangulation accuracy at ranges close to ship. The expected 1 sigma X_{ST} accuracy is computed for input to a Kalman filter which combines the X_{ST} data with inertial data.

INERTIAL DATA PROCESSING

Inertial data is taken from the three orthogonal accelerometers. The accelerometer axes are assumed not to coincide with the X_{ST}, Y_{ST}, Z_{ST} coordinate system so the ships and aircraft heading references are used to resolve the aircraft accelerations into the X_{ST}, Y_{ST}, Z_{ST} coordinates. Each of the resolved accelerations ($\ddot{X}_{IS}$, $\ddot{Y}_{IS}$, $\ddot{Z}_{IS}$) goes through a double intergration to obtain inertial rate ($\dot{X}_{IS}$, $\dot{Y}_{IS}$, $\dot{Z}_{IS}$) and inertial position (X_{IS}, Y_{IS}, Z_{IS}) respectively.

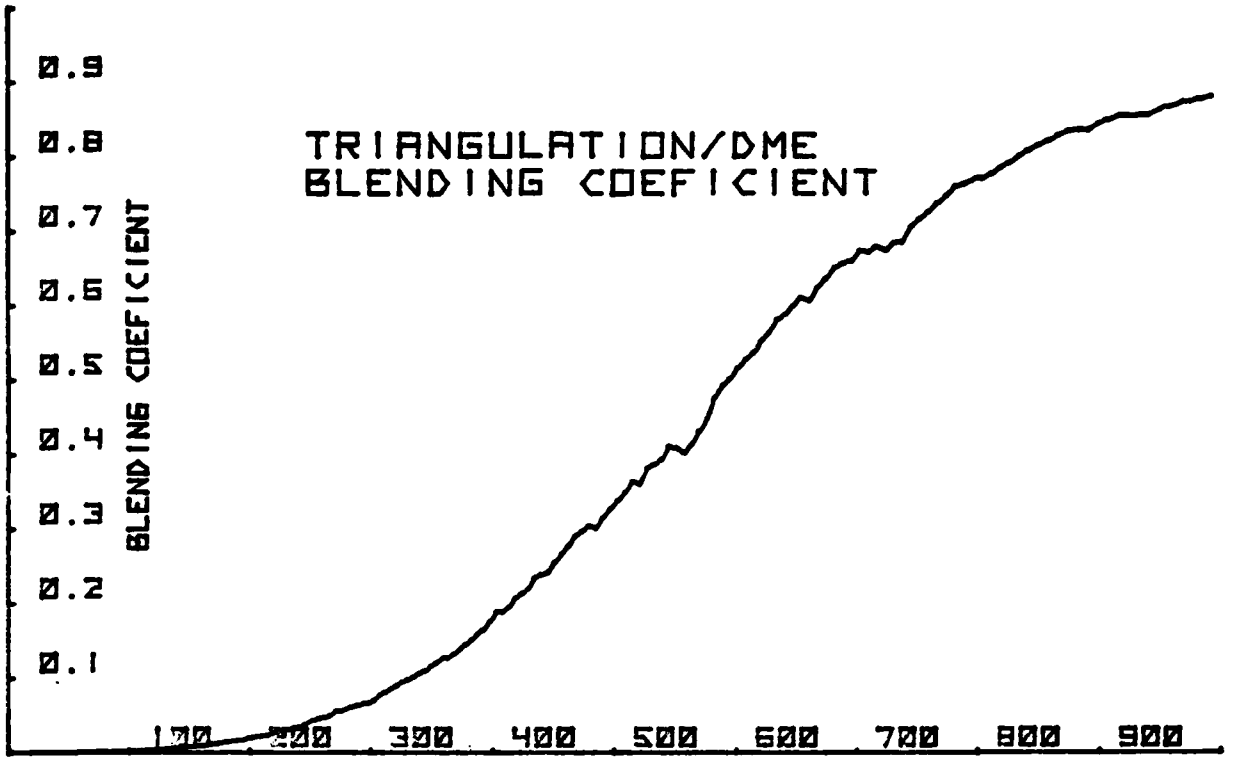
TRIANGULATION/DME
BLENDING COEFICIENT
BLENDING COEFICIENT
0.9
0.8
0.7
0.6
0.5
0.4
0.3
0.2
0.1
100
200
300
400
500
600
700
800
900

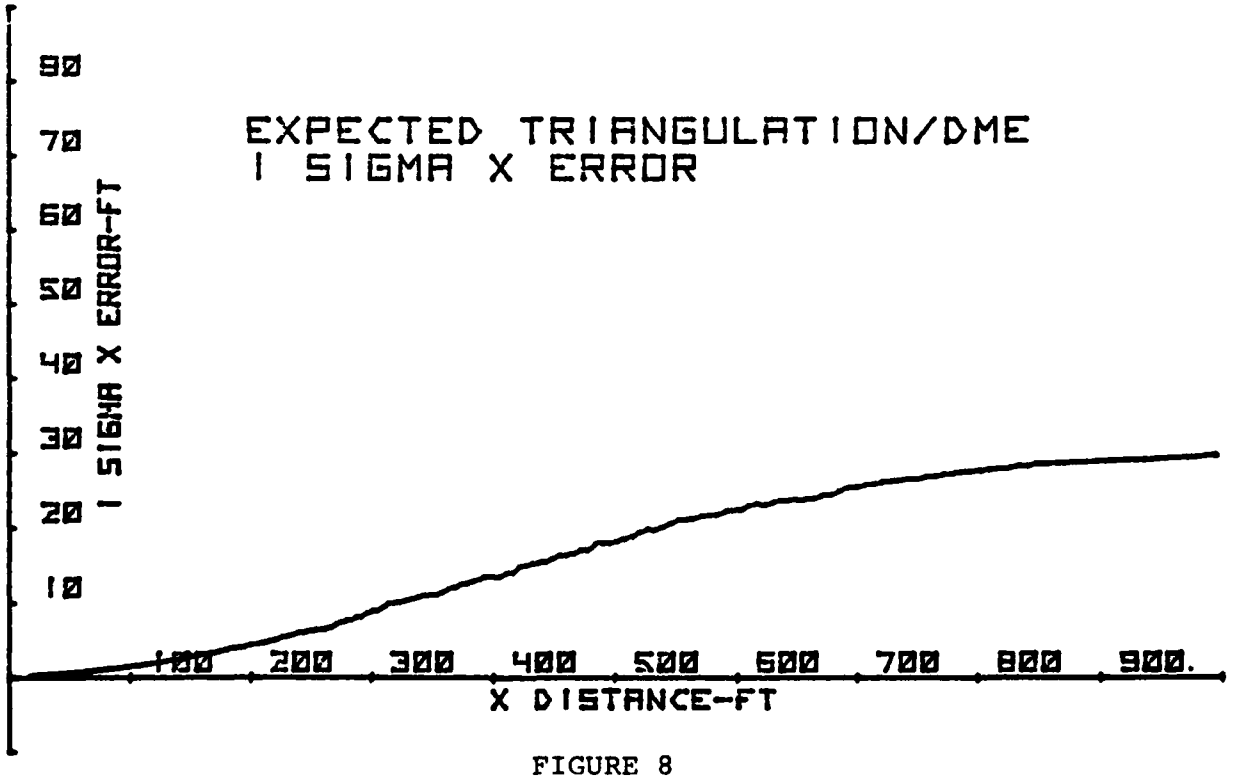
EXPECTED TRIANGULATION/DME
1 SIGMA X ERROR
1 SIGMA X ERROR-FT
90
70
60
50
40
30
20
10
100
200
300
400
500
600
700
800
900.
X DISTANCE-FT

FIGURE 8

The ships vertical acceleration (sensed on the ship and data linked to aircraft) is subtracted from the aircraft vertical acceleration to obtain relative acceleration between ship and plane prior to going through the integration process. This is done because of the relatively large heave components expected. The same is not done for the X and Y accelerations, i.e., the landing platform surge and sway fluctuations are ignored.

Note that Figure 6 shows the integrators and Kalman filter only for the X component. A similar mechanization is assumed for the Y and Z components. The following discussion centers on the X component, but is equally valid for the Y and Z components as well.

The distance integrator is initialized at the start of the trajectory using the first computed X_{ST} measurement. The rate integration is initialized using the difference between two X_{ST} measurements spaced 1 second apart.

KALMAN FILTER

Output error of the integrators is shown in Figure 9. The X rate error ($\dot{X}_{IS}$) is seen to have a bias essentially equal to the initialization error with a barely noticeable drift as a function of time (or distance). The noise component is seen to be quite small. Noise component of the X error (X_{IS}) is also seen to be small, but a much more noticeable drift as function of time occurs.

The purpose of the Kalman filter, therefore, is to estimate the bias error in the inertial position and rate (X_{IS} and $\dot{X}_{IS}$) using the computed X_{ST} measurement. The biases are then subtracted from the inertial measurements to obtain low noise and low bias position and velocity estimates.

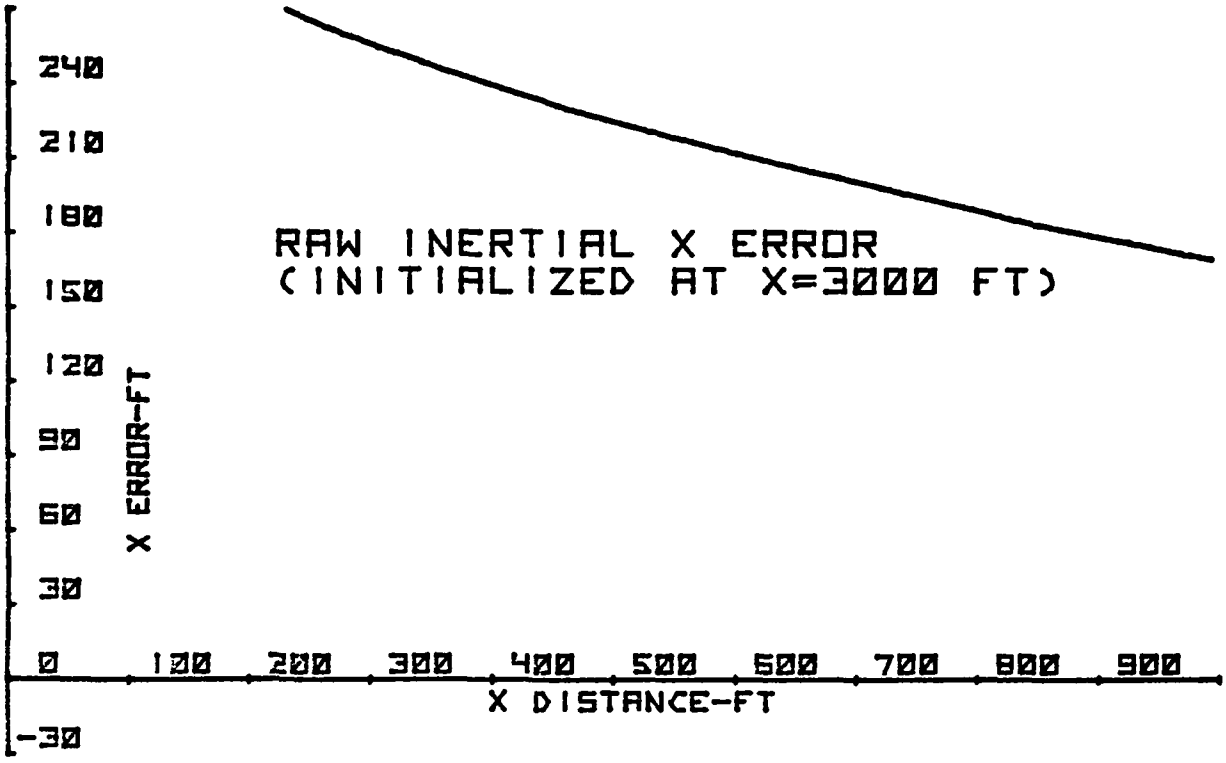
RAW INERTIAL X ERROR
(INITIALIZED AT X=3000 FT)
240
210
180
150
120
90
60
30
X ERROR-FT
0
100
200
300
400
500
600
700
800
900
X DISTANCE-FT
-30

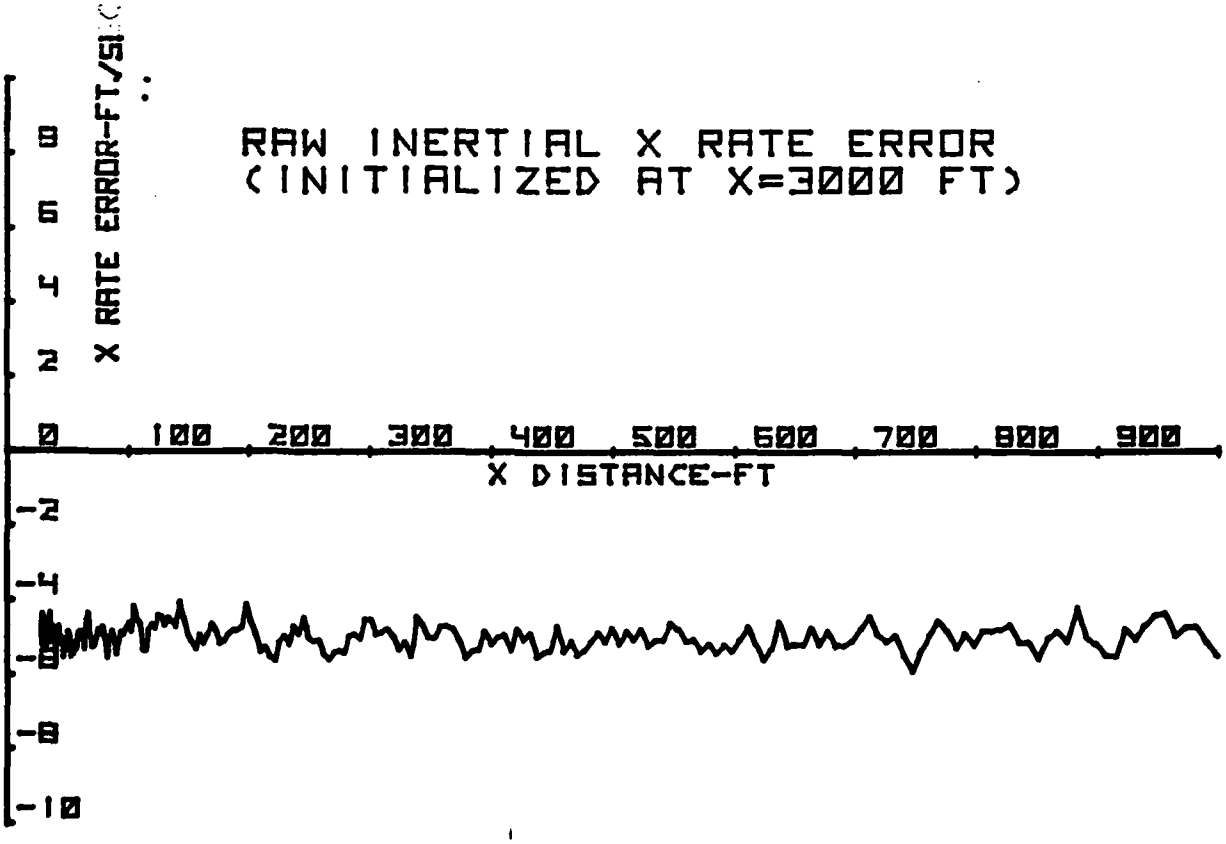
RAW INERTIAL X RATE ERROR
(INITIALIZED AT X=3000 FT)
X RATE ERROR-FT/SI
8
6
4
2
0
100
200
300
400
500
600
700
800
900
X DISTANCE-FT
-2
-4
-6
-8
-10

FIGURE 9

The filter's input consists of the difference between inertial position X_{IS} and the X_{ST} measurement, i.e., the raw inertial error. Also input to the filter is the expected 1 sigma X_{ST} accuracy (which is also the accuracy of the input raw inertial error).

The filter generates two outputs; inertial position bias estimate and inertial velocity bias estimate. Several additional parameters are also internally computed. These parameters are: (1) prediction of the position bias and velocity bias for the next computational cycle and (2) the expected accuracy of that prediction.

The predicted estimates are combined with the input data in a manner similar to the way triangulation range was combined with DME range. A weighing coefficient is computed based on the relative expected accuracies of the predicted versus input data. The weighing coefficient combines a portion of the input data with a portion of the predicted estimate to arrive at an optimum estimate of the output variables.

Figure 10 shows the filter weighing coefficients from 3,000 feet range to touchdown. The position weighing coefficient is seen to have a value of nearly 1 at the start of the trajectory. This implies that the output is formed mostly from the input data with very small percentage from the predicted estimate. As time goes on, the predicted estimate becomes more and more accurate so that only a small portion of the input data is used to form the output estimate. Within 300 feet from touchdown, the input data becomes more and more accurate because of the increasing accuracy of the triangulation measurement. This is reflected in the weighing coefficient by increasing the percentage of input data used to form the output in relation to the predicted estimate.

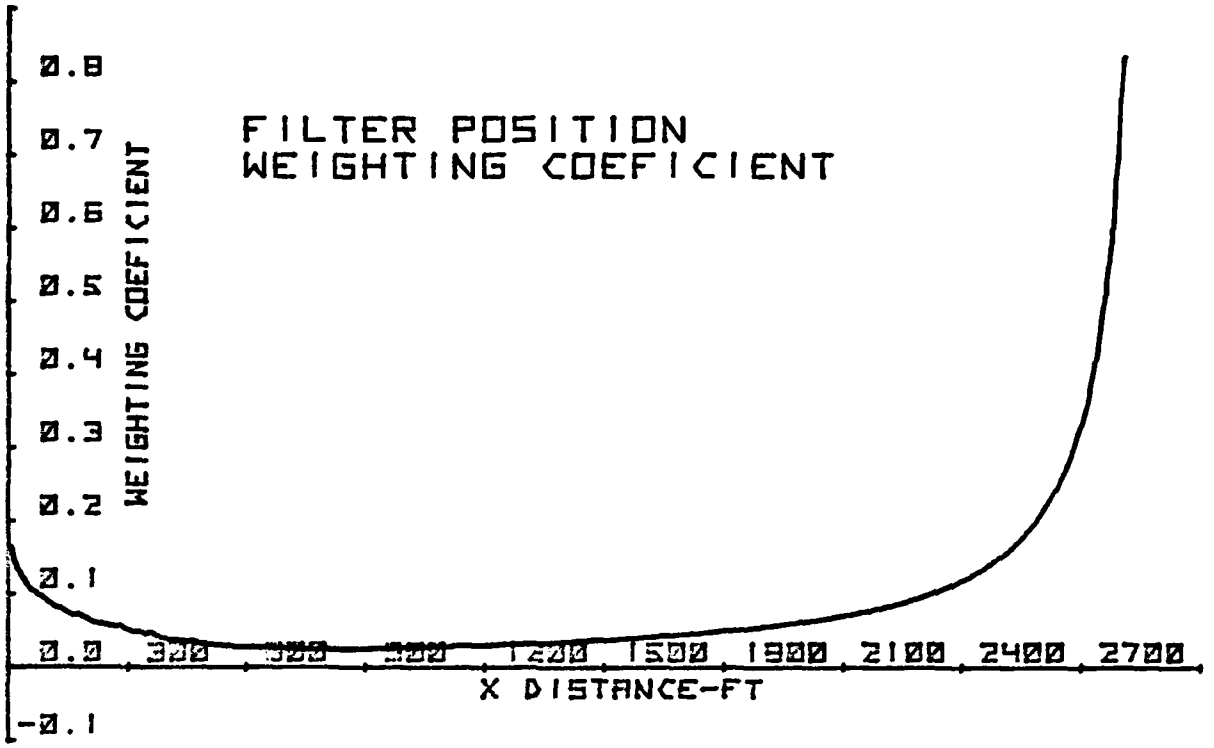
FILTER POSITION
WEIGHTING COEFICIENT
WEIGHTING COEFICIENT
0.8
0.7
0.6
0.5
0.4
0.3
0.2
0.1
0.0
-0.1
1200
1500
1800
2100
2400
2700
X DISTANCE-FT

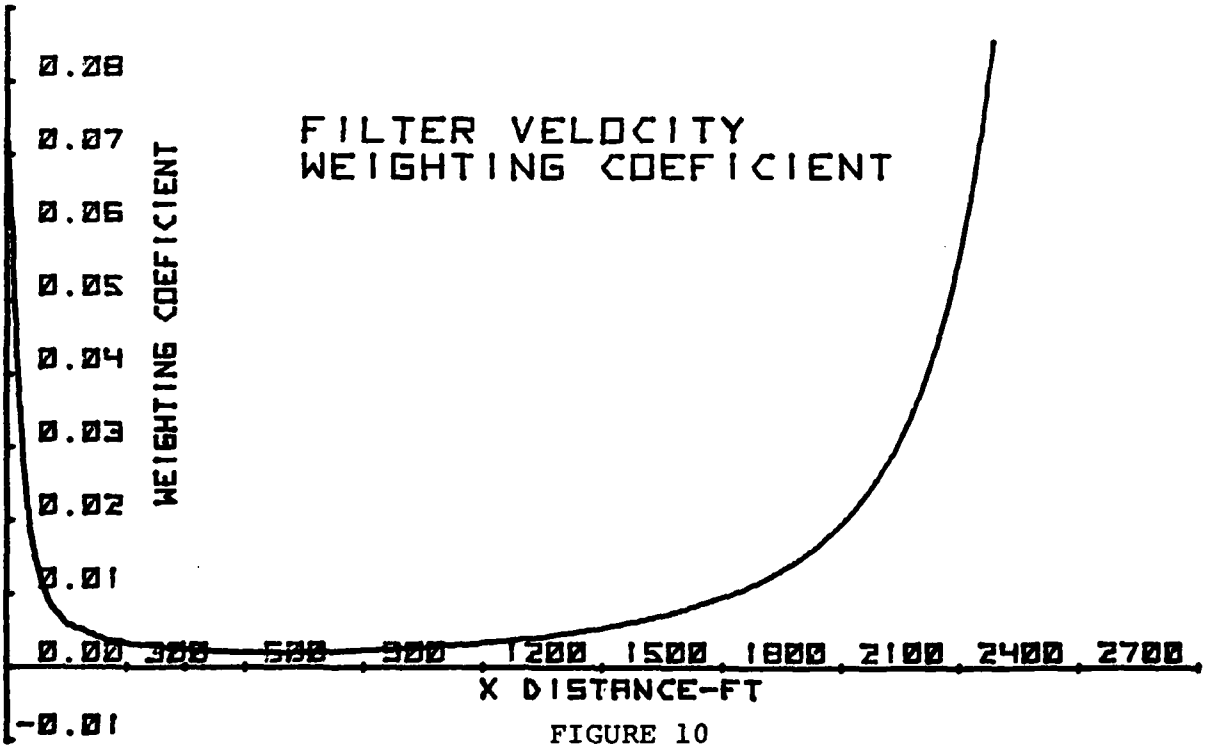
FILTER VELOCITY
WEIGHTING COEFICIENT
WEIGHTING COEFICIENT
0.08
0.07
0.06
0.05
0.04
0.03
0.02
0.01
0.00
-0.01
1200
1500
1800
2100
2400
2700
X DISTANCE-FT

FIGURE 10

The output position bias estimate and velocity bias estimate is subtracted from the respective inertial position and inertial velocity in order to obtain the smoothed position and smoothed velocity estimates.

It should be noted that there is no averaging done on the inertial data and, therefore, practically no lag associated with the smoothed outputs due to a sudden aircraft acceleration. The only expected lag is due to the sampling interval of the integrators, which was arbitrarily set at .1 seconds.

Filter settling characteristics when initialized from a cold start are shown in Figure 11. Smoothed X position is useable as soon as the integrators are initialized (it takes 1 second to initialize the integrators). Smoothed X velocity gets within 4 ft/sec of final value in less than 4 seconds from start.

F. SIMULATION OUTPUTS

Position and rate accuracies for a simulation run utilizing nominal parameter values (see Table I) and DME #1 are given in Fiugres 12 through 14. The X parameter (Figure 12) is seen to be relatively noise free. The bias error is essentially the bias of the triangulation/DME measurement and tends to zero as touchdown is neared.

X rate error contains a bias error between 1 and 2 ft/sec primarily due to the changing bias in the X parameter. Noise is low, less than 1/2 ft/sec.

Accuracies in the Y and Z parameters are primarily determined by the biases in the angle measurements. Accuracies are better than 1 foot within 600 feet of touchdown. Rate accuracies have noise components of 1/3 ft/sec. Rate bias is typically less than 1/3 ft. sec.

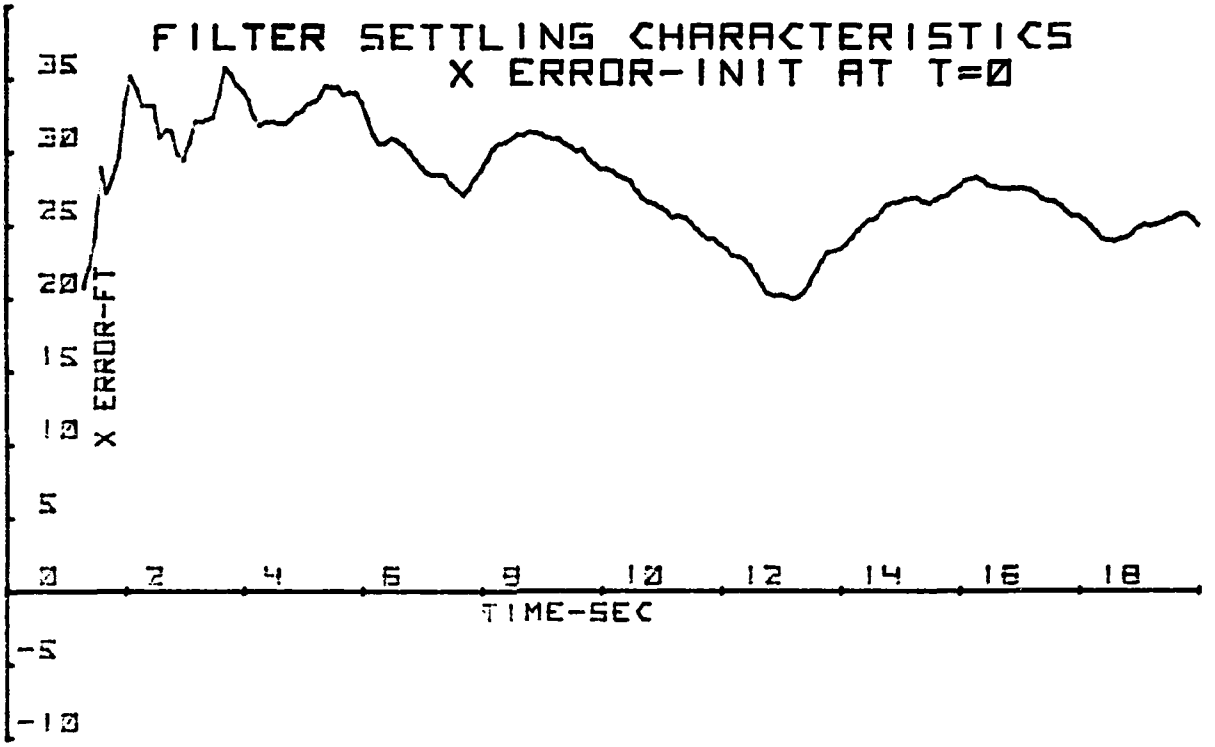
FILTER SETTLING CHARACTERISTICS
X ERROR-INIT AT T=0
X ERROR-FT
TIME-SEC
35
30
25
20
15
10
5
0
-5
-10
2
4
6
8
10
12
14
16
18

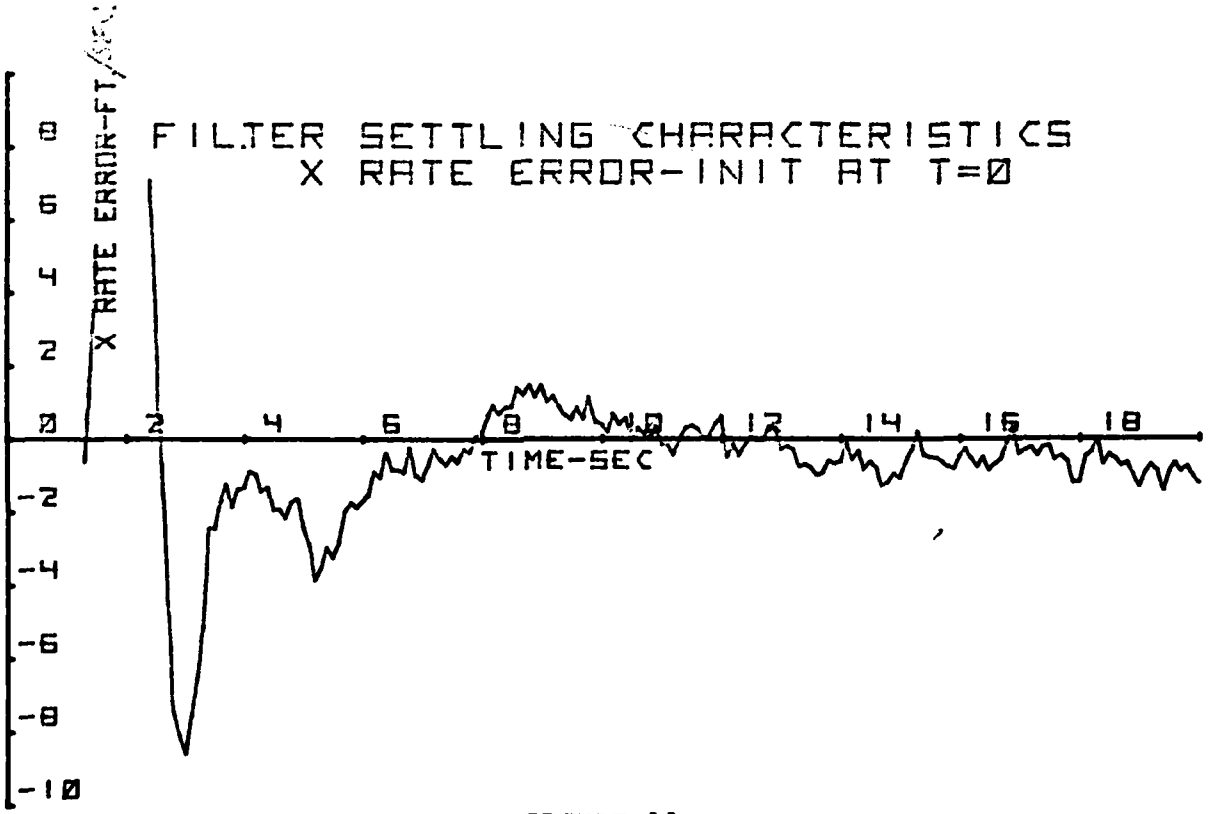
FILTER SETTLING CHARACTERISTICS
X RATE ERROR-INIT AT T=0
X RATE ERROR-FT/SEC
TIME-SEC
8
6
4
2
0
-2
-4
-6
-8
-10
2
4
6
8
10
12
14
16
18

FIGURE 11

Accuracies for the X and X rate parameters for a simulation run utilizing nominal parameter values and DME #2 is shown in Figure 15.

Here, the combination of large DME bias (80 feet) coupled with a large time correlated DME noise component (70 feet with a time constant of 5 seconds) generated rate biases in excess of 16 ft/sec. As demonstrated by this example, although this system mechanization is capable of smoothing large noise components in the DME and triangulation data, it does have a hard time smoothing out slowly varying fluctuations such as encountered when using DME #2.

G. COMPILATION OF STATISTICS

Twenty individual runs (similar to Figures 12 through 15) are performed in order to generate the accuracy statistics. The statistics are compiled during 3 segments of the trajectory each segment being 2.5 seconds long, starting at 1,000 feet, 300 feet and 40 feet distance, respectively. Figure 16 shows the X accuracy during these segments for several individual runs.

RSS error (bias plus noise) is computed for each of the trajectory segments using data from the 20 runs. The computed RSS error constitutes a single point in the sensitivity analysis plots. Another point is generated by changing one of the sensor parameters and repeating the 20 simulation runs. Figure 18 shows a sample plot of X error sensitivity to changes in heading error.

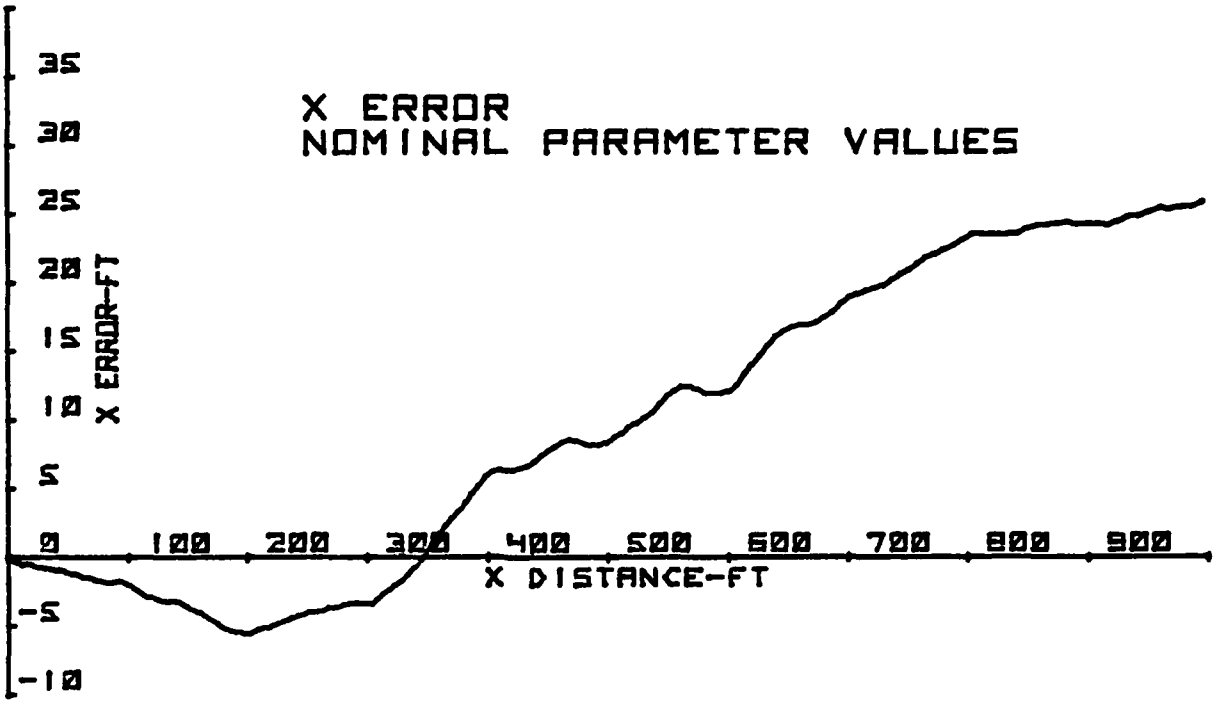

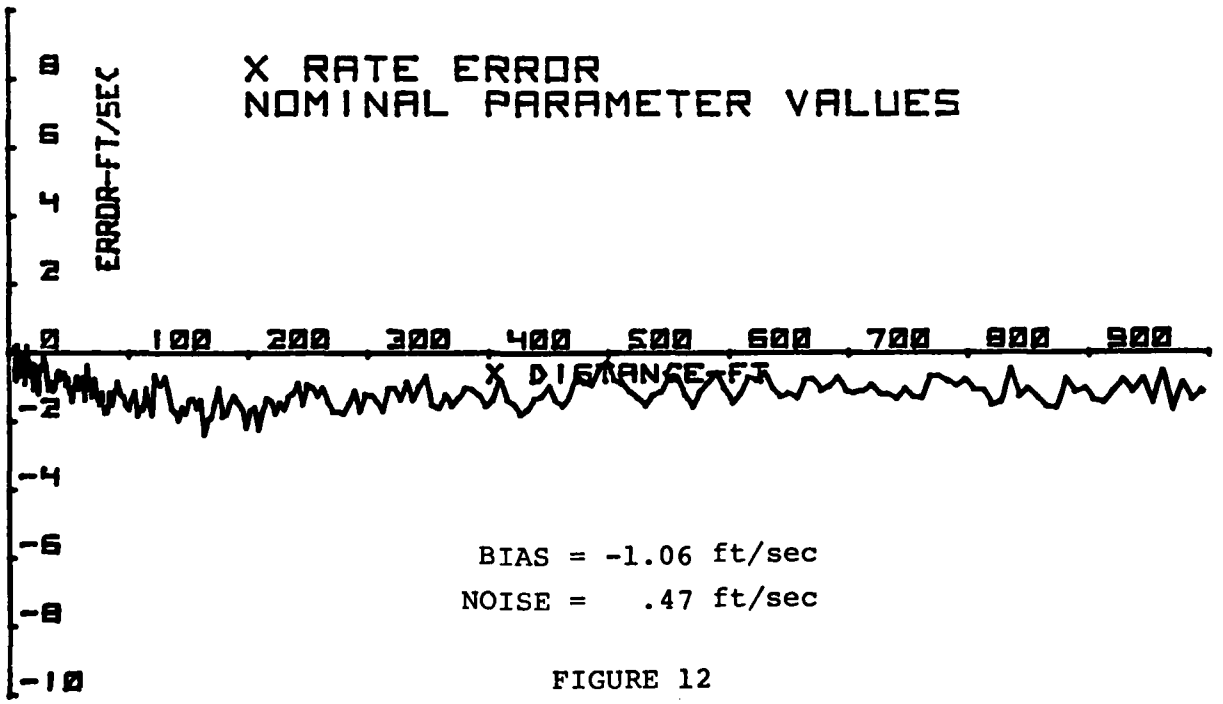

BIAS = -1.06 ft/sec

NOISE = .47 ft/sec

FIGURE 12

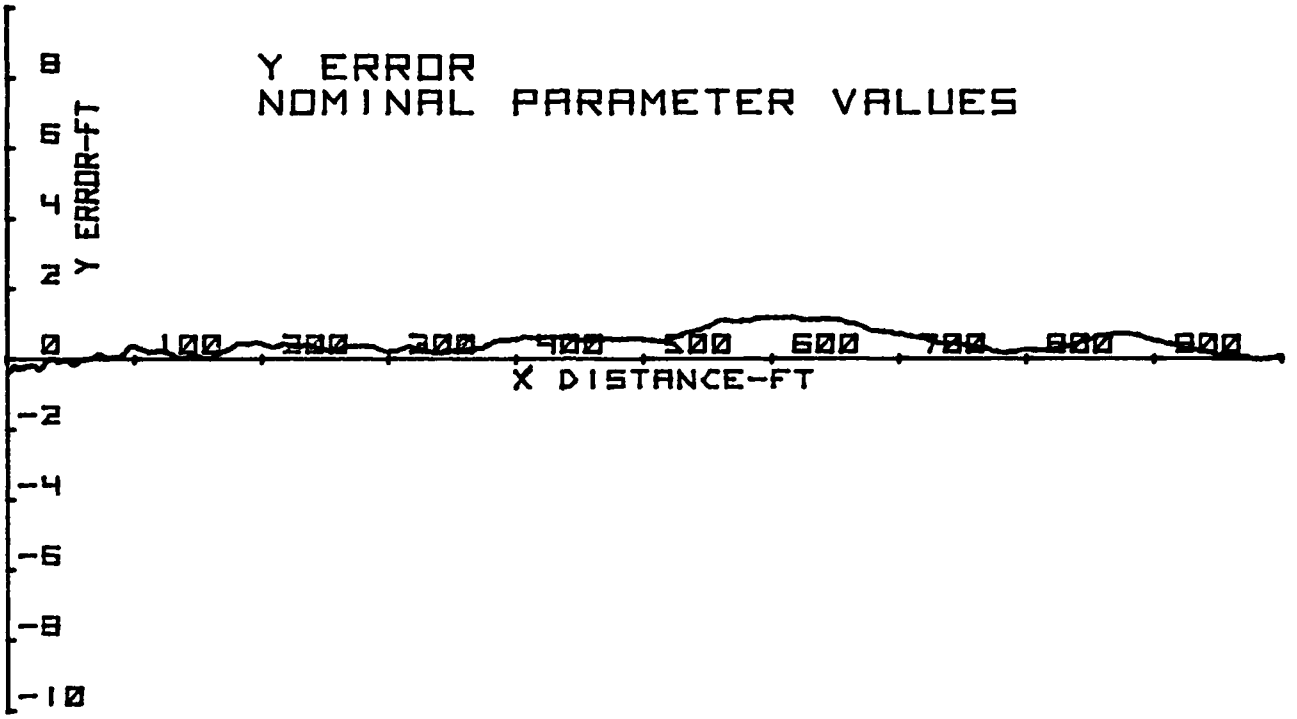

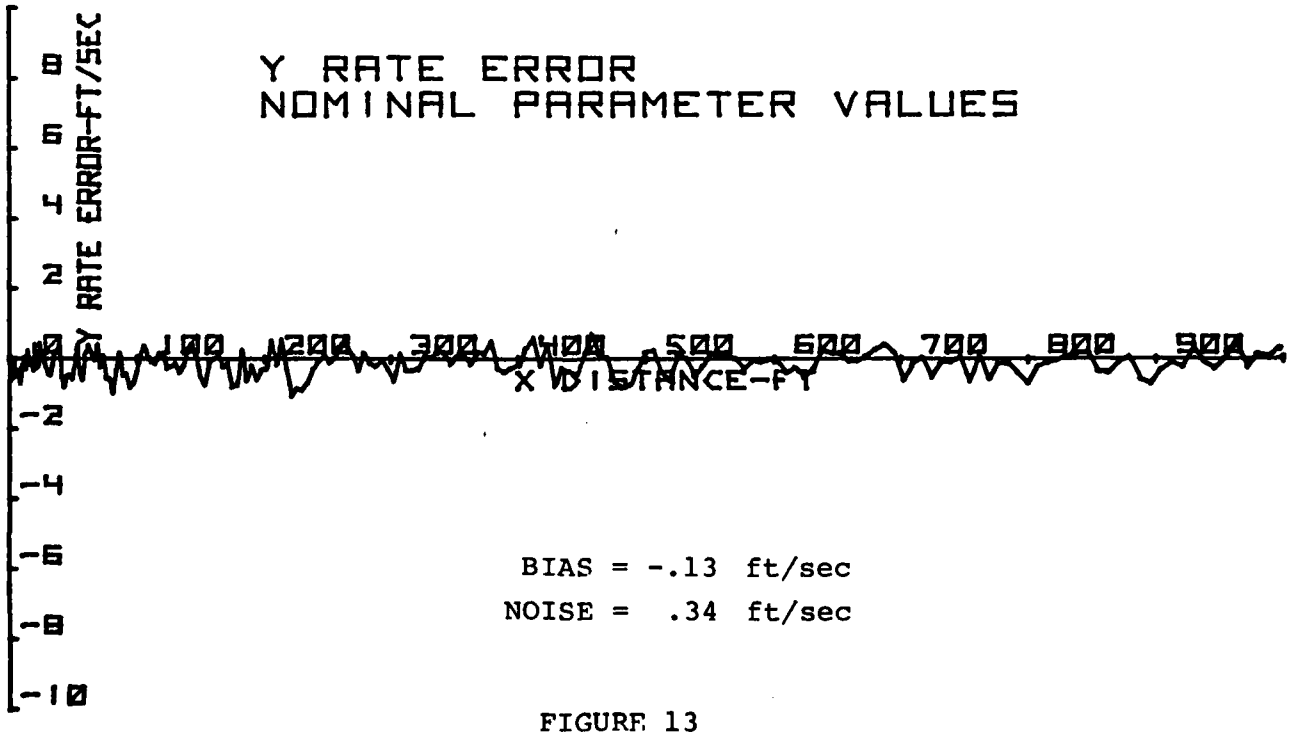

BIAS = -.13 ft/sec

NOISE = .34 ft/sec

FIGURE 13

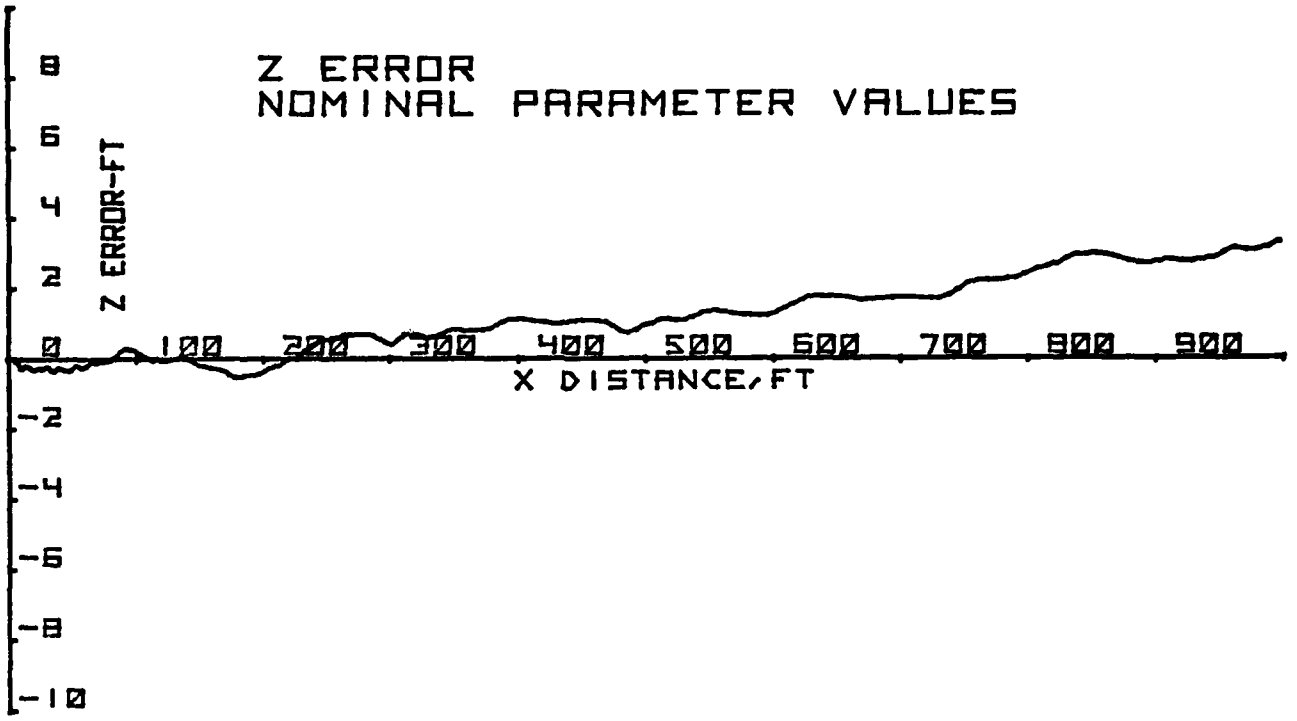

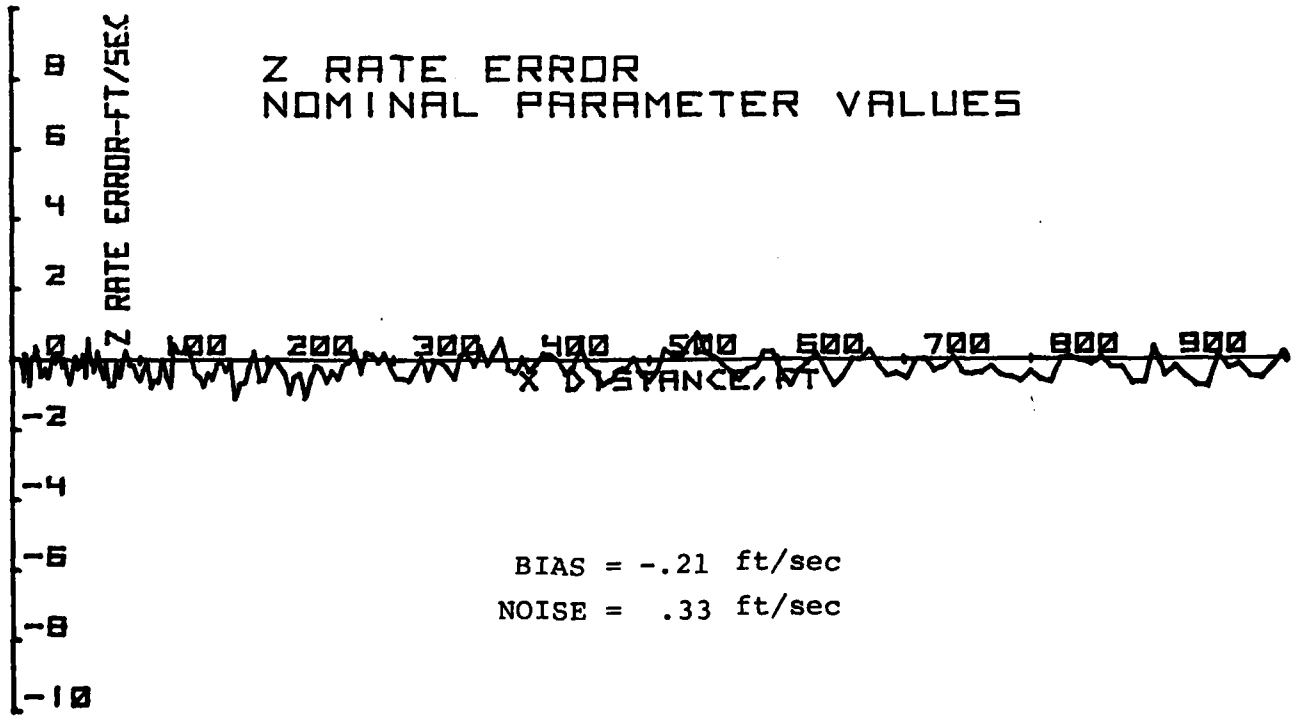

BIAS = -.21 ft/sec

NOISE = .33 ft/sec

FIGURE 14

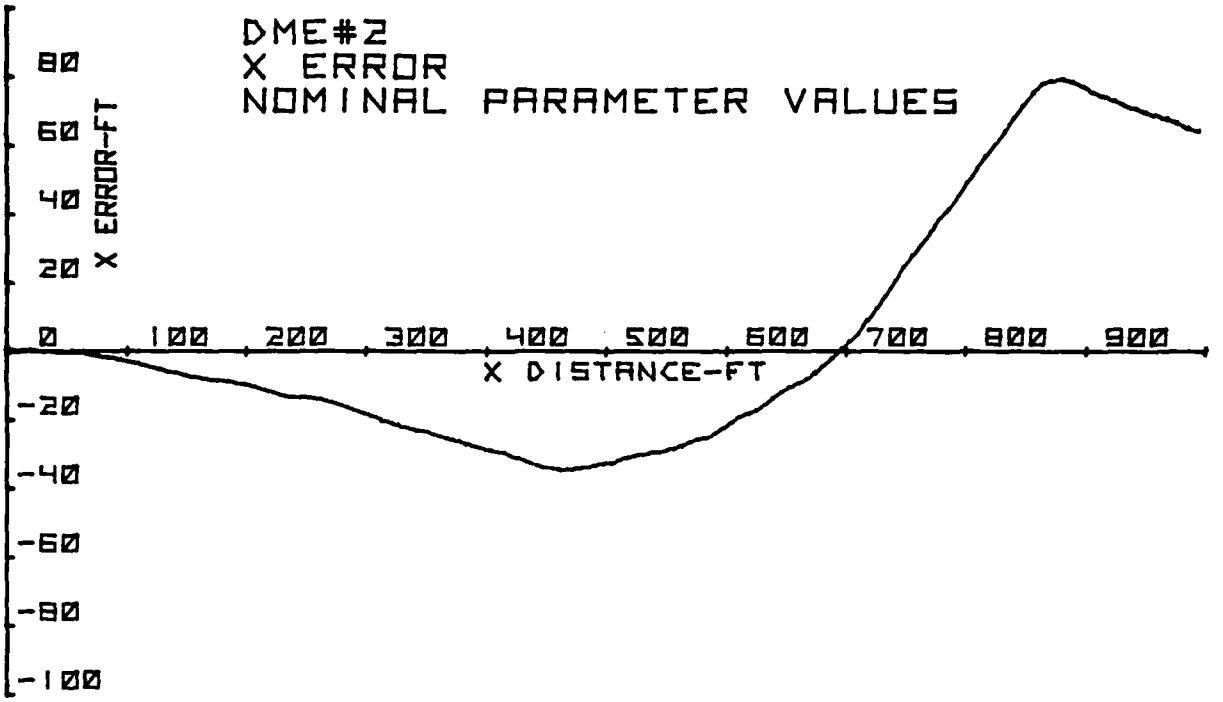

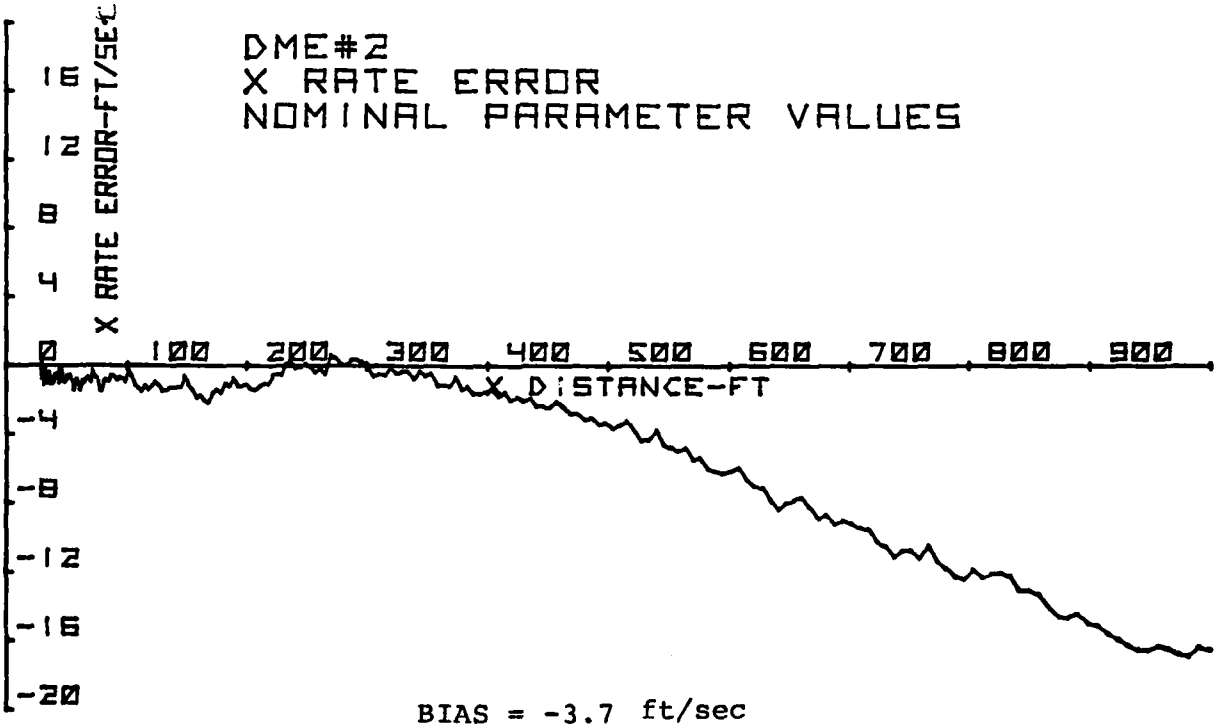

BIAS = -3.7 ft/sec

NOISE = -4.8 ft/sec

FIGURE 15

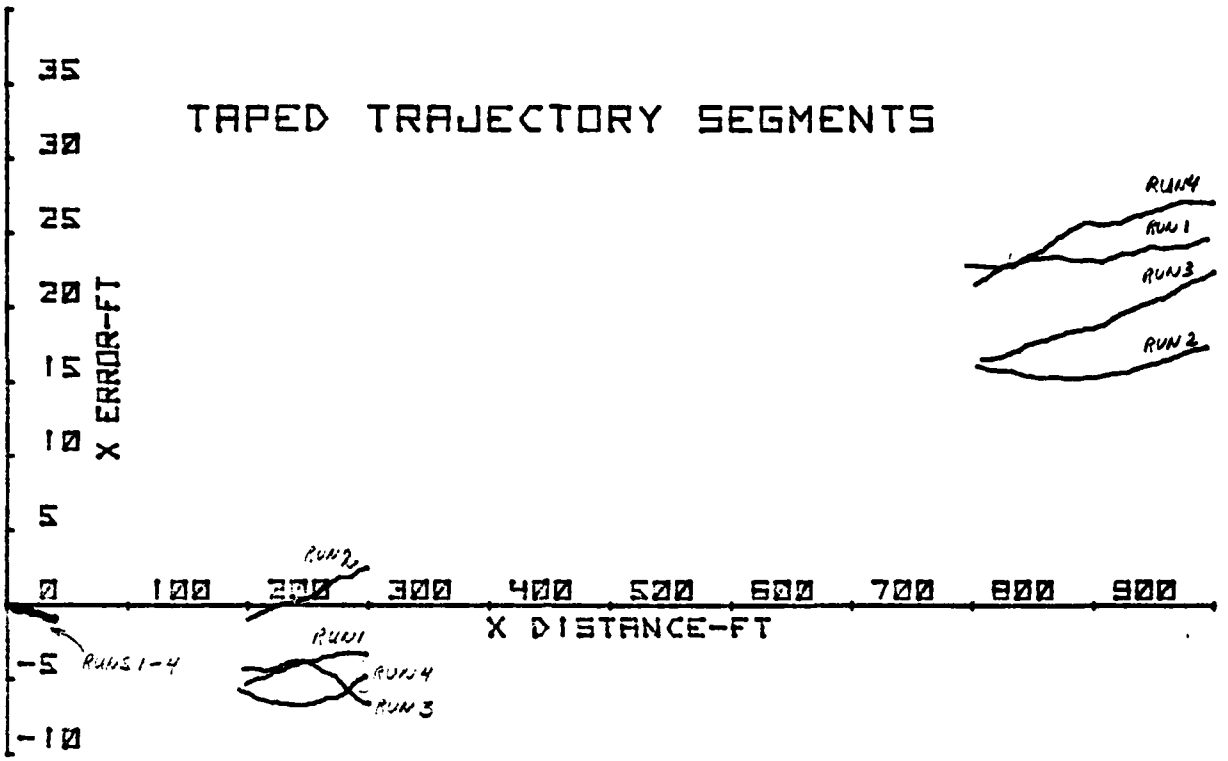
TAPED TRAJECTORY SEGMENTS
35
30
25
20
15
10
5
0
-5
-10
X ERROR-FT
100
200
300
400
500
600
700
800
900
X DISTANCE-FT
RUN 4
RUN 1
RUN 3
RUN 2
RUNS 1-4

FIGURE 16

III. SIMULATION RESULTS

Simulation results are presented in two parts. The first part, Figures 17 through 72, contains position and rate error sensitivities to changes in airborne sensor parameters. Platform motion is not included in these simulations.

Parameters analyzed are as follows:

(1) Difference in error between ships and airborne heading references

(2) DME bias error

(3) Airborne accelerometer bias

(4) DME error correlation time constant

(5) Angle error correlation time constant

The second part of the results, Figures 73 through 106, deals with position and rate error sensitivities to changes in ship motion sensor parameters. Platform motion is included in these simulations.

Parameters analyzed include:

(1) Pitch sensor bias

(2) Roll sensor bias

(3) Ships vertical accelerometer bias

A. SENSITIVITIES TO AIRBORNE SENSOR PARAMETERS

HEADING ERROR (FIGURES 17 - 25)

Sensitivity of X error to the error difference between the ships and airborne heading references (Figure 18) shows a modest increase when heading error is varied from 1 degree to 10 degrees. Largest percentage increase in X error occurs near touchdown. At 40 feet range, X error increases from .55 feet to 1.21 feet.

X rate error (Figure 19) similarly changes with heading error. At 40 feet, range X rate error increases from .74 ft/sec to 1.4 ft/sec when heading error changes from 1 degree to 10 degrees.

Y error and Y rate error (Figures 21 and 22) also show an increase with increasing heading error, but accuracies near touchdown are better than 1 foot and 1 ft/sec even for heading errors of 10 degrees.

X errors and X rate errors utilizing DME #2 is given in Figures 24 and 25. At ranges beyond 300 feet, very little difference in error are seen mainly because other error sources swamp out the contribution due to heading. X

error at 1,000 feet range is typically 90 feet. X rate error is typically 9 ft/sec. At 40 feet range and 10 degree heading error, X error becomes .63 feet and X rate error is 1 ft/sec. The apparently better performance at close range of DME #2 system versus DME #1 is due to transitioning to triangulation guidance much earlier in range.

Sensitivity of the Z and Z rate parameters versus heading error were not performed since heading inaccuracy does not impact measurement of aircraft vertical accelerations.

DME BIAS ERROR (FIGURES 26 - 37)

Sensitivities of position and rate accuracy to changes in DME bias were performed by fixing the triangulation/DME blending parameters such that the blending coefficient was optimized for a DME with a 30 foot bias. The actual bias, however, was varied from 10 to 120 feet.

Results of the X error sensitivity are given in Figure 27. As expected, X error varies linearly with DME bias at longer ranges, having the least effect near touchdown. It is interesting to note that at 300 feet range, X error for a 30 foot DME bias is lower than the X error for a 10 foot DME bias. This is probably because the triangulation/DME blending is "tuned" for a 30 foot DME bias.

Increasing the DME bias had the most effect on the X rate accuracy around 300 feet range (Figure 28). The slope in the X error bias which occurs during transition from DME to triangulation appears to effect the X rate accuracy most.

Y error and Y rate error were minimally effected (Figures 30 and 31). Z error increased at longer range with little effect near touchdown. Z rate accuracy was likewise minimally effected.

X and X rate accuracies for a DME #2 system (Figures 36 and 37) did not show appreciable increases due to increasing DME bias. The large time correlated noise component of DME #2 appears to be swamping out this source of error. An increase in X rate error around 300 feet range is noticeable.

ACCELEROMETER BIAS (FIGURES 38 - 49)

Accelerometer bias did not seem to have much impact on position and rate accuracies for accelerometer bias levels up to 1,000 microG's. At 10,000 microG'S (.01G), all position and rate accuracies developed a fixed offset which was fairly constant from run to run.

X error bias at 40 feet range for example changed from -.31 feet to 1.69 feet when the accelerometer bias increased from 1,000 to 10,000 microG's. X rate accuracy bias at 40 feet likewise increased from -.47 ft/sec to 1.52 ft/sec.

The Y and Z position and rate errors suffered a similar shift in bias of approximately 2 feet and 2 ft/sec respectively.

X and X rate accuracies utilizing DME #2 do not seem to show much change with changing accelerometer bias probably because of the masking effect of other larger sources of error.

DME CORRELATION TIME CONSTANT (FIGURES 50 - 61)

Increasing the DME error correlation time constant from .5 seconds to 10 seconds had the greatest impact on X accuracy around 300 feet range (Figure 51). X error at 300 feet increased from 2 feet to 18 feet. Most of the error increase was in the form of a bias which changed

from run to run. X error increase at 1,000 feet range can also be seen, but is not quite as pronounced as at 300 feet.

X rate error increased somewhat at 1,000 feet range (from 1 ft/sec to 1.6 ft/sec). Very little effect is seen at 300 feet and 40 feet.

Y and Z position and rates (Figures 53 - 57) did not show much sensitivity to this error parameter.

X error utilizing DME #2 also showed a pronounced increase as the correlation time constant was changed from 5 seconds to 20 seconds (Figure 60) especially at 300 feet range. X rate error was also increased, although not quite as pronounced.

ANGLE CORRELATION TIME CONSTANT (FIGURES 62 - 72)

Changing the angle correlation time constant from .5 seconds to 5 seconds had minimal effect on all position and rate errors. Maximum effect was observed at long ranges, 1,000 feet, for the Y error and Z error.

Y error at 1,000 feet increased from .95 feet to 1.54 feet. Z error increased from 3.25 feet to 3.69 feet.

B. SENSITIVITY TO SHIP MOTION SENSOR PARAMETERS

PITCH SENSOR BIAS

Pitch sensor bias was varied from a nominal value of .05 degrees up to a maximum of .15 degrees. The only noticeable effect on position and rate accuracies was an increase in the Z error at 1,000 feet from 3.78 feet to 5.5 feet. (Figure 80). Most of the increase was due to a shift in Z bias.

In addition to the normal Z output which is relative to the touchdown point, an absolute Z estimate (referenced to the next position of the touchdown point) was computed. This, in effect, is an indirect way of measuring heave.

The absolute Z estimate is performed by not subtracting the ships vertical acceleration from the airborne vertical acceleration. Figure 82 shows a typical run utilizing nominal parameters. Figures 83 and 84 show the absolute Z and Z rate sensitivity to pitch sensor bias. Absolute Z accuracy near touchdown was measured to be 2.86 feet at .05 degree pitch sensor bias, increasing to 3.87 feet at .15 degree pitch sensor bias. The absolute Z accuracy appeared to be highly dependent on the exact structure of heave fluctuation.

Absolute Z rate did not appear sensitive to pitch bias, staying at approximately 1/2 ft/sec.

ROLL SENSOR BIAS (FIGURES 85 - 95)

Changing roll sensor bias from .05 to .15 degrees had no significant effect on any of the position and rate accuracies.

Absolute Z error appeared to decrease with increasing roll bias, but this is most probably attributed to an inadequate number of runs to completely characterize the heave fluctuation.

VERTICAL ACCELEROMETER BIAS (FIGURES 102 - 106)

As expected, increasing the bias of the ships vertical accelerometer effected only the Z and Z rate error.

The Z and Z rate errors did not change appreciably until the accelerometer bias increased to 10,000 microG's. At that point, both Z and Z rate developed a fixed offset of approximately -3 feet and -3 ft/sec respectively. Also, the Z error developed a fluctuation due to the inadequate filtering of the heave component (see Figure 102).

C. SUMMARY AND CONSLUSIONS

System mechanization utilizing nominal parameters and DME #1 had no problems meeting 1 foot position and 1 ft/sec rate accuracies near touchdown.

Rate accuracies at longer ranges were within 1 ft/sec; more than adequate for autoland flight control.

The assumed angle sensor accuracies of .1 degree bias, .07 degree noise were adequate. Changes in noise correlation time constant did not appear to make much difference in position and rate accuracies. Operating frequency for the angle sensors should, therefore, be dictated mostly by the physical size of the scanning antennas.

X rate accuracy utilizing DME #2 was marginal at longer ranges. One sigma amplitude of the time correlated noise component should, therefore, be limited to 10 or 15 feet. Operating frequency should be as high as possible in order to minimize the noise correlation time constant. DME bias error should be held within 60 feet in order to limit the X rate bias shift during the transition from DME to triangulation guidance.

Airborne accelerometer biases should be within 1,000 microG's so as not to introduce position and rate biases.

Difference in error between shipboard and airborne heading reference had minimal effect on system accuracy. A 5 degree error limit will yield satisfactory results.

Shipboard vertical accelerometer bias should be held to within 1,000 microG's so as to minimize height and height rate biases. Shipboard pitch and roll sensors did not have much effect on output accuracy. A .15 degree bias allowance for pitch and roll will yield satisfactory system performance.

IV. SIMULATION DATA - SENSITIVITIES TO AIRBORNE SENSOR ERROR PARAMETERS

A. SENSITIVITY TO DIFFERENCE IN HEADING ERROR

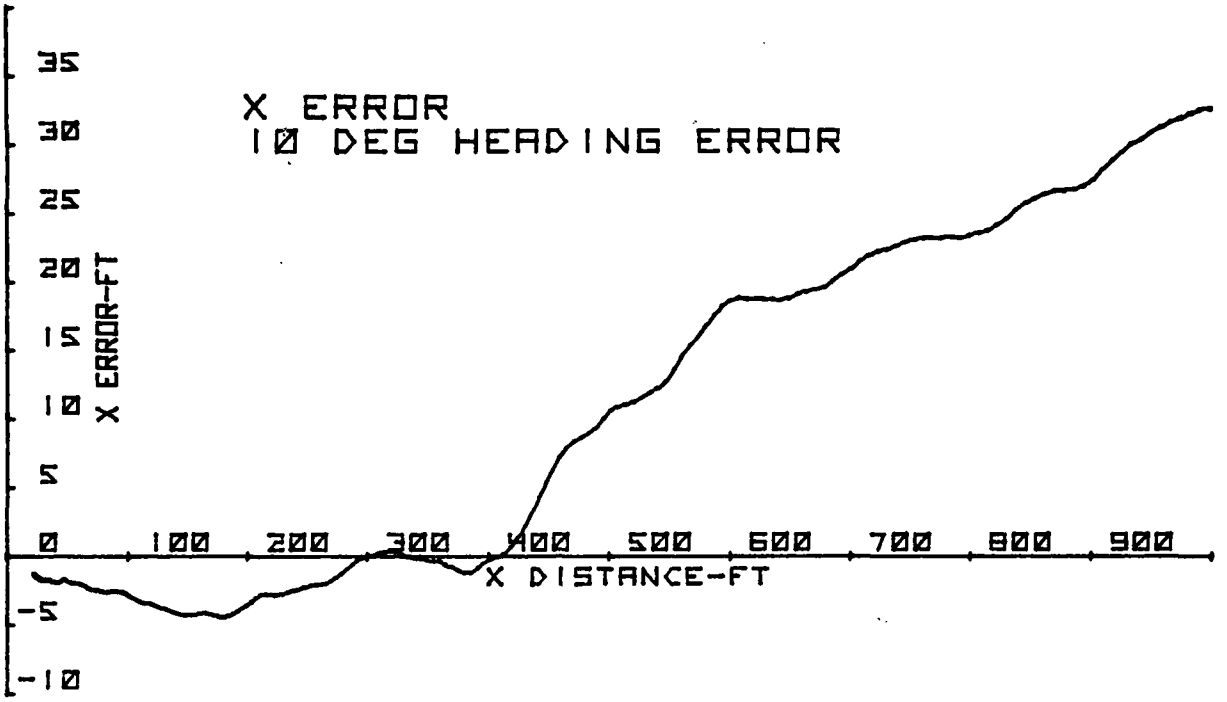

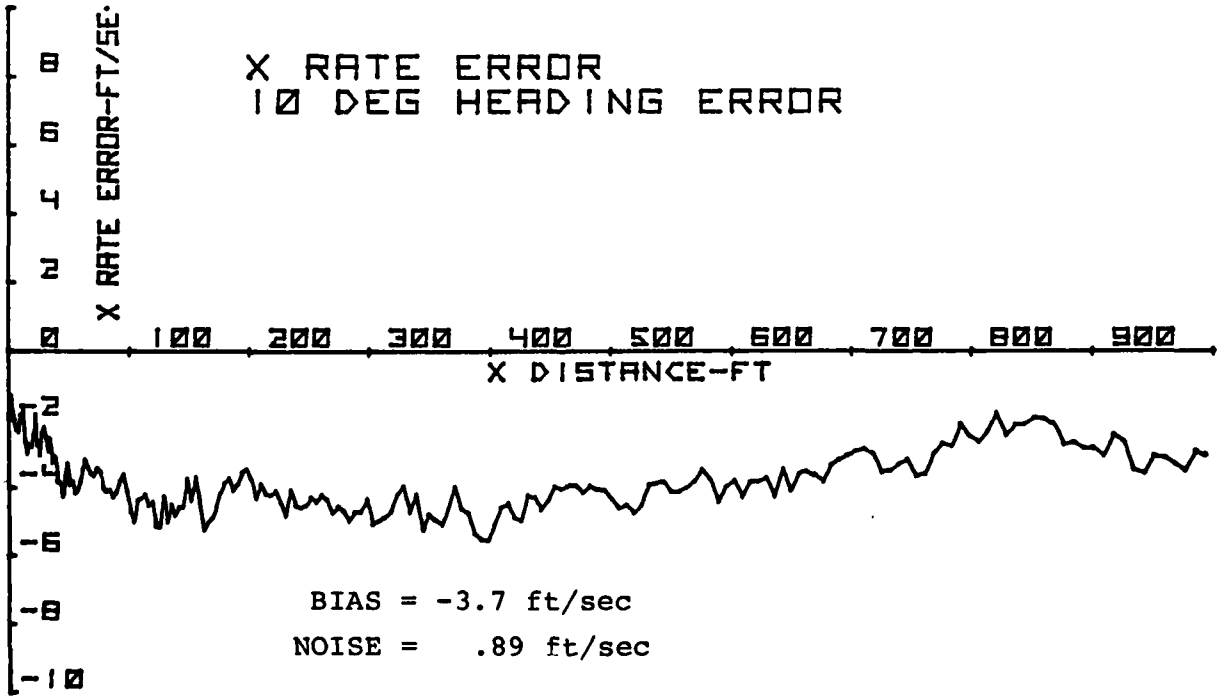

BIAS = -3.7 ft/sec

NOISE = .89 ft/sec

FIGURE 17

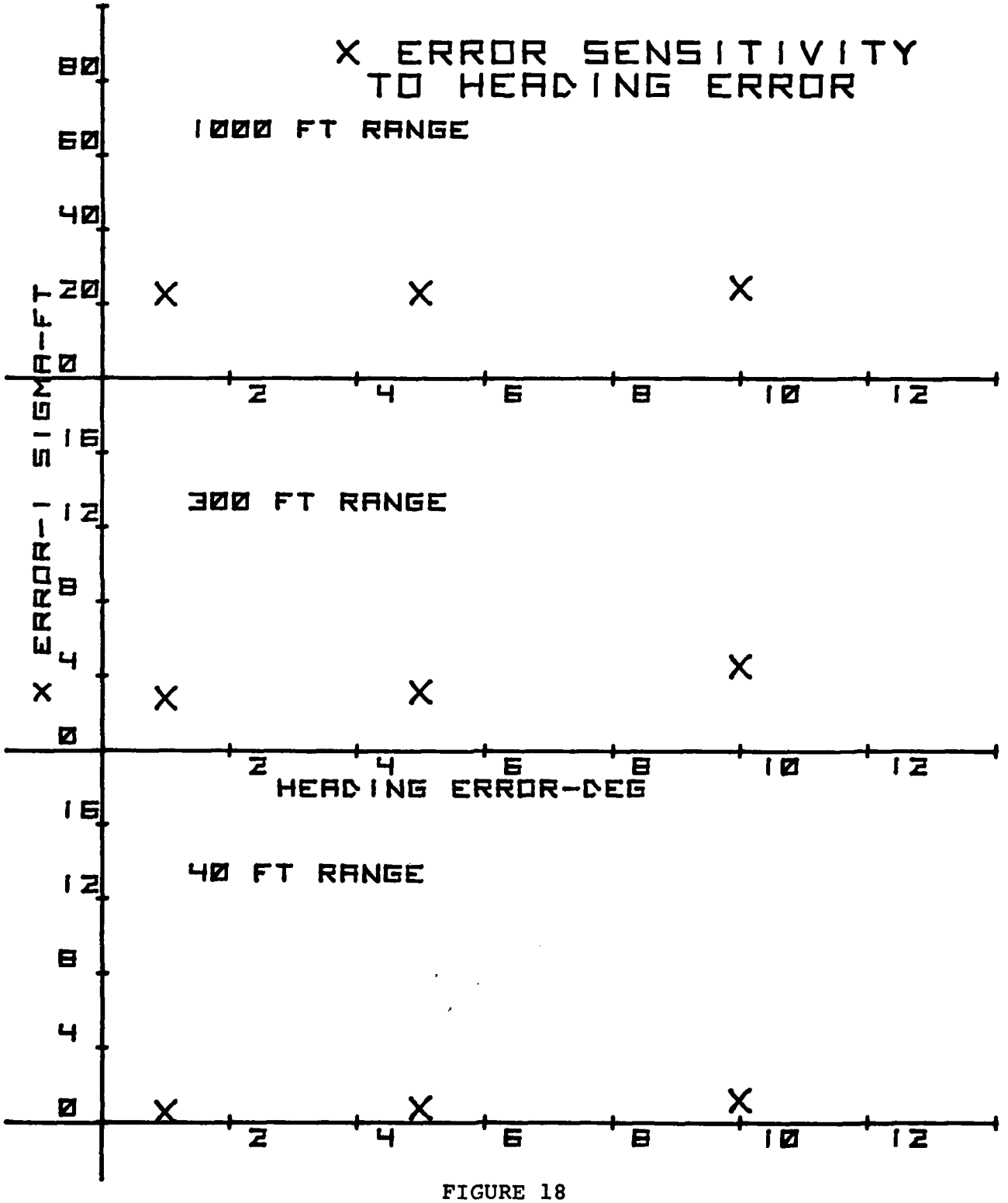
X ERROR SENSITIVITY
TO HEADING ERROR
1000 FT RANGE
300 FT RANGE
40 FT RANGE
X ERROR-1 SIGMA-FT
HEADING ERROR-DEG
80
60
40
20
0
16
12
8
4
0
2
4
6
8
10
12

FIGURE 18

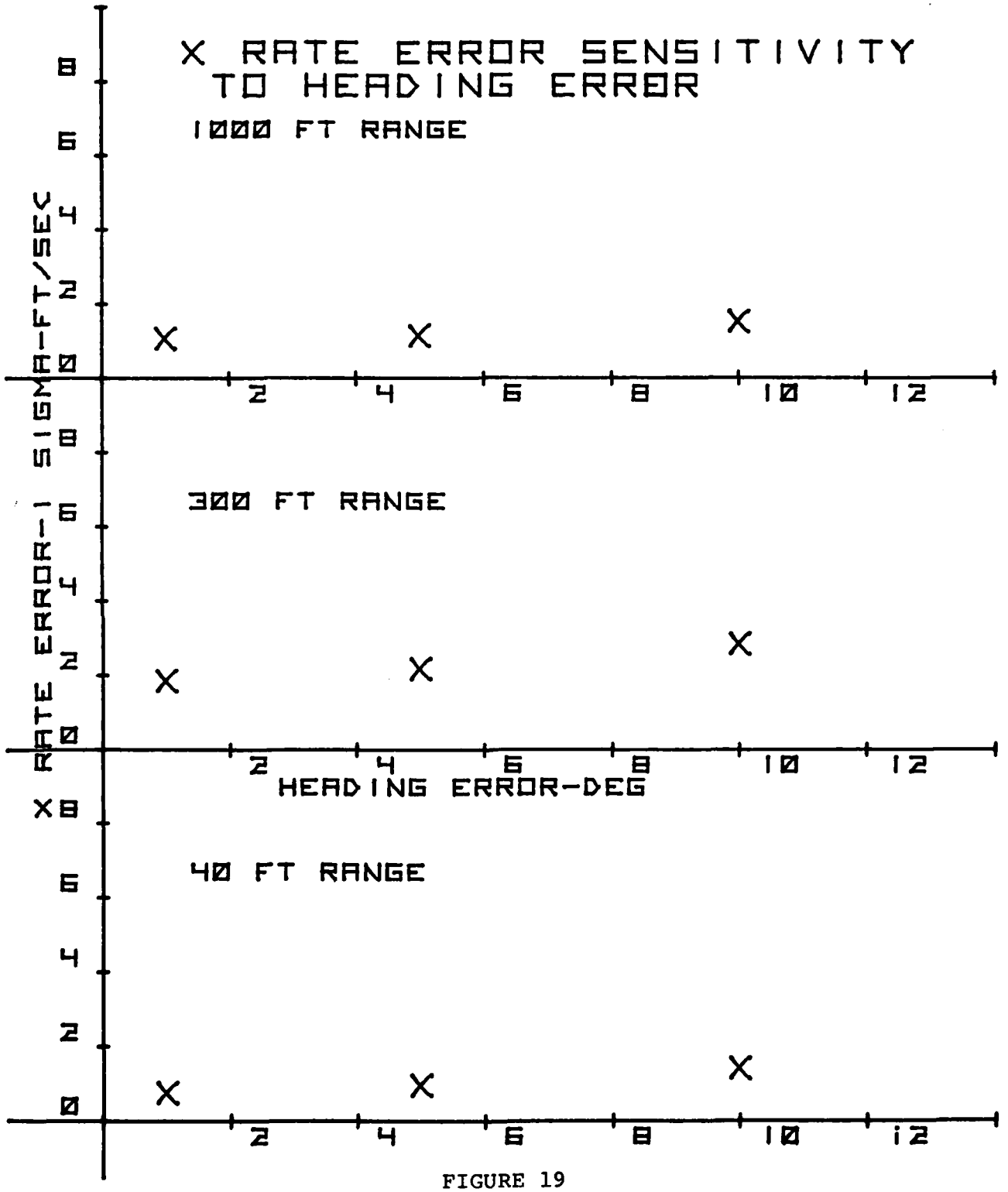
X RATE ERROR SENSITIVITY
TO HEADING ERROR
1000 FT RANGE
300 FT RANGE
40 FT RANGE
X RATE ERROR-1 SIGMA-FT/SEC
HEADING ERROR-DEG
0
2
4
6
8
10
12

FIGURE 19

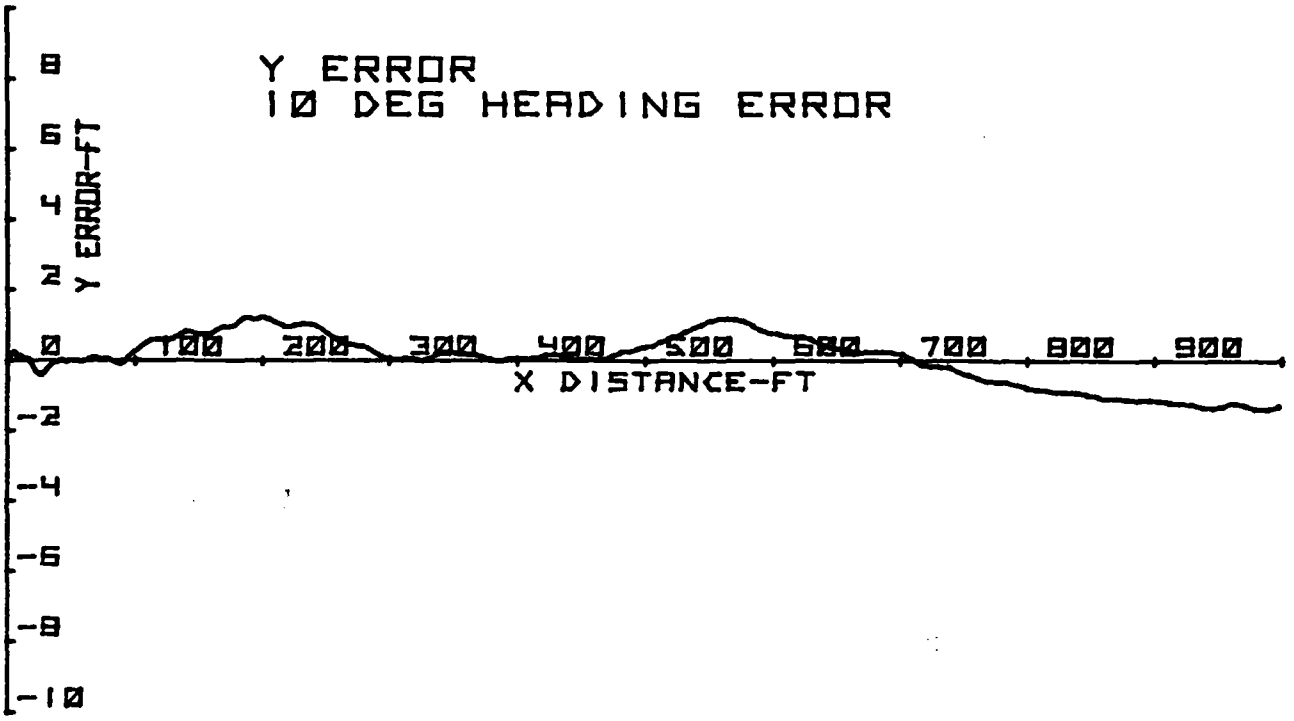

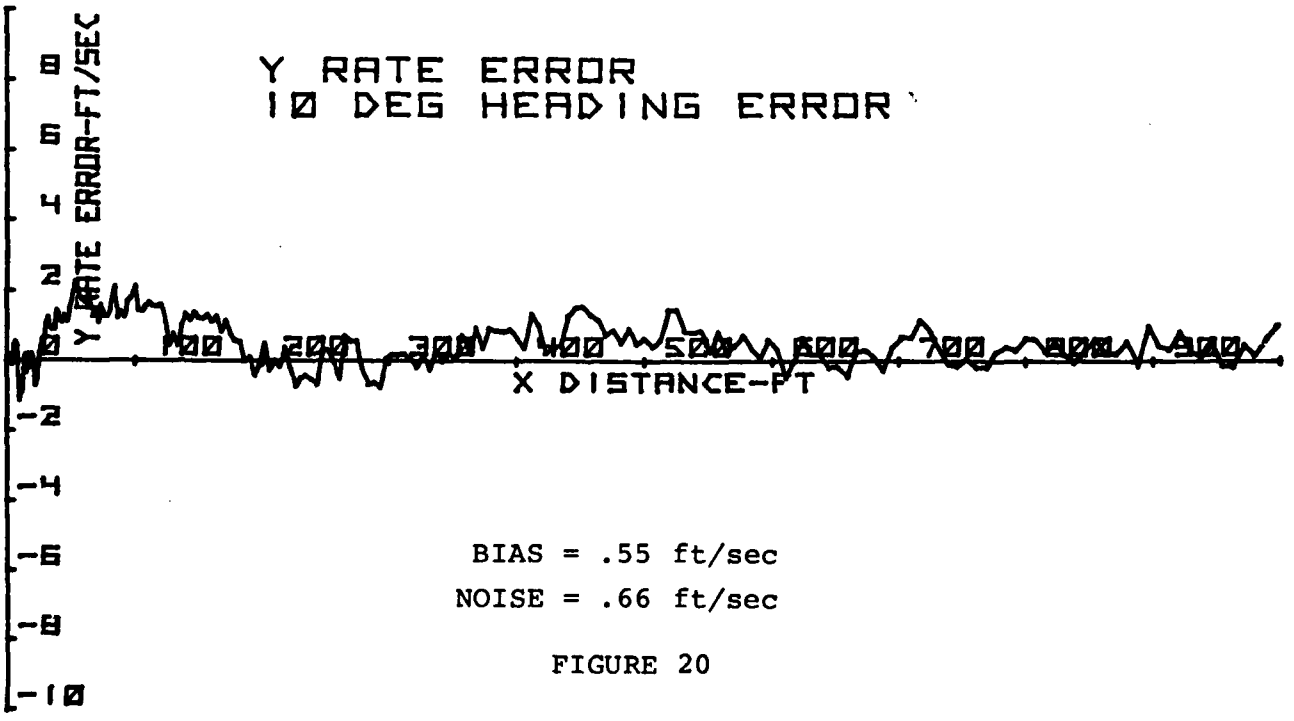

BIAS = .55 ft/sec

NOISE = .66 ft/sec

FIGURE 20

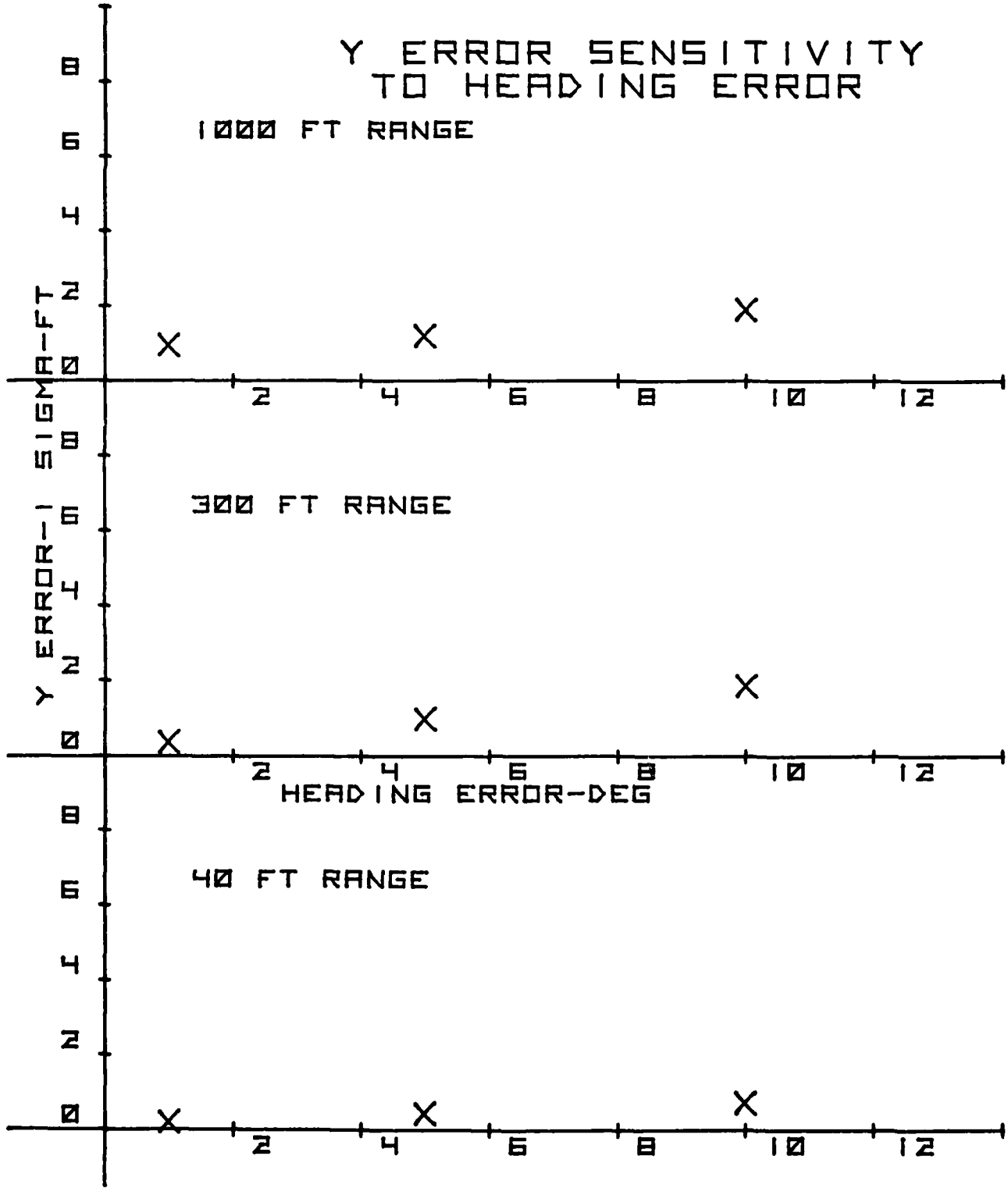
Y ERROR SENSITIVITY
TO HEADING ERROR
1000 FT RANGE
300 FT RANGE
40 FT RANGE
Y ERROR-1 SIGMA-FT
HEADING ERROR-DEG
0
2
4
6
8
10
12

FIGURE 21

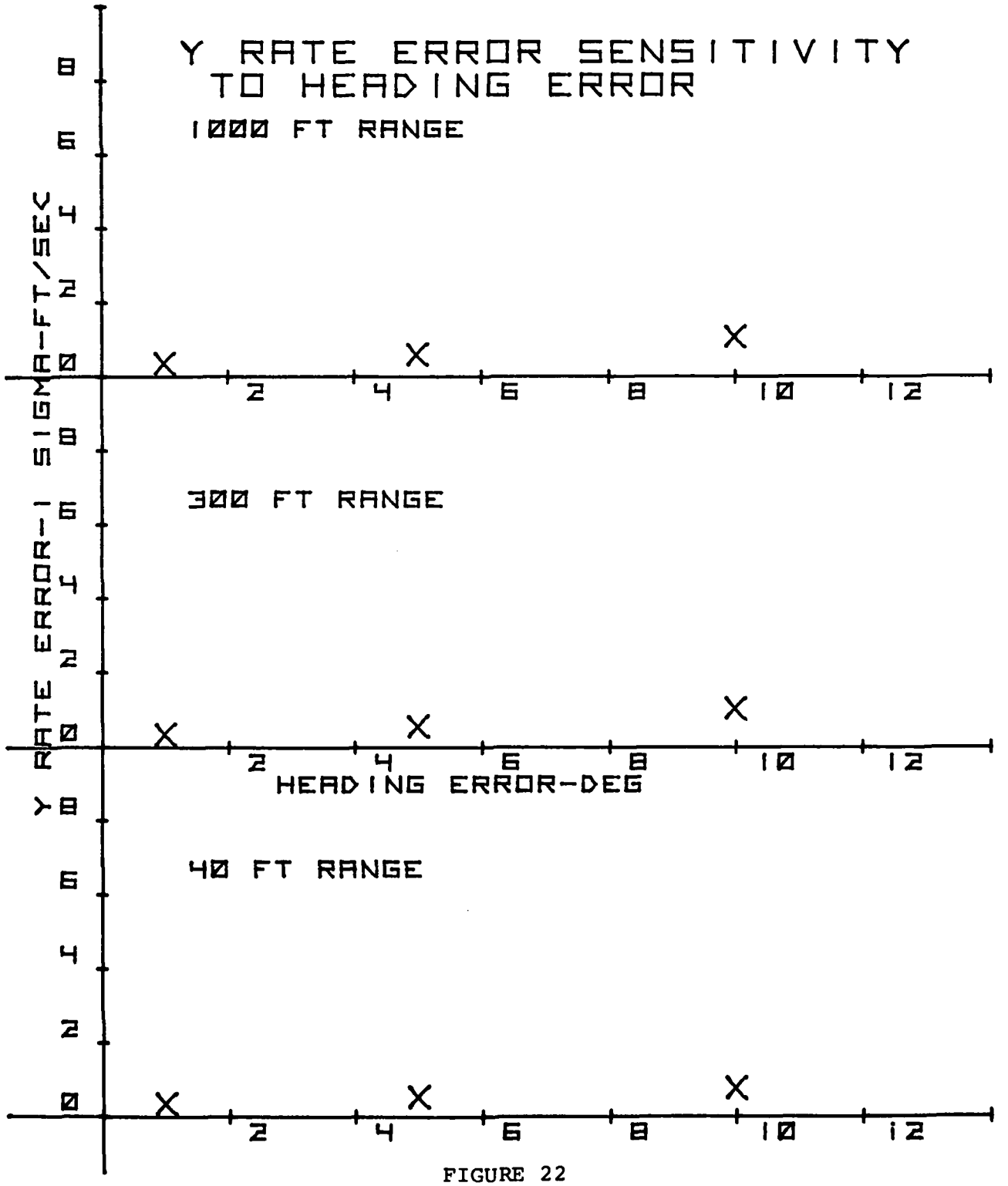
Y RATE ERROR SENSITIVITY
TO HEADING ERROR
1000 FT RANGE
300 FT RANGE
40 FT RANGE
Y RATE ERROR-1 SIGMA-FT/SEC
HEADING ERROR-DEG
0
2
4
6
8
10
12

FIGURE 22

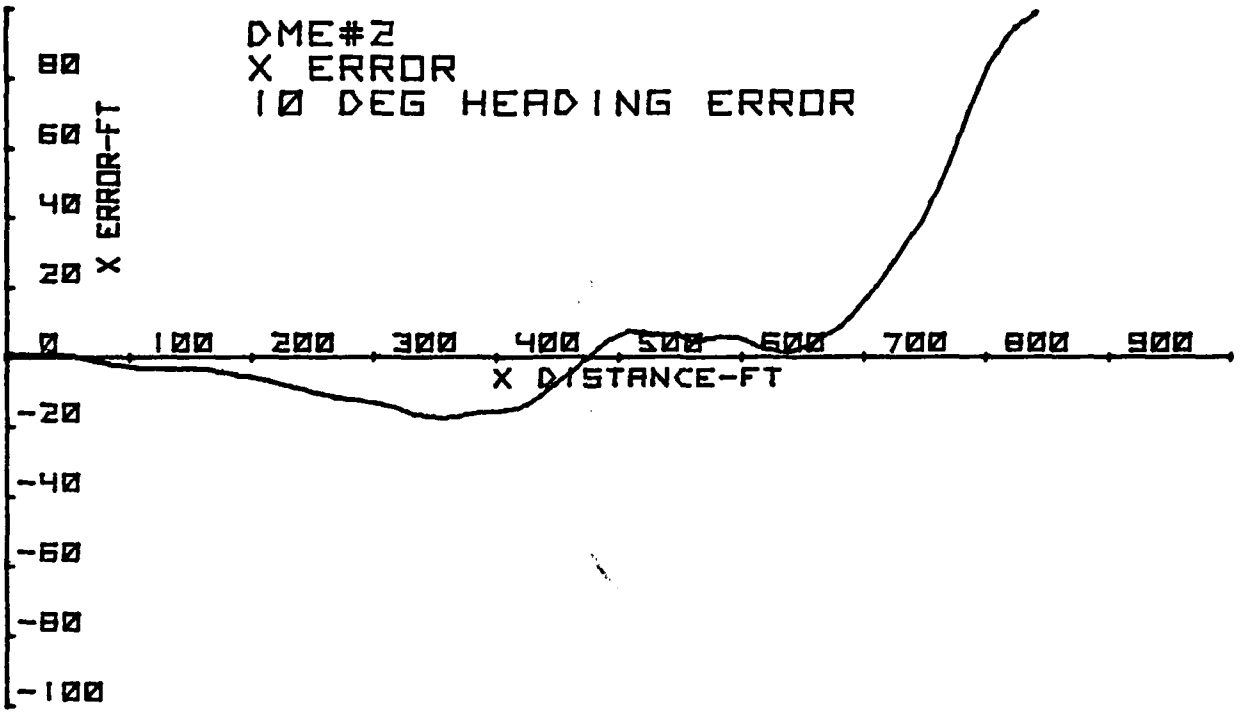
DME#2
X ERROR
10 DEG HEADING ERROR
X ERROR-FT
80
60
40
20
0
100
200
300
400
500
600
700
800
900
X DISTANCE-FT
-20
-40
-60
-80
-100

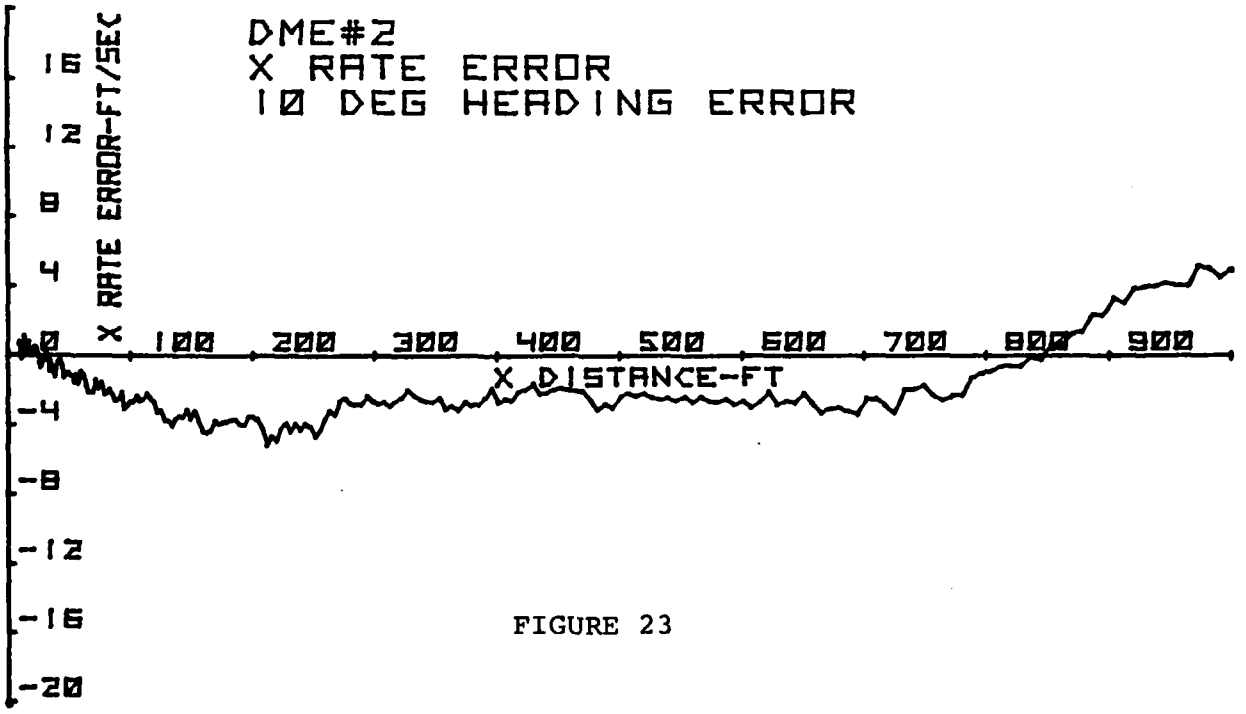
DME#2
X RATE ERROR
10 DEG HEADING ERROR
X RATE ERROR-FT/SEC
16
12
8
4
0
100
200
300
400
500
600
700
800
900
X DISTANCE-FT
-4
-8
-12
-16
-20

FIGURE 23

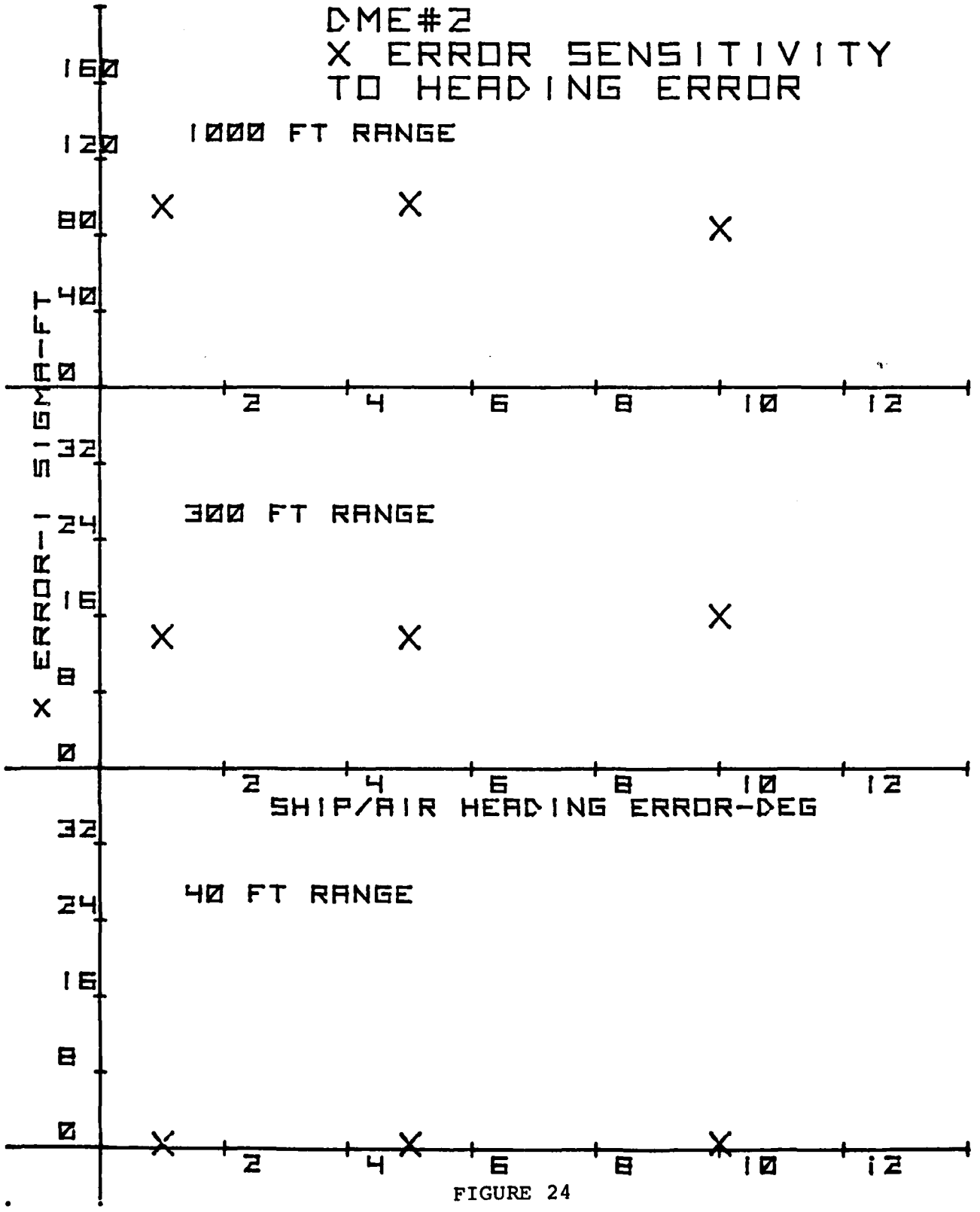
DME#2
X ERROR SENSITIVITY
TO HEADING ERROR
1000 FT RANGE
300 FT RANGE
40 FT RANGE
X ERROR-1 SIGMA-FT
SHIP/AIR HEADING ERROR-DEG
160
120
80
40
0
32
24
16
8
0
2
4
6
8
10
12

FIGURE 24

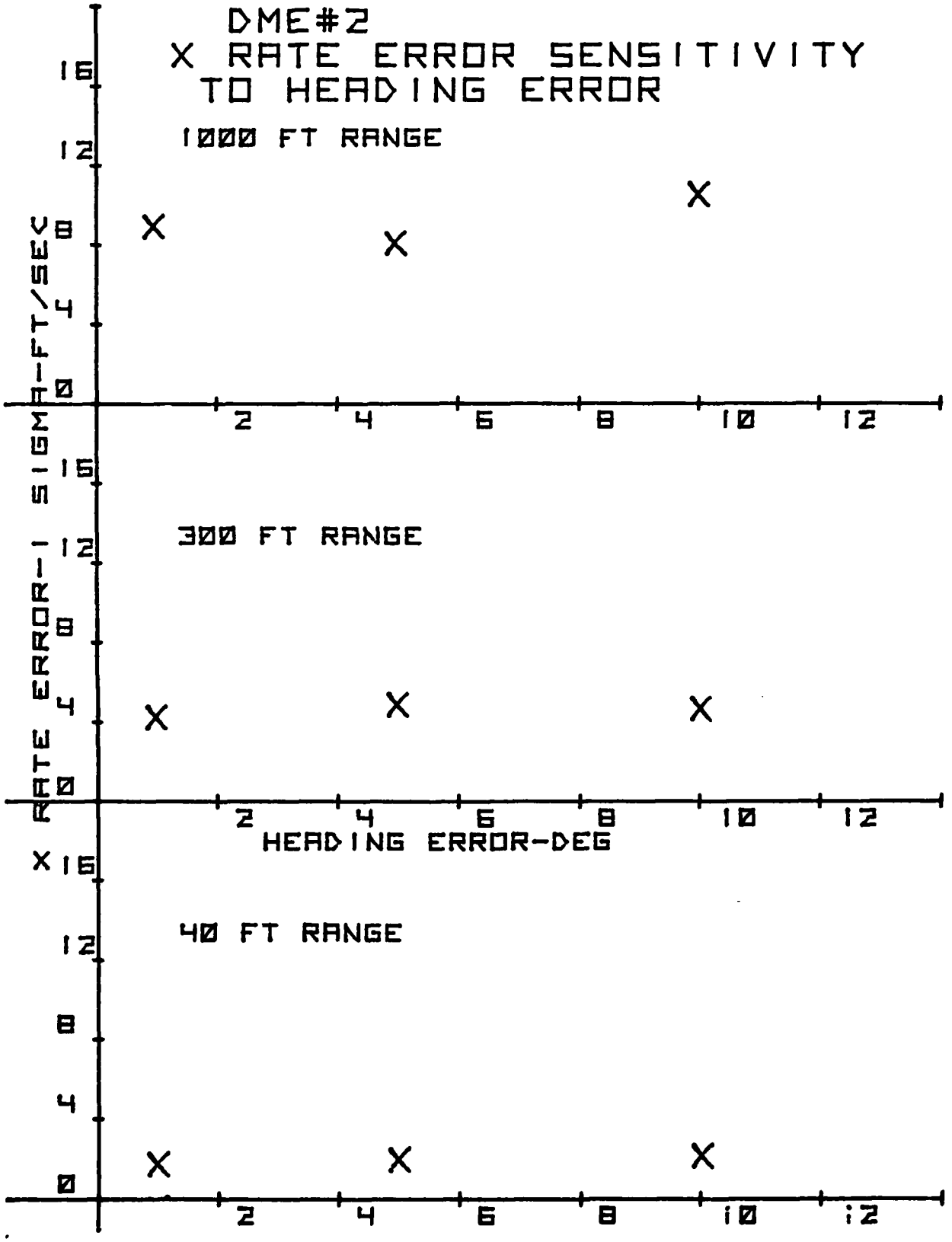
DME#2
X RATE ERROR SENSITIVITY
TO HEADING ERROR
1000 FT RANGE
300 FT RANGE
40 FT RANGE
X RATE ERROR-1 SIGMA-FT/SEC
HEADING ERROR-DEG
0
4
8
12
16
2
4
6
8
10
12

FIGURE 25

B. SENSITIVITY TO DME BIAS ERROR

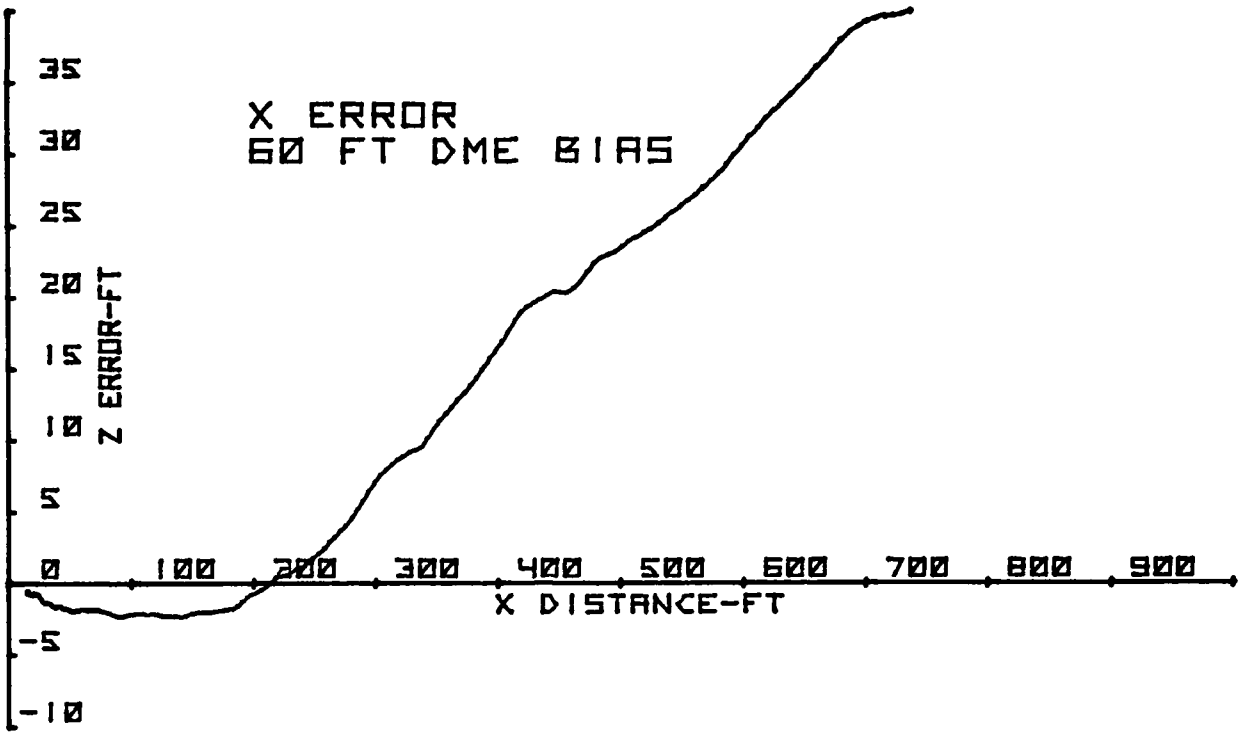

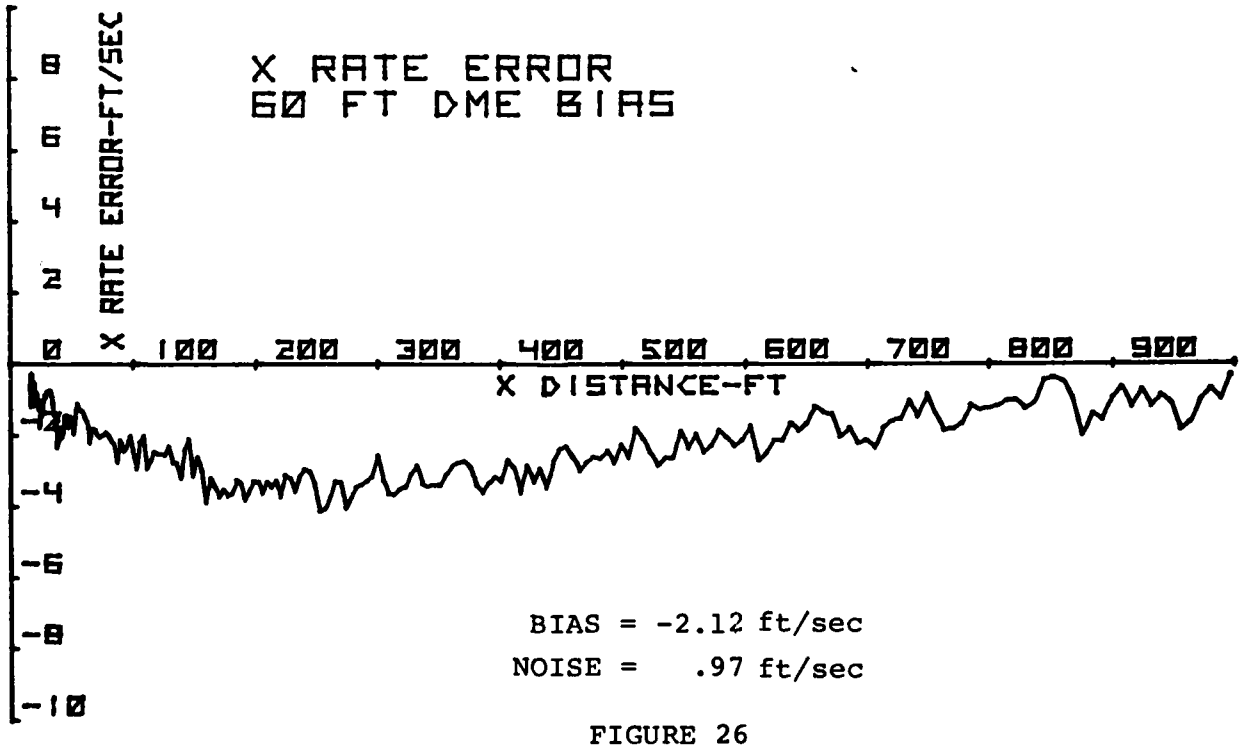

BIAS = -2.12 ft/sec

NOISE = .97 ft/sec

FIGURE 26

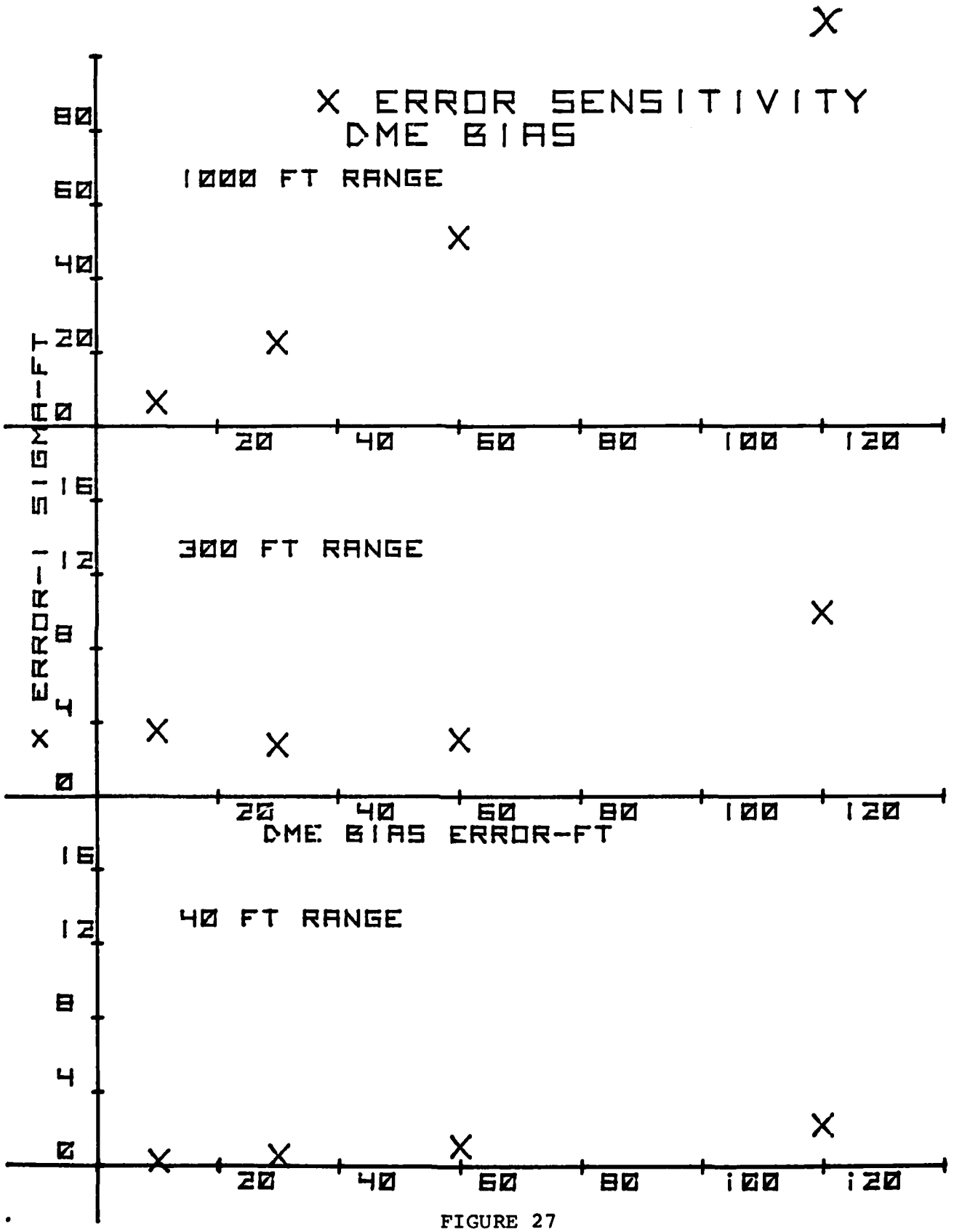
X ERROR SENSITIVITY
DME BIAS
1000 FT RANGE
300 FT RANGE
40 FT RANGE
X ERROR-1 SIGMA-FT
DME BIAS ERROR-FT
0
4
8
12
16
20
40
60
80
100
120

FIGURE 27

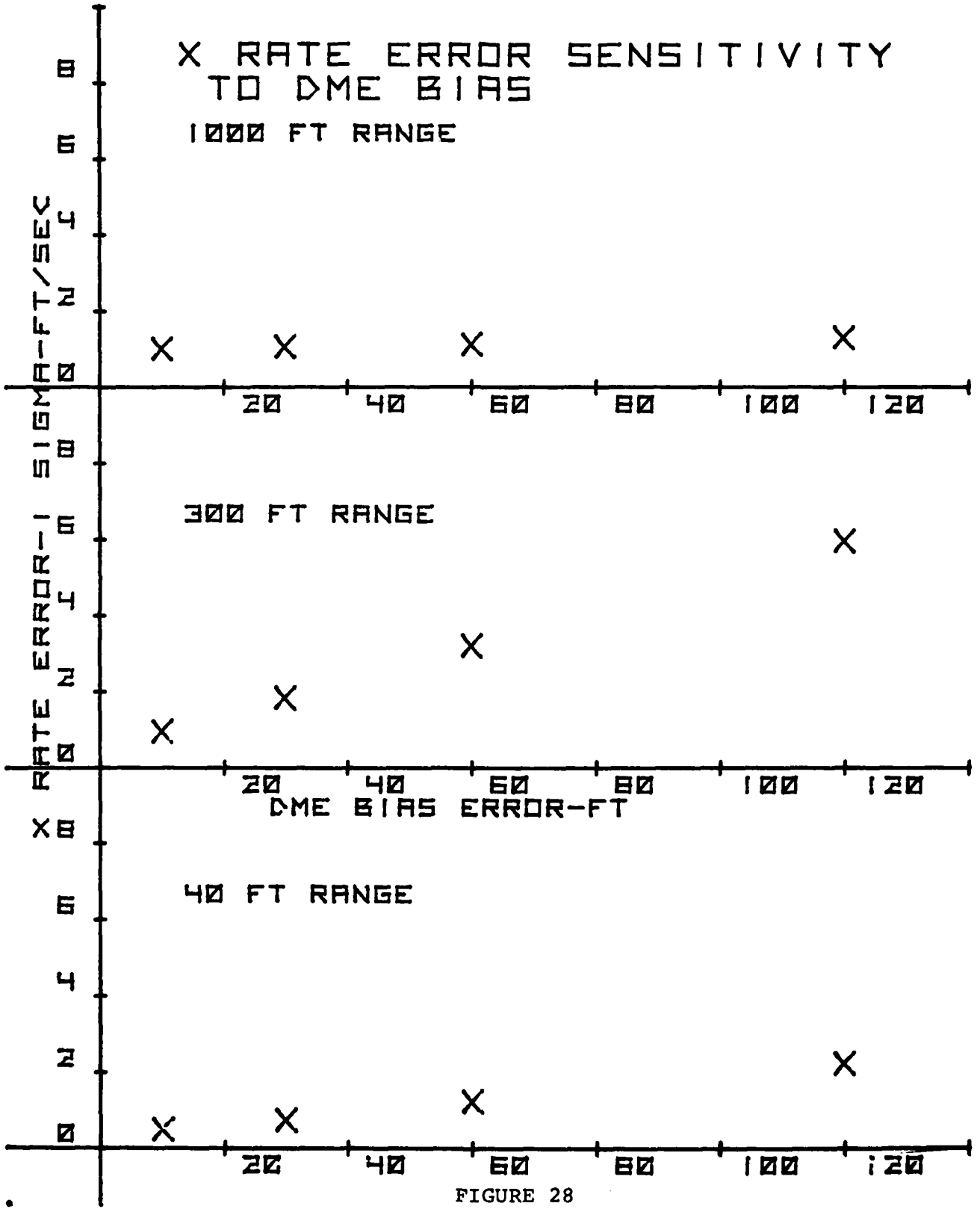
X RATE ERROR SENSITIVITY
TO DME BIAS
1000 FT RANGE
300 FT RANGE
40 FT RANGE
X RATE ERROR-1 SIGMA-FT/SEC
DME BIAS ERROR-FT
0
20
40
60
80
100
120

FIGURE 28

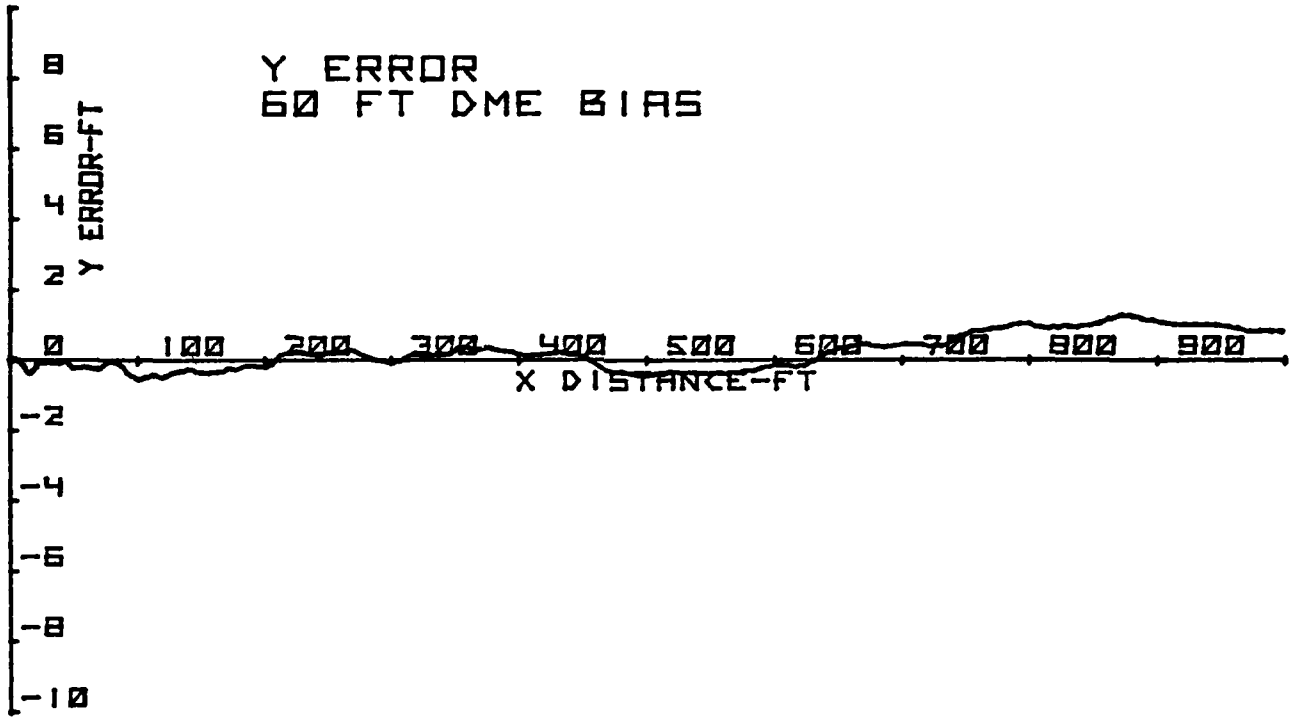

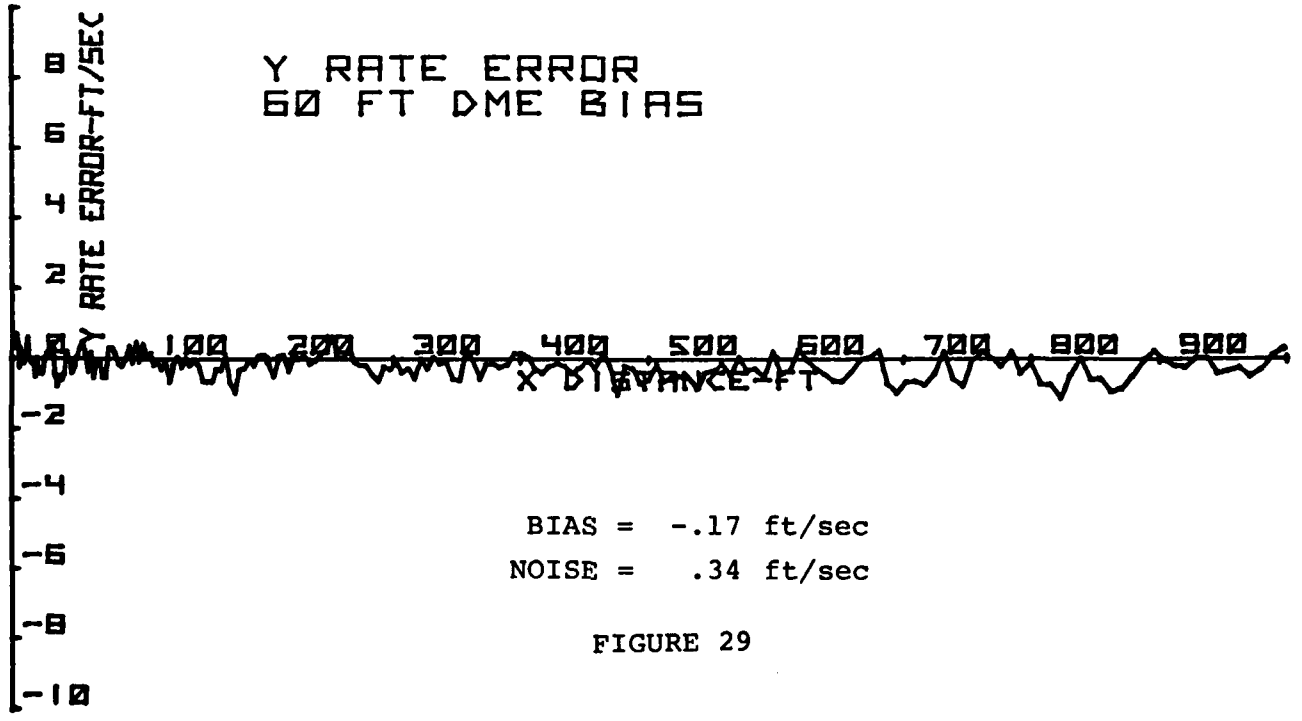

BIAS = -.17 ft/sec

NOISE = .34 ft/sec

FIGURE 29

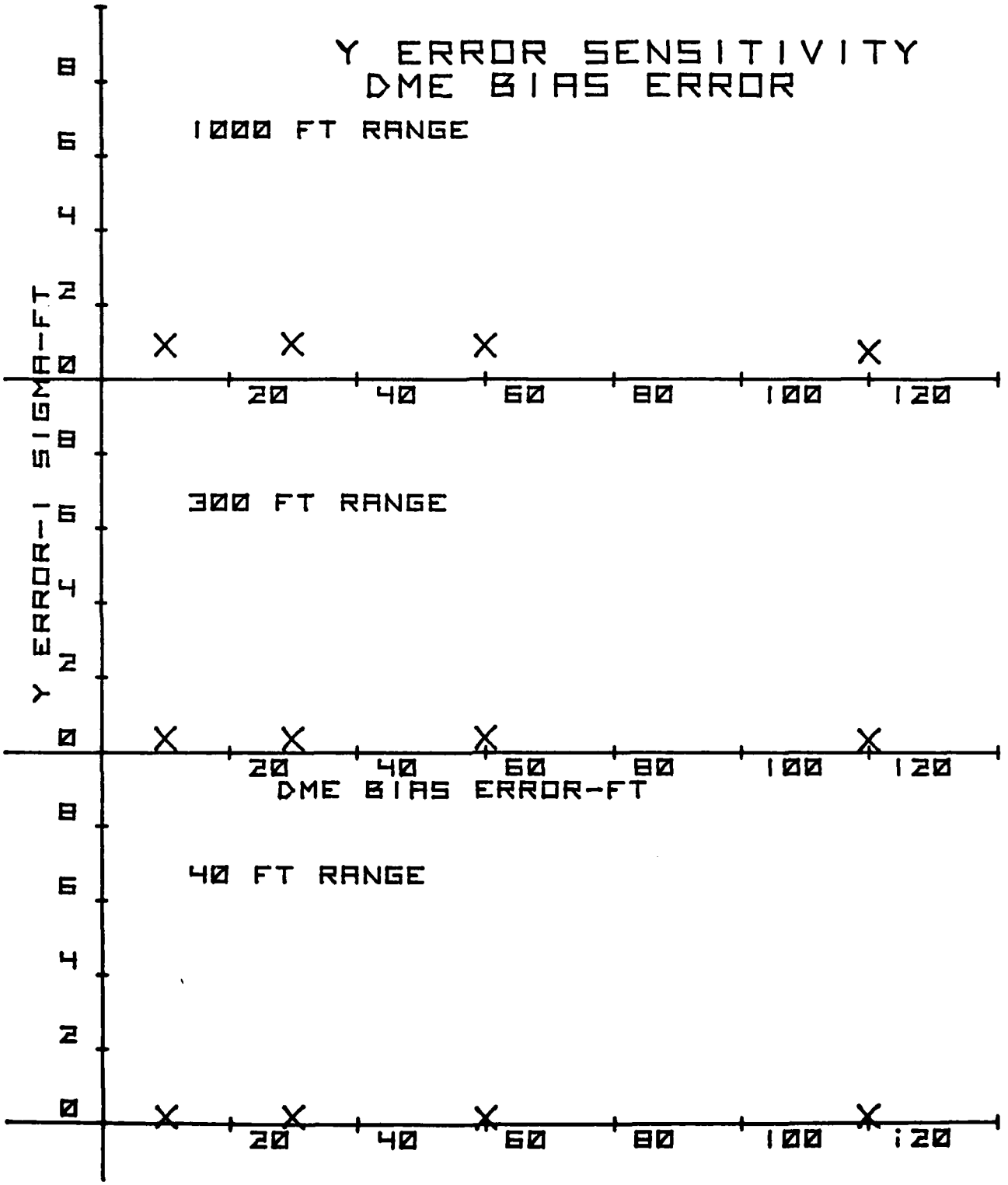
Y ERROR SENSITIVITY
DME BIAS ERROR
1000 FT RANGE
300 FT RANGE
40 FT RANGE
Y ERROR-1 SIGMA-FT
DME BIAS ERROR-FT
0
2
4
6
8
20
40
60
80
100
120

FIGURE 30

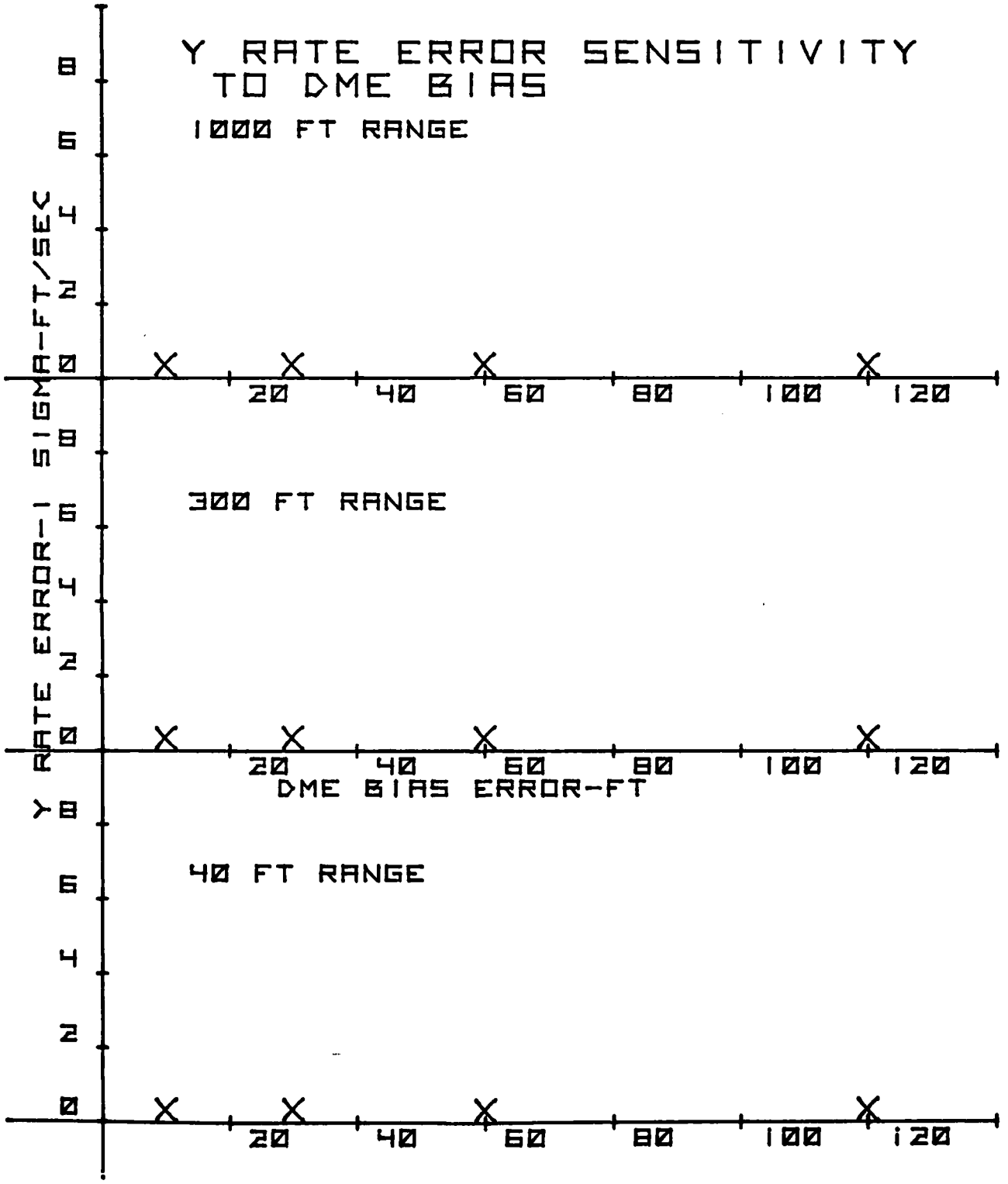
Y RATE ERROR SENSITIVITY
TO DME BIAS
1000 FT RANGE
300 FT RANGE
40 FT RANGE
Y RATE ERROR-1 SIGMA-FT/SEC
0
2
4
6
8
20
40
60
80
100
120
DME BIAS ERROR-FT

FIGURE 31

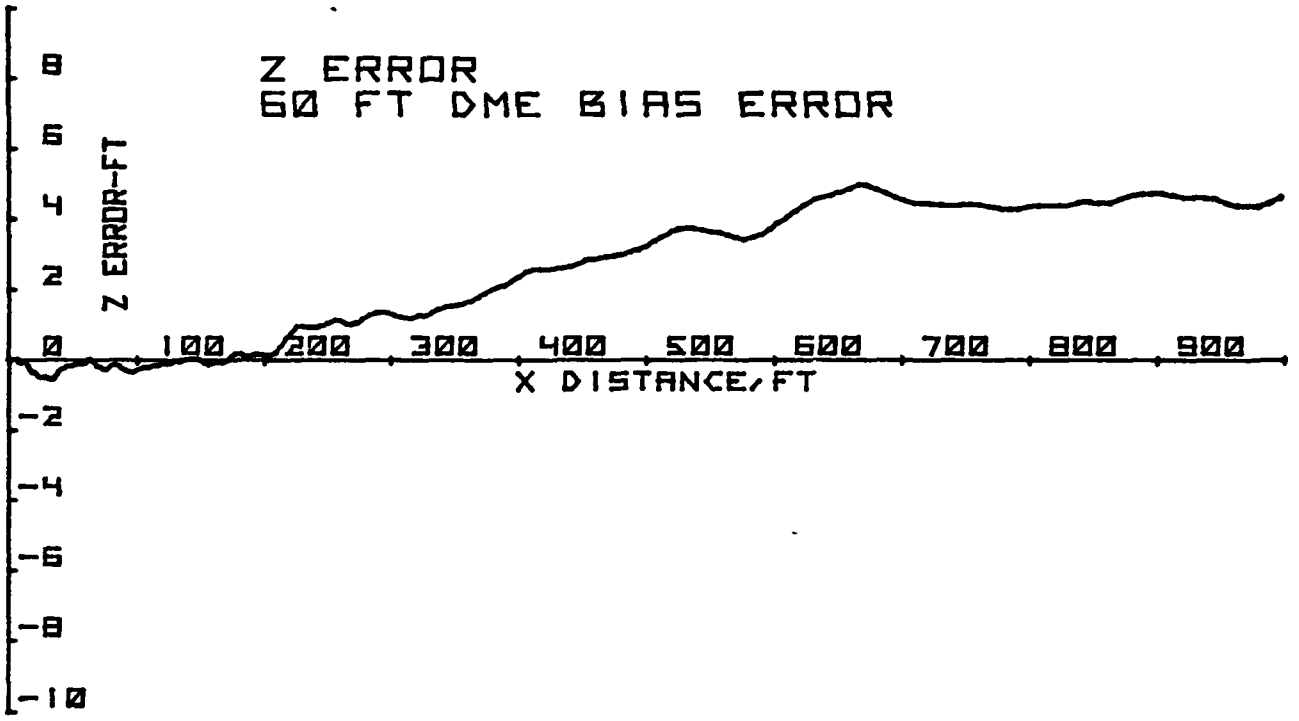

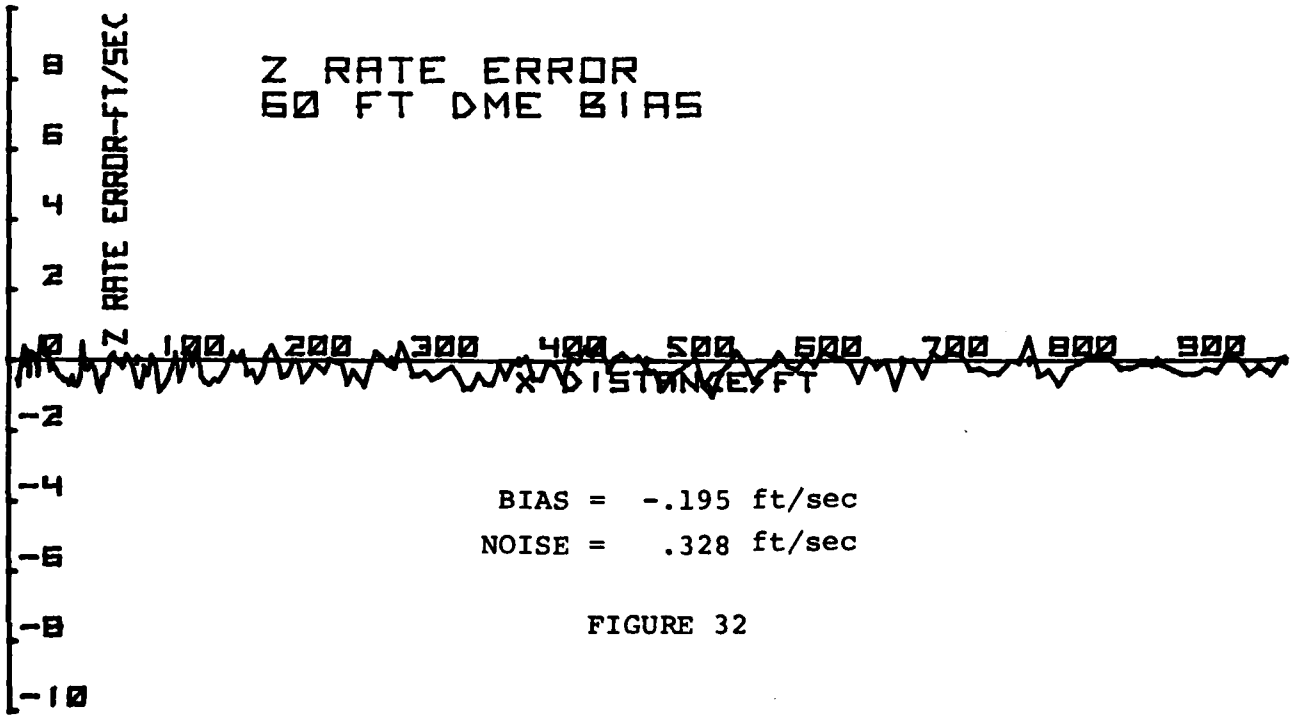

BIAS = -.195 ft/sec

NOISE = .328 ft/sec

FIGURE 32

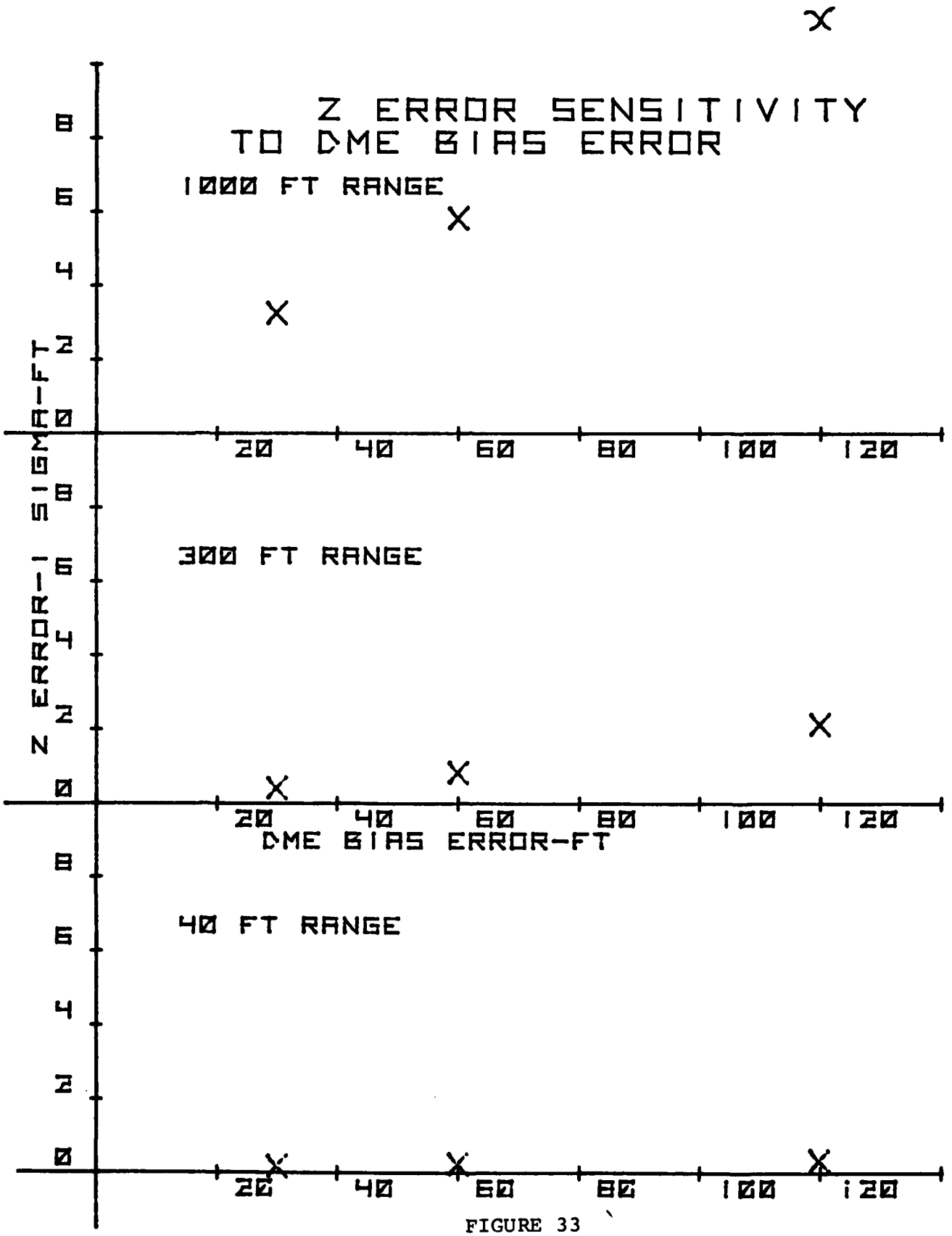
Z ERROR SENSITIVITY
TO DME BIAS ERROR
1000 FT RANGE
300 FT RANGE
40 FT RANGE
Z ERROR-1 SIGMA-FT
DME BIAS ERROR-FT
0
2
4
6
8
20
40
60
80
100
120

FIGURE 33

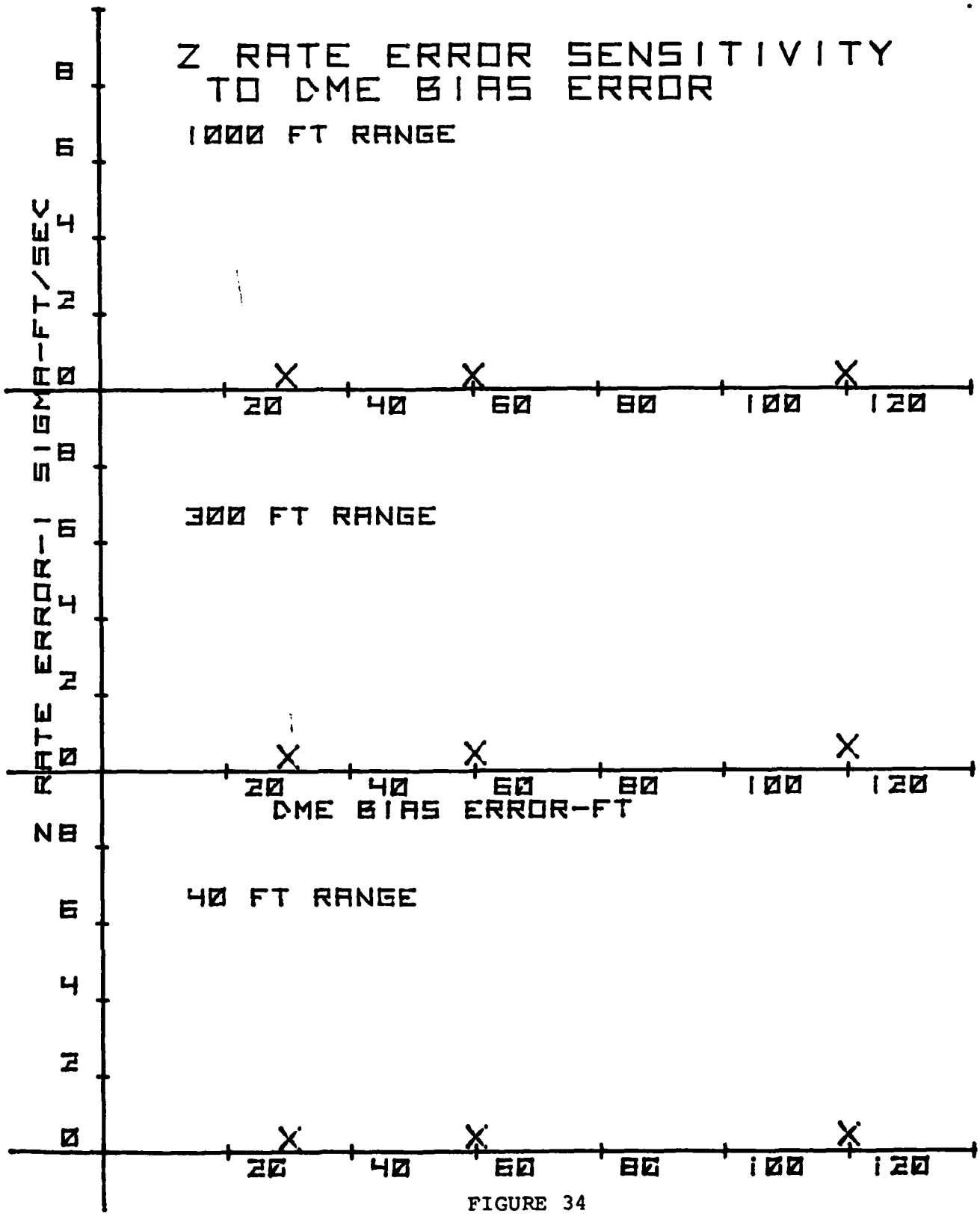
Z RATE ERROR SENSITIVITY
TO DME BIAS ERROR
1000 FT RANGE
300 FT RANGE
40 FT RANGE
Z RATE ERROR-1 SIGMA-FT/SEC
DME BIAS ERROR-FT
0
2
4
6
8
20
40
60
80
100
120

FIGURE 34

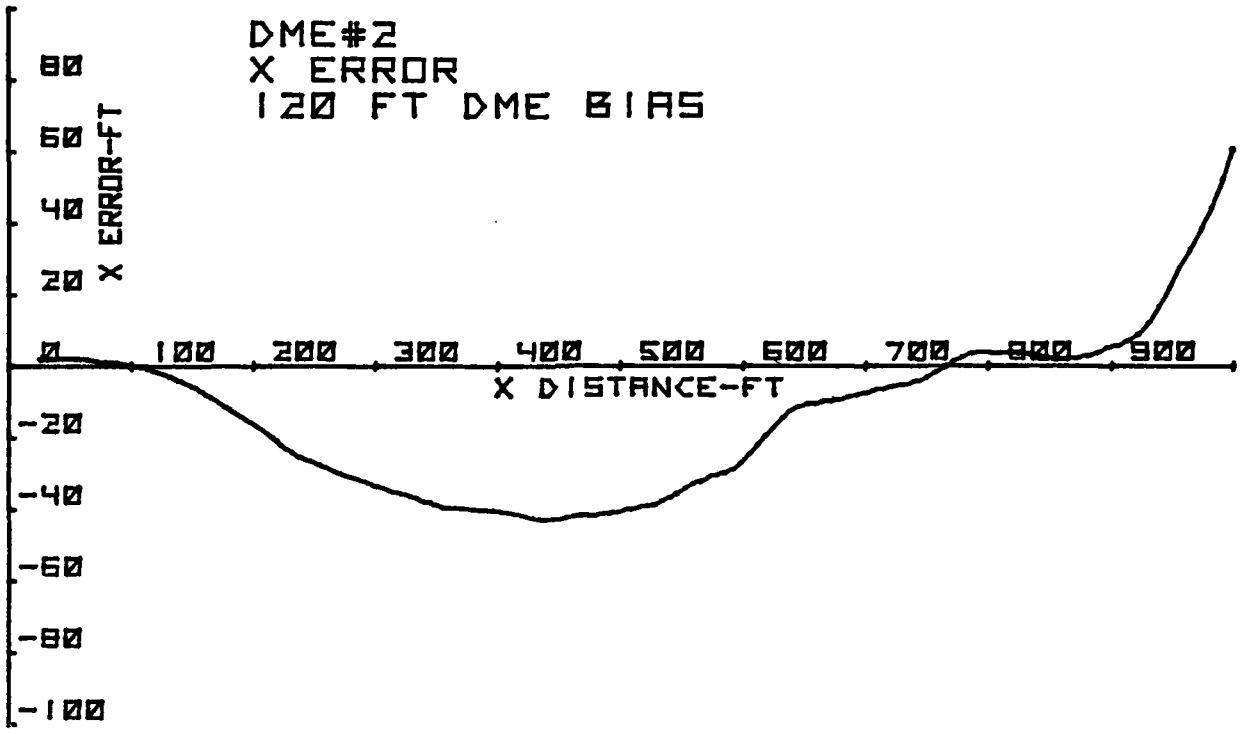
DME#2
X ERROR
120 FT DME BIAS
X ERROR-FT
80
60
40
20
0
100
200
300
400
500
600
700
800
900
X DISTANCE-FT
-20
-40
-60
-80
-100

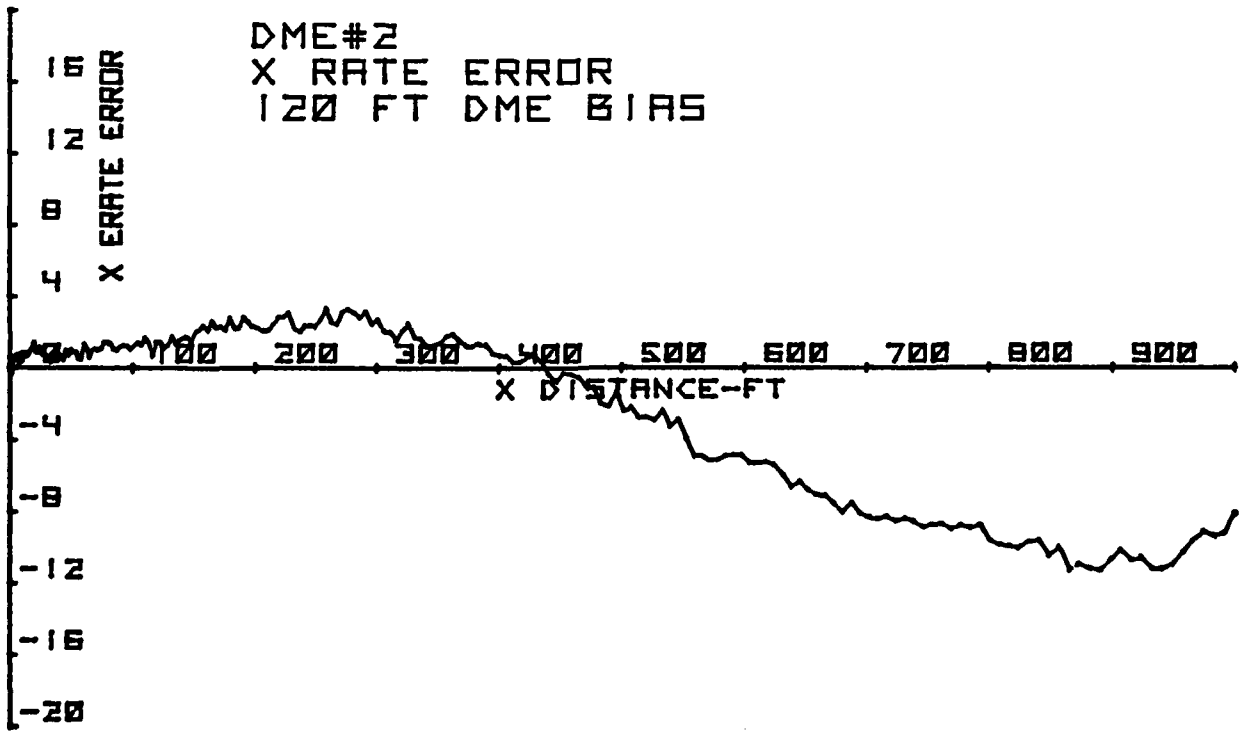
DME#2
X RATE ERROR
120 FT DME BIAS
X ERATE ERROR
16
12
8
4
0
100
200
300
400
500
600
700
800
900
X DISTANCE-FT
-4
-8
-12
-16
-20

FIGURE 35

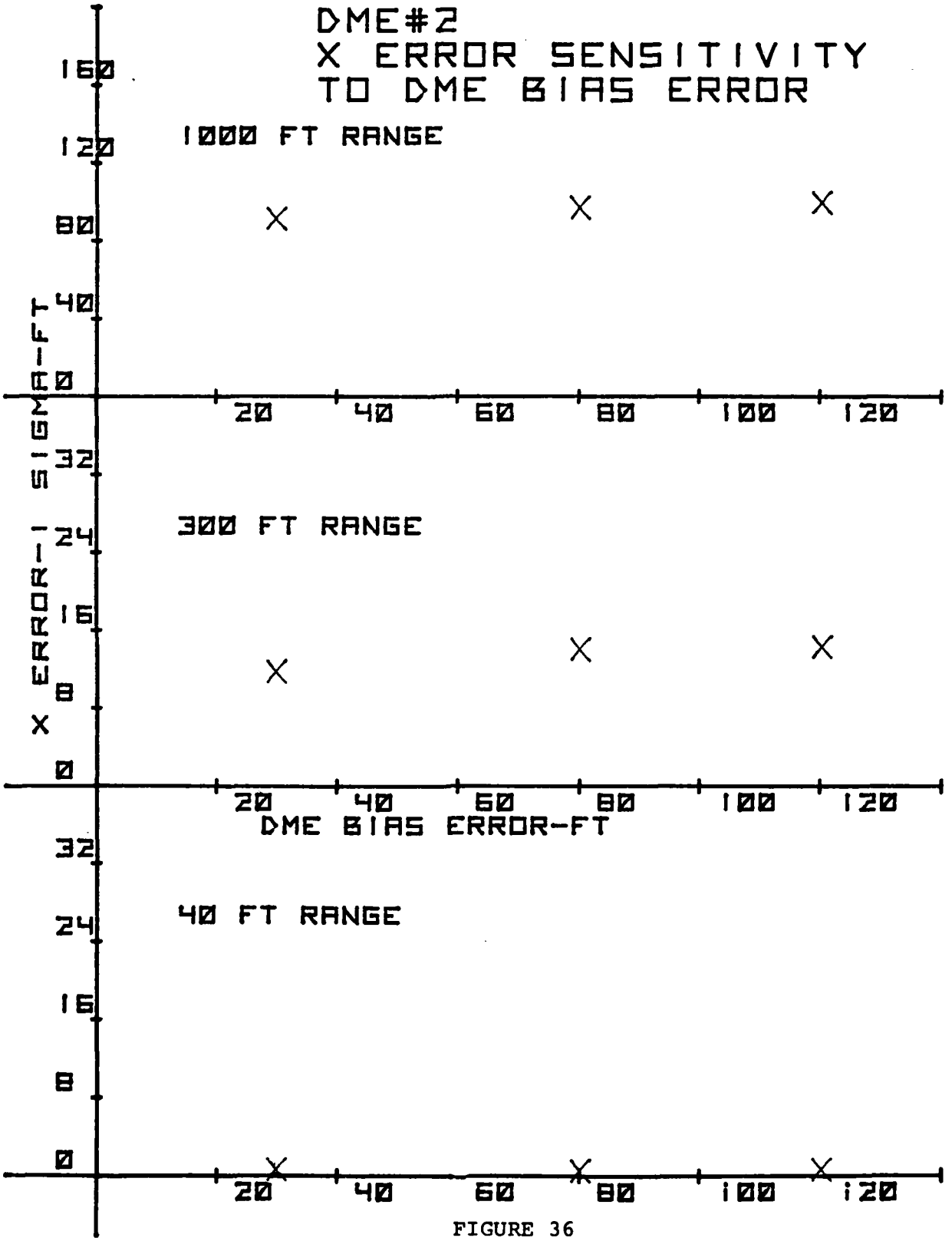
DME#2
X ERROR SENSITIVITY
TO DME BIAS ERROR
1000 FT RANGE
300 FT RANGE
40 FT RANGE
X ERROR-1 SIGMA-FT
DME BIAS ERROR-FT
160
120
80
40
0
32
24
16
8
0
20
40
60
80
100
120

FIGURE 36

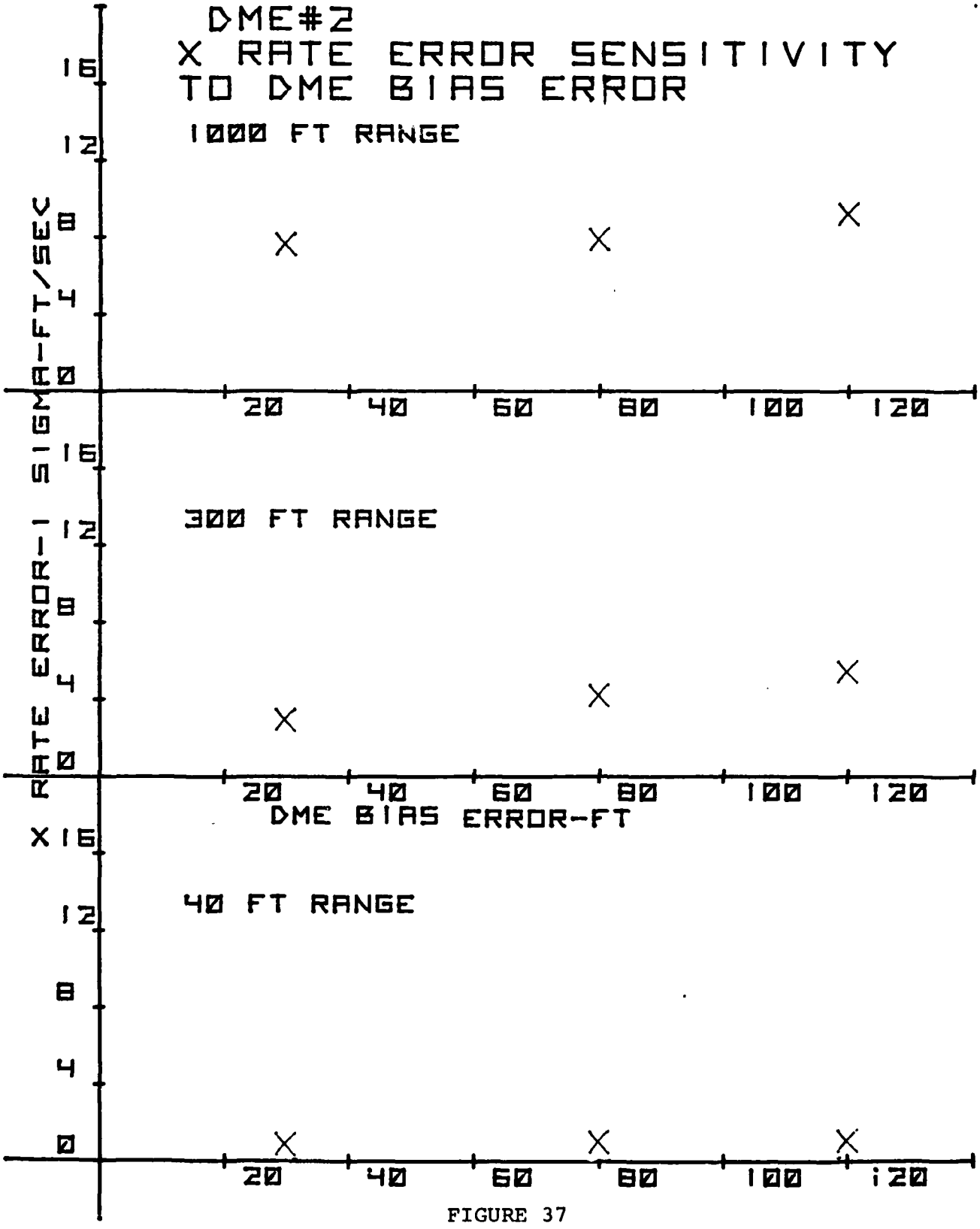
DME#2
X RATE ERROR SENSITIVITY
TO DME BIAS ERROR
1000 FT RANGE
300 FT RANGE
40 FT RANGE
X RATE ERROR-1 SIGMA-FT/SEC
DME BIAS ERROR-FT
0
4
8
12
16
20
40
60
80
100
120

FIGURE 37

C. SENSITIVITY TO ACCELEROMETER BIAS ERROR

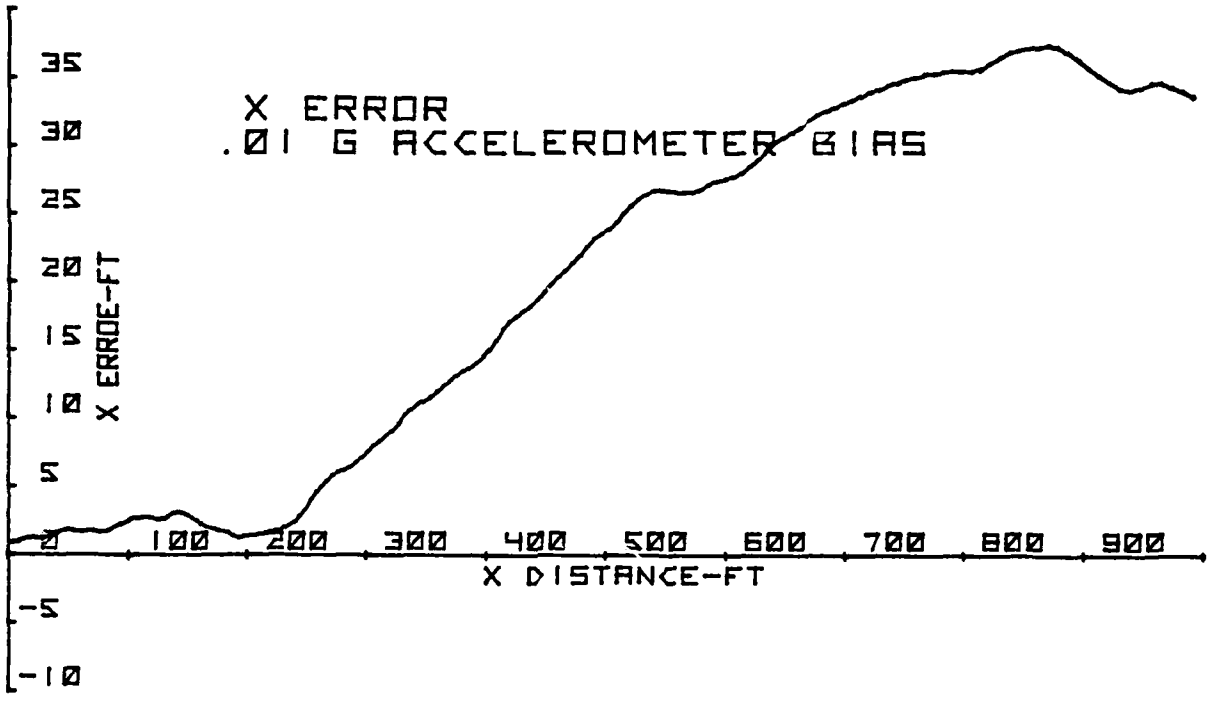
X ERROR
.01 G ACCELEROMETER BIAS
X ERROR-FT
35
30
25
20
15
10
5
0
-5
-10
100
200
300
400
500
600
700
800
900
X DISTANCE-FT

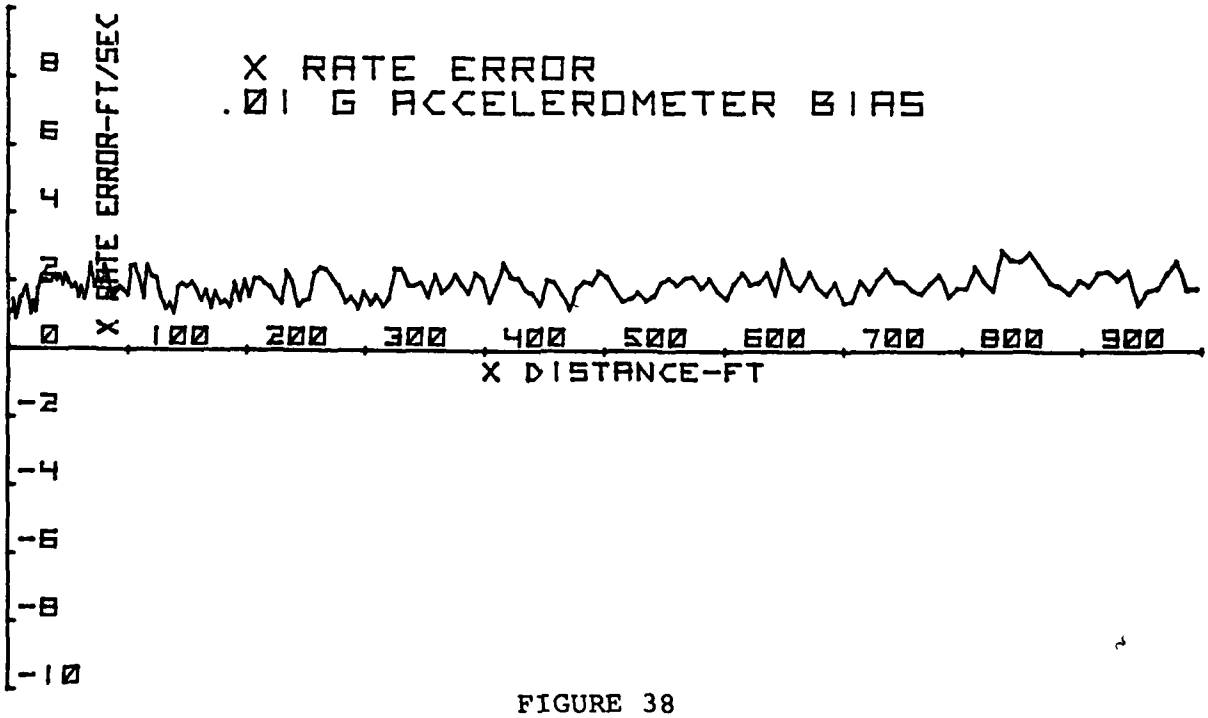
X RATE ERROR
.01 G ACCELEROMETER BIAS
X RATE ERROR-FT/SEC
8
6
4
2
0
-2
-4
-6
-8
-10
100
200
300
400
500
600
700
800
900
X DISTANCE-FT

FIGURE 38

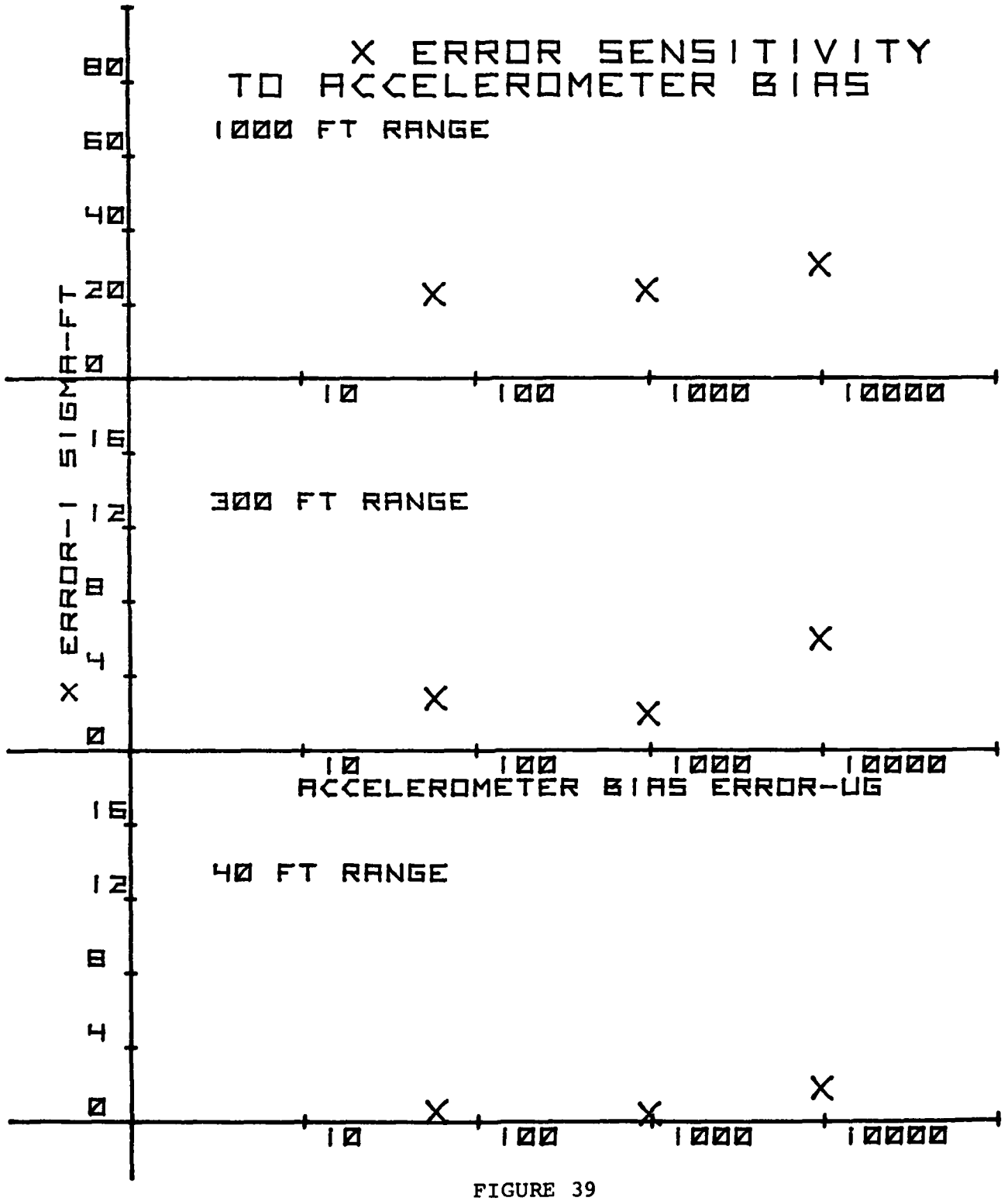
X ERROR SENSITIVITY
TO ACCELEROMETER BIAS
1000 FT RANGE
300 FT RANGE
40 FT RANGE
X ERROR-1 SIGMA-FT
80
60
40
20
0
16
12
8
4
0
16
12
8
4
0
10
100
1000
10000
ACCELEROMETER BIAS ERROR-UG

FIGURE 39

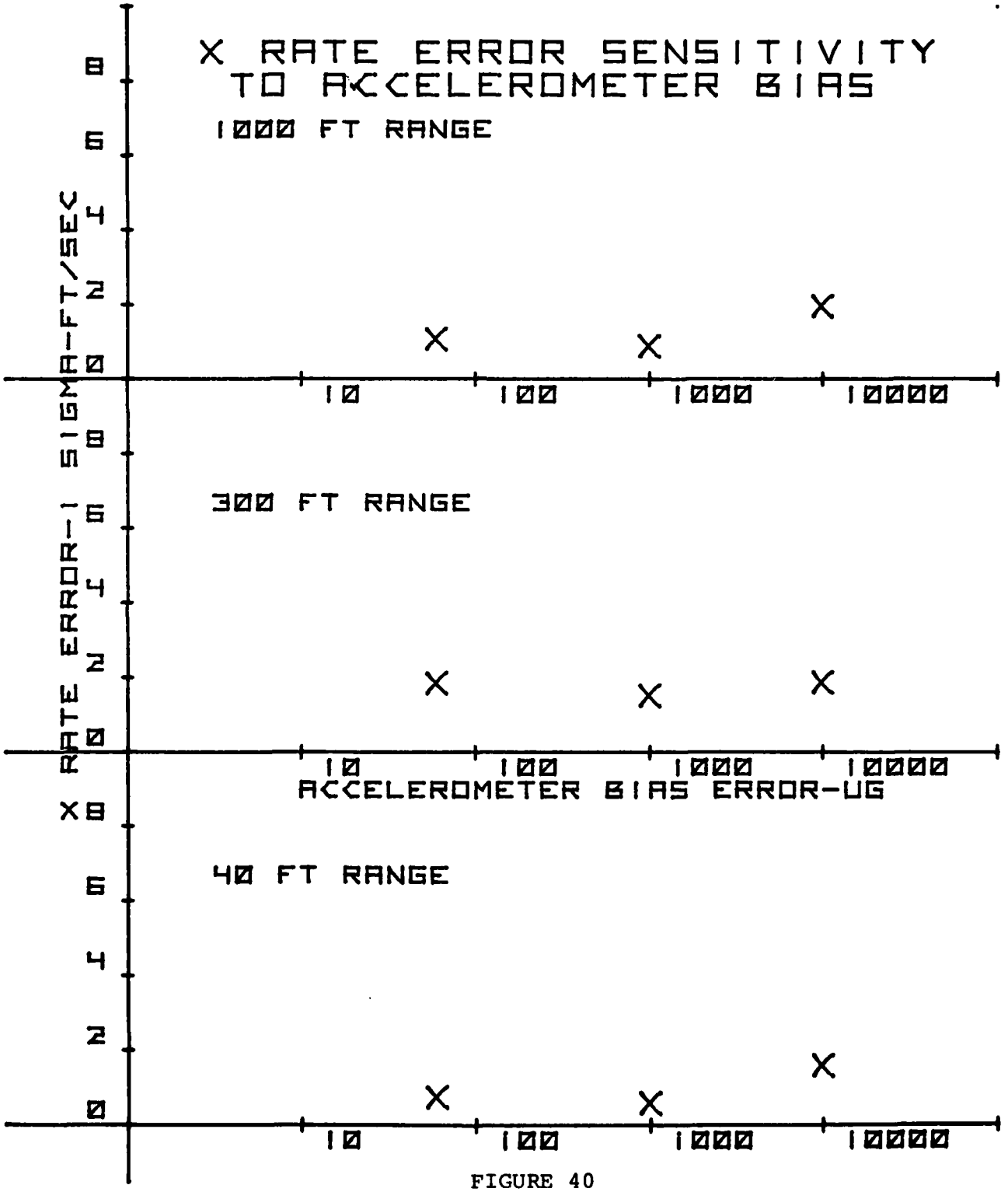
X RATE ERROR SENSITIVITY
TO ACCELEROMETER BIAS
1000 FT RANGE
300 FT RANGE
40 FT RANGE
X RATE ERROR-1 SIGMA-FT/SEC
ACCELEROMETER BIAS ERROR-UG
10
100
1000
10000

FIGURE 40

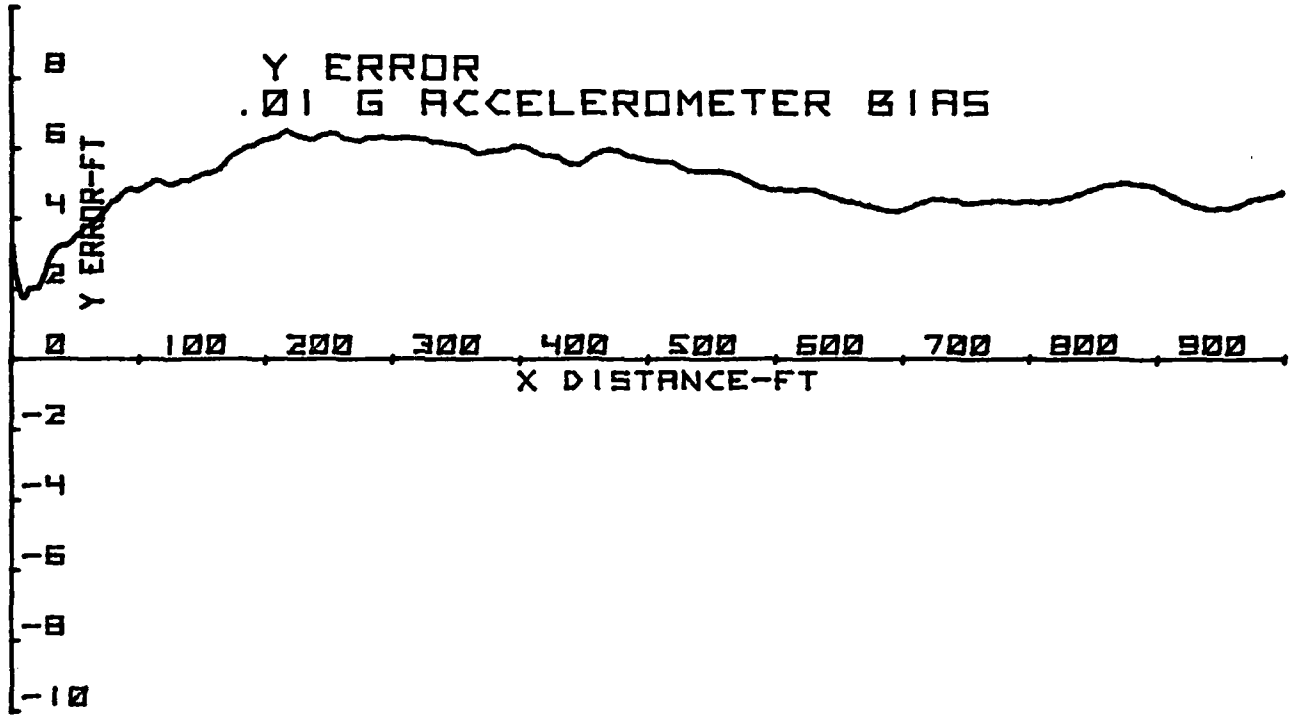
Y ERROR
.01 G ACCELEROMETER BIAS
Y ERROR-FT
8
6
4
2
0
100
200
300
400
500
600
700
800
900
X DISTANCE-FT
-2
-4
-6
-8
-10

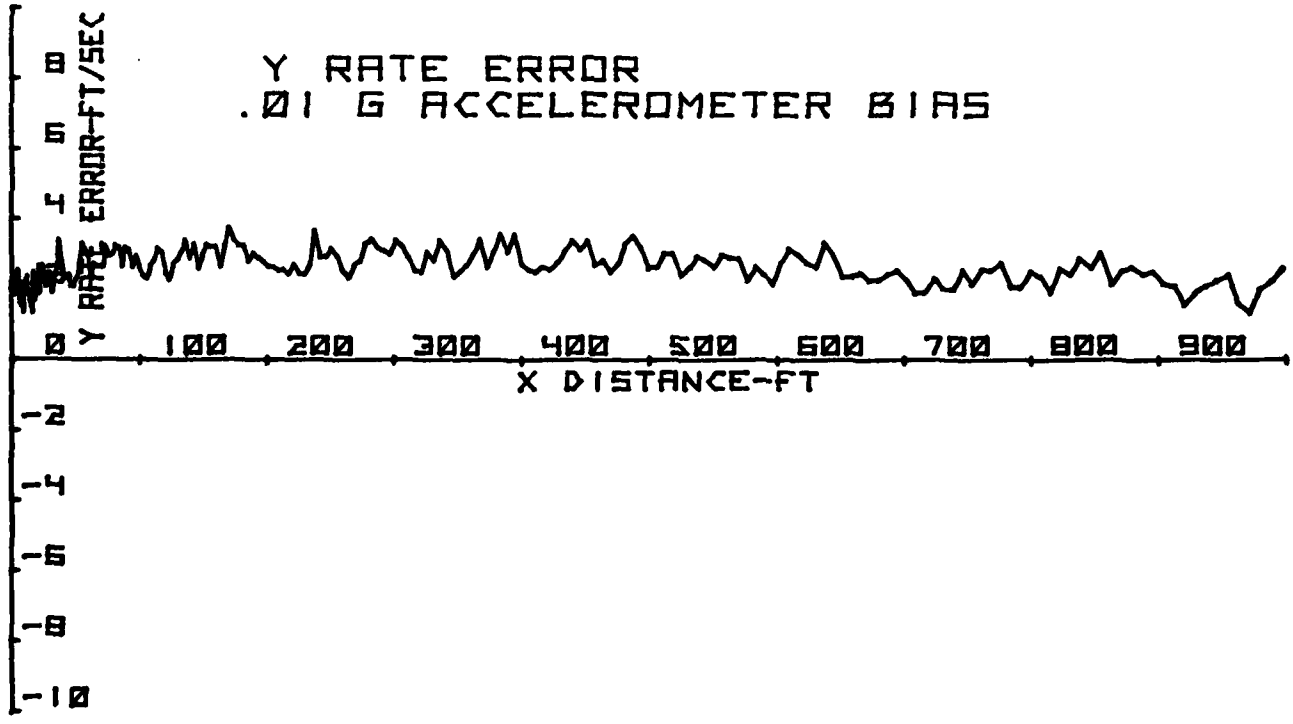
Y RATE ERROR
.01 G ACCELEROMETER BIAS
Y RATE ERROR-FT/SEC
8
6
4
0
100
200
300
400
500
600
700
800
900
X DISTANCE-FT
-2
-4
-6
-8
-10

FIGURE 41

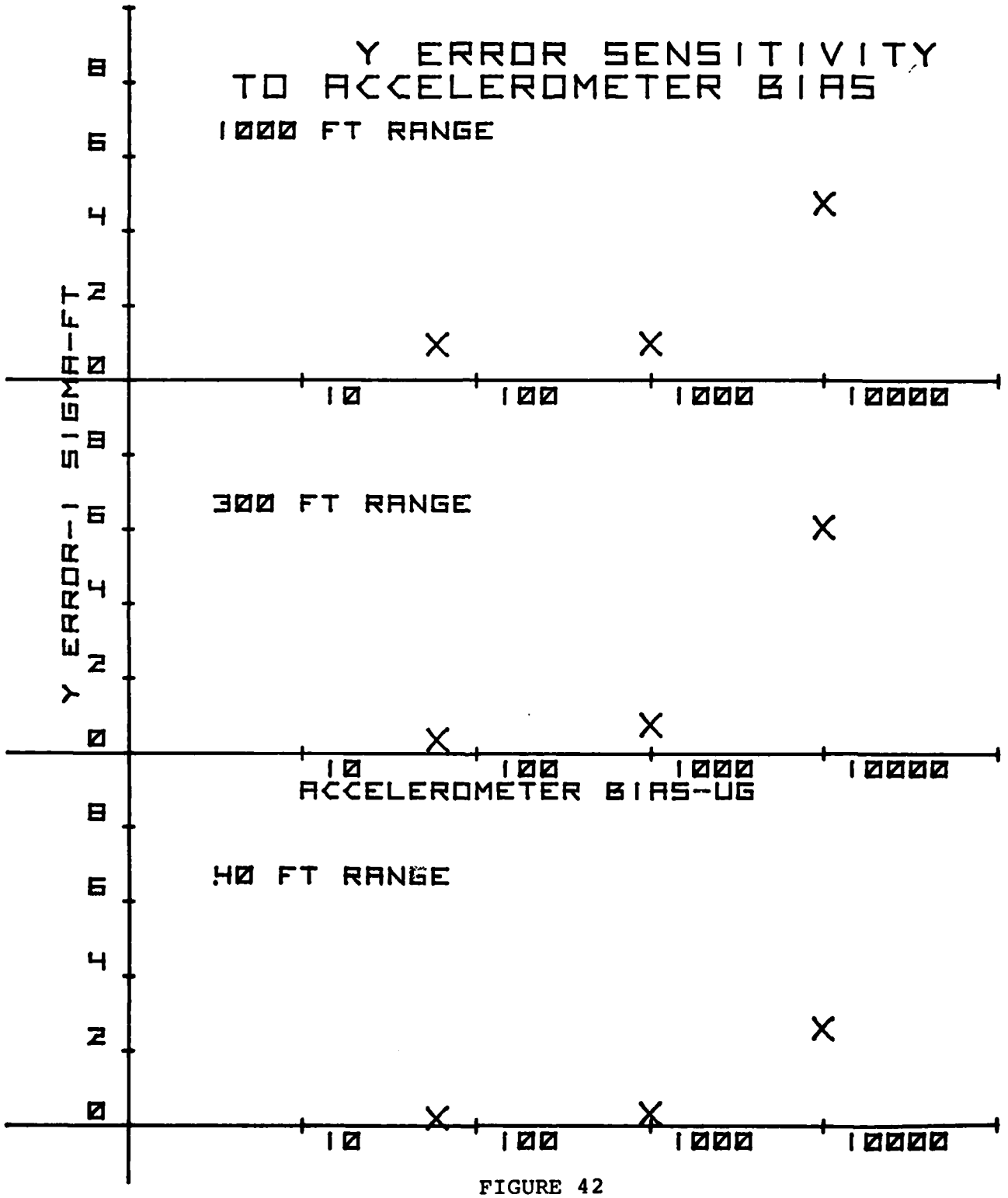
Y ERROR SENSITIVITY
TO ACCELEROMETER BIAS
1000 FT RANGE
300 FT RANGE
40 FT RANGE
Y ERROR-1 SIGMA-FT
0
2
4
6
8
10
100
1000
10000
ACCELEROMETER BIAS-UG

FIGURE 42

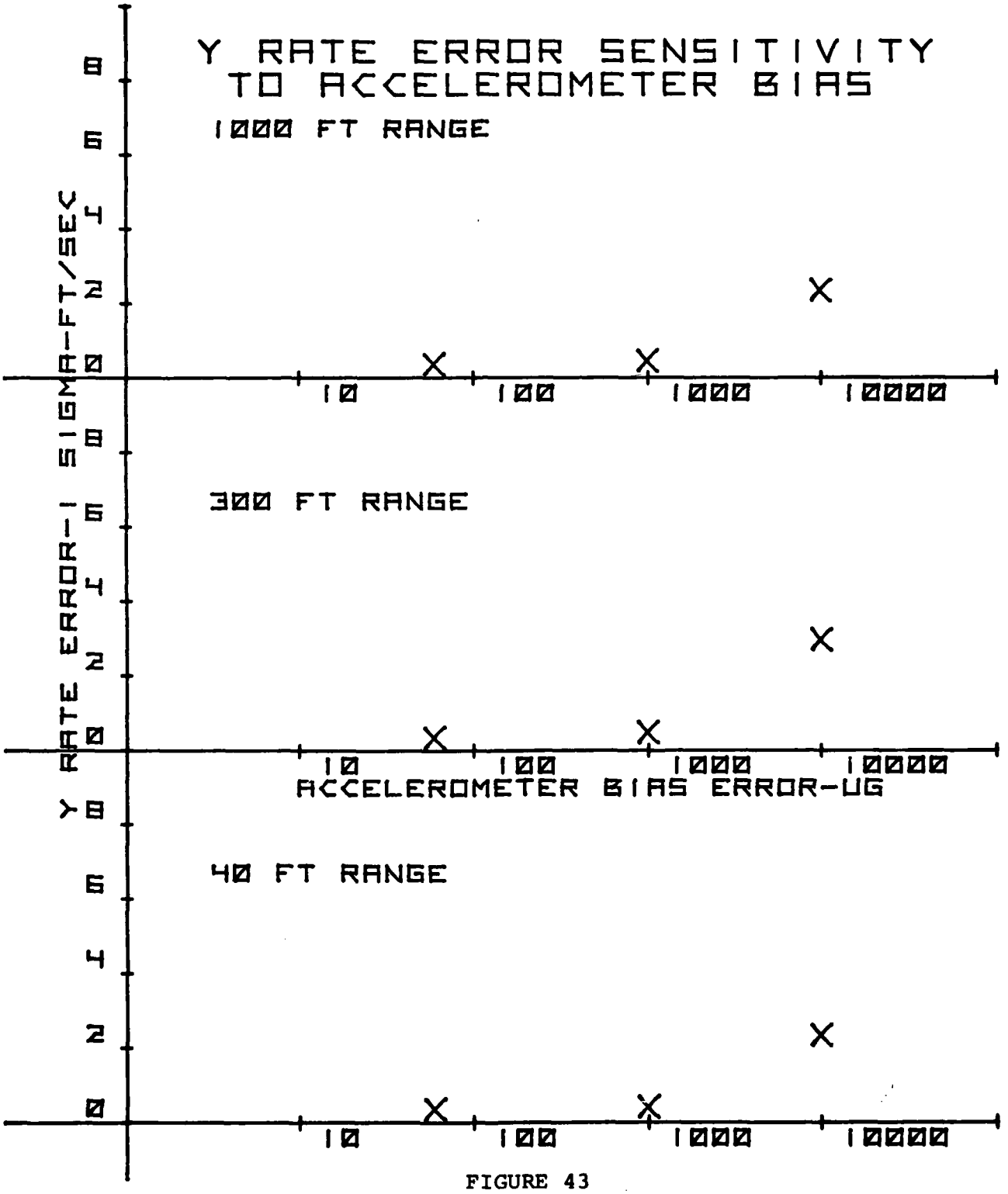
Y RATE ERROR SENSITIVITY
TO ACCELEROMETER BIAS
1000 FT RANGE
300 FT RANGE
40 FT RANGE
Y RATE ERROR-1 SIGMA-FT/SEC
ACCELEROMETER BIAS ERROR-UG
0
2
4
6
8
10
100
1000
10000

FIGURE 43

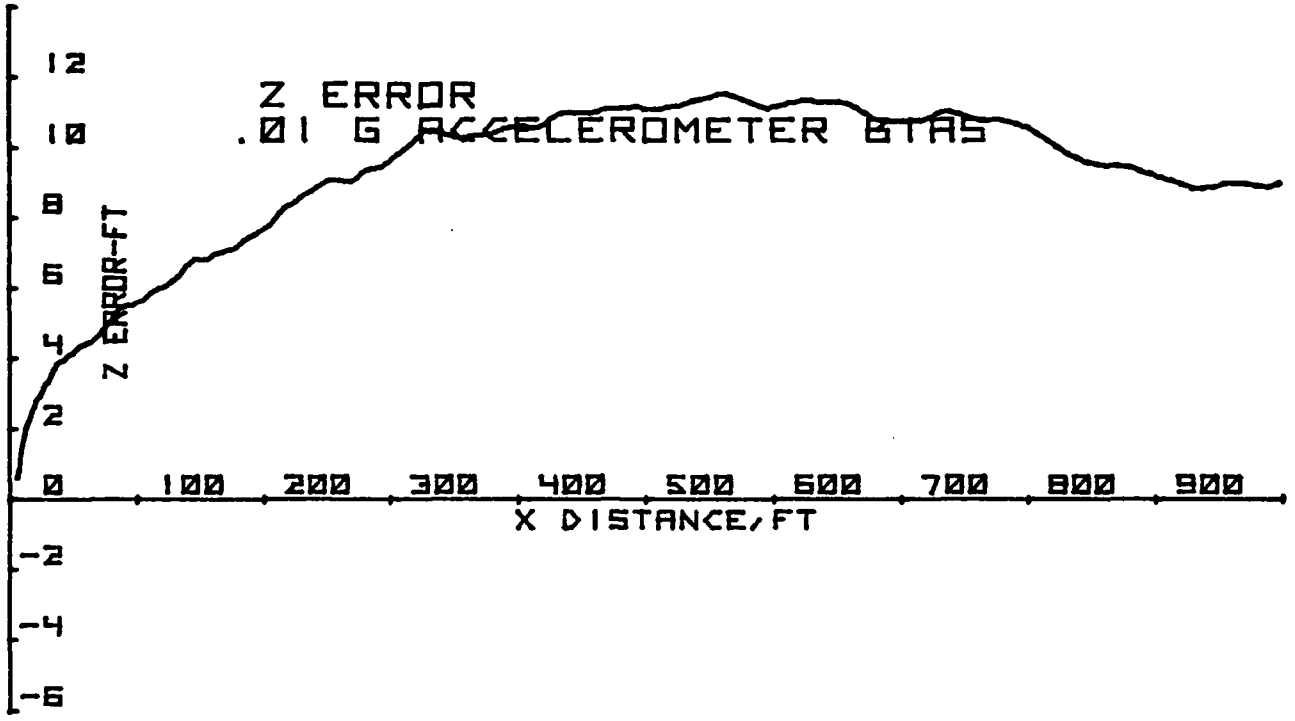

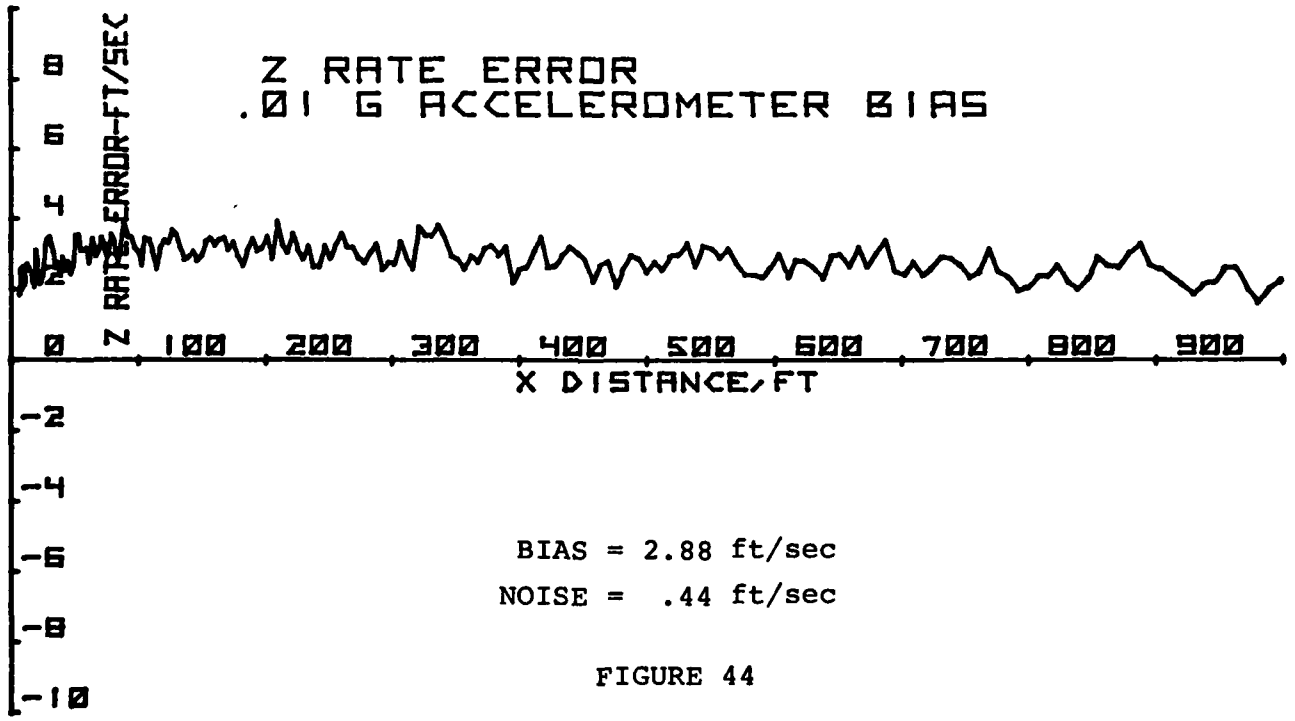

BIAS = 2.88 ft/sec

NOISE = .44 ft/sec

FIGURE 44

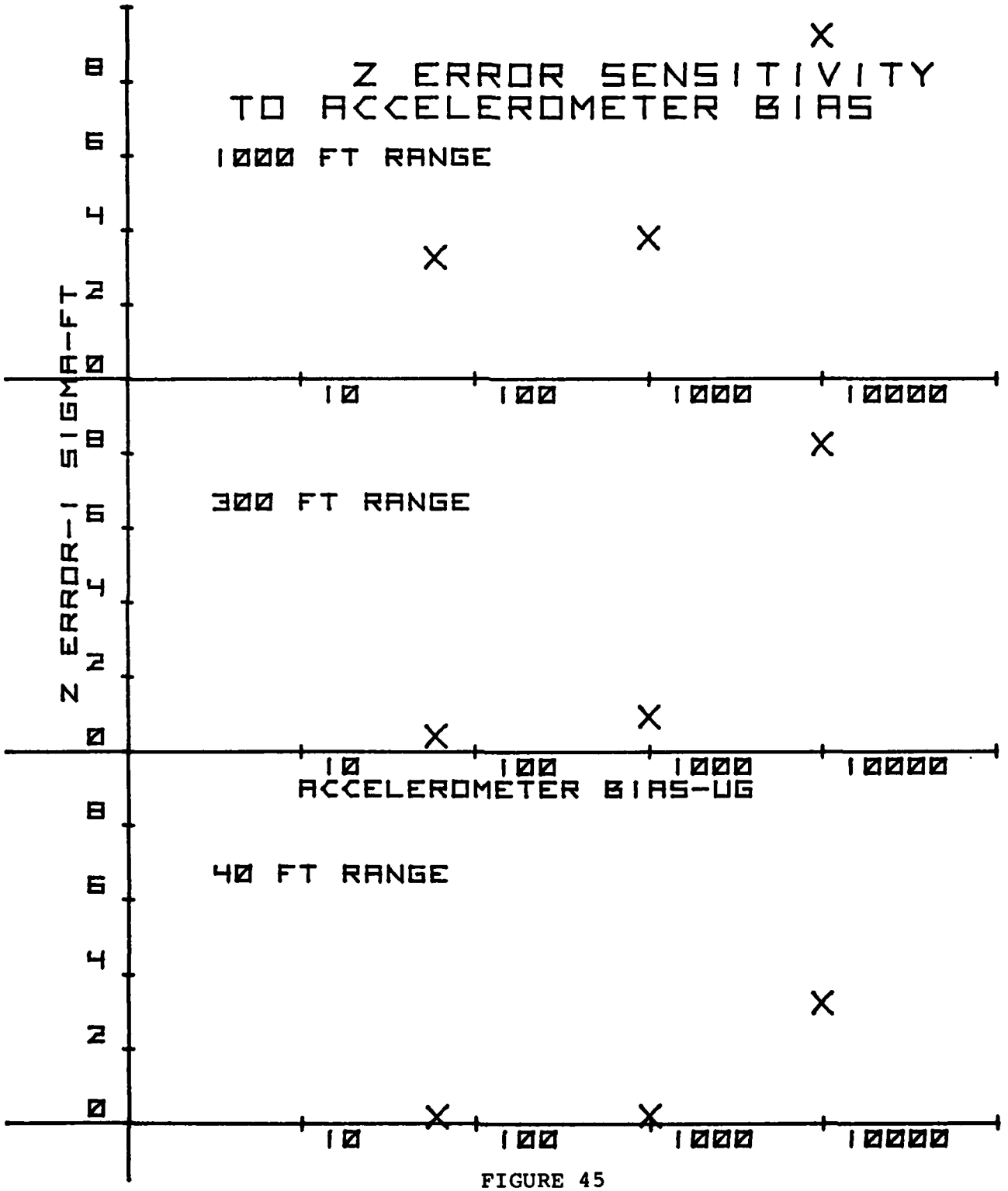
Z ERROR SENSITIVITY
TO ACCELEROMETER BIAS
1000 FT RANGE
300 FT RANGE
40 FT RANGE
Z ERROR-1 SIGMA-FT
0
2
4
6
8
10
100
1000
10000
ACCELEROMETER BIAS-UG

FIGURE 45

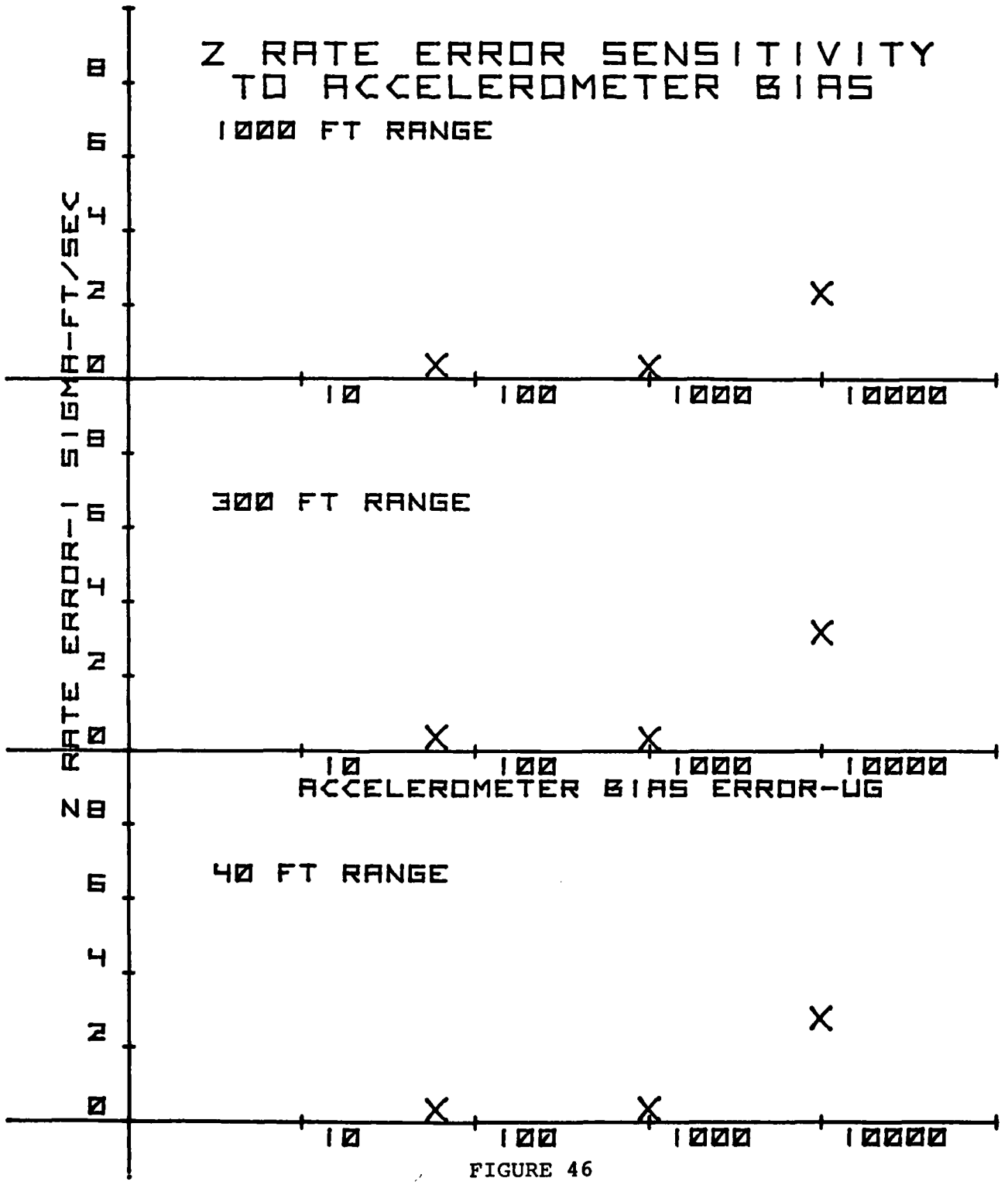
Z RATE ERROR SENSITIVITY
TO ACCELEROMETER BIAS
1000 FT RANGE
300 FT RANGE
40 FT RANGE
Z RATE ERROR-1 SIGMA-FT/SEC
ACCELEROMETER BIAS ERROR-UG
0
2
4
6
8
10
100
1000
10000

FIGURE 46

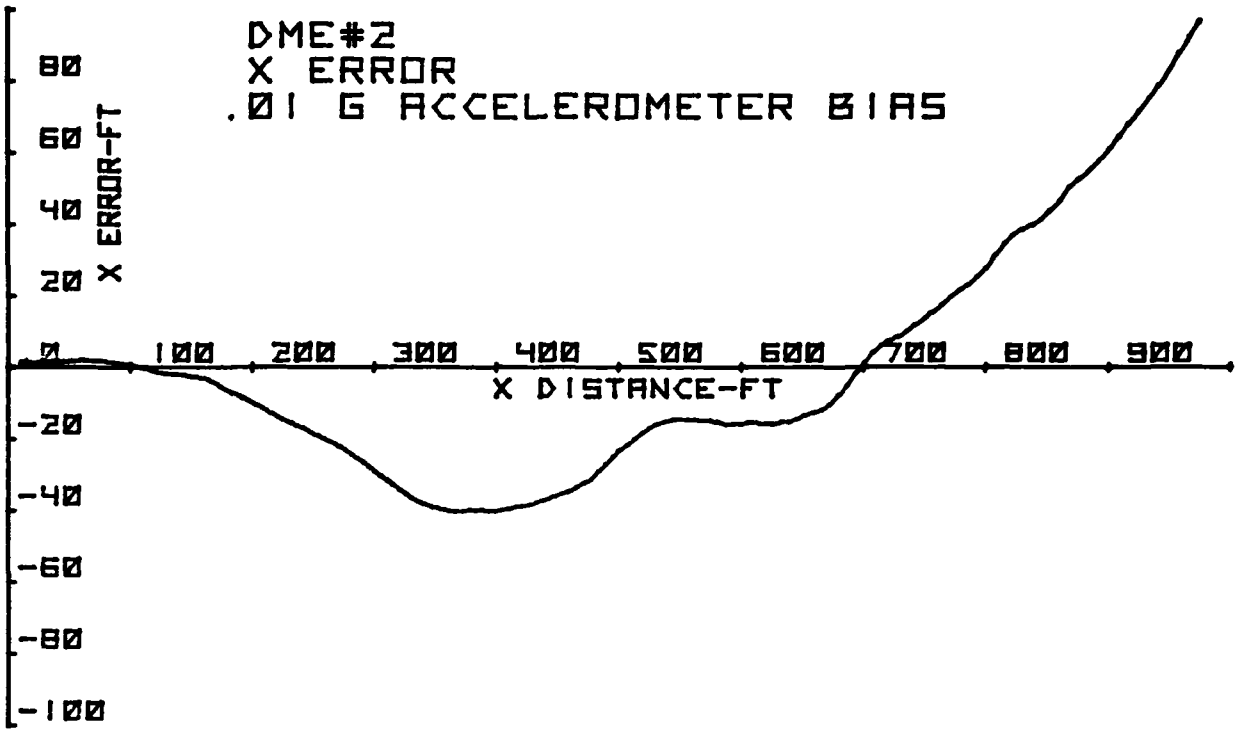
DME#2
X ERROR
.01 G ACCELEROMETER BIAS
X ERROR-FT
80
60
40
20
0
100
200
300
400
500
600
700
800
900
X DISTANCE-FT
-20
-40
-60
-80
-100

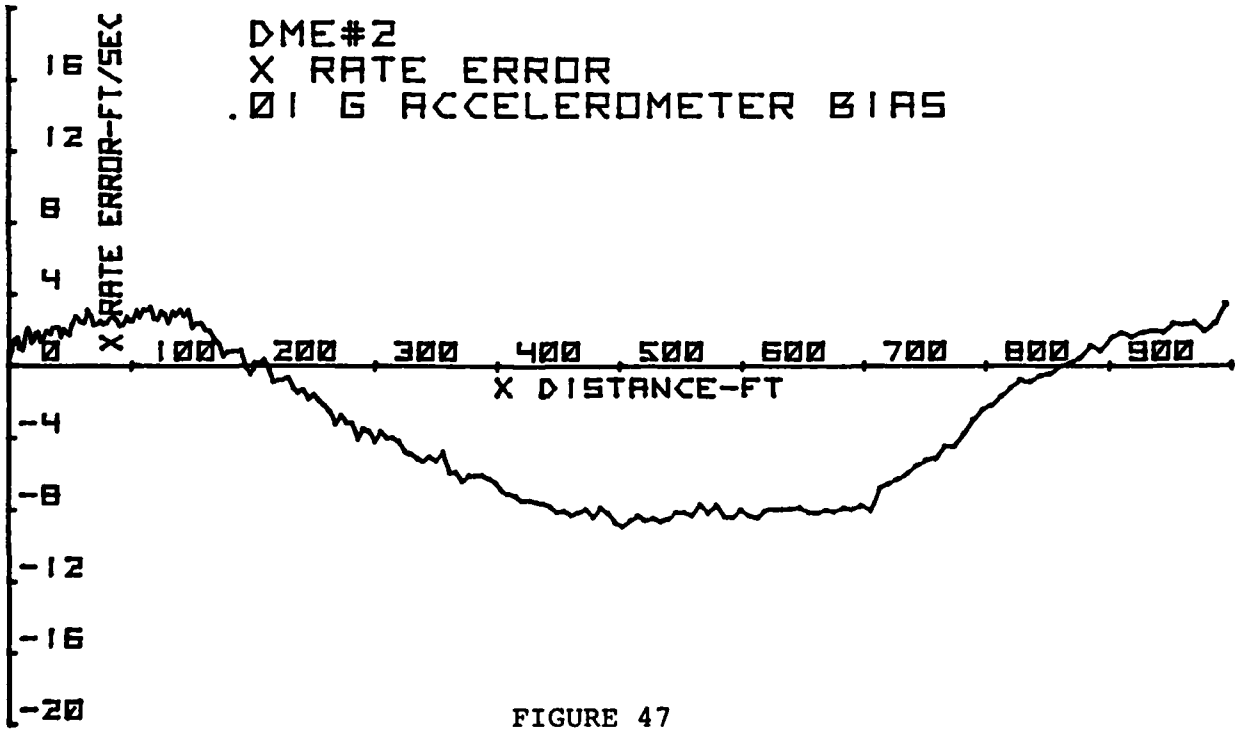
DME#2
X RATE ERROR
.01 G ACCELEROMETER BIAS
X RATE ERROR-FT/SEC
16
12
8
4
0
100
200
300
400
500
600
700
800
900
X DISTANCE-FT
-4
-8
-12
-16
-20

FIGURE 47

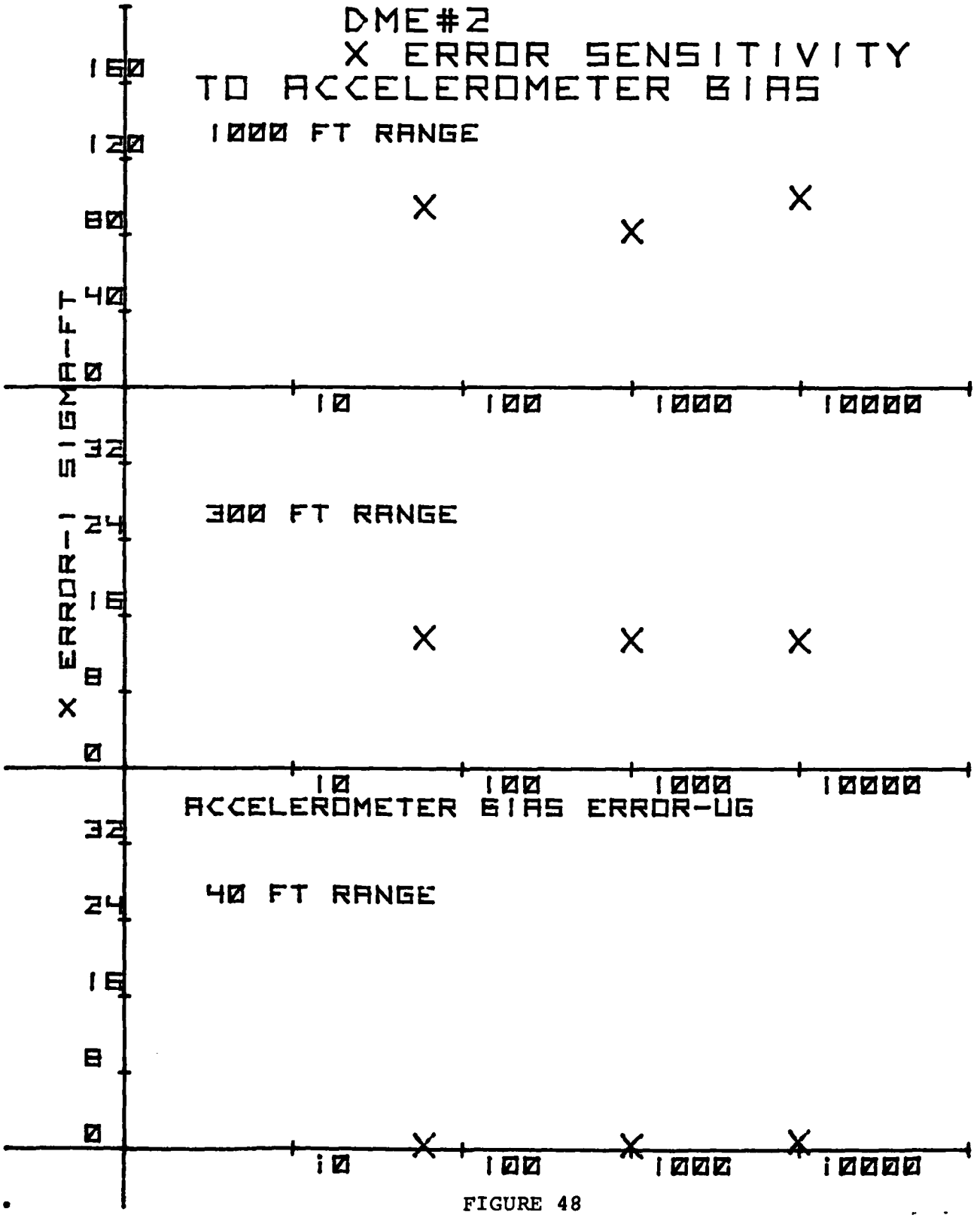
DME#2
X ERROR SENSITIVITY
TO ACCELEROMETER BIAS
1000 FT RANGE
300 FT RANGE
40 FT RANGE
X ERROR-1 SIGMA-FT
ACCELEROMETER BIAS ERROR-UG
160
120
80
40
0
32
24
16
8
0
10
100
1000
10000

FIGURE 48

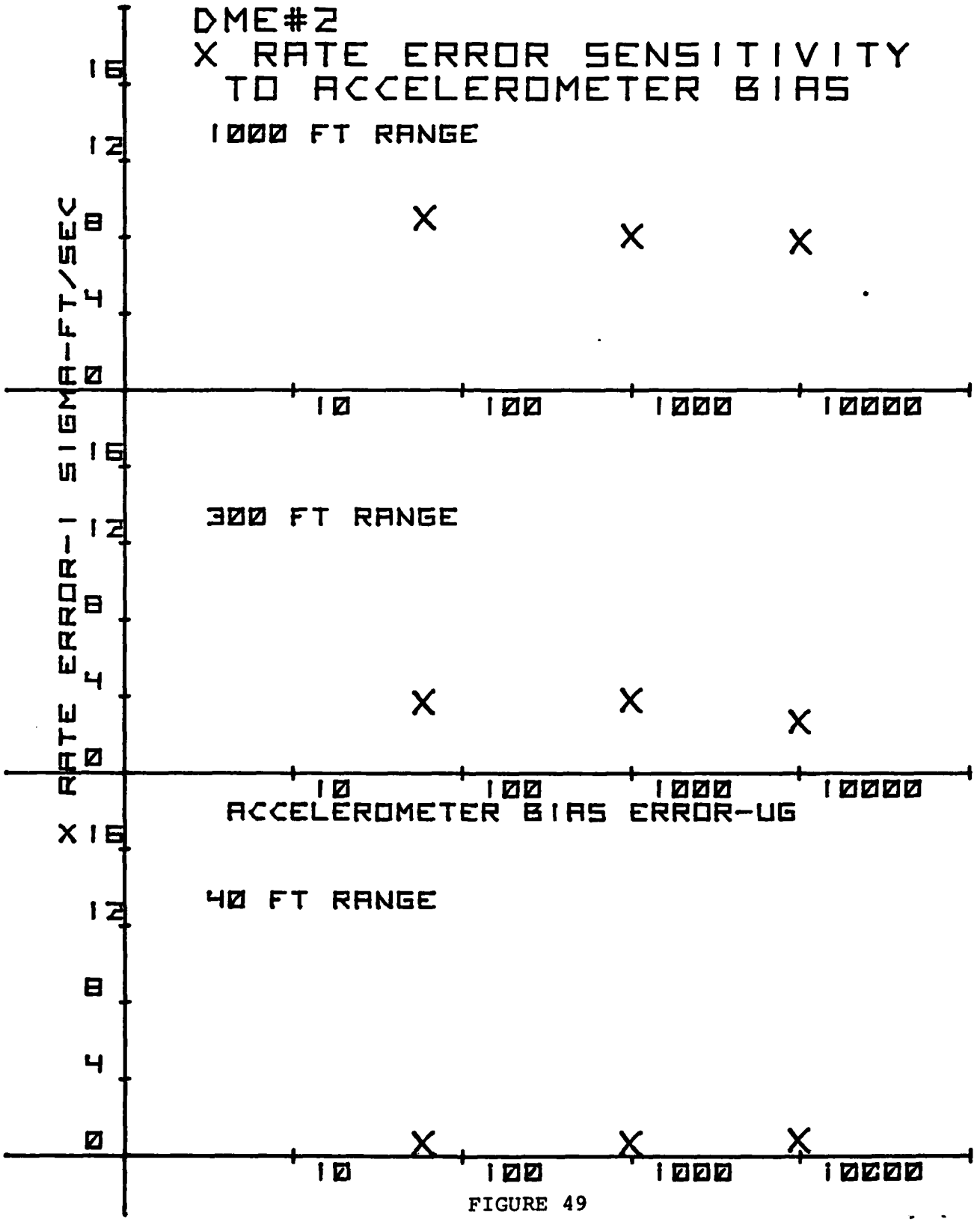
DME#2
X RATE ERROR SENSITIVITY
TO ACCELEROMETER BIAS
1000 FT RANGE
300 FT RANGE
40 FT RANGE
X RATE ERROR-1 SIGMA-FT/SEC
ACCELEROMETER BIAS ERROR-UG
0
4
8
12
16
10
100
1000
10000

FIGURE 49

D. SENSITIVITY TO DME ERROR CORRELATION TIME CONSTANT

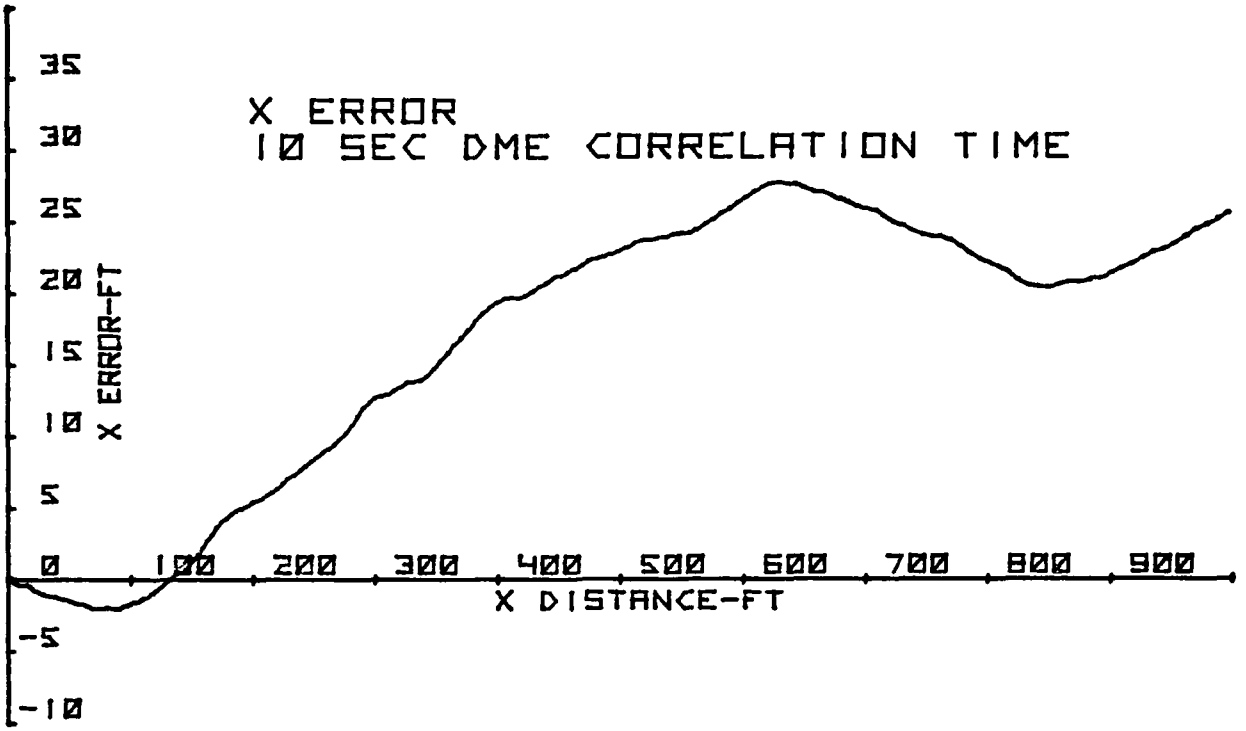

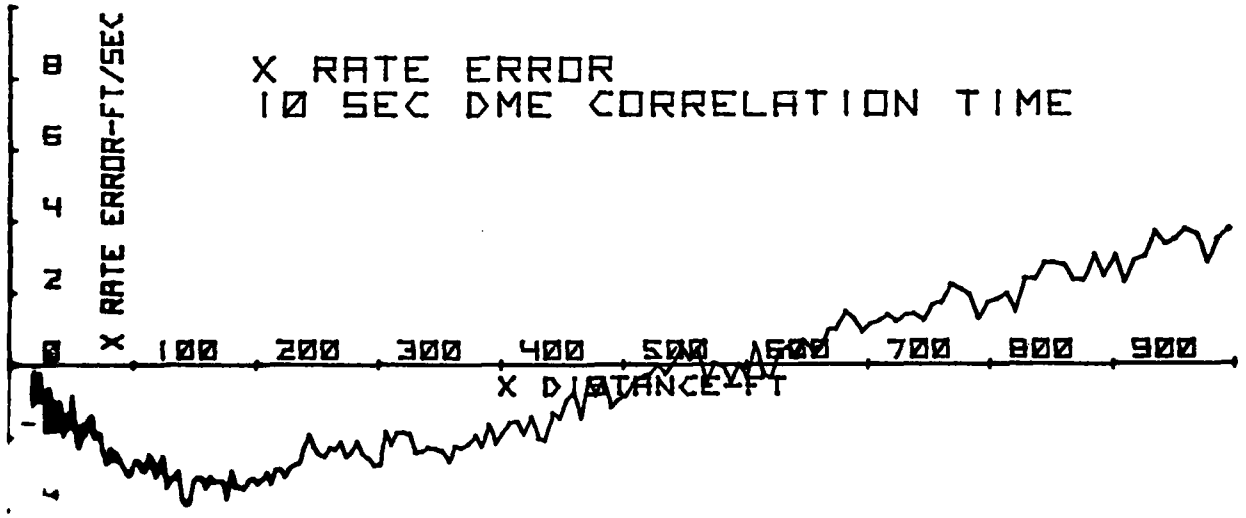

BIAS = -.99 ft/sec

NOISE = 1.90 ft/sec

FIGURE 50

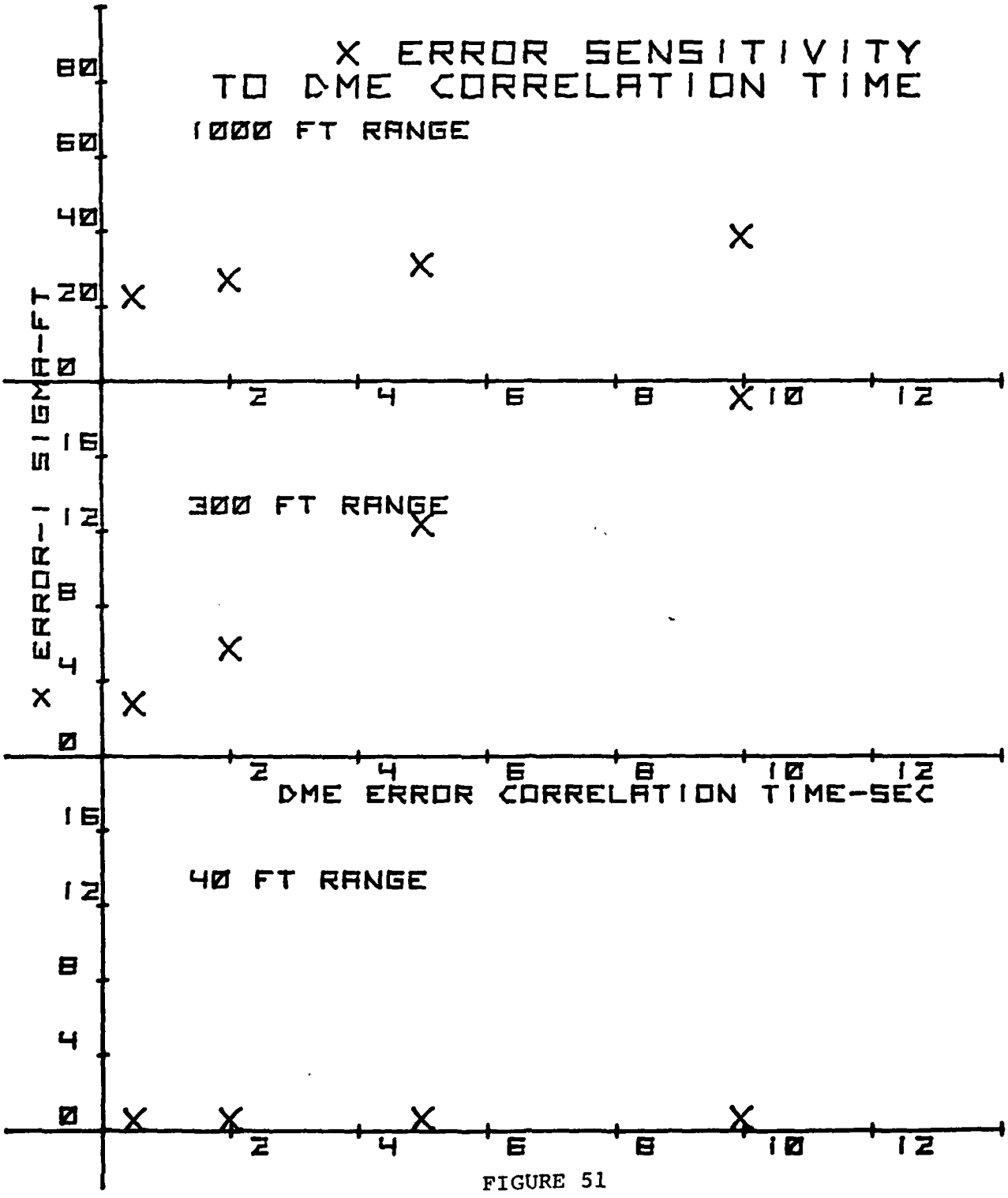
X ERROR SENSITIVITY
TO DME CORRELATION TIME
1000 FT RANGE
300 FT RANGE
40 FT RANGE
X ERROR-1 SIGMA-FT
DME ERROR CORRELATION TIME-SEC
80
60
40
20
0
16
12
8
4
0
2
4
6
8
10
12

FIGURE 51

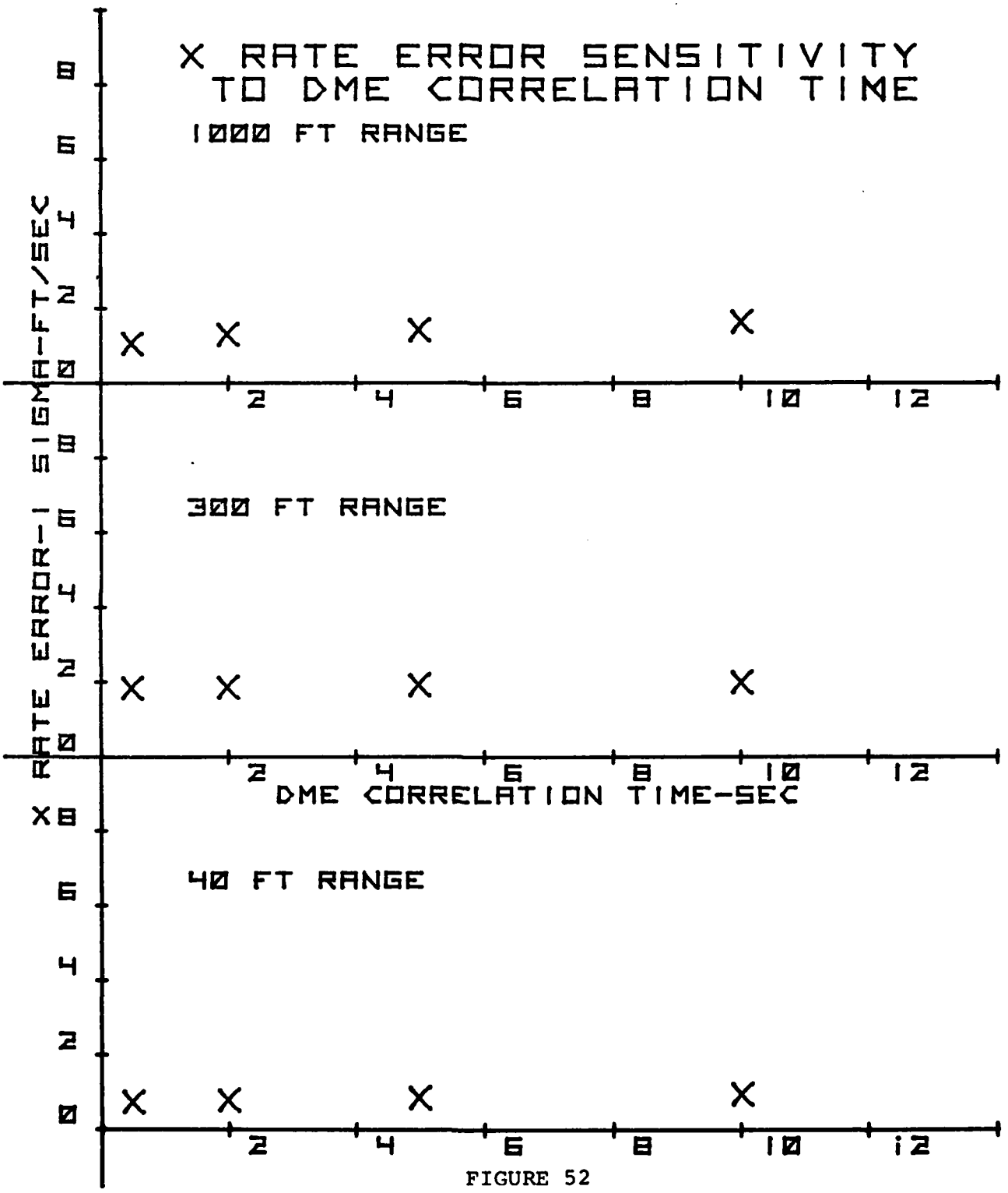
X RATE ERROR SENSITIVITY
TO DME CORRELATION TIME
1000 FT RANGE
300 FT RANGE
40 FT RANGE
X RATE ERROR-1 SIGMA-FT/SEC
DME CORRELATION TIME-SEC
0
2
4
6
8
10
12

FIGURE 52

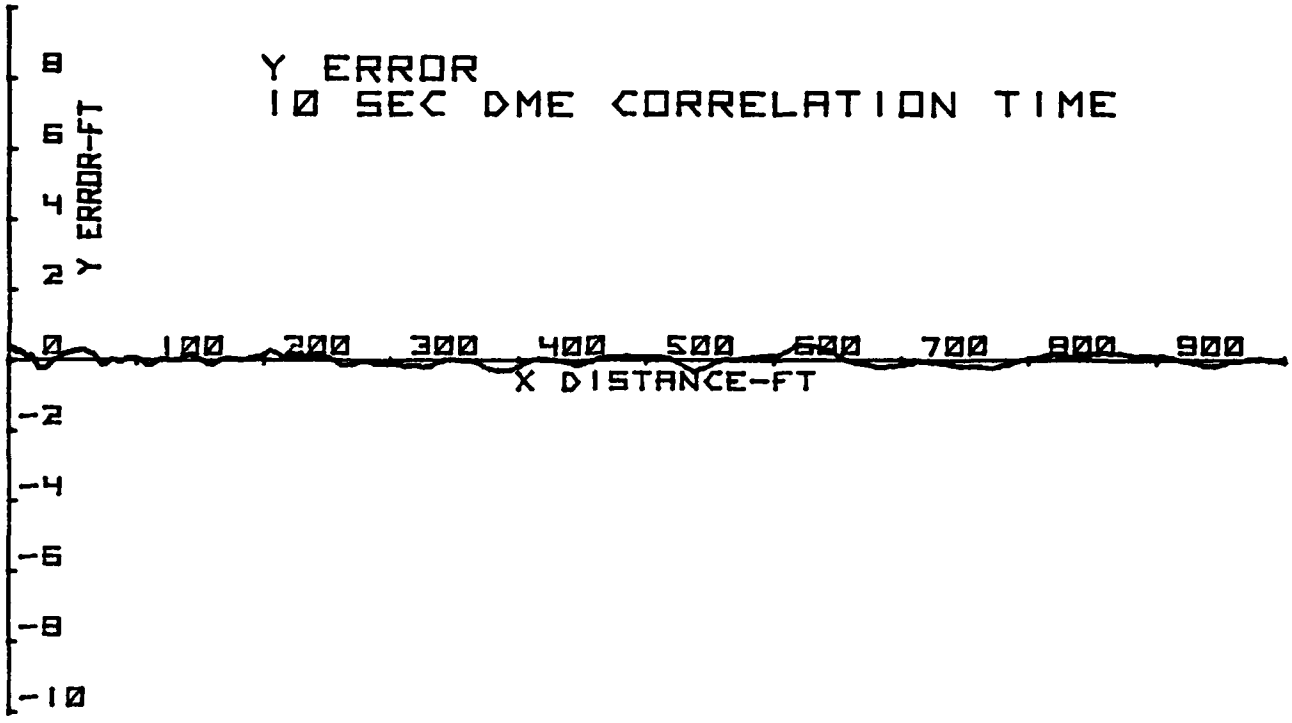

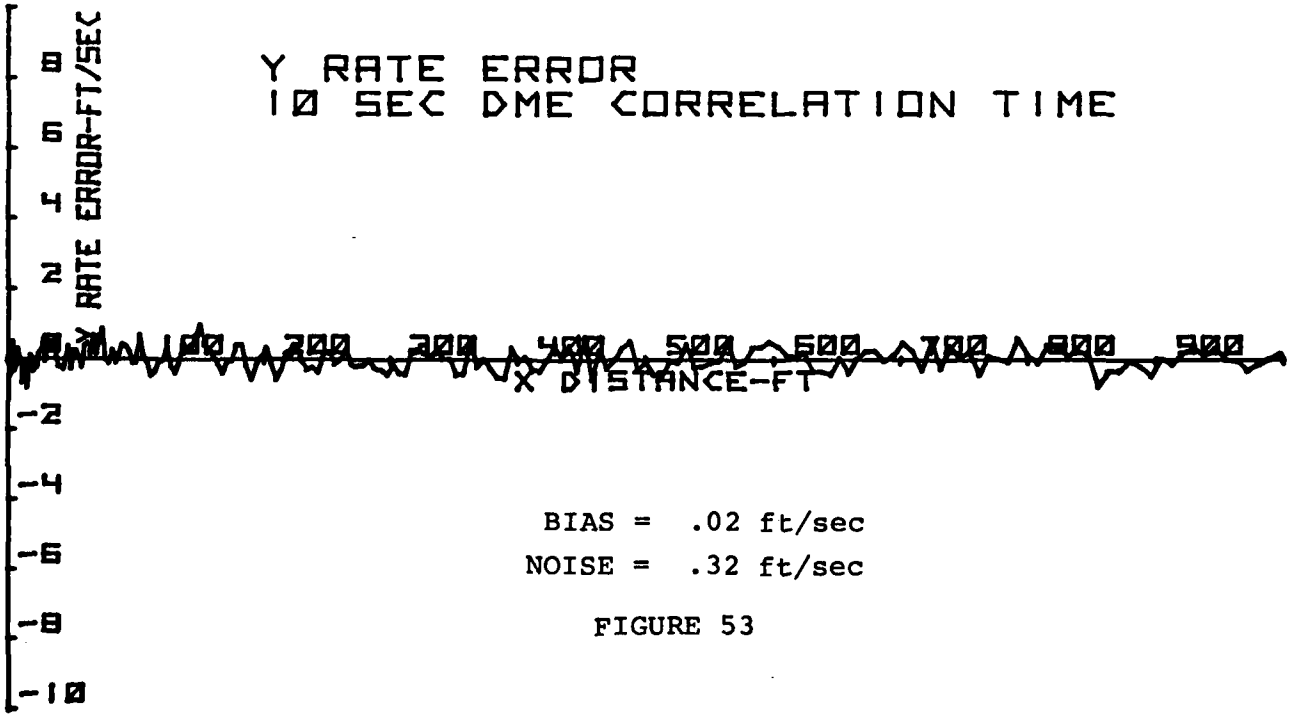

BIAS = .02 ft/sec

NOISE = .32 ft/sec

FIGURE 53

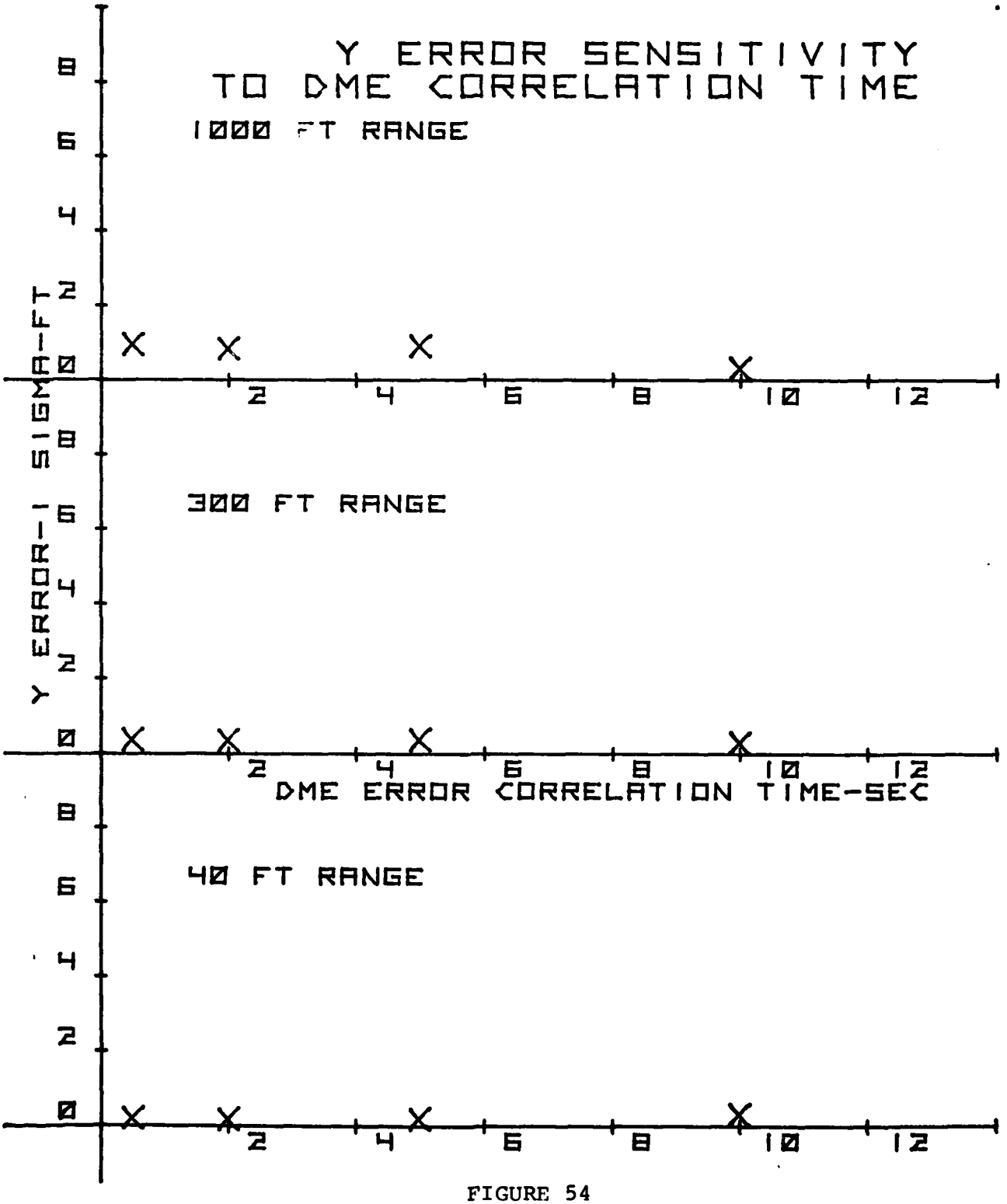
Y ERROR SENSITIVITY
TO DME CORRELATION TIME
1000 FT RANGE
300 FT RANGE
40 FT RANGE
Y ERROR-1 SIGMA-FT
0
2
4
6
8
10
12
DME ERROR CORRELATION TIME-SEC

FIGURE 54

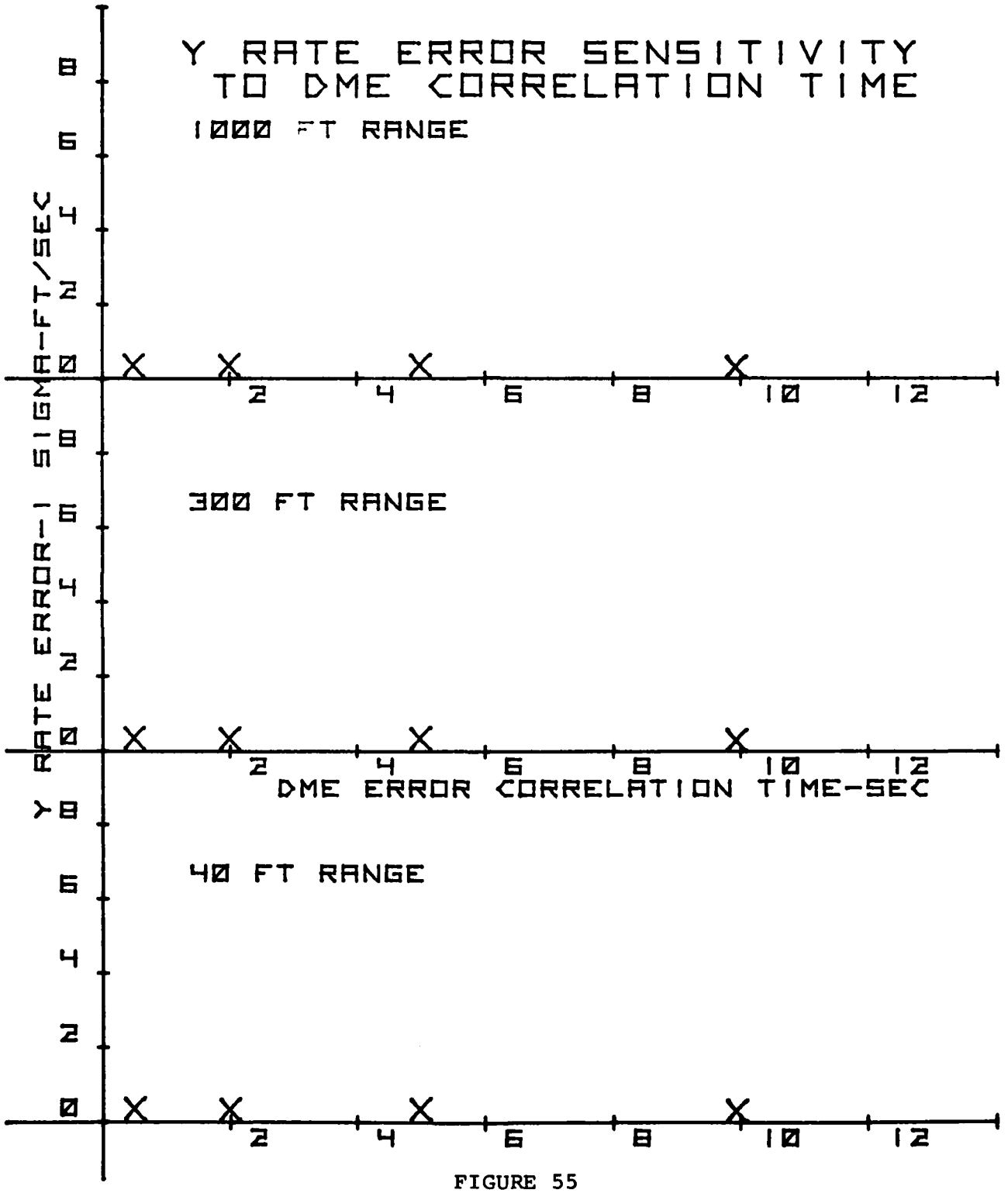
Y RATE ERROR SENSITIVITY
TO DME CORRELATION TIME
1000 FT RANGE
300 FT RANGE
40 FT RANGE
Y RATE ERROR-1 SIGMA-FT/SEC
DME ERROR CORRELATION TIME-SEC
0
2
4
6
8
10
12

FIGURE 55

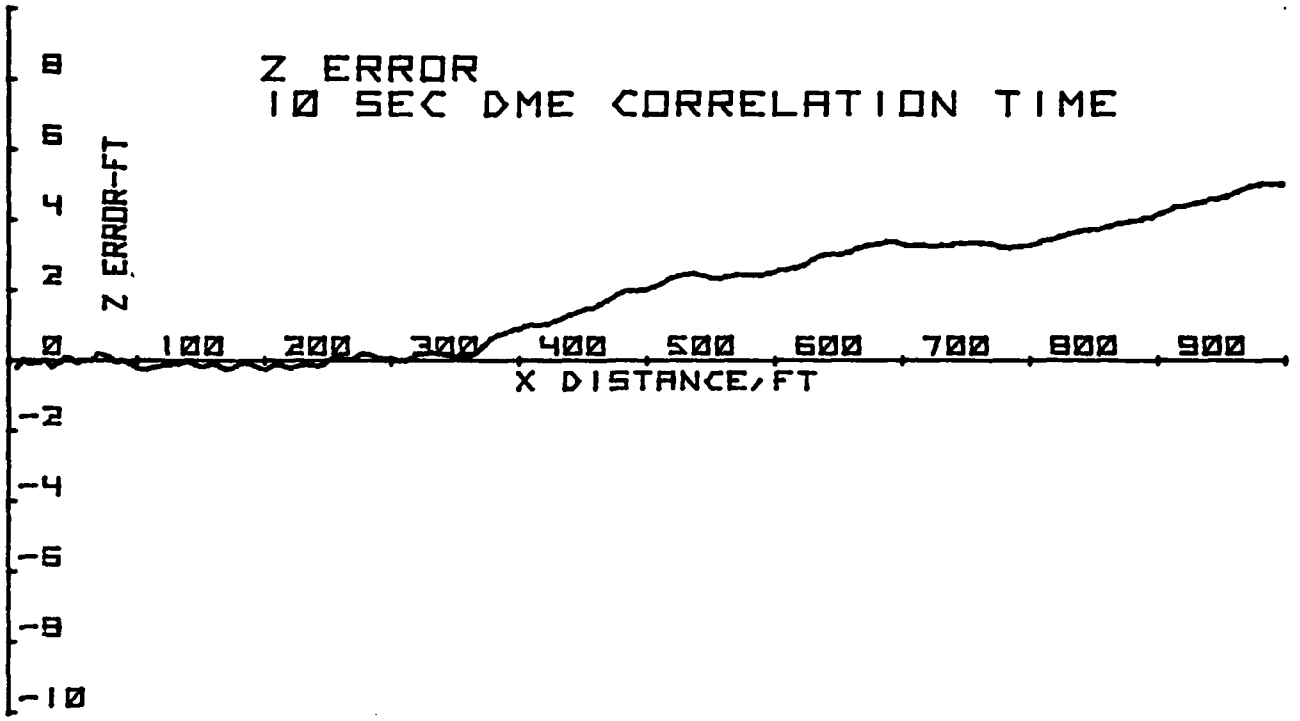

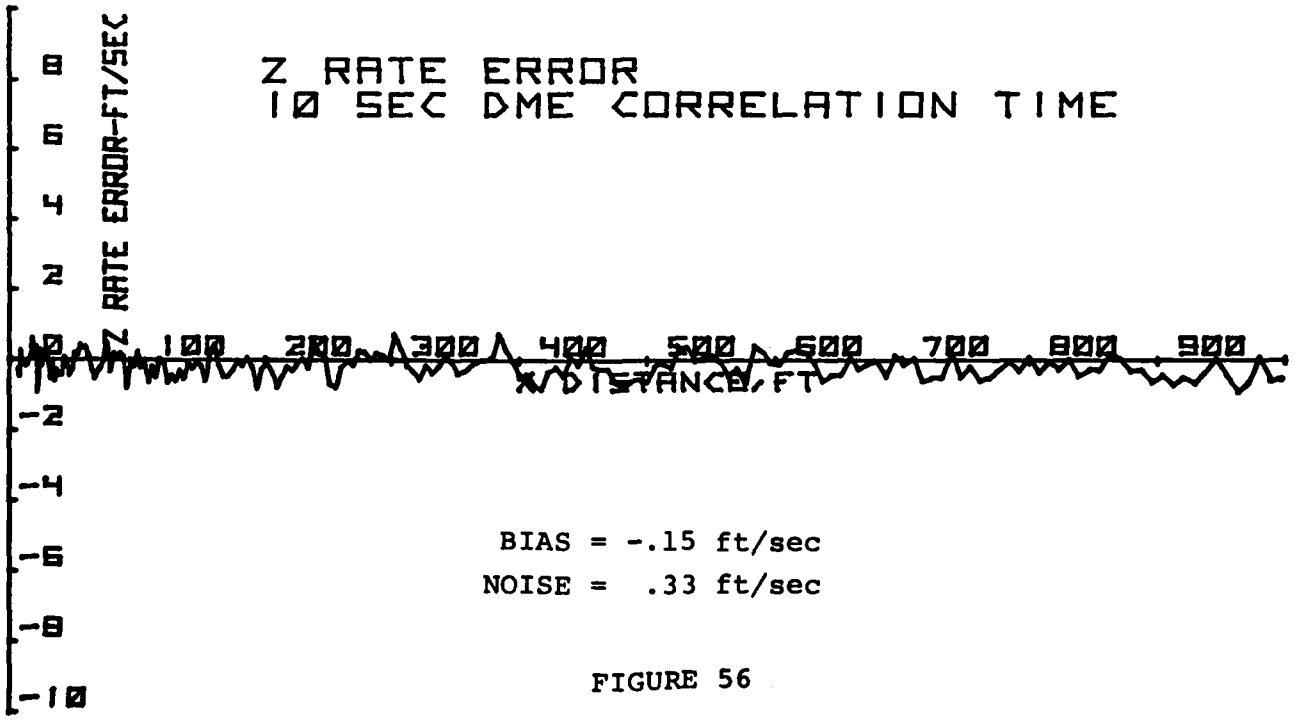

BIAS = -.15 ft/sec
NOISE = .33 ft/sec

FIGURE 56

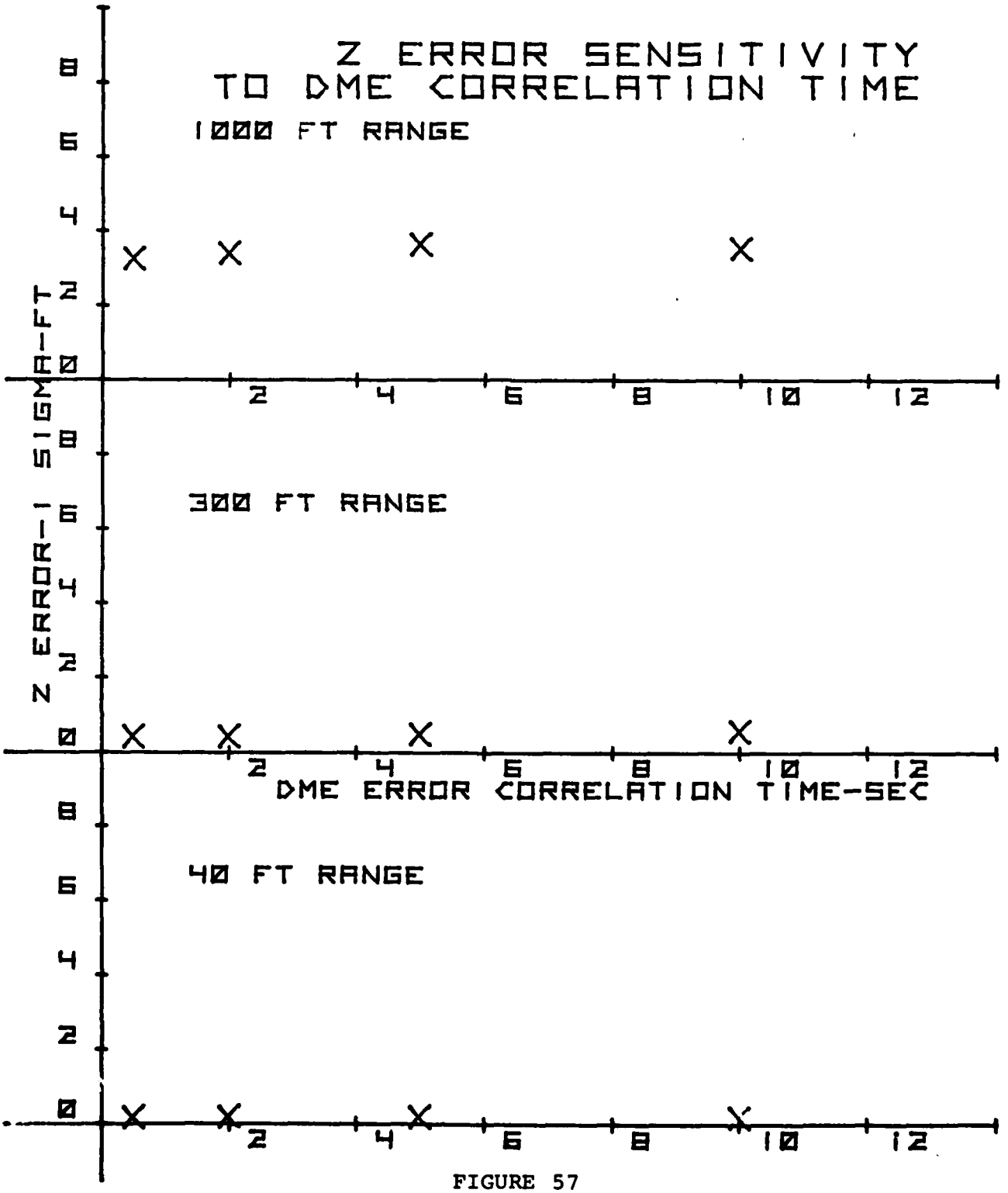
Z ERROR SENSITIVITY
TO DME CORRELATION TIME
1000 FT RANGE
300 FT RANGE
40 FT RANGE
Z ERROR-1 SIGMA-FT
DME ERROR CORRELATION TIME-SEC
0
2
4
6
8
10
12

FIGURE 57

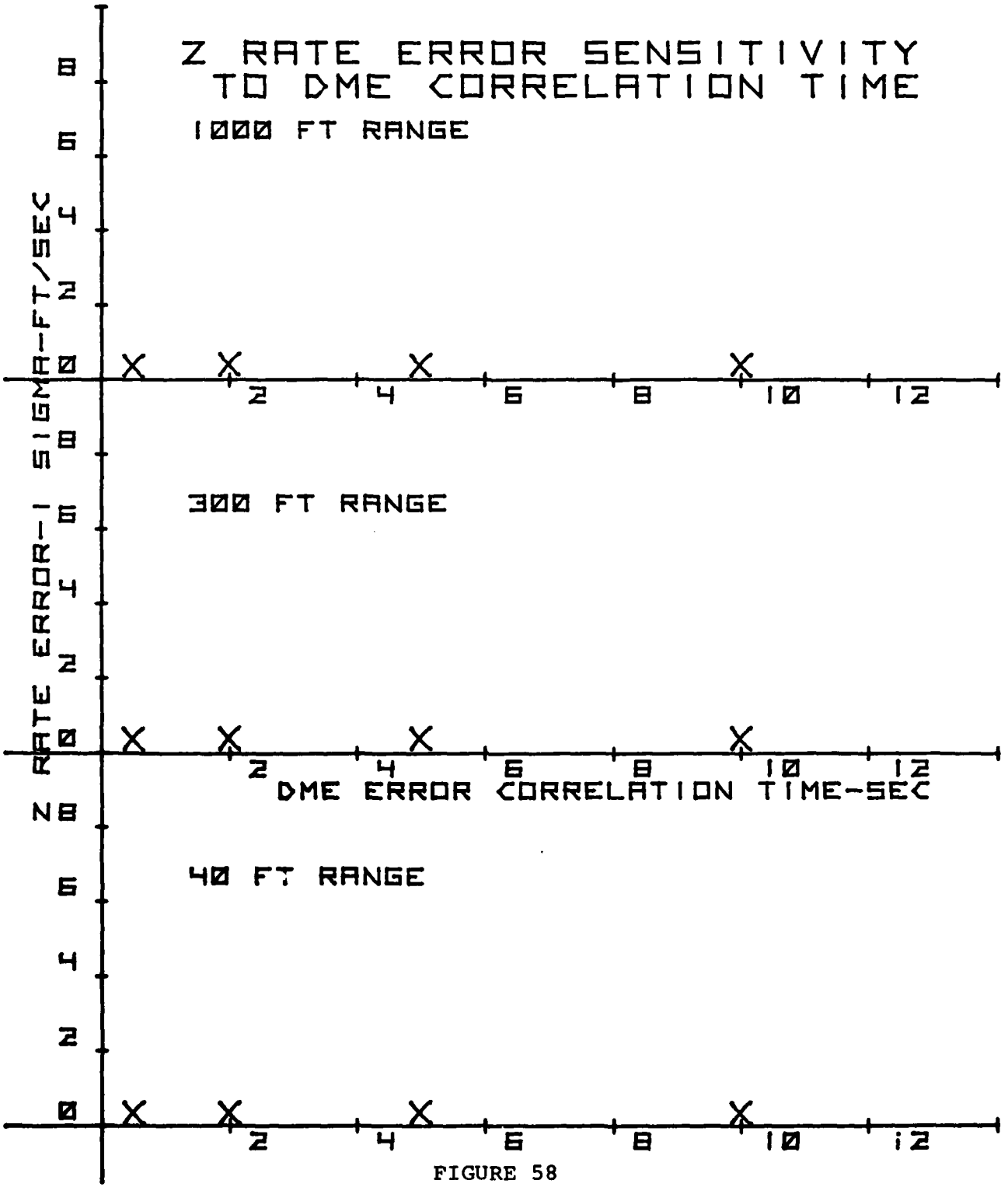
Z RATE ERROR SENSITIVITY
TO DME CORRELATION TIME
1000 FT RANGE
300 FT RANGE
40 FT RANGE
Z RATE ERROR-1 SIGMA-FT/SEC
DME ERROR CORRELATION TIME-SEC
0
2
4
6
8
10
12

FIGURE 58

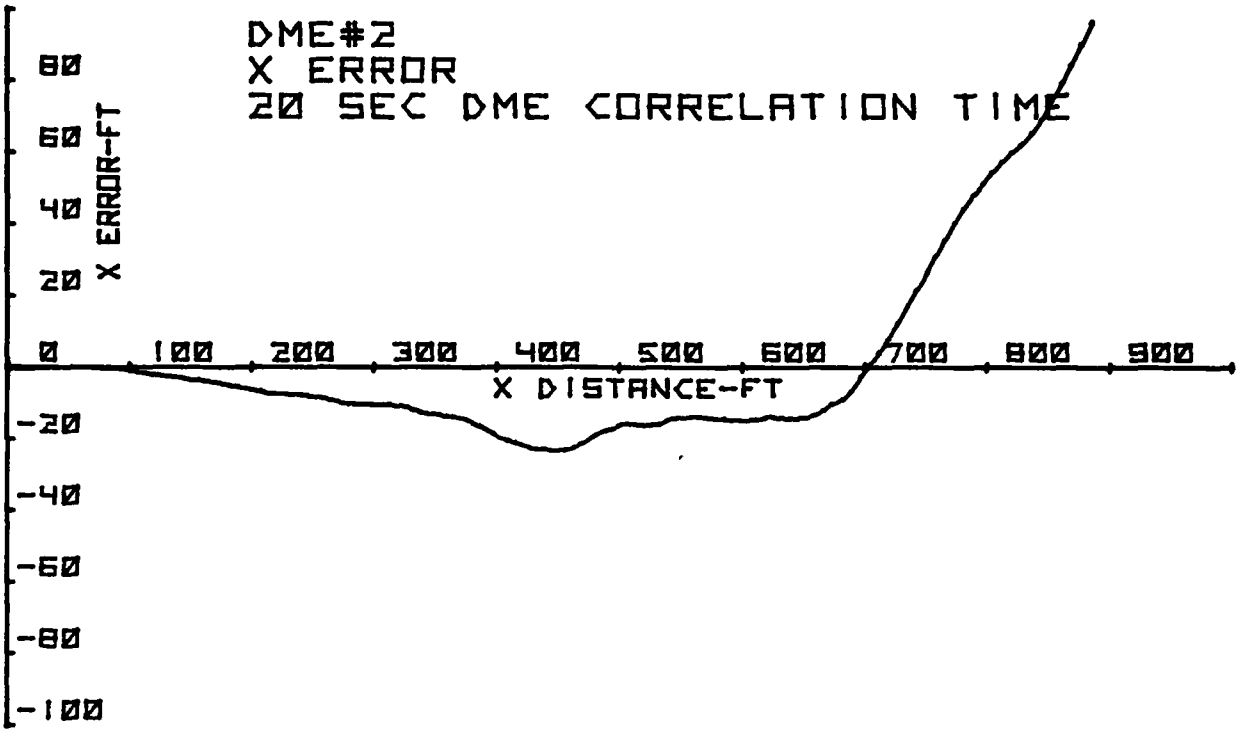
DME#2
X ERROR
20 SEC DME CORRELATION TIME
X ERROR-FT
80
60
40
20
0
100
200
300
400
500
600
700
800
900
X DISTANCE-FT
-20
-40
-60
-80
-100

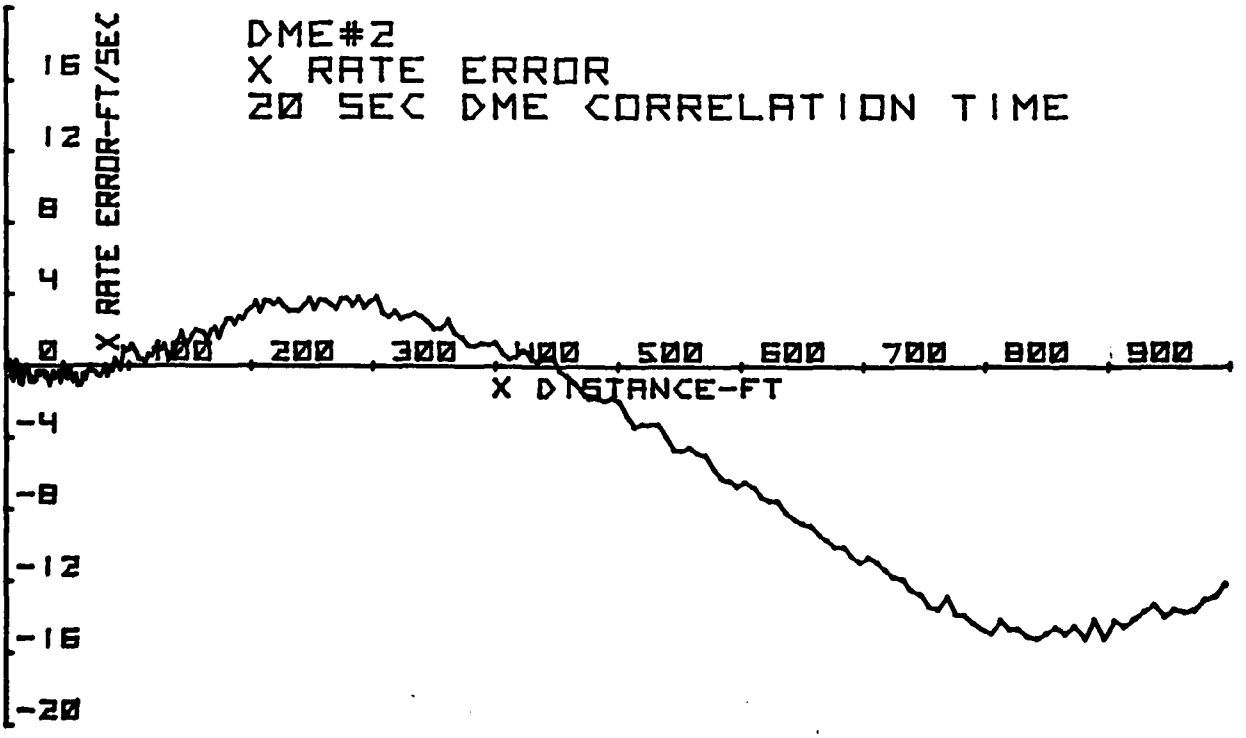
DME#2
X RATE ERROR
20 SEC DME CORRELATION TIME
X RATE ERROR-FT/SEC
16
12
8
4
0
100
200
300
400
500
600
700
800
900
X DISTANCE-FT
-4
-8
-12
-16
-20

FIGURE 59

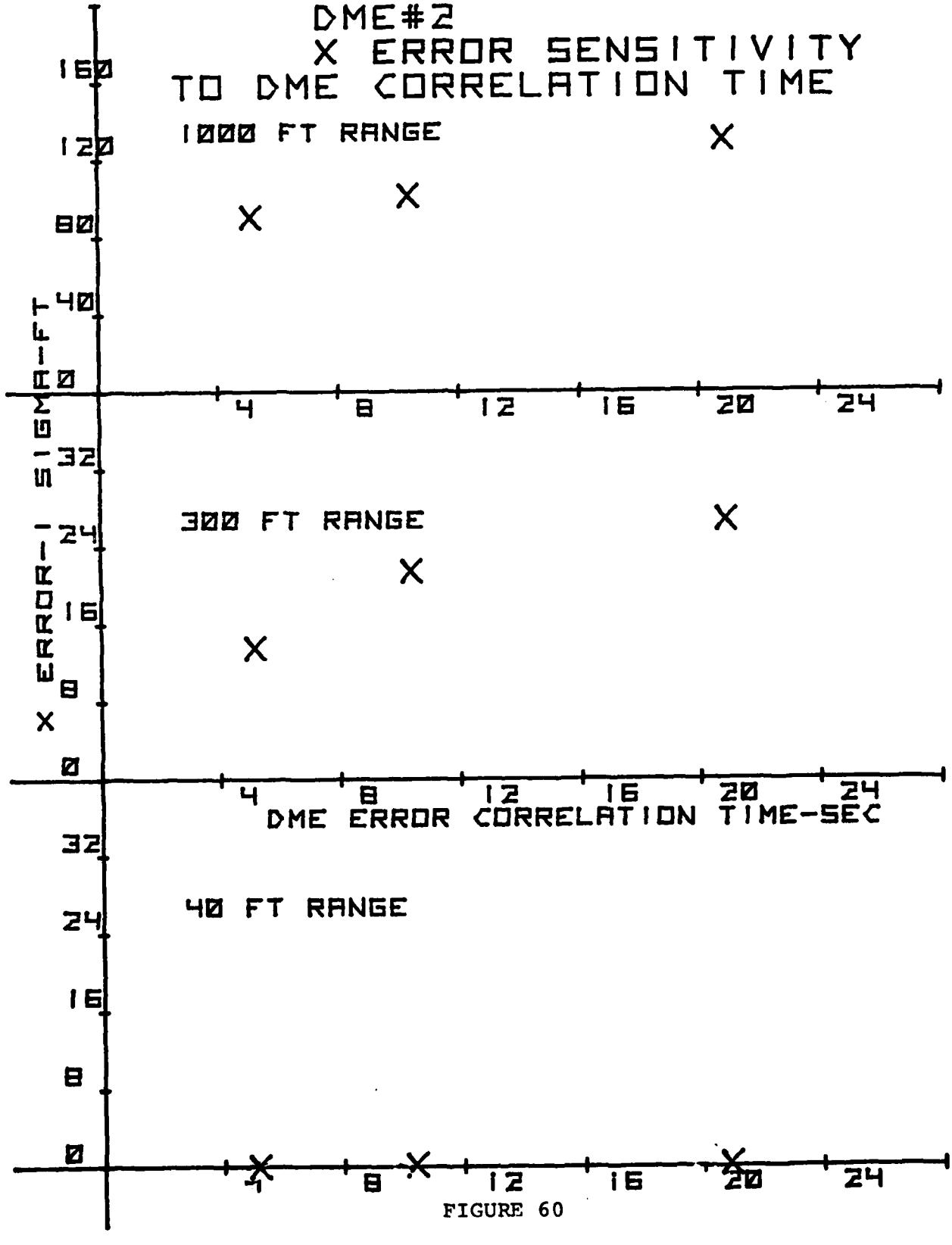
DME#2
X ERROR SENSITIVITY
TO DME CORRELATION TIME
1000 FT RANGE
300 FT RANGE
40 FT RANGE
X ERROR-1 SIGMA-FT
DME ERROR CORRELATION TIME-SEC
160
120
80
40
0
32
24
16
8
0
4
8
12
16
20
24

FIGURE 60

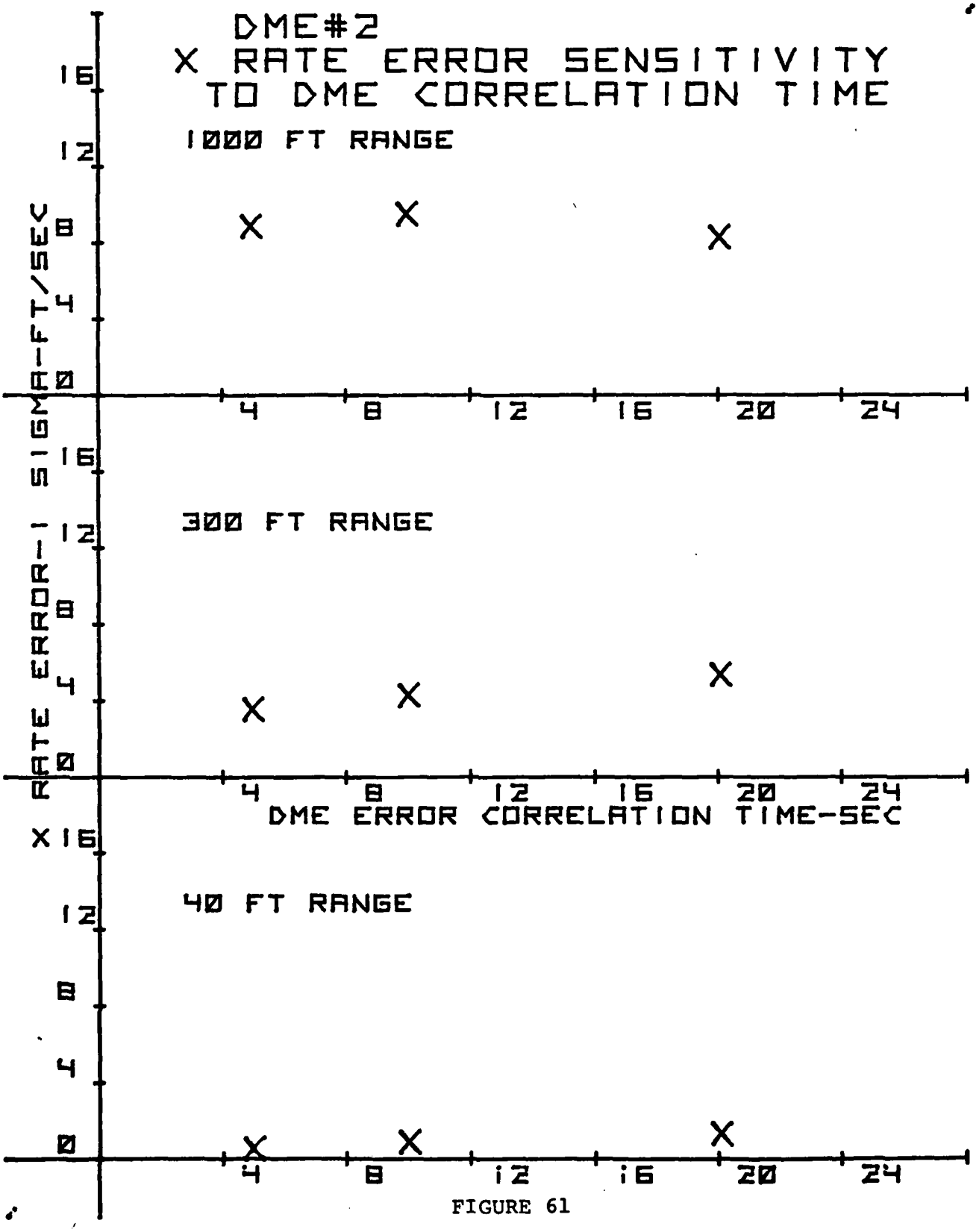
DME#2
X RATE ERROR SENSITIVITY
TO DME CORRELATION TIME
1000 FT RANGE
300 FT RANGE
40 FT RANGE
X RATE ERROR-1 SIGMA-FT/SEC
DME ERROR CORRELATION TIME-SEC
0
4
8
12
16
20
24

FIGURE 61

E. SENSITIVITY TO ANGLE ERROR CORRELATION TIME CONSTANT

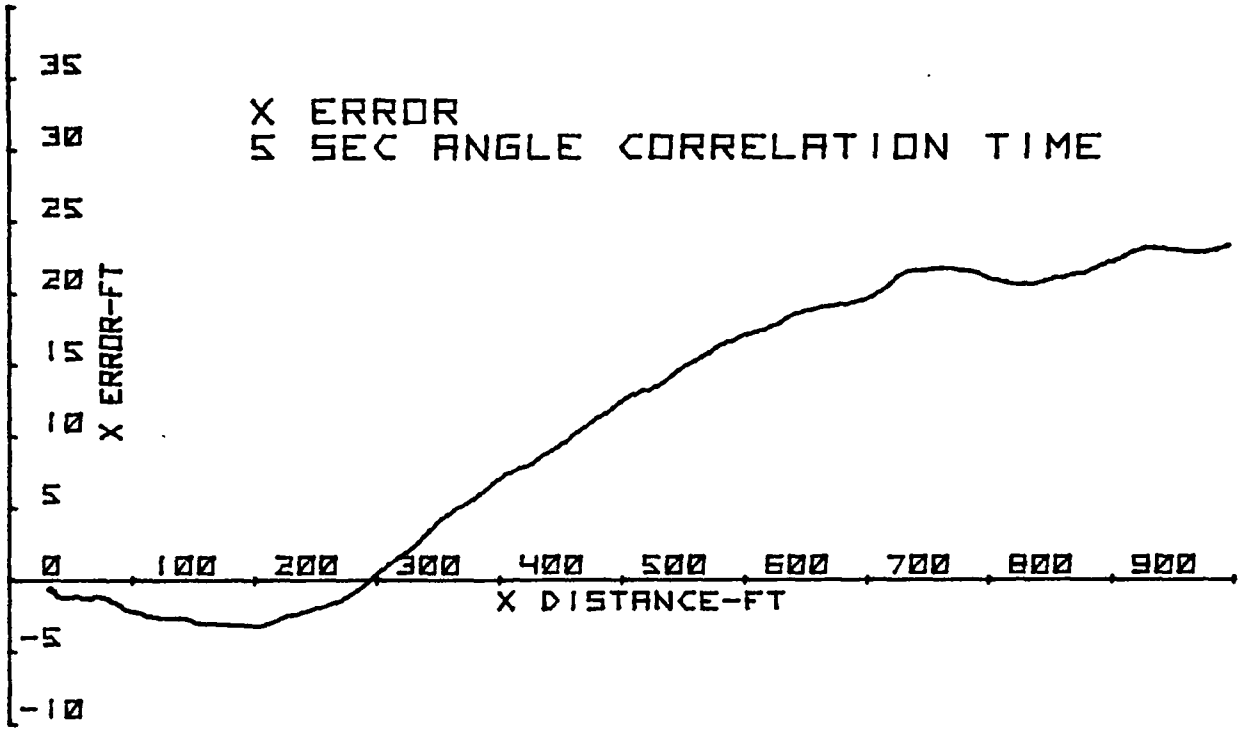

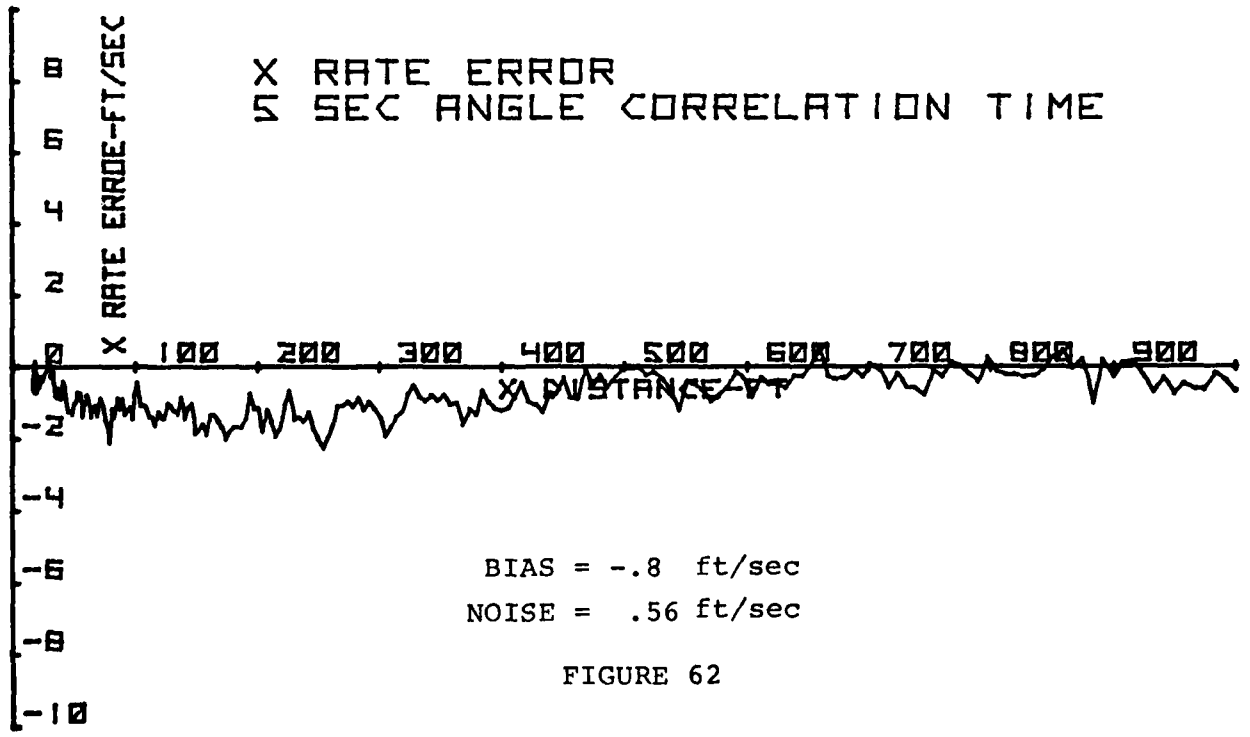

BIAS = -.8 ft/sec

NOISE = .56 ft/sec

FIGURE 62

AD-A084 037 EATON CORP DEER PARK NY AIL DIV F/G 17/7
SIMULATION OF PRECISION AIRCRAFT POSITIONING SYSTEM UTILIZING T--ETC(U)
MAR 78 A CHARYCH N00123-76-C-1322
UNCLASSIFIED NL

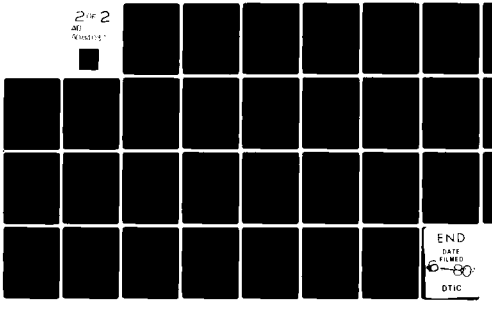

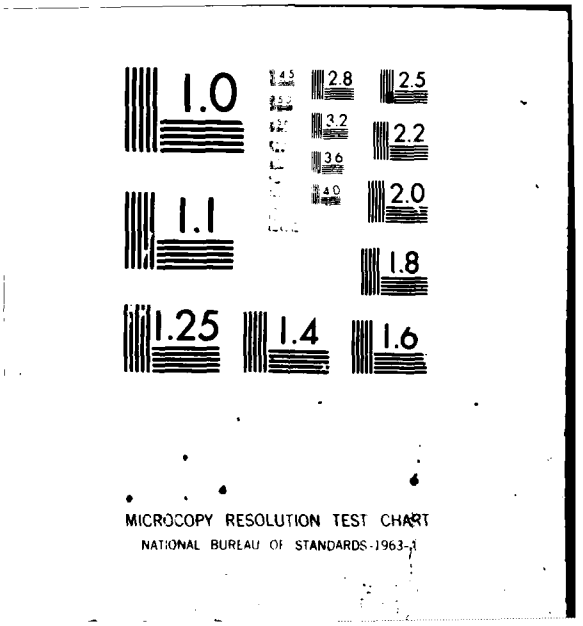
1.0
1.1
1.25
1.4
1.6
1.8
2.0
2.2
2.5
2.8
3.2
3.6
4.0
MICROCOPY RESOLUTION TEST CHART
NATIONAL BUREAU OF STANDARDS-1963-A

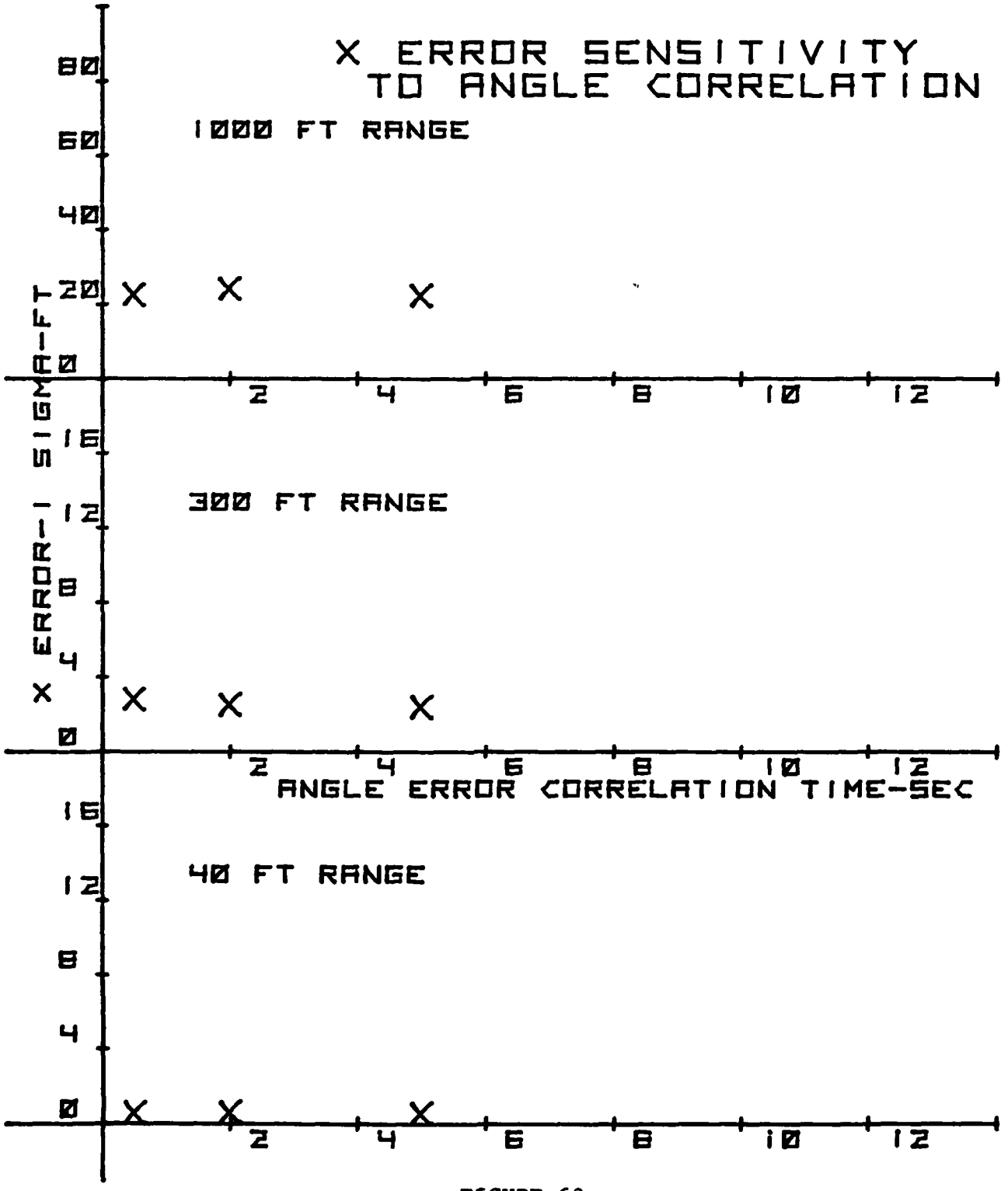
X ERROR SENSITIVITY
TO ANGLE CORRELATION
1000 FT RANGE
300 FT RANGE
40 FT RANGE
X ERROR-1 SIGMA-FT
ANGLE ERROR CORRELATION TIME-SEC
0
20
40
60
80
4
8
12
16
2
4
6
8
10
12

FIGURE 63

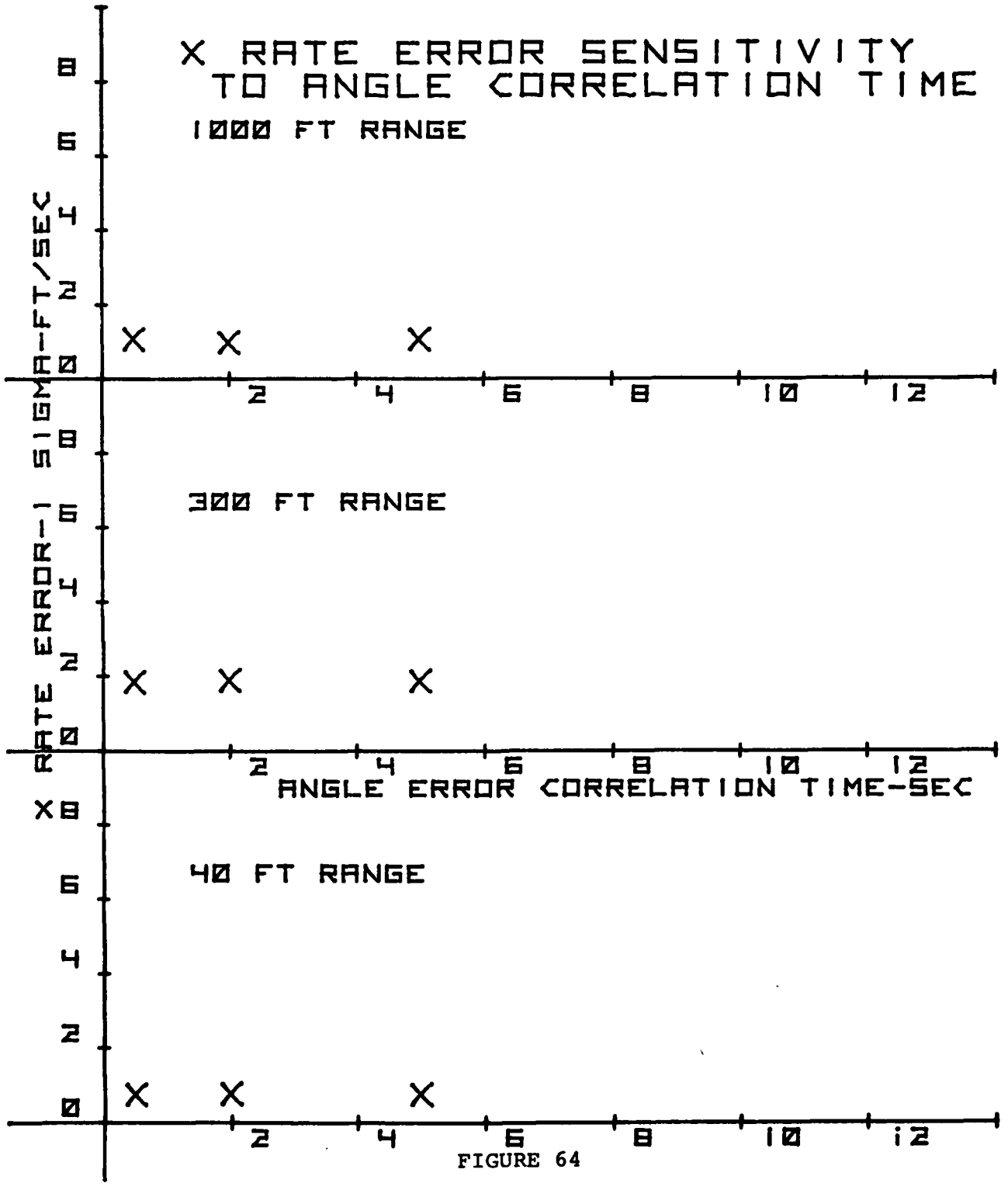
X RATE ERROR SENSITIVITY
TO ANGLE CORRELATION TIME
1000 FT RANGE
300 FT RANGE
40 FT RANGE
X RATE ERROR-1 SIGMA-FT/SEC
ANGLE ERROR CORRELATION TIME-SEC
0
2
4
6
8
10
12

FIGURE 64

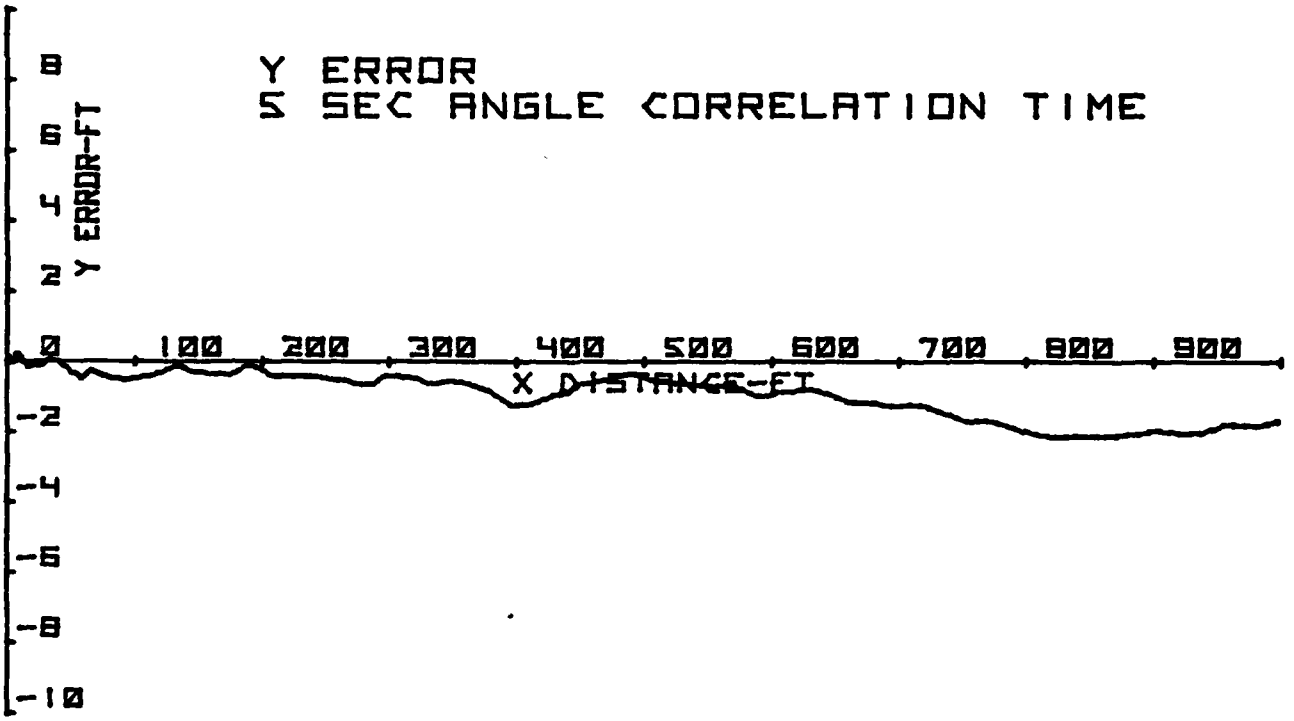

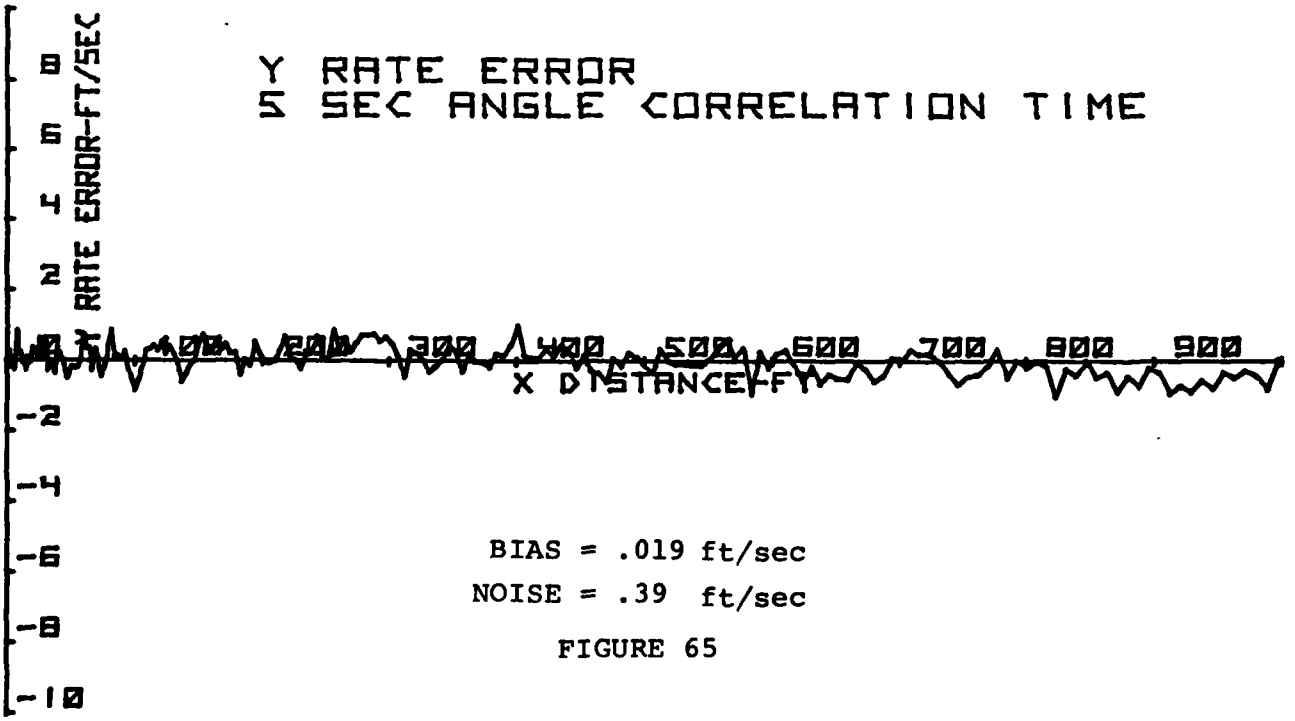

BIAS = .019 ft/sec

NOISE = .39 ft/sec

FIGURE 65

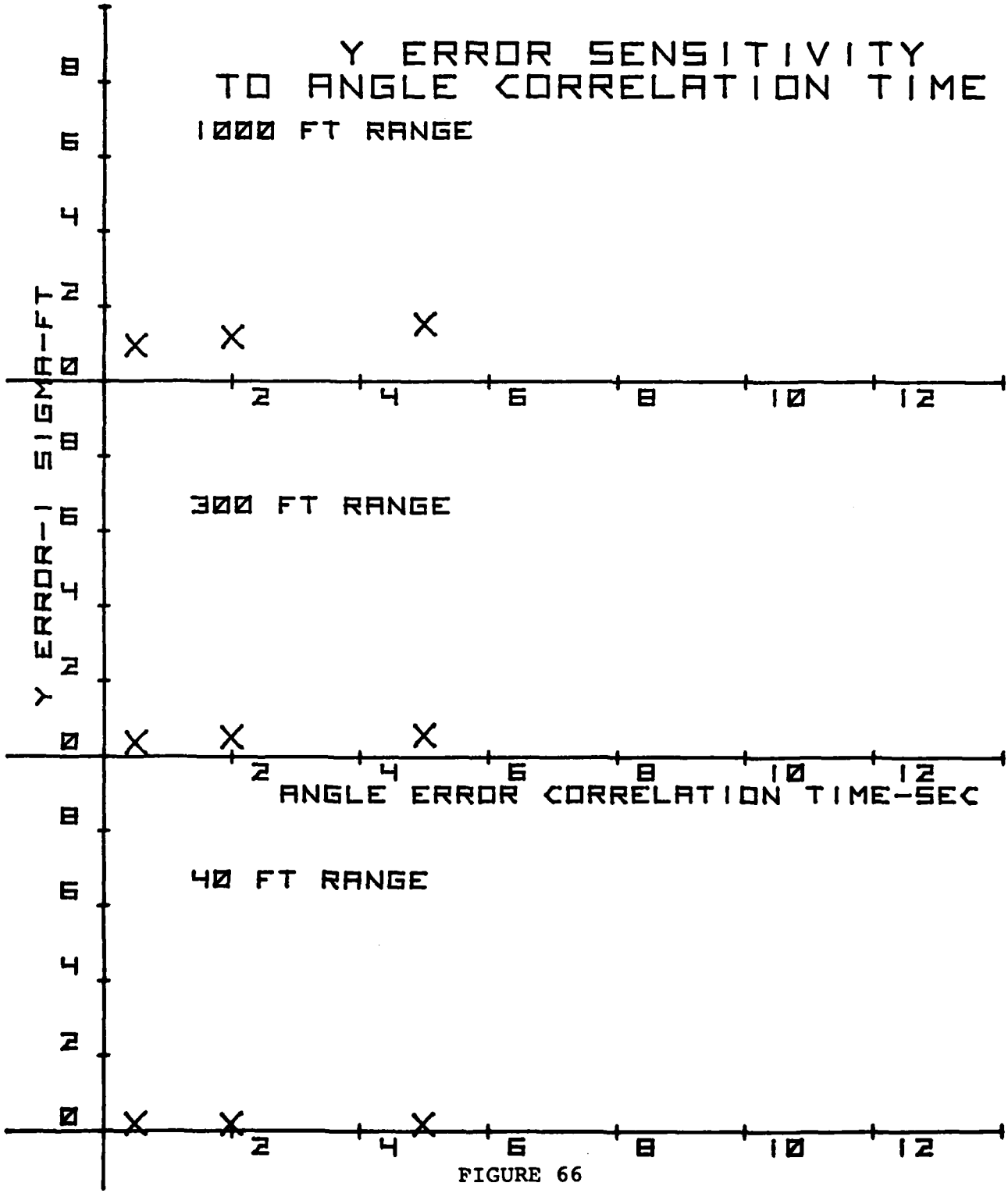
Y ERROR SENSITIVITY
TO ANGLE CORRELATION TIME
1000 FT RANGE
300 FT RANGE
40 FT RANGE
Y ERROR-1 SIGMA-FT
ANGLE ERROR CORRELATION TIME-SEC
0
2
4
6
8
10
12

FIGURE 66

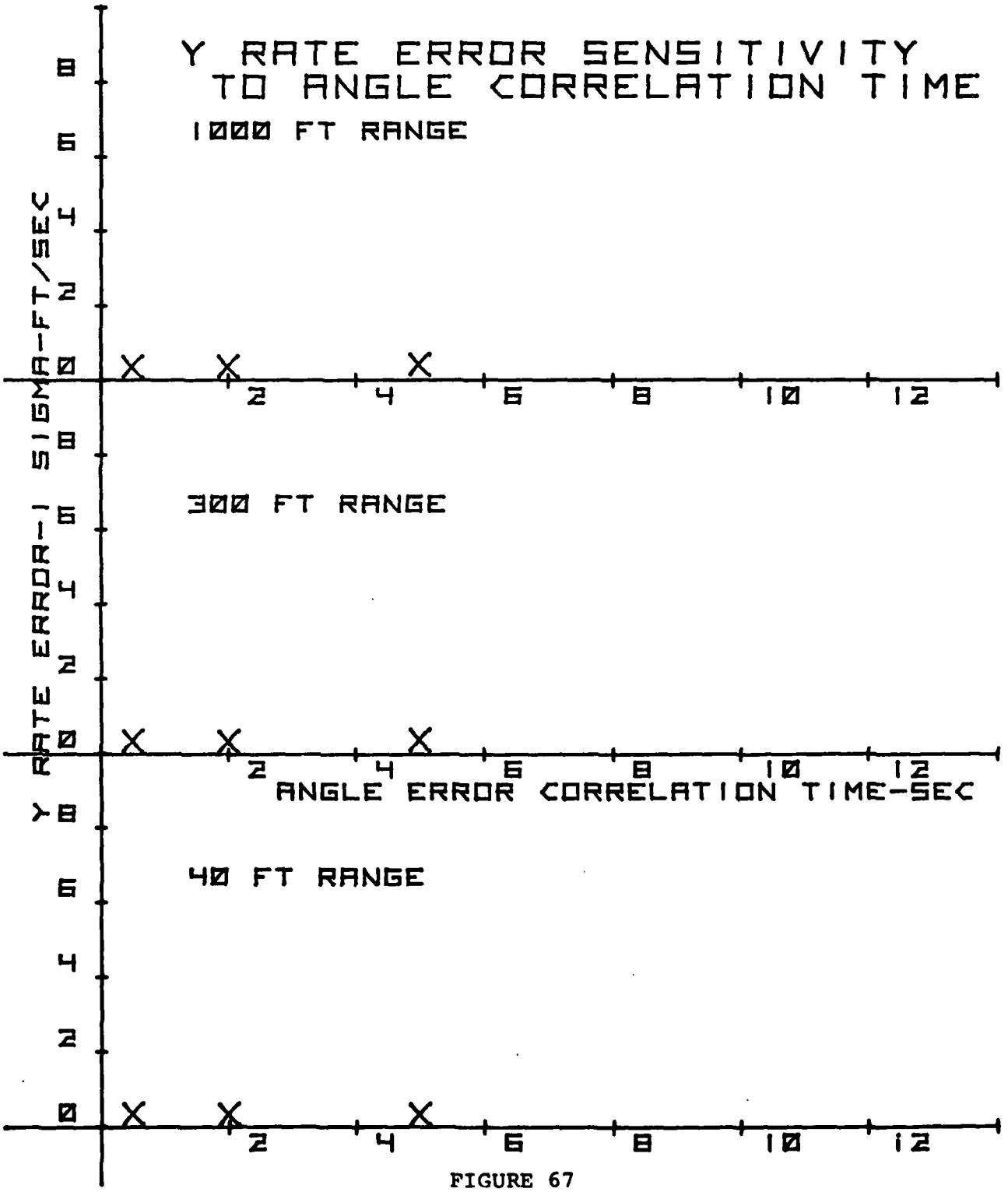
Y RATE ERROR SENSITIVITY
TO ANGLE CORRELATION TIME
1000 FT RANGE
300 FT RANGE
40 FT RANGE
Y RATE ERROR-1 SIGMA-FT/SEC
ANGLE ERROR CORRELATION TIME-SEC
0
2
4
6
8
10
12

FIGURE 67

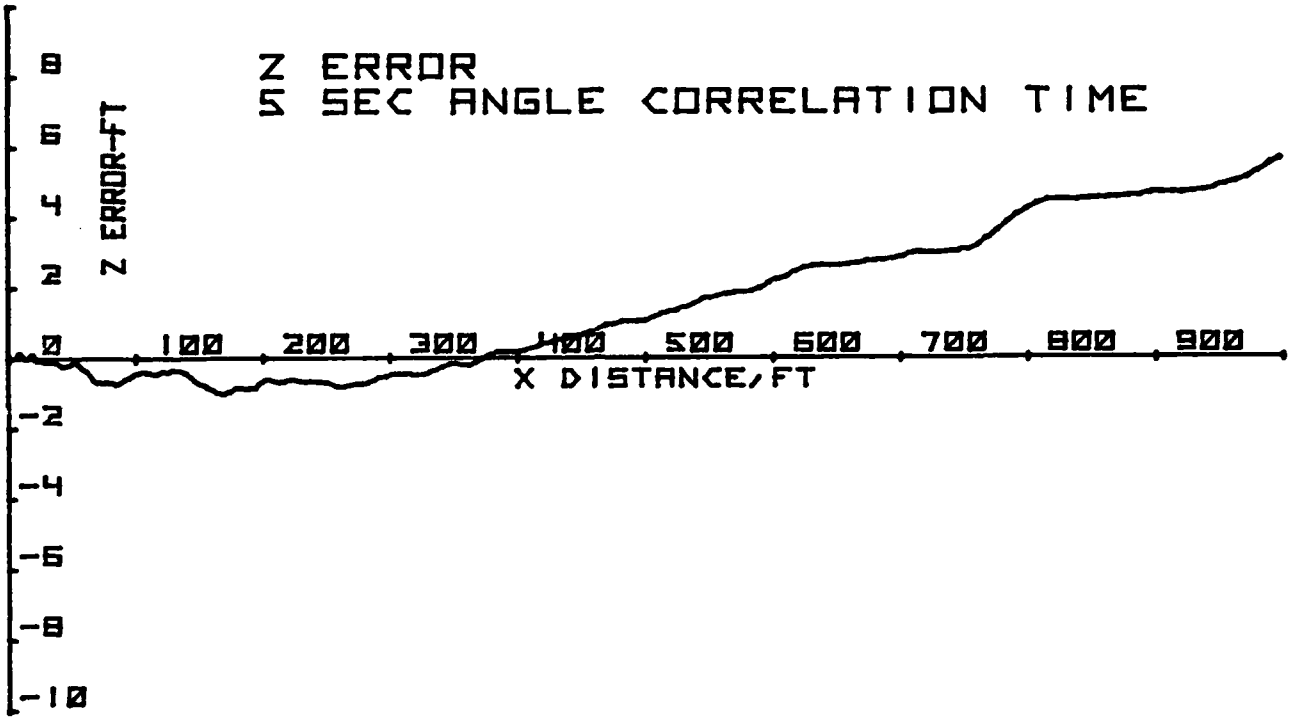

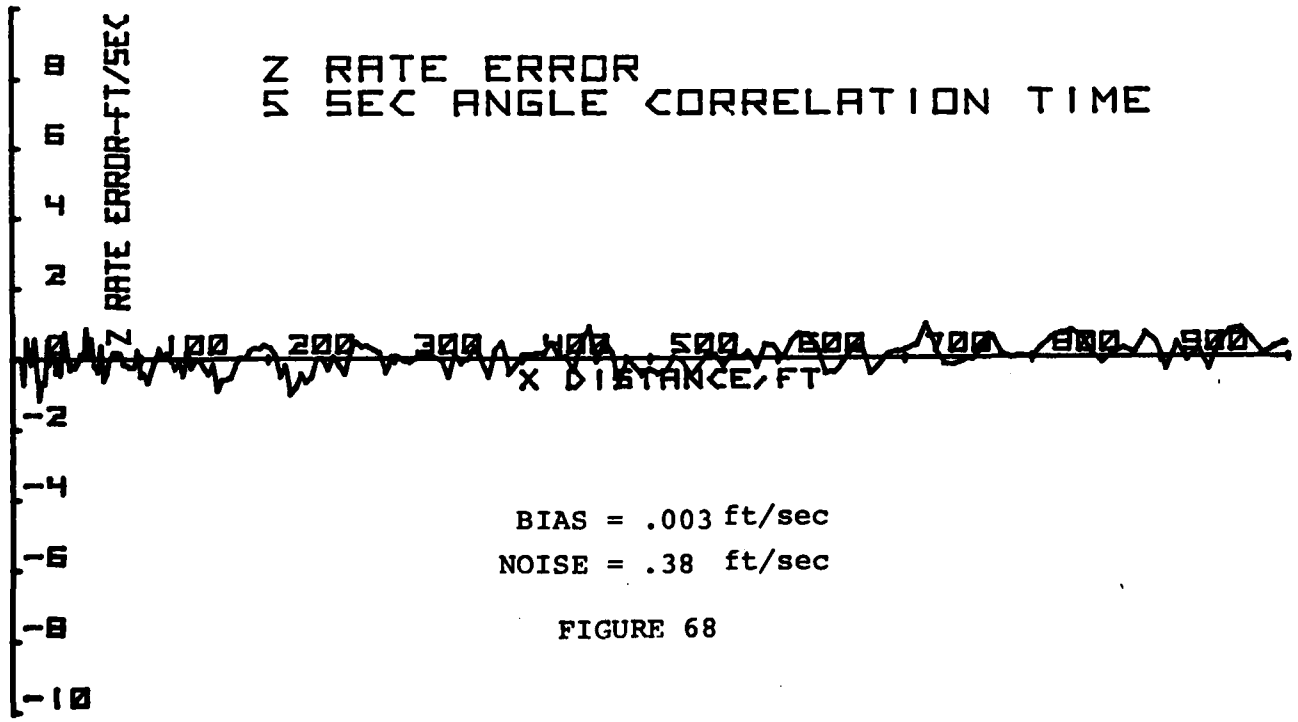

BIAS = .003 ft/sec

NOISE = .38 ft/sec

FIGURE 68

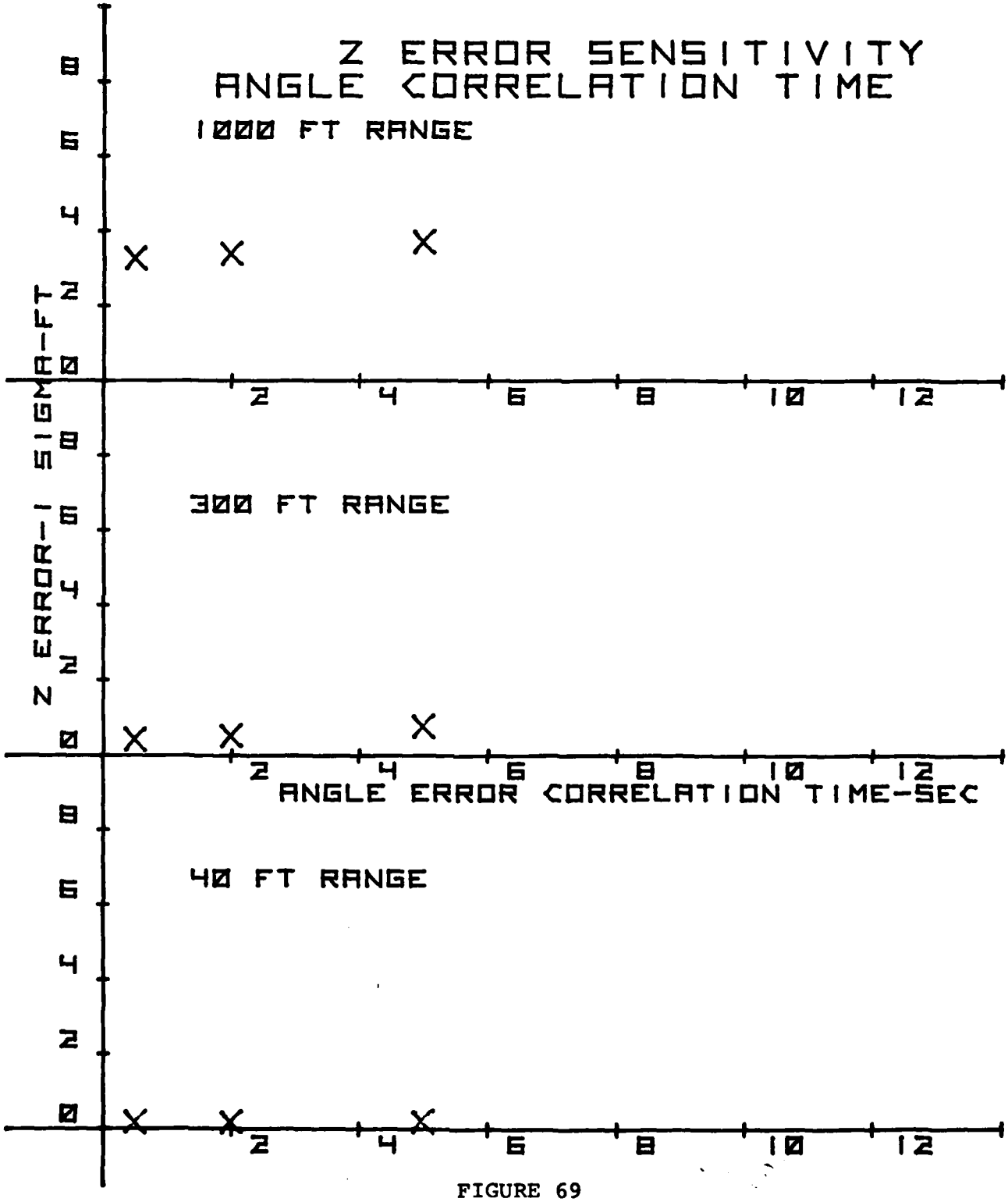
Z ERROR SENSITIVITY
ANGLE CORRELATION TIME
1000 FT RANGE
300 FT RANGE
40 FT RANGE
Z ERROR-1 SIGMA-FT
0
2
4
6
8
10
12
ANGLE ERROR CORRELATION TIME-SEC

FIGURE 69

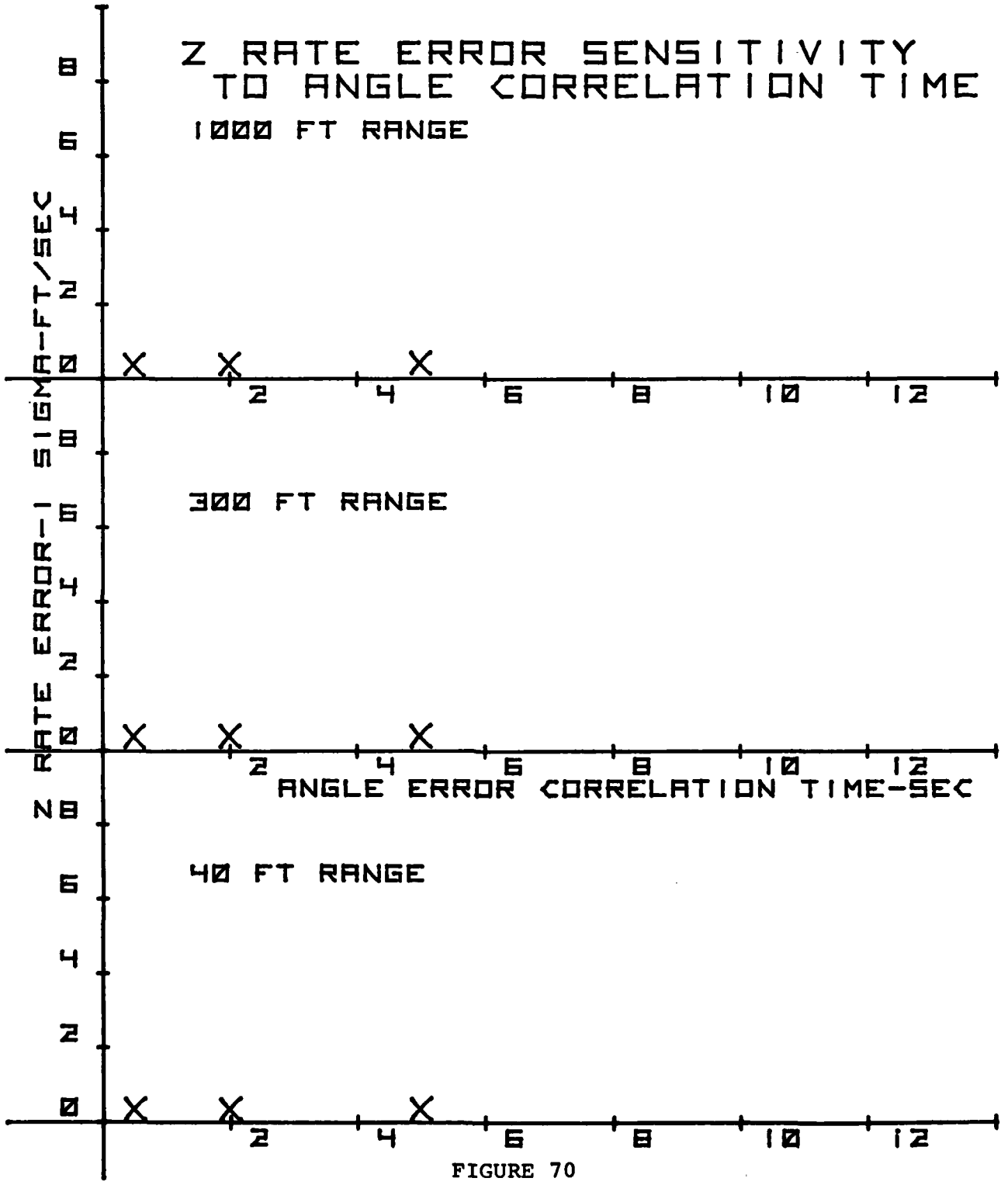
Z RATE ERROR SENSITIVITY
TO ANGLE CORRELATION TIME
1000 FT RANGE
300 FT RANGE
40 FT RANGE
Z RATE ERROR-1 SIGMA-FT/SEC
ANGLE ERROR CORRELATION TIME-SEC
0
2
4
6
8
10
12

FIGURE 70

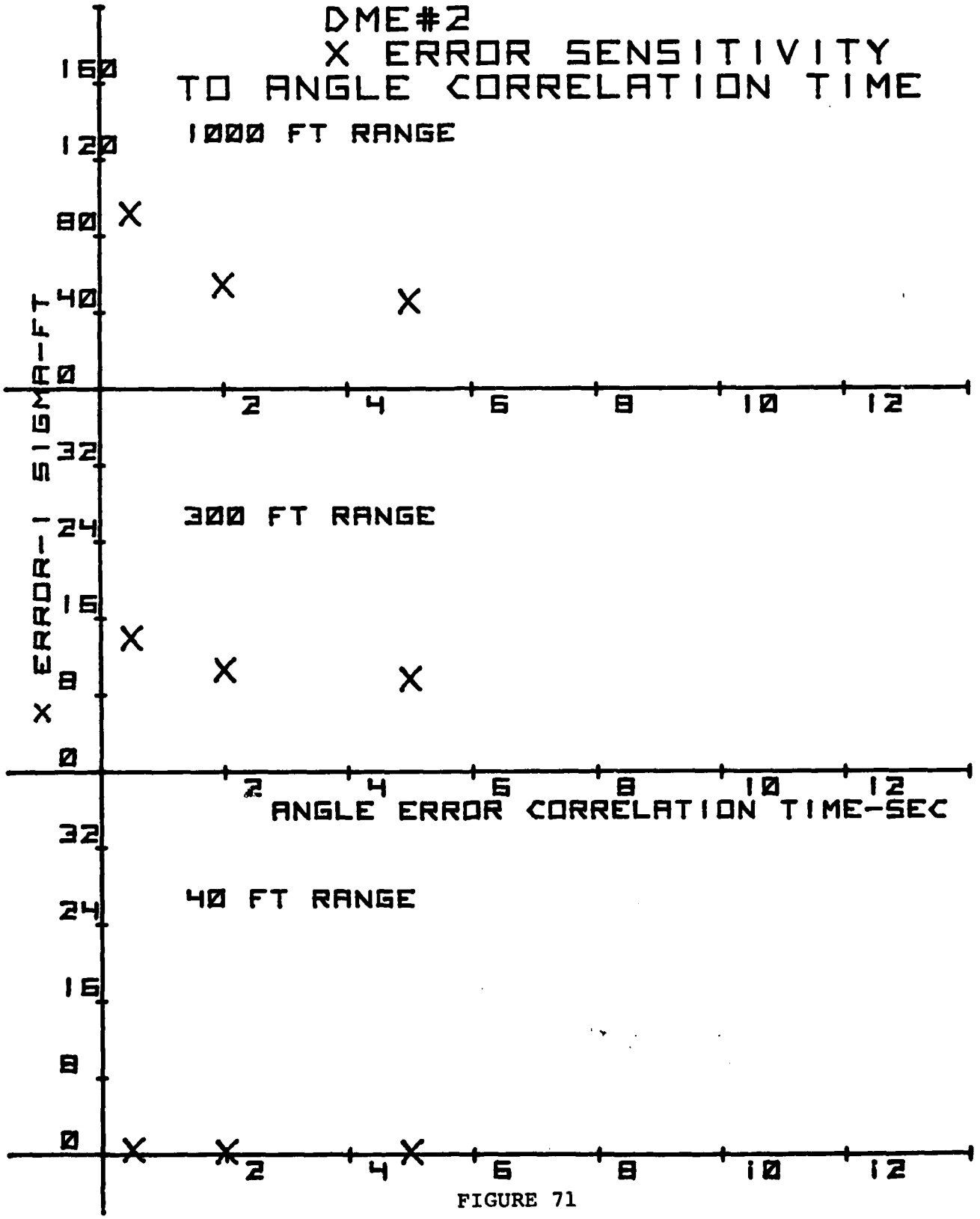
DME#2
X ERROR SENSITIVITY
TO ANGLE CORRELATION TIME
1000 FT RANGE
300 FT RANGE
40 FT RANGE
X ERROR-1 SIGMA-FT
ANGLE ERROR CORRELATION TIME-SEC
160
120
80
40
0
32
24
16
8
0
2
4
6
8
10
12

FIGURE 71

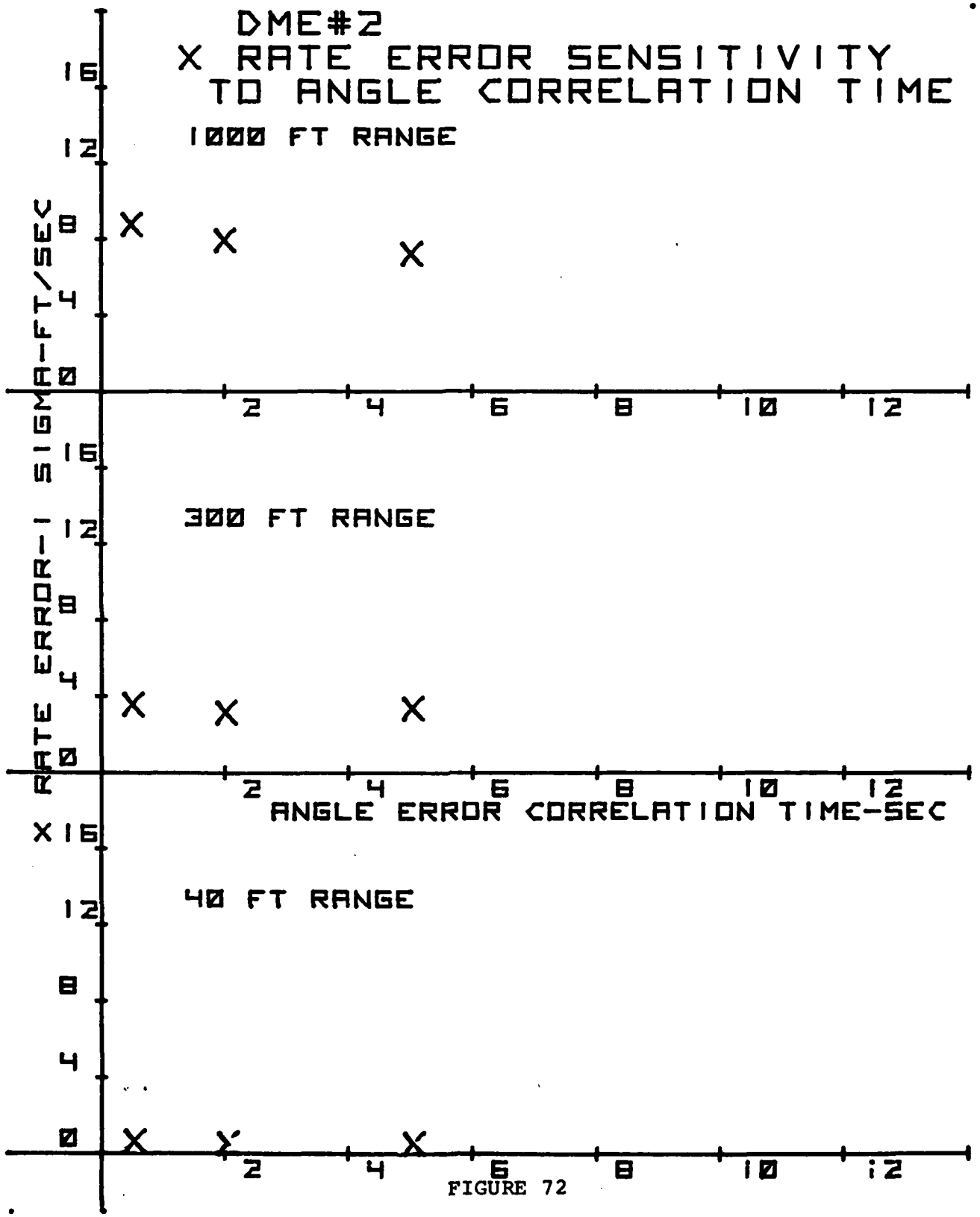
DME#2
X RATE ERROR SENSITIVITY
TO ANGLE CORRELATION TIME
1000 FT RANGE
300 FT RANGE
40 FT RANGE
X RATE ERROR-1 SIGMA-FT/SEC
ANGLE ERROR CORRELATION TIME-SEC
0
4
8
12
16
2
4
6
8
10
12

FIGURE 72

V. SIMULATION DATA - SENSITIVITIES TO SHIP MOTION SENSOR ERROR PARAMETERS

A. SENSITIVITY TO PITCH SENSOR BIAS ERROR

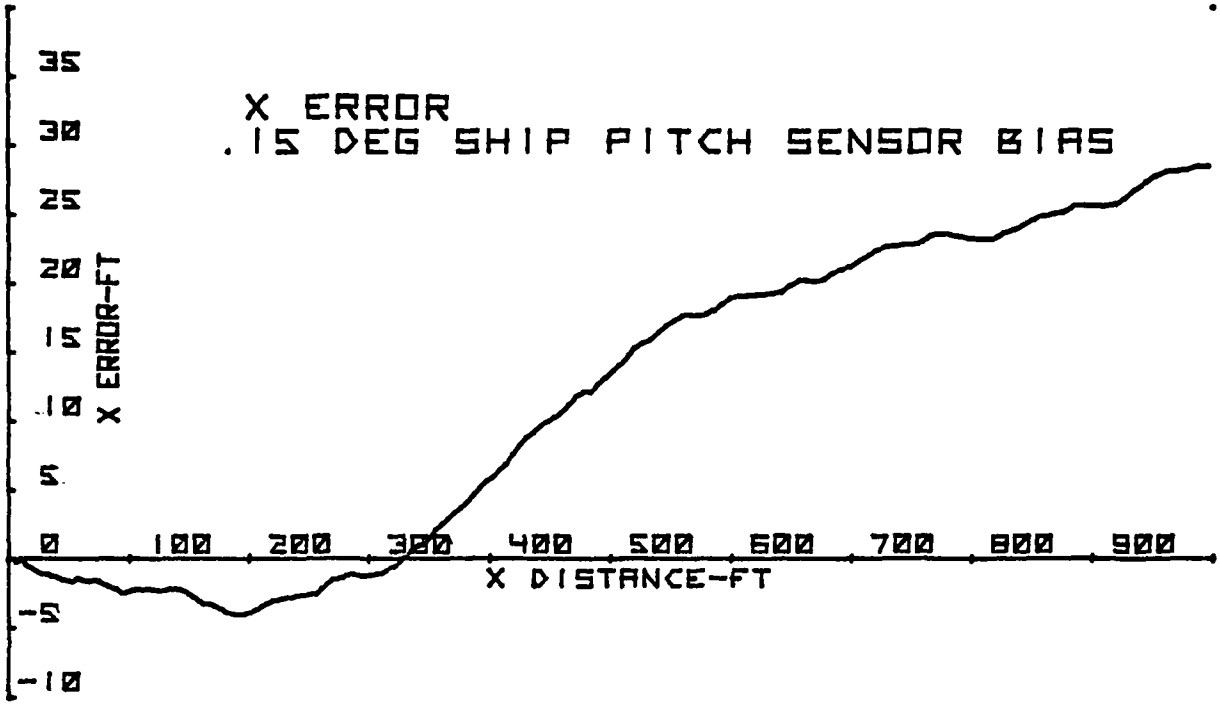
X ERROR
.15 DEG SHIP PITCH SENSOR BIAS
X ERROR-FT
35
30
25
20
15
10
5
0
100
200
300
400
500
600
700
800
900
X DISTANCE-FT
-5
-10

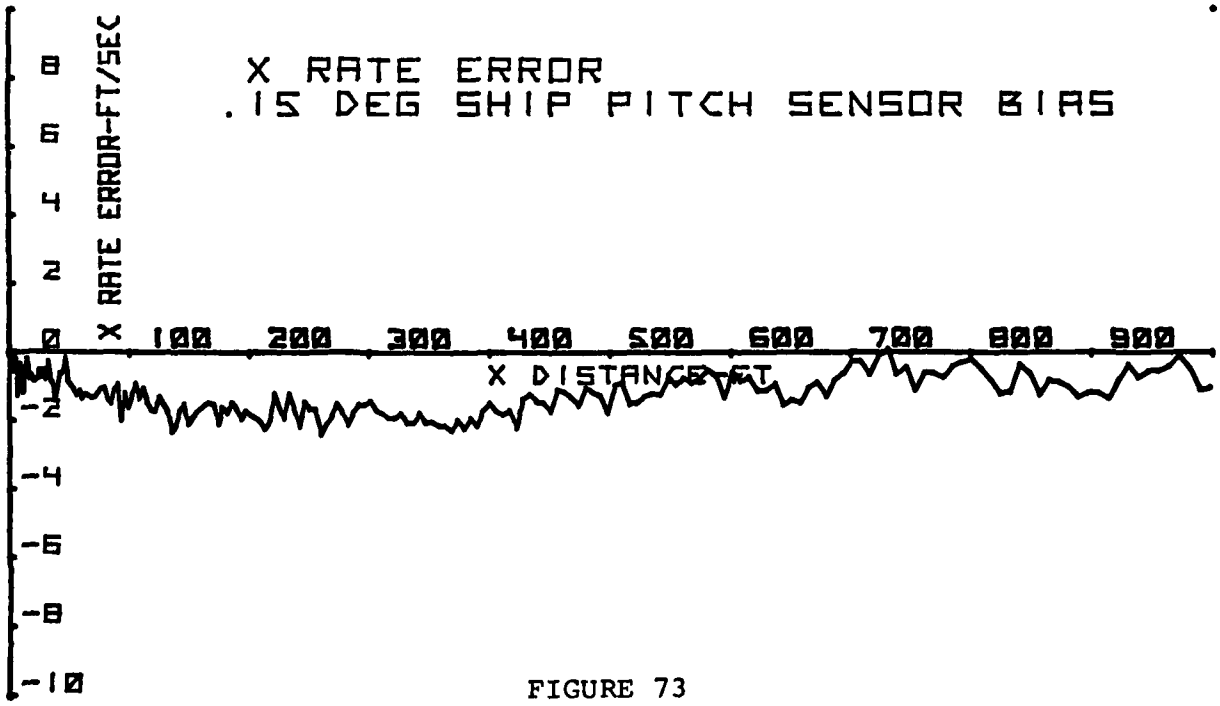
X RATE ERROR
.15 DEG SHIP PITCH SENSOR BIAS
X RATE ERROR-FT/SEC
8
6
4
2
0
100
200
300
400
500
600
700
800
900
X DISTANCE-FT
-2
-4
-6
-8
-10

FIGURE 73

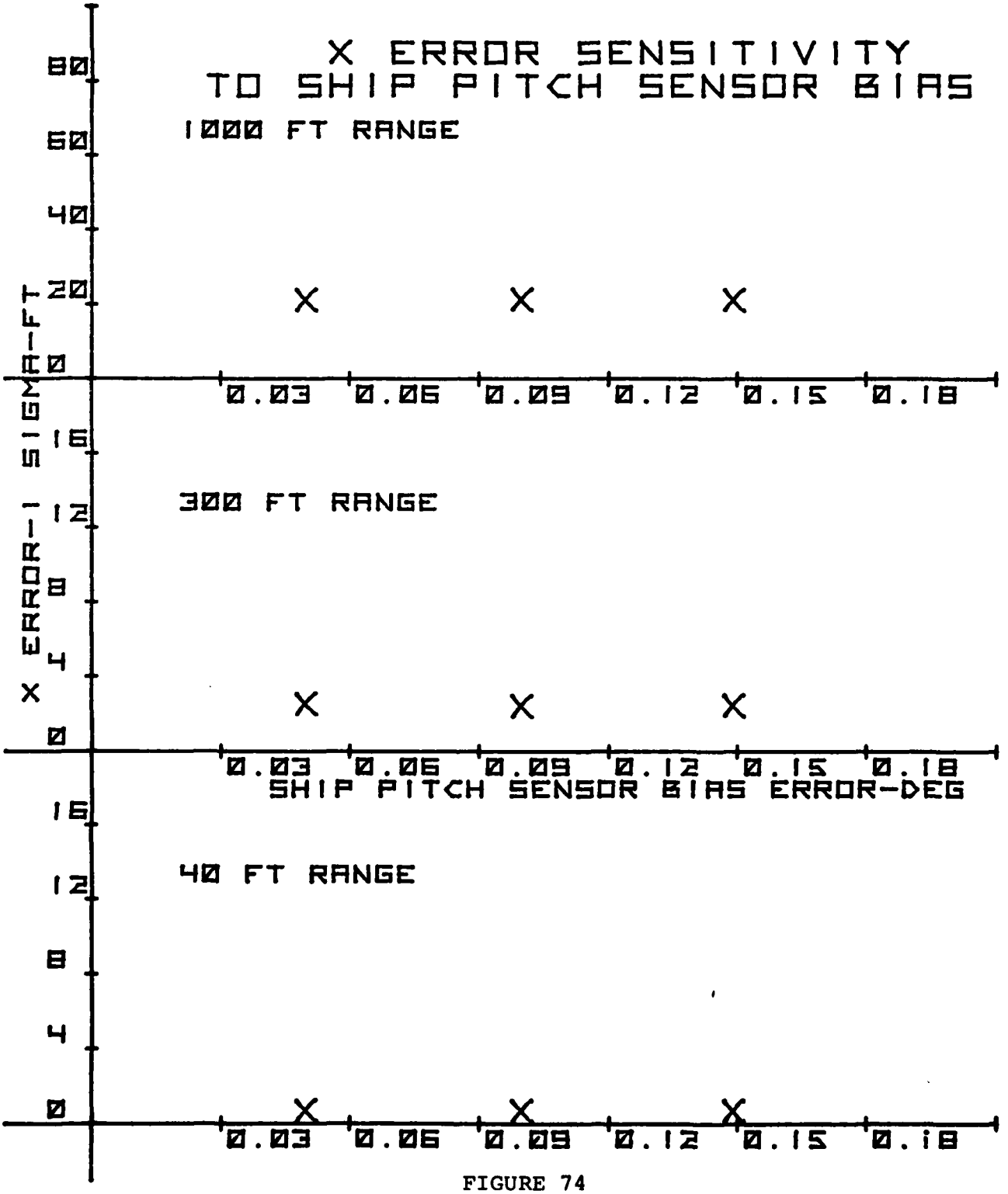
X ERROR SENSITIVITY
TO SHIP PITCH SENSOR BIAS
1000 FT RANGE
300 FT RANGE
40 FT RANGE
X ERROR-1 SIGMA-FT
80
60
40
20
0
16
12
8
4
0
16
12
8
4
0
0.03
0.06
0.09
0.12
0.15
0.18
SHIP PITCH SENSOR BIAS ERROR-DEG

FIGURE 74

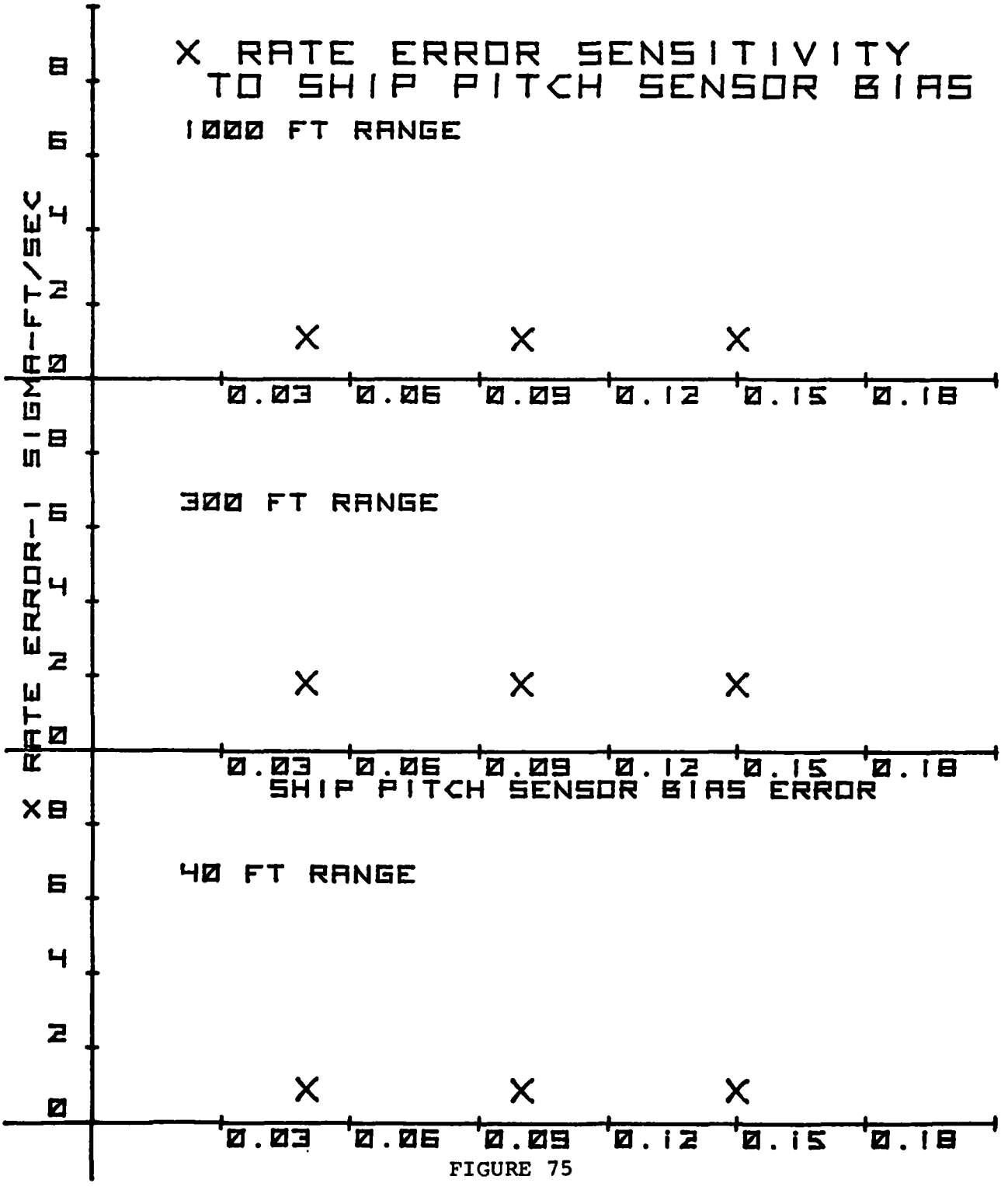
X RATE ERROR SENSITIVITY
TO SHIP PITCH SENSOR BIAS
1000 FT RANGE
300 FT RANGE
40 FT RANGE
X RATE ERROR-1 SIGMA-FT/SEC
0
2
4
6
8
0.03
0.06
0.09
0.12
0.15
0.18
SHIP PITCH SENSOR BIAS ERROR

FIGURE 75

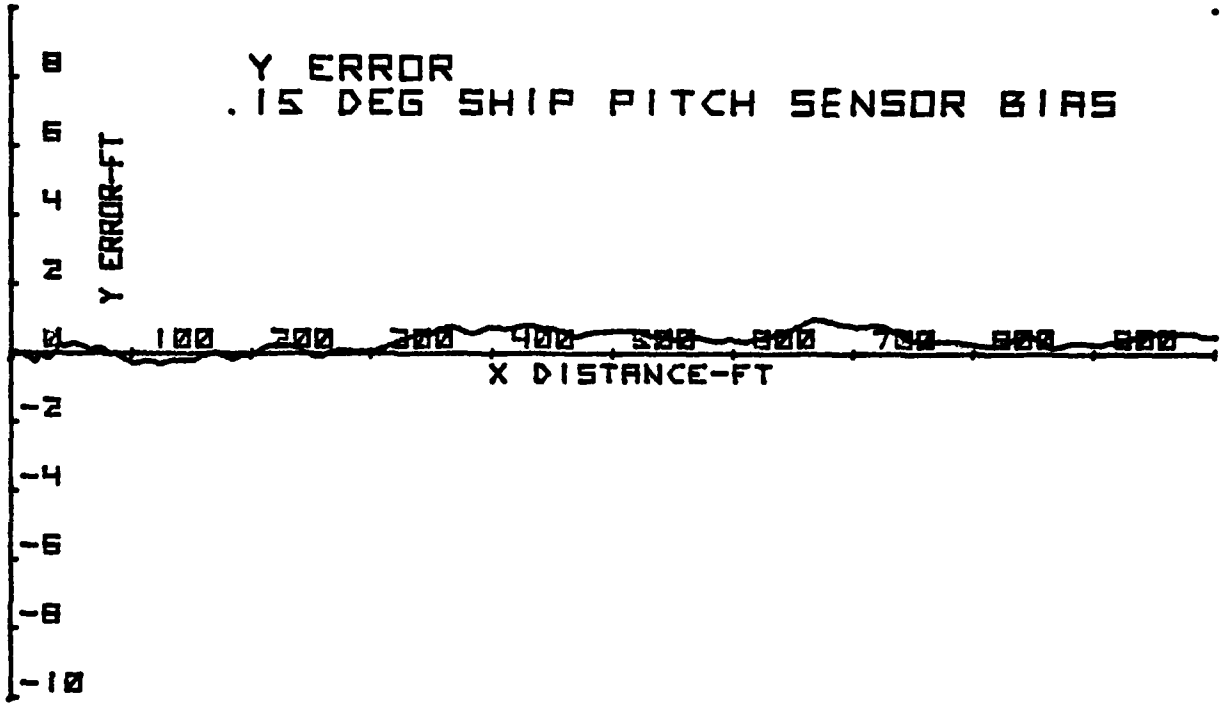
Y ERROR
.15 DEG SHIP PITCH SENSOR BIAS
Y ERROR-FT
8
6
4
2
0
-2
-4
-6
-8
-10
100
200
300
400
500
600
700
800
900
X DISTANCE-FT

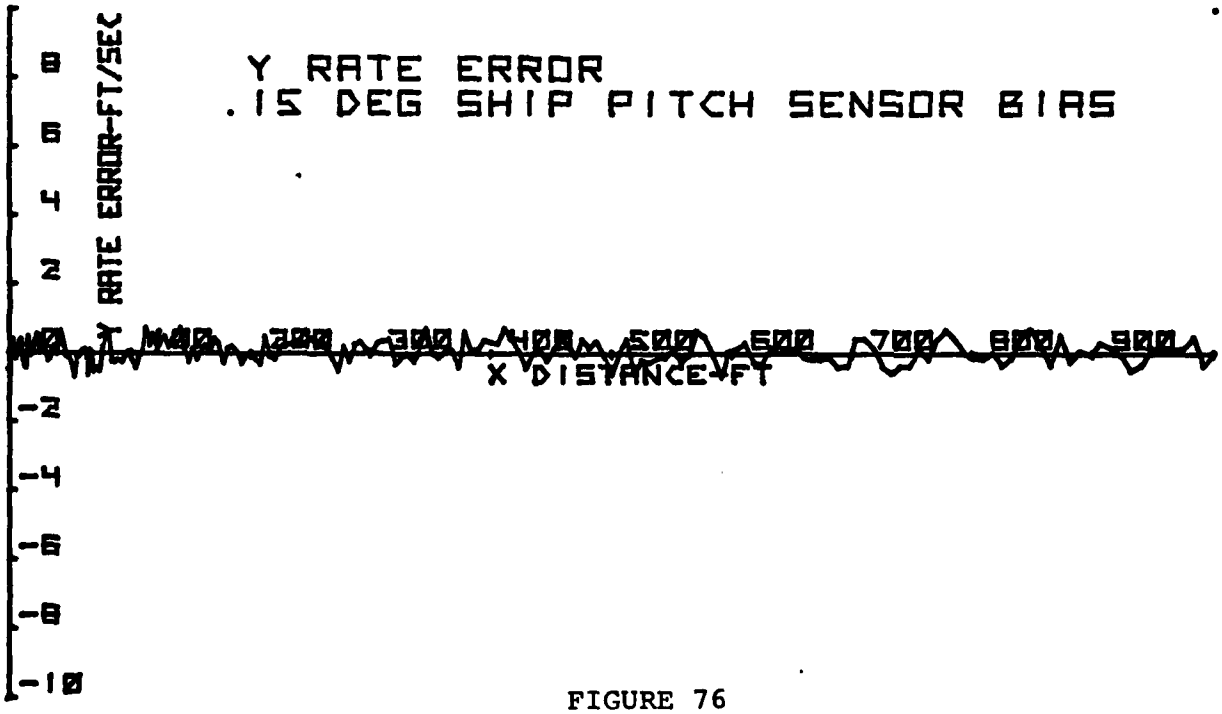
Y RATE ERROR
.15 DEG SHIP PITCH SENSOR BIAS
Y RATE ERROR-FT/SEC
8
6
4
2
0
-2
-4
-6
-8
-10
100
200
300
400
500
600
700
800
900
X DISTANCE-FT

FIGURE 76

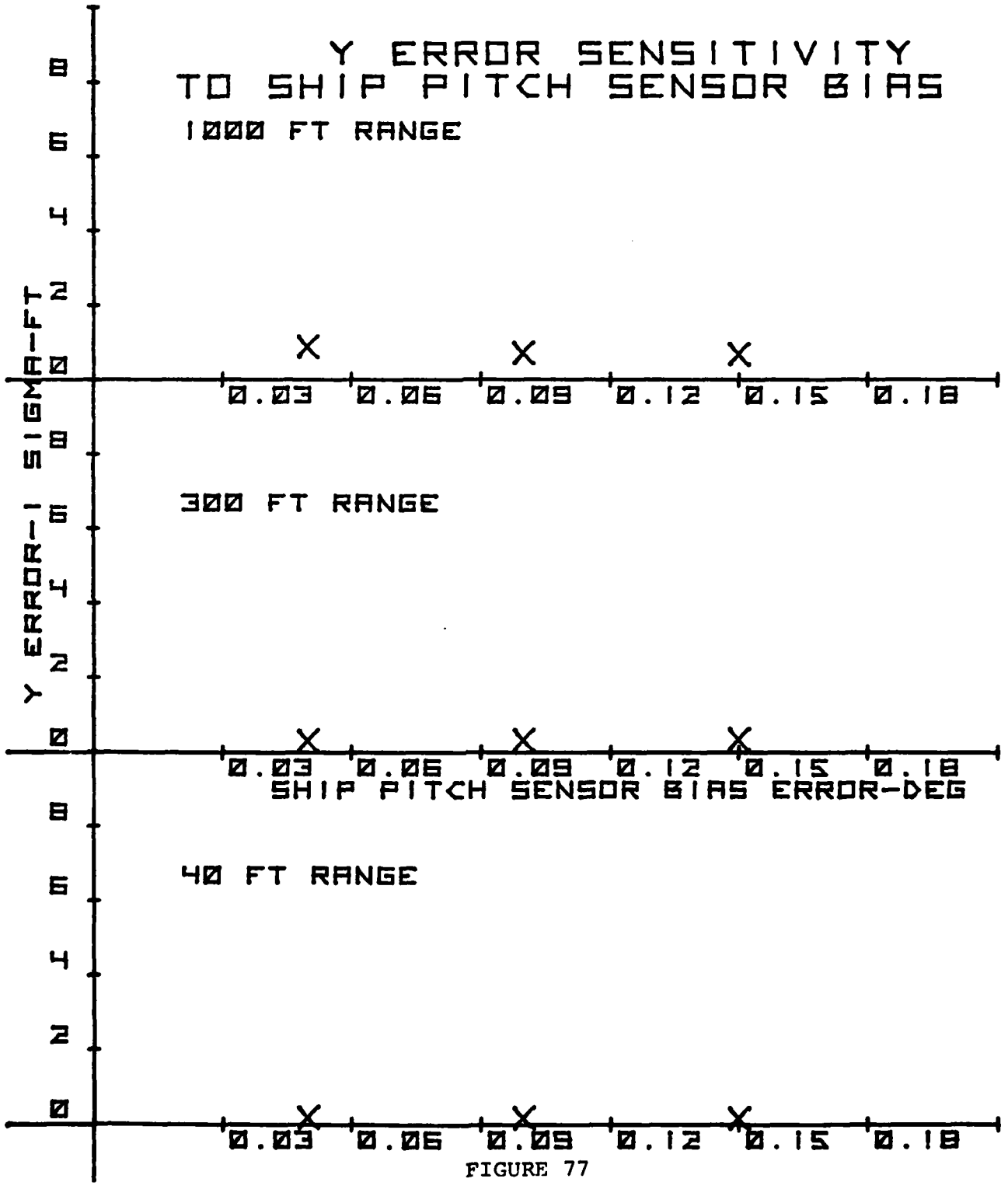
Y ERROR SENSITIVITY
TO SHIP PITCH SENSOR BIAS
1000 FT RANGE
300 FT RANGE
40 FT RANGE
Y ERROR-1 SIGMA-FT
0
2
4
6
8
0.03
0.06
0.09
0.12
0.15
0.18
SHIP PITCH SENSOR BIAS ERROR-DEG

FIGURE 77

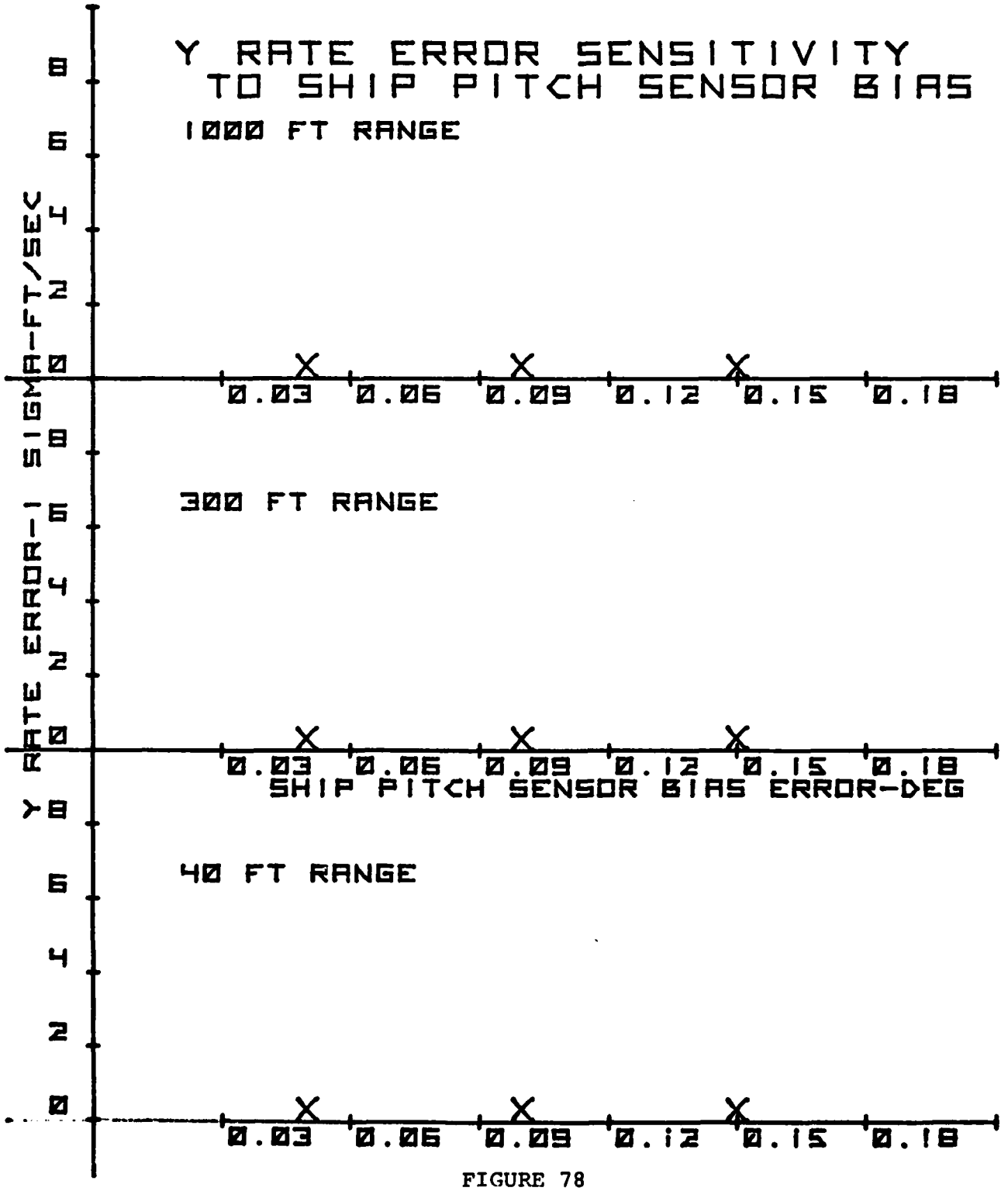
Y RATE ERROR SENSITIVITY
TO SHIP PITCH SENSOR BIAS
1000 FT RANGE
300 FT RANGE
40 FT RANGE
Y RATE ERROR-1 SIGMA-FT/SEC
0
2
4
6
8
0.03
0.06
0.09
0.12
0.15
0.18
SHIP PITCH SENSOR BIAS ERROR-DEG

FIGURE 78

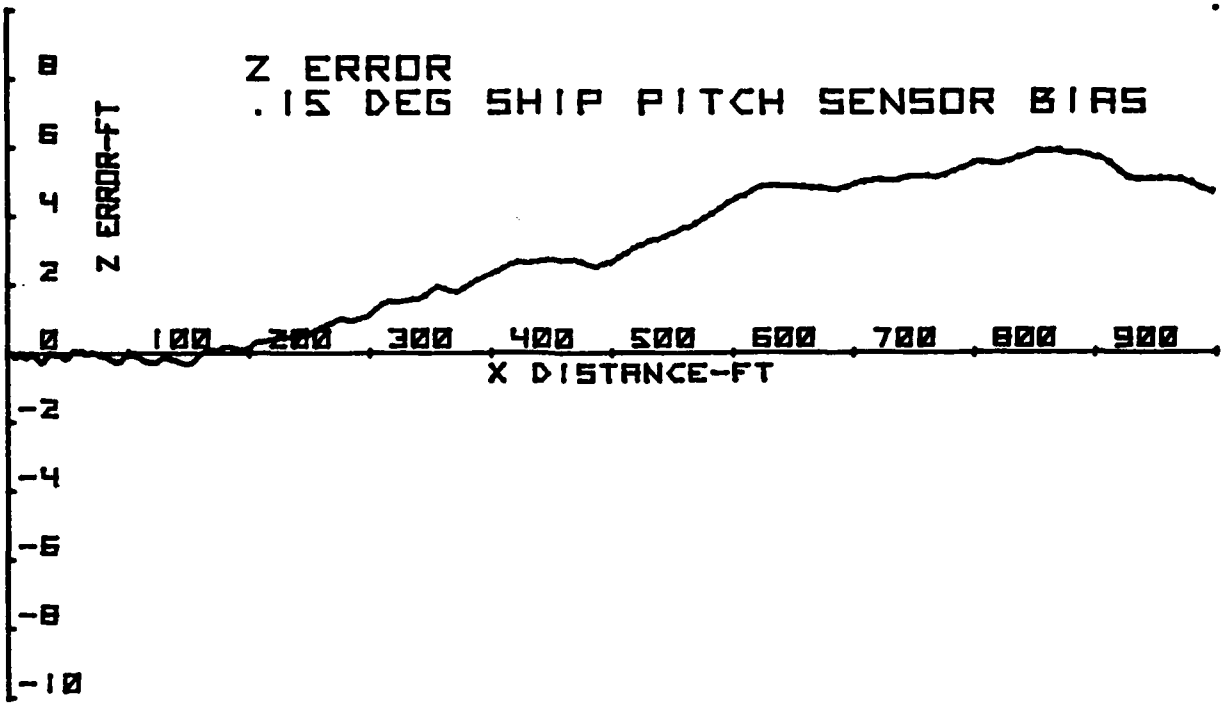

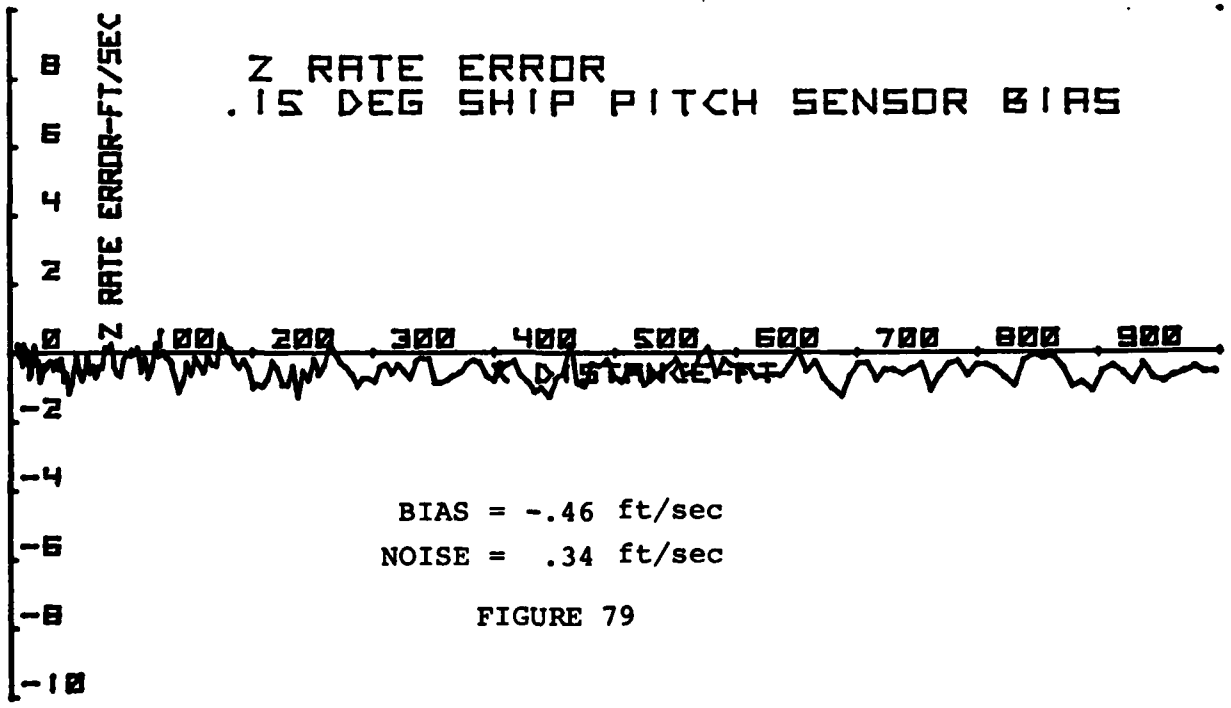

BIAS = -.46 ft/sec

NOISE = .34 ft/sec

FIGURE 79

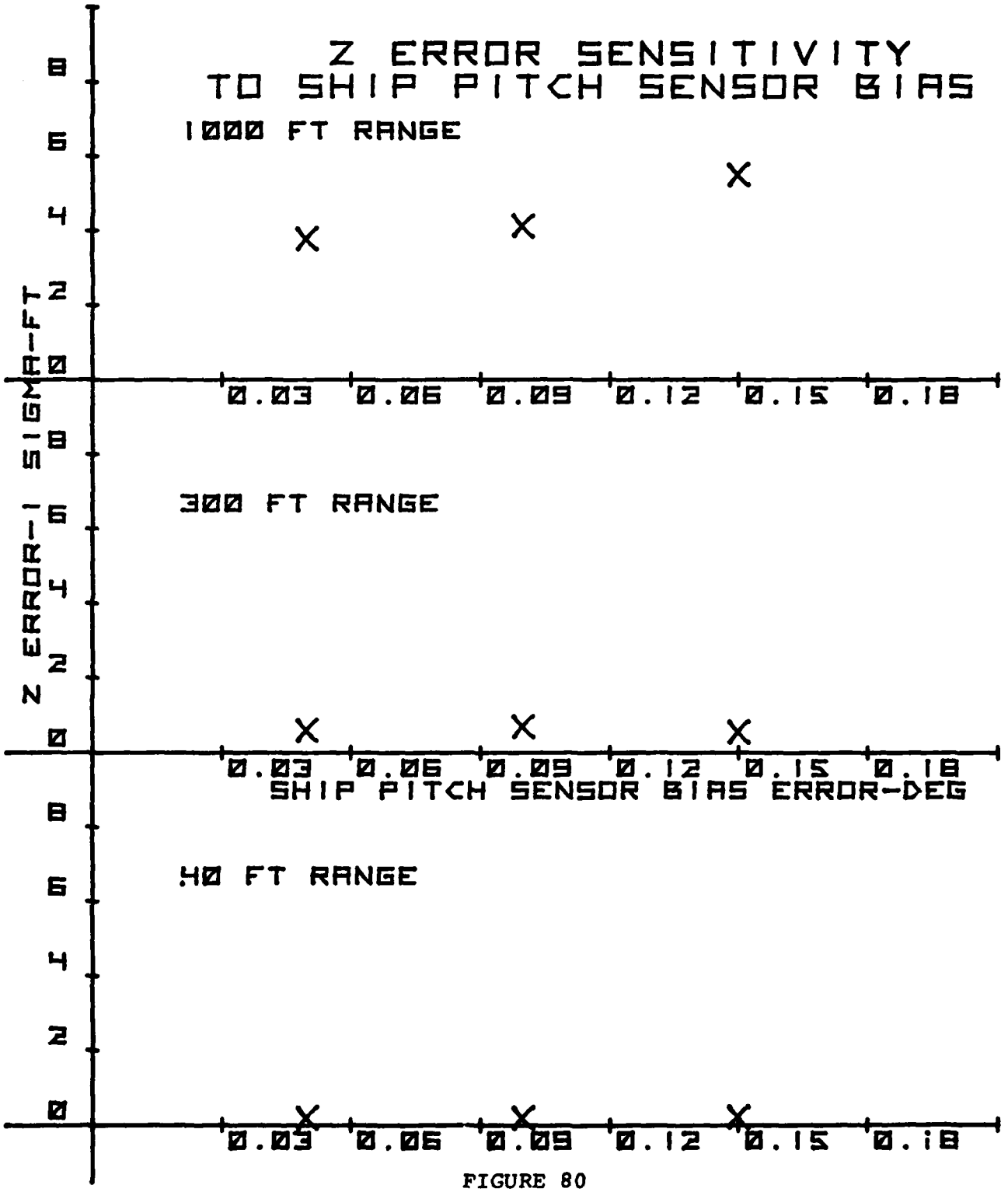
Z ERROR SENSITIVITY
TO SHIP PITCH SENSOR BIAS
1000 FT RANGE
300 FT RANGE
40 FT RANGE
Z ERROR-1 SIGMA-FT
0
2
4
6
8
0.03
0.06
0.09
0.12
0.15
0.18
SHIP PITCH SENSOR BIAS ERROR-DEG

FIGURE 80

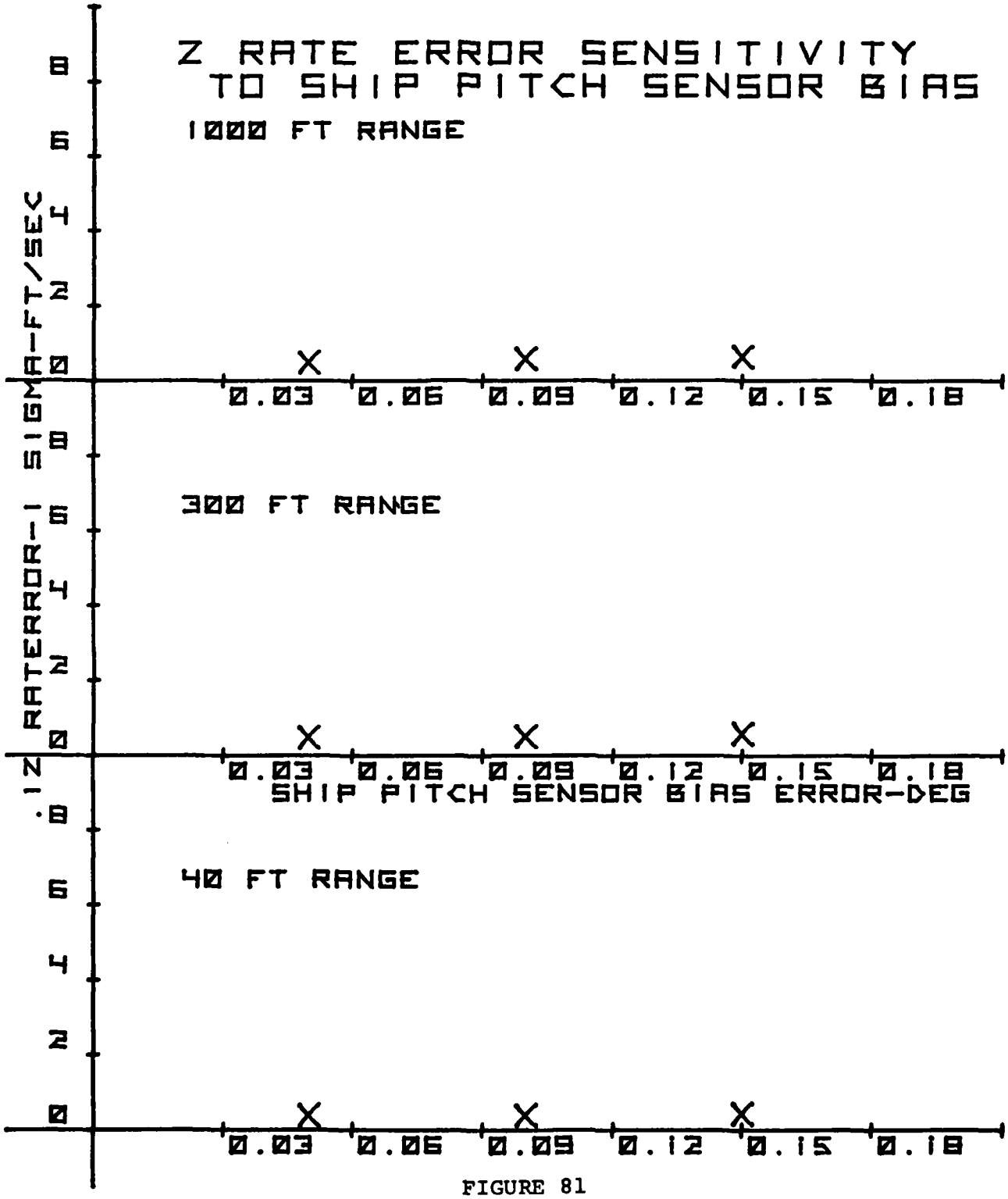
Z RATE ERROR SENSITIVITY
TO SHIP PITCH SENSOR BIAS
1000 FT RANGE
300 FT RANGE
40 FT RANGE
RATERROR-1 SIGMA-FT/SEC
.12
.8
.6
.4
.2
0
0.03
0.06
0.09
0.12
0.15
0.18
SHIP PITCH SENSOR BIAS ERROR-DEG

FIGURE 81

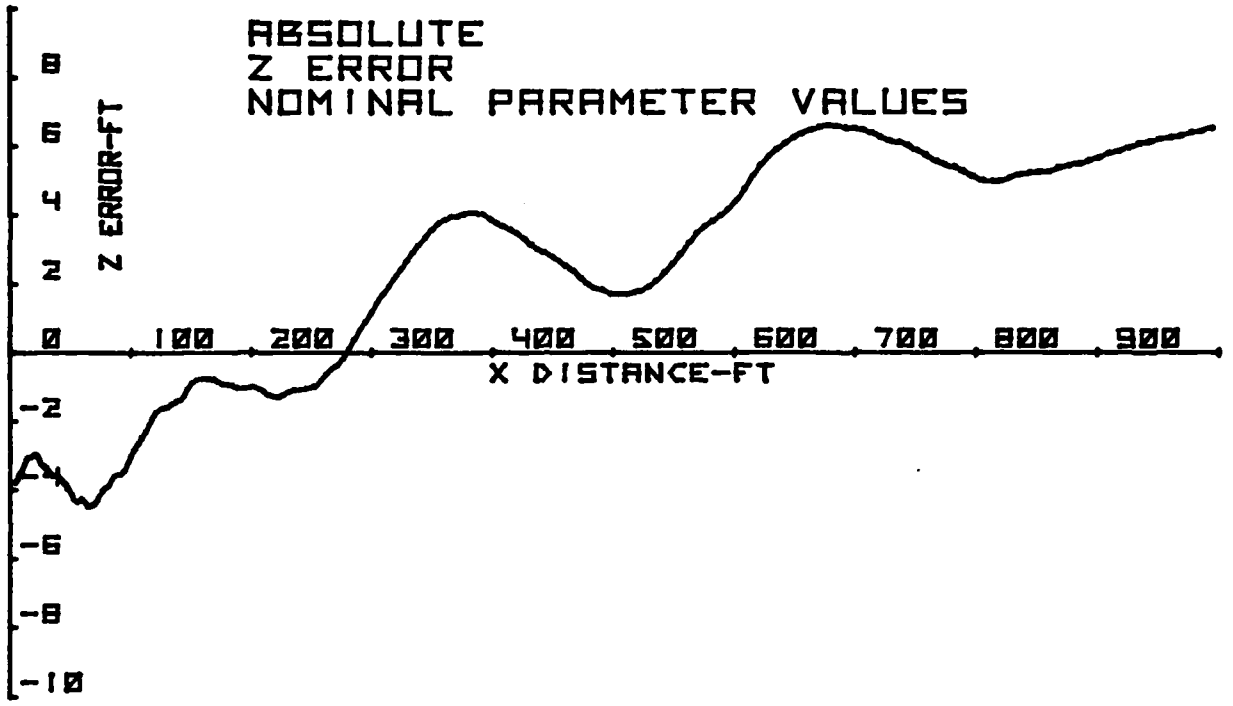
ABSOLUTE
Z ERROR
NOMINAL PARAMETER VALUES
Z ERROR-FT
8
6
4
2
0
-2
-6
-8
-10
100
200
300
400
500
600
700
800
900
X DISTANCE-FT

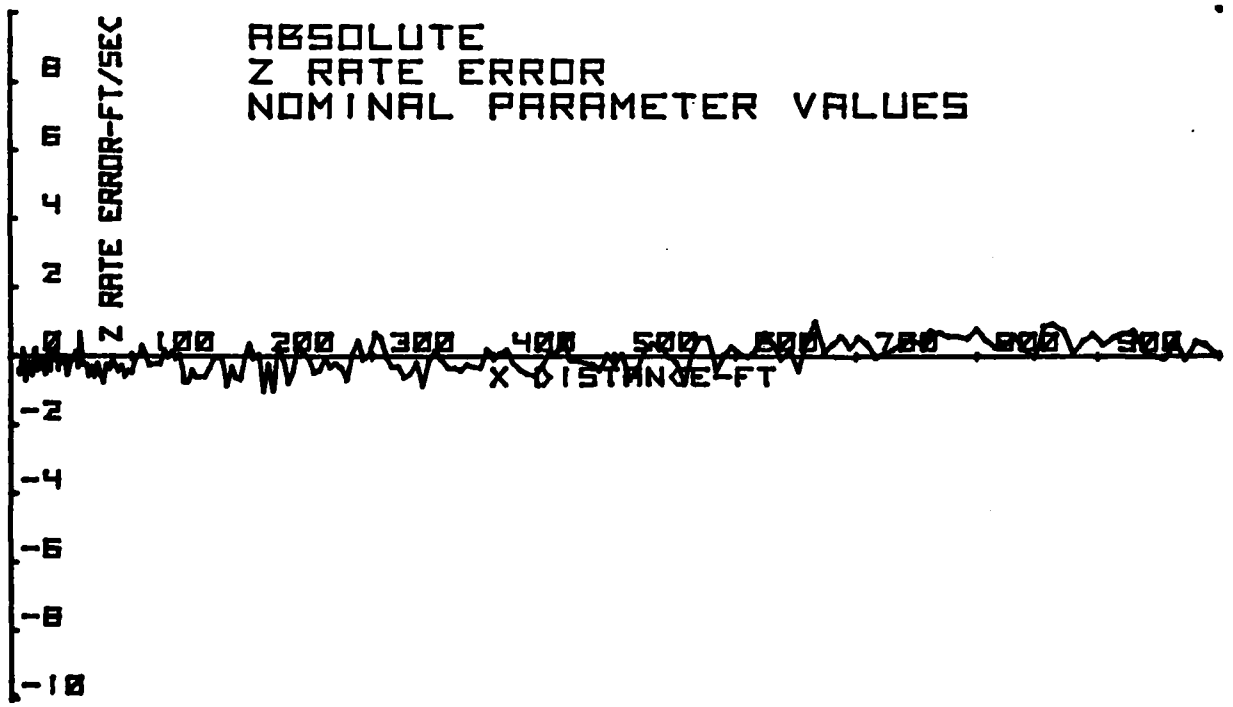
ABSOLUTE
Z RATE ERROR
NOMINAL PARAMETER VALUES
Z RATE ERROR-FT/SEC
8
6
4
2
0
-2
-4
-6
-8
-10
100
200
300
400
500
X DISTANCE-FT

FIGURE 82

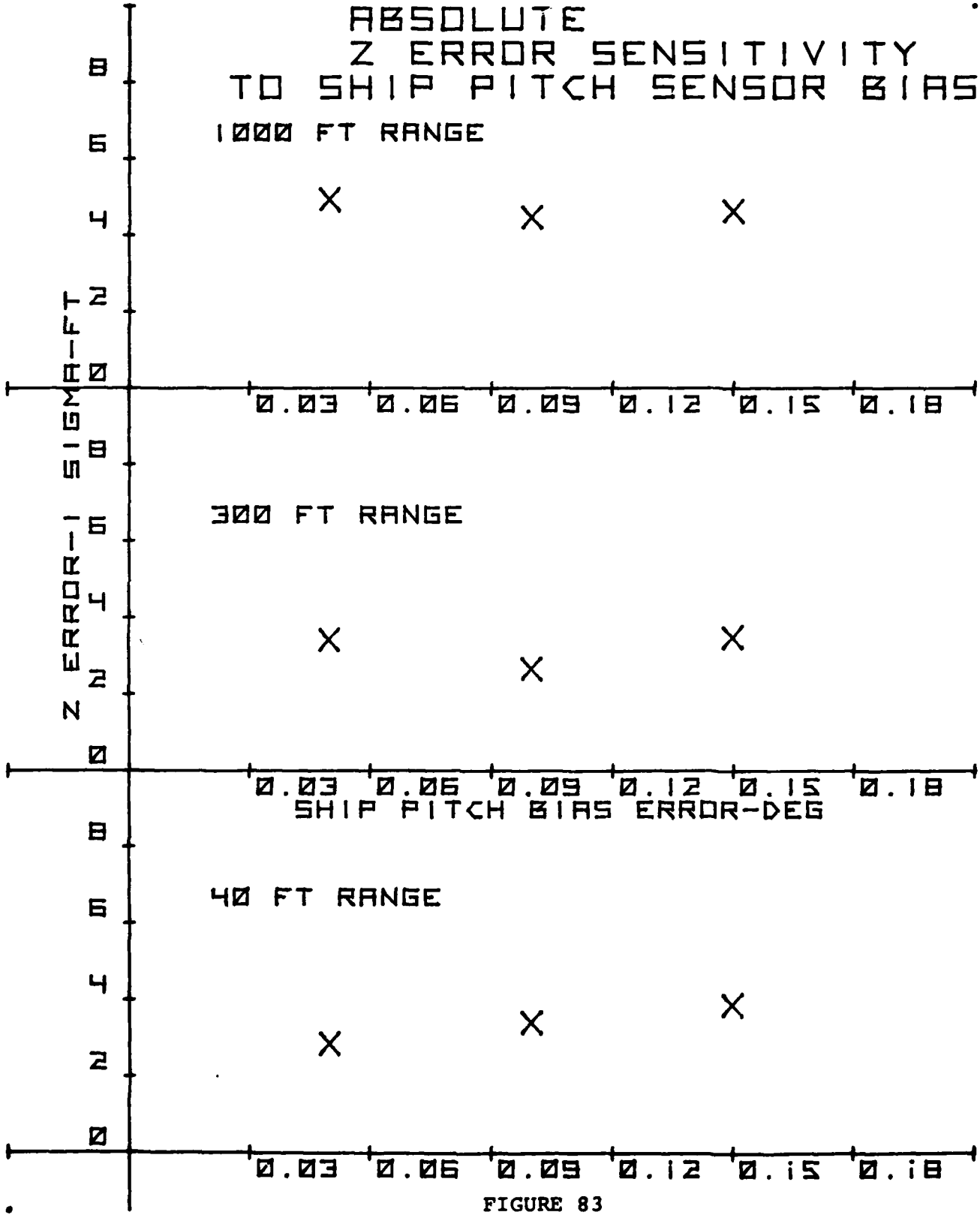
ABSOLUTE
Z ERROR SENSITIVITY
TO SHIP PITCH SENSOR BIAS
1000 FT RANGE
300 FT RANGE
40 FT RANGE
Z ERROR-1 SIGMA-FT
0
2
4
6
8
0.03
0.06
0.09
0.12
0.15
0.18
SHIP PITCH BIAS ERROR-DEG

FIGURE 83

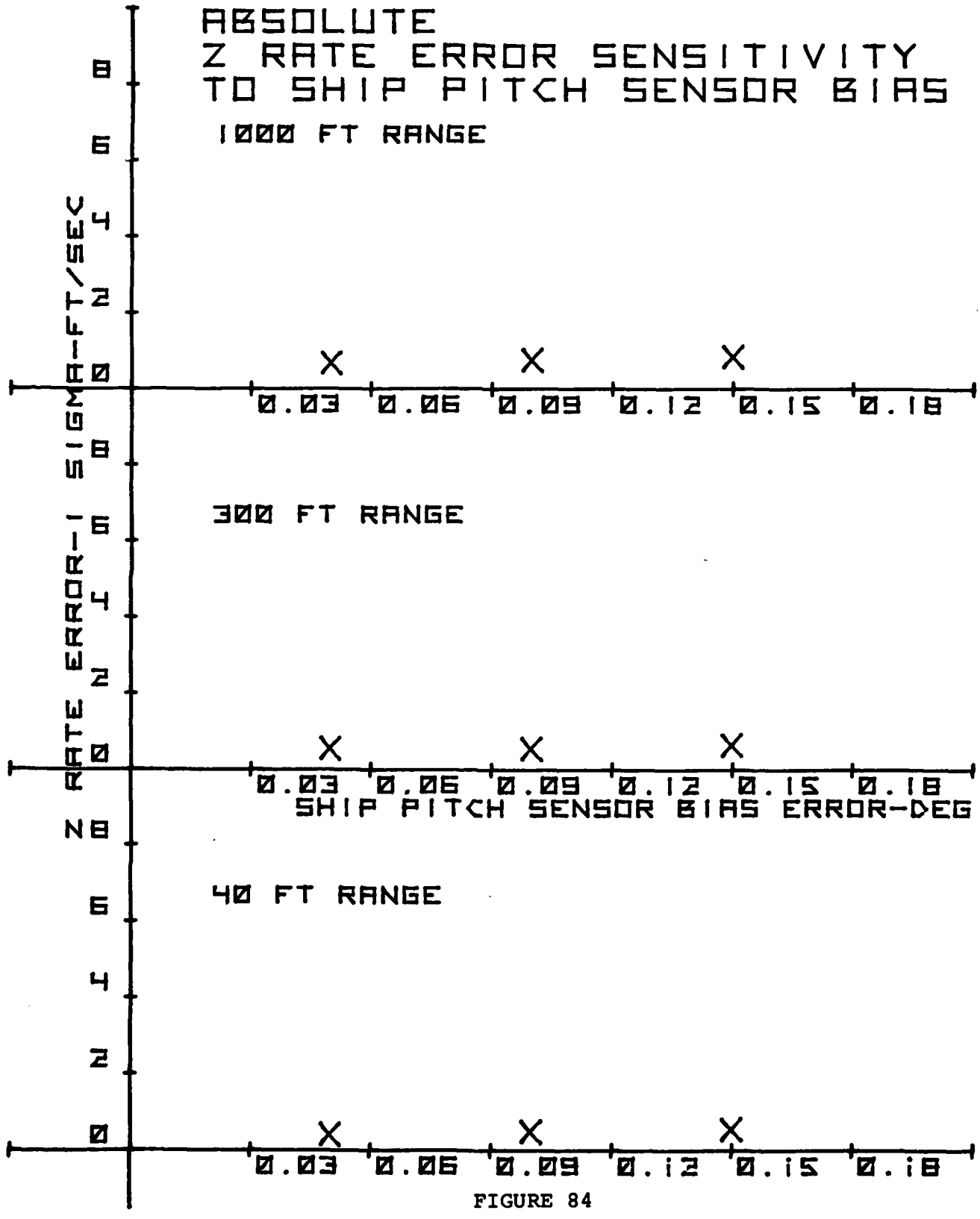
ABSOLUTE
Z RATE ERROR SENSITIVITY
TO SHIP PITCH SENSOR BIAS
1000 FT RANGE
300 FT RANGE
40 FT RANGE
Z RATE ERROR-1 SIGMA-FT/SEC
8
6
4
2
0
0.03
0.06
0.09
0.12
0.15
0.18
SHIP PITCH SENSOR BIAS ERROR-DEG

FIGURE 84

B. SENSITIVITY TO ROLL SENSOR BIAS ERROR

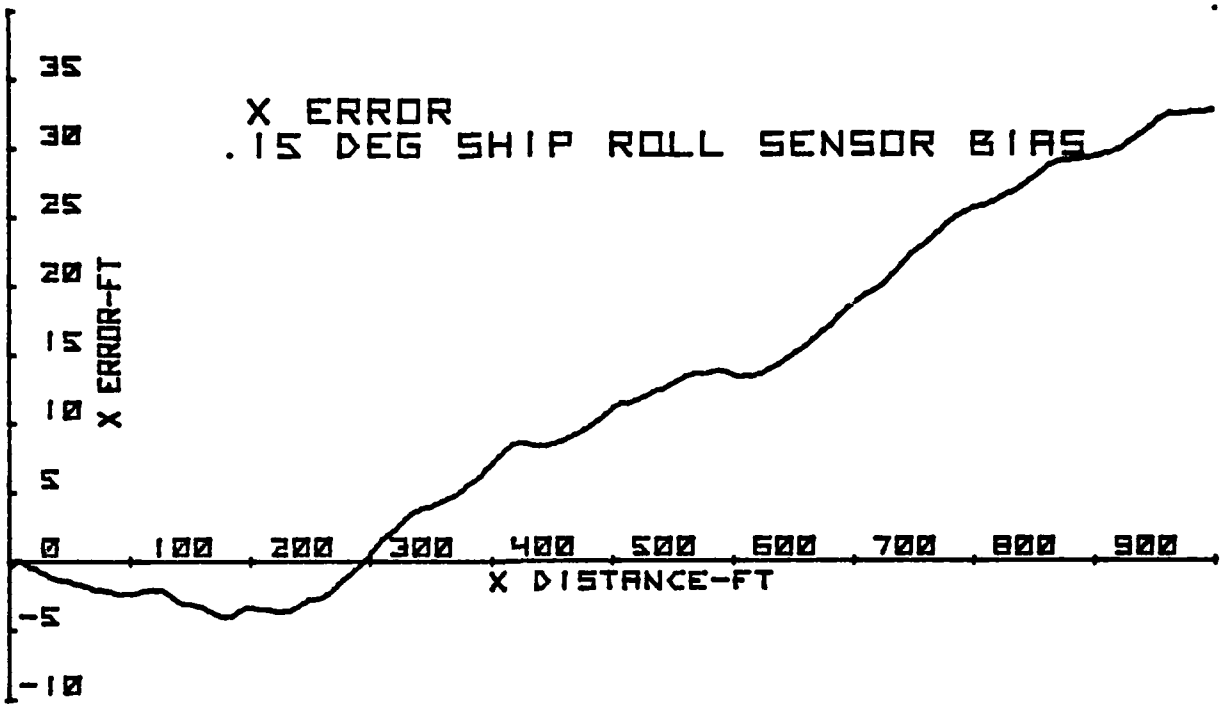
X ERROR
.15 DEG SHIP ROLL SENSOR BIAS
X ERROR-FT
35
30
25
20
15
10
5
0
-5
-10
100
200
300
400
500
600
700
800
900
X DISTANCE-FT

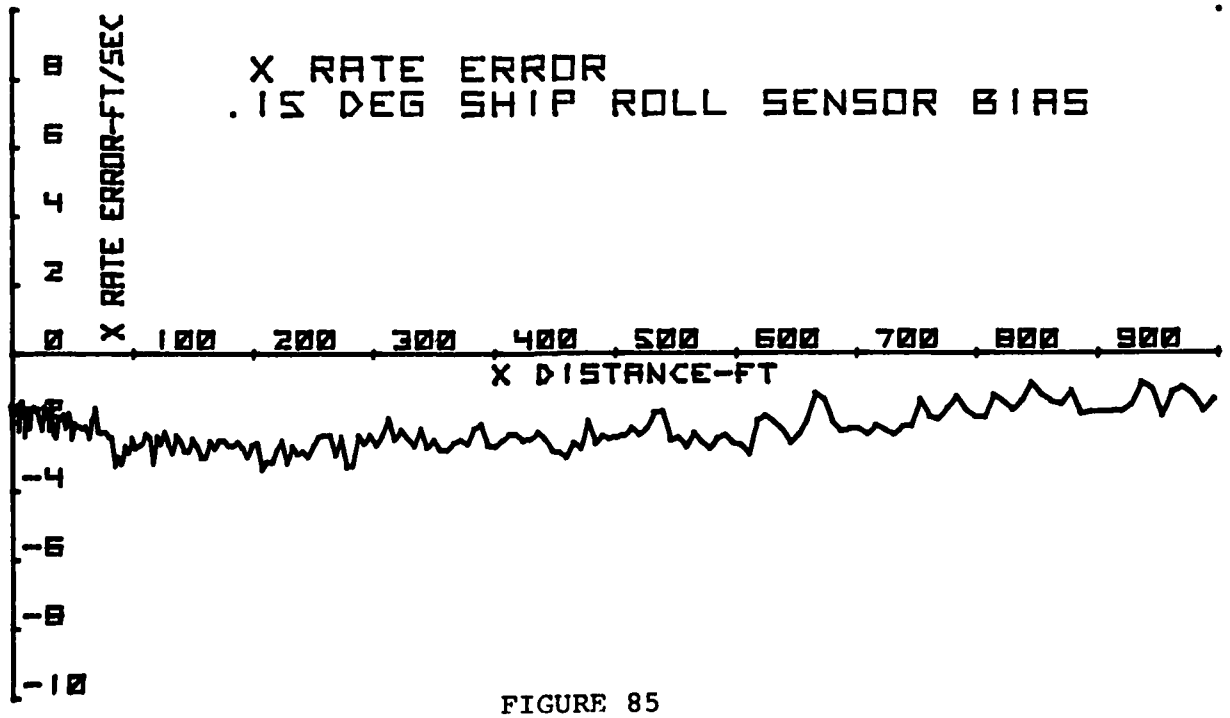
X RATE ERROR
.15 DEG SHIP ROLL SENSOR BIAS
X RATE ERROR-FT/SEC
8
6
4
2
0
-4
-6
-8
-10
100
200
300
400
500
600
700
800
900
X DISTANCE-FT

FIGURE 85

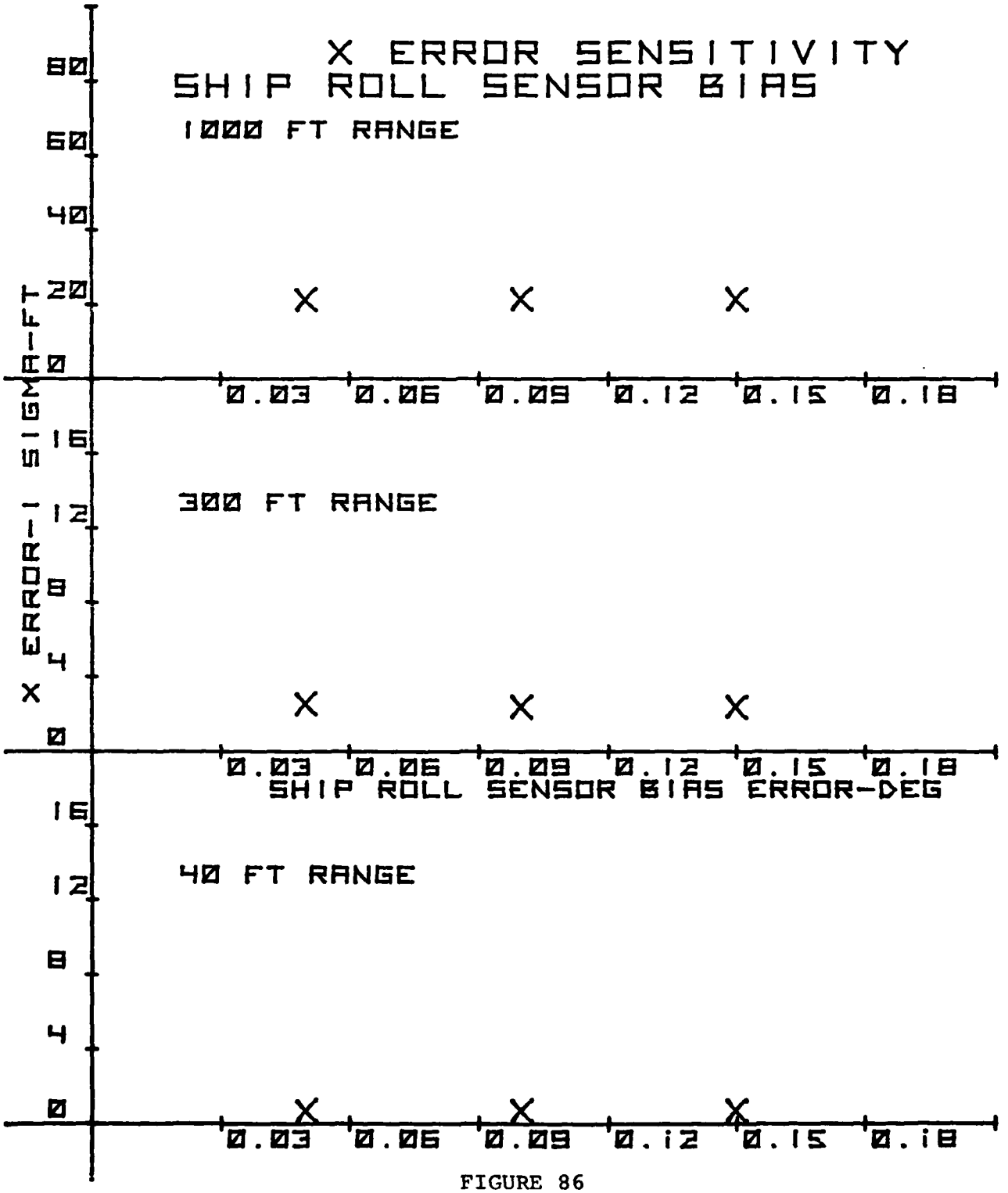
X ERROR SENSITIVITY
SHIP ROLL SENSOR BIAS
1000 FT RANGE
300 FT RANGE
40 FT RANGE
X ERROR-1 SIGMA-FT
SHIP ROLL SENSOR BIAS ERROR-DEG
0
4
8
12
16
20
40
60
80
0.03
0.06
0.09
0.12
0.15
0.18

FIGURE 86

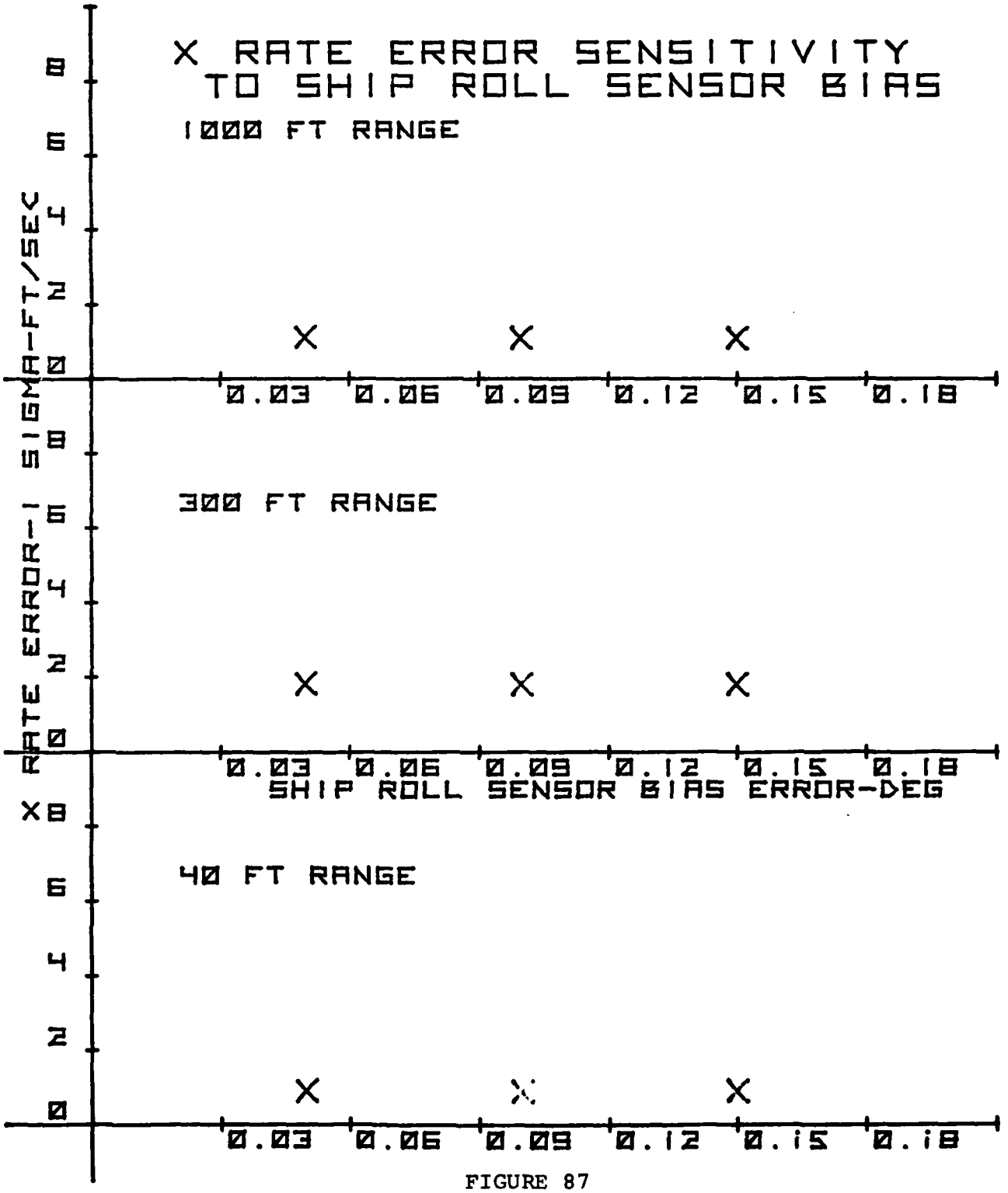
X RATE ERROR SENSITIVITY
TO SHIP ROLL SENSOR BIAS
1000 FT RANGE
300 FT RANGE
40 FT RANGE
X RATE ERROR-1 SIGMA-FT/SEC
0
2
4
6
8
0.03
0.06
0.09
0.12
0.15
0.18
SHIP ROLL SENSOR BIAS ERROR-DEG

FIGURE 87

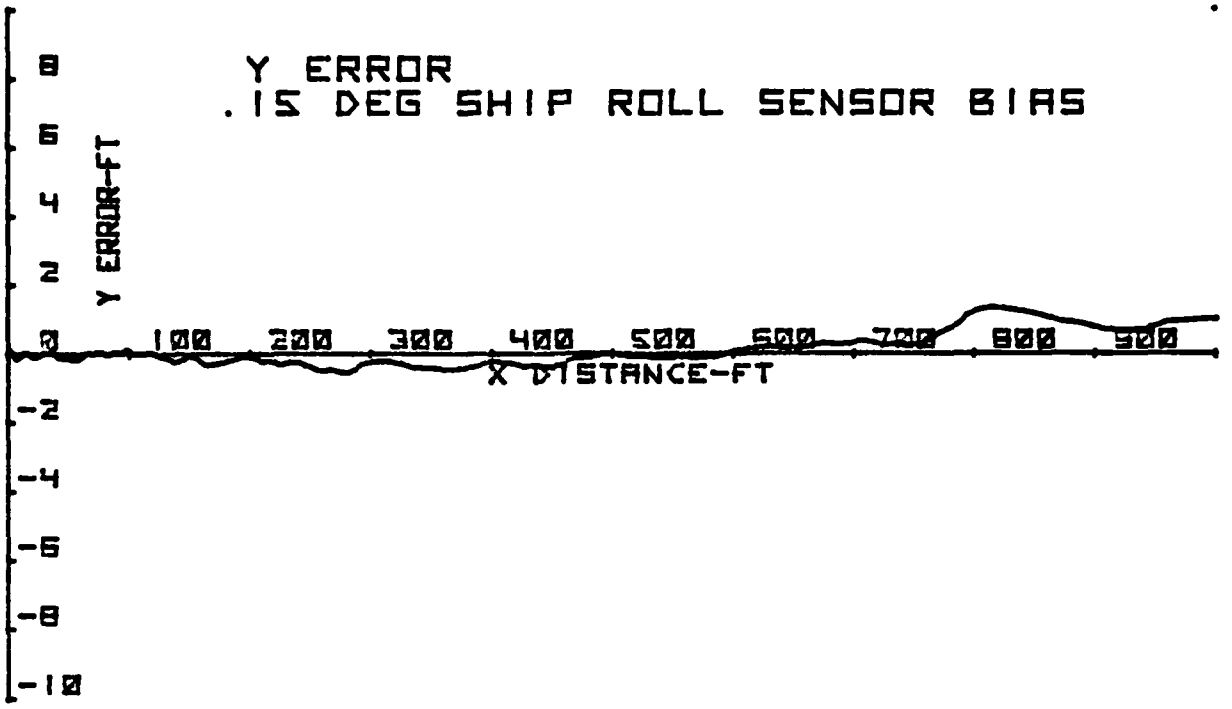
Y ERROR
.15 DEG SHIP ROLL SENSOR BIAS
Y ERROR-FT
8
6
4
2
0
-2
-4
-6
-8
-10
100
200
300
400
500
600
700
800
900
X DISTANCE-FT

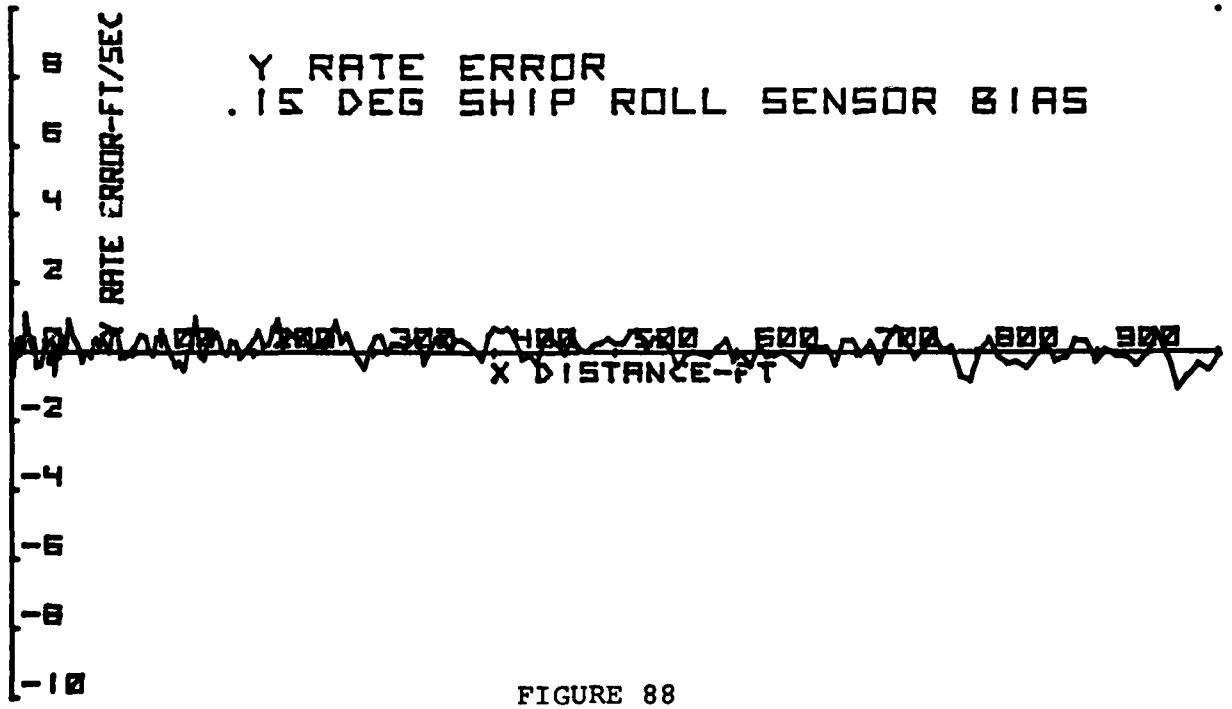
Y RATE ERROR
.15 DEG SHIP ROLL SENSOR BIAS
Y RATE ERROR-FT/SEC
8
6
4
2
0
-2
-4
-6
-8
-10
X DISTANCE-FT

FIGURE 88

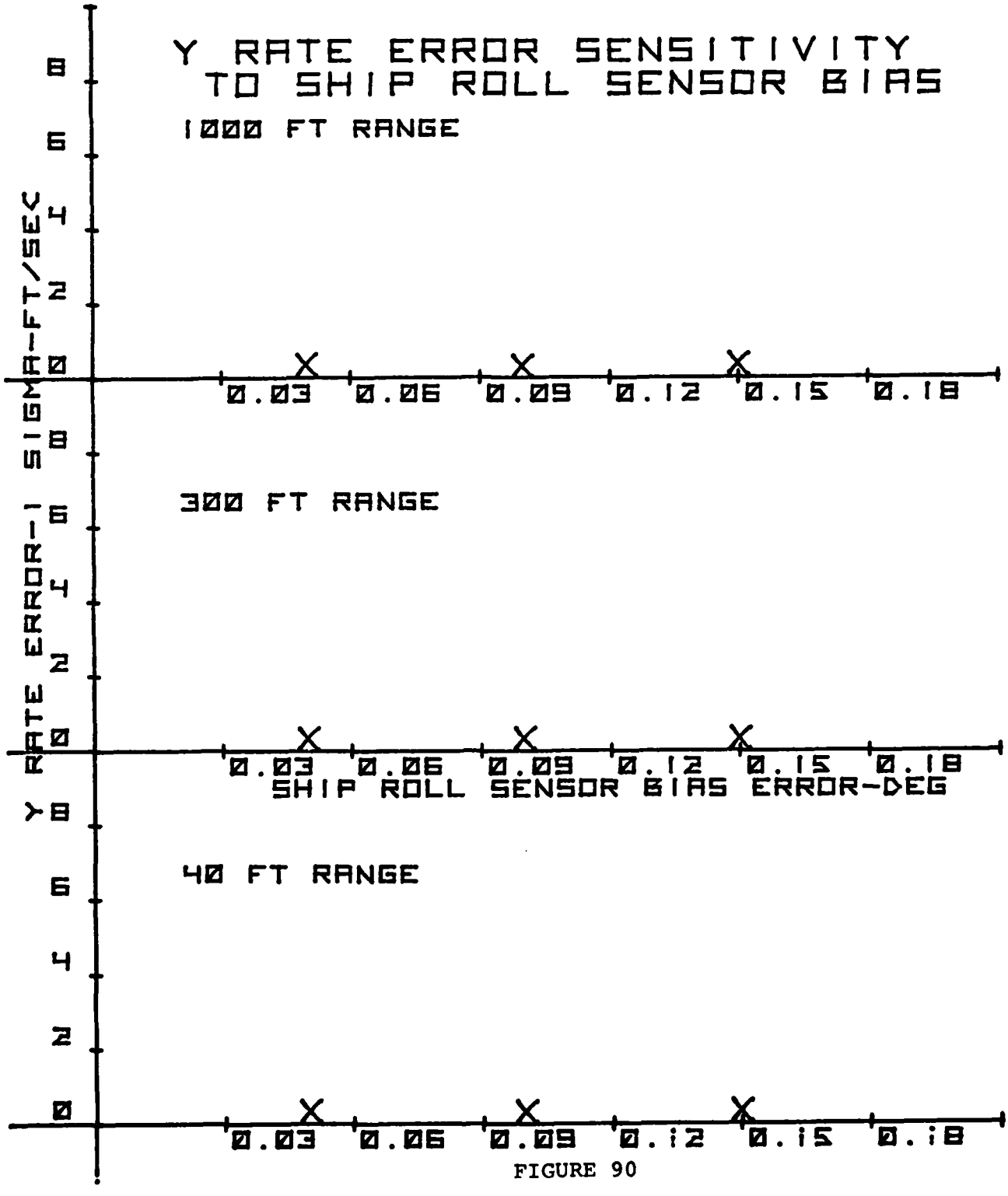
Y RATE ERROR SENSITIVITY
TO SHIP ROLL SENSOR BIAS
1000 FT RANGE
300 FT RANGE
40 FT RANGE
Y RATE ERROR-1 SIGMA-FT/SEC
0
2
4
6
8
0.03
0.06
0.09
0.12
0.15
0.18
SHIP ROLL SENSOR BIAS ERROR-DEG

FIGURE 90

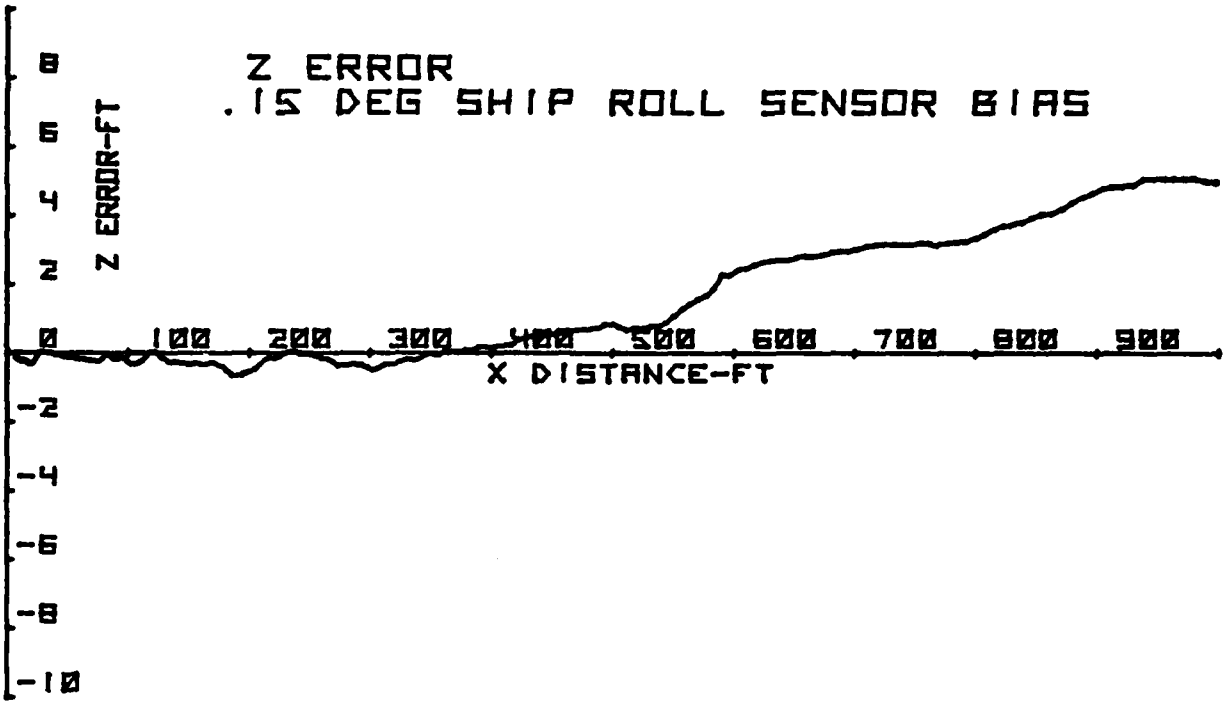

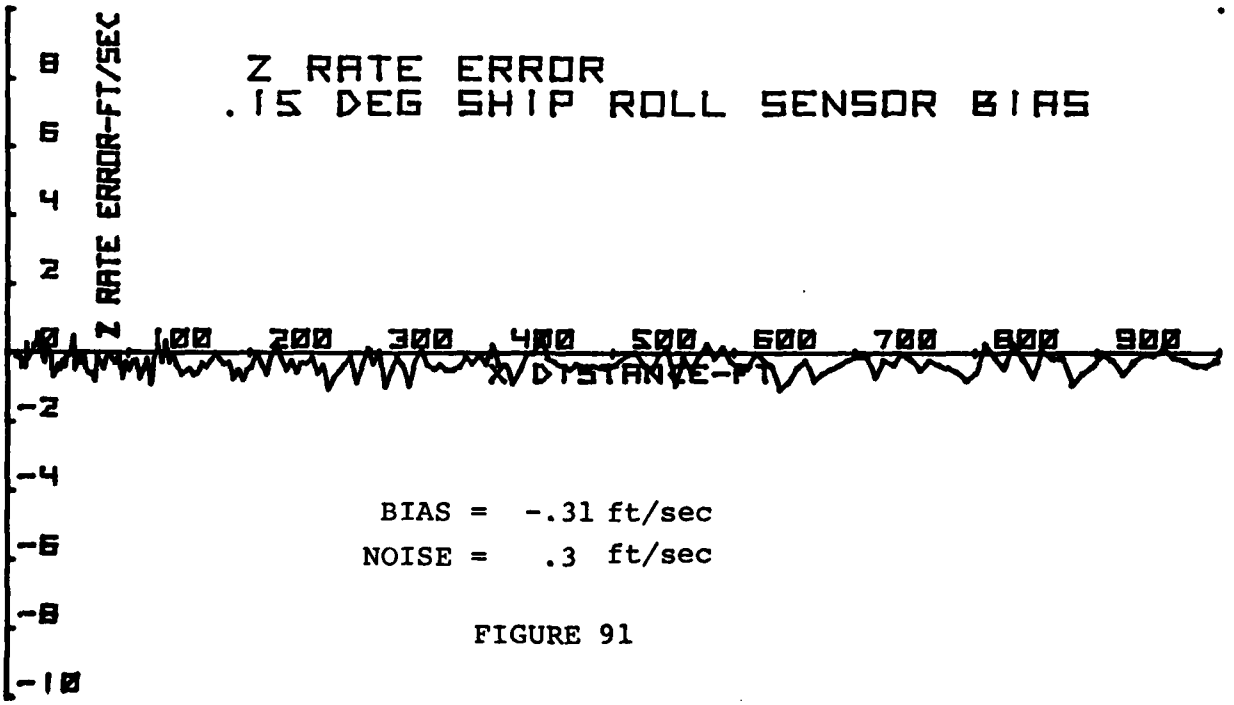

BIAS = -.31 ft/sec

NOISE = .3 ft/sec

FIGURE 91

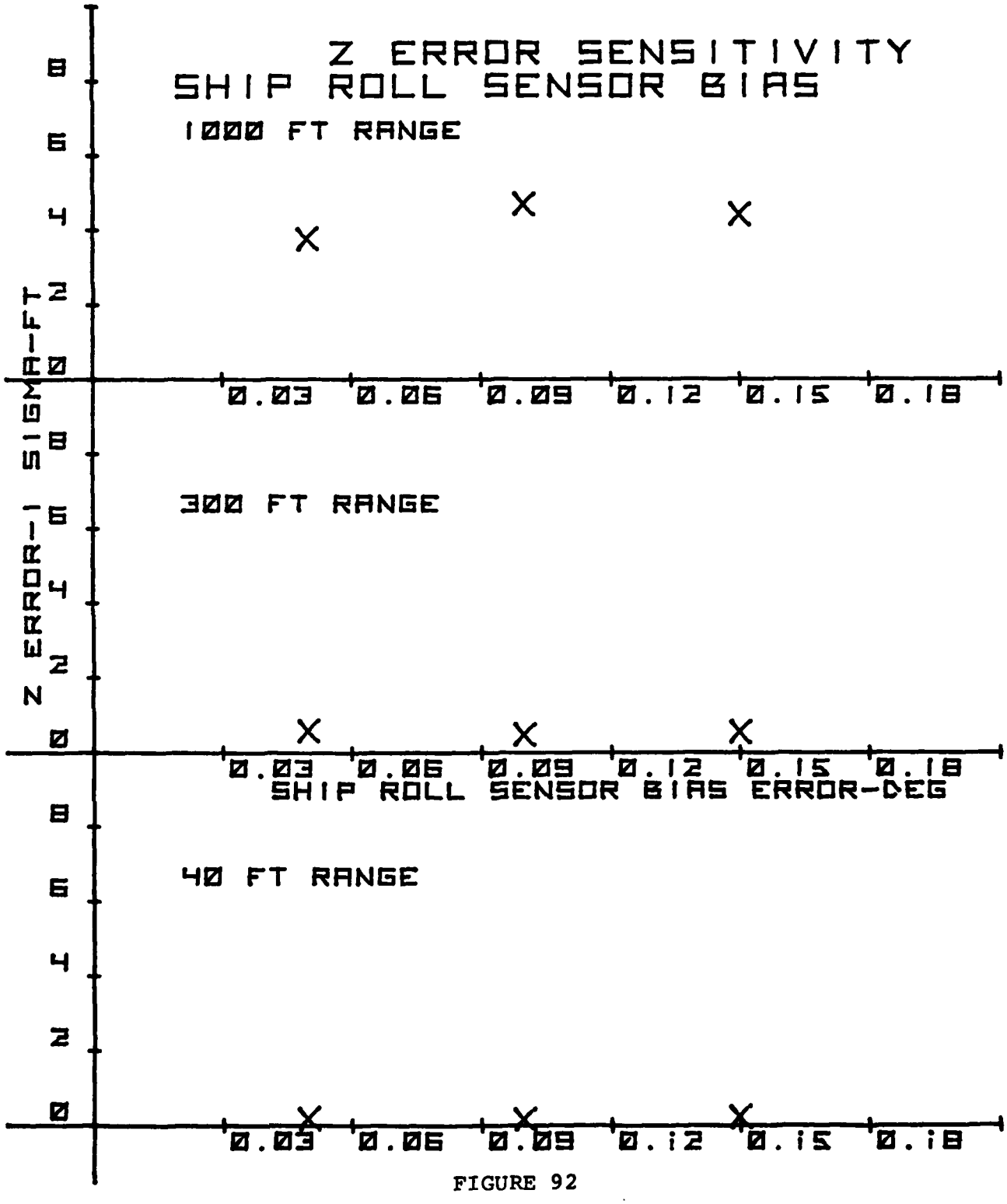
Z ERROR SENSITIVITY
SHIP ROLL SENSOR BIAS
1000 FT RANGE
300 FT RANGE
40 FT RANGE
Z ERROR-1 SIGMA-FT
0
2
4
6
8
0.03
0.06
0.09
0.12
0.15
0.18
SHIP ROLL SENSOR BIAS ERROR-DEG

FIGURE 92

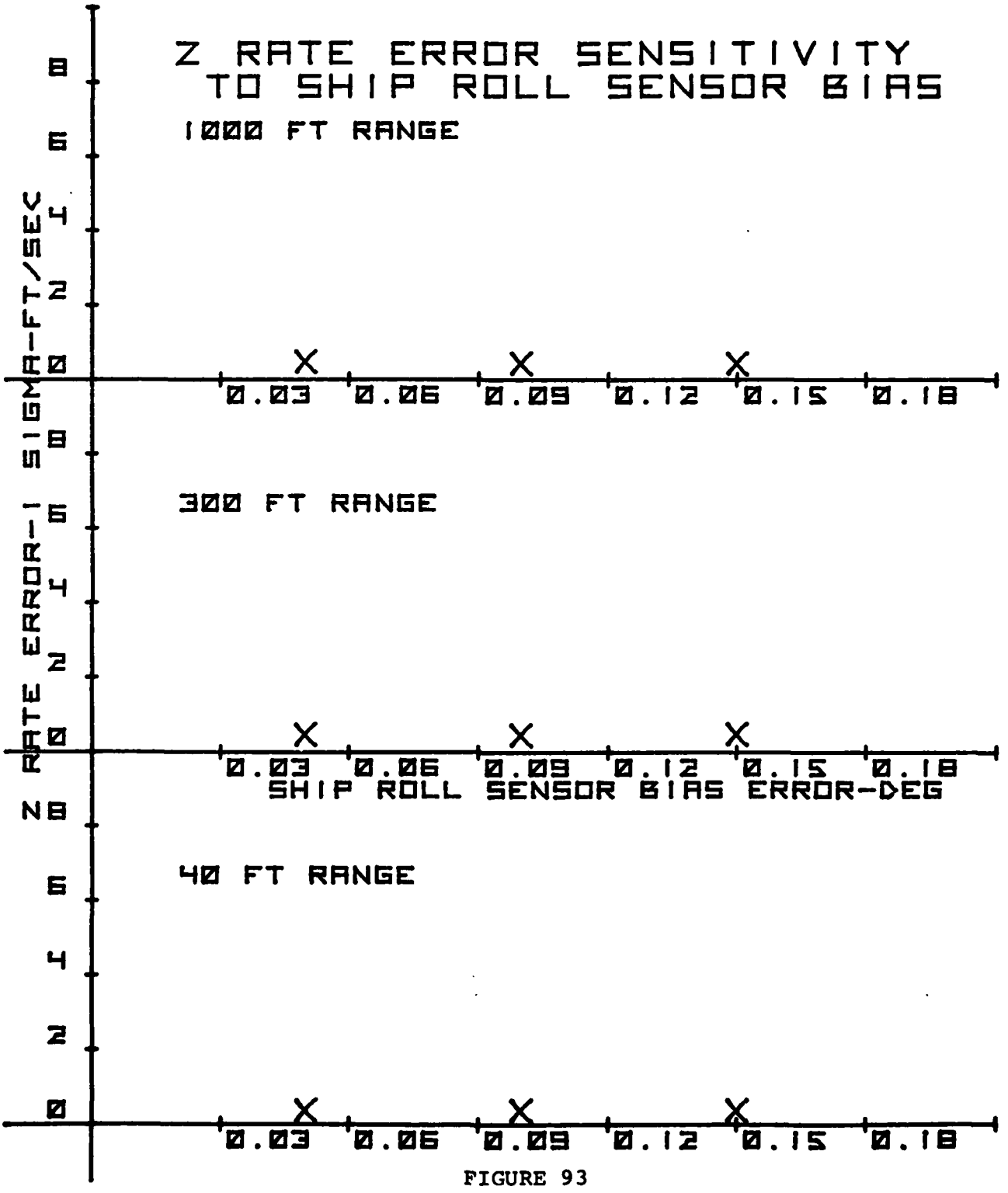
Z RATE ERROR SENSITIVITY
TO SHIP ROLL SENSOR BIAS
1000 FT RANGE
300 FT RANGE
40 FT RANGE
Z RATE ERROR-1 SIGMA-FT/SEC
0
2
4
6
8
0.03
0.06
0.09
0.12
0.15
0.18
SHIP ROLL SENSOR BIAS ERROR-DEG

FIGURE 93

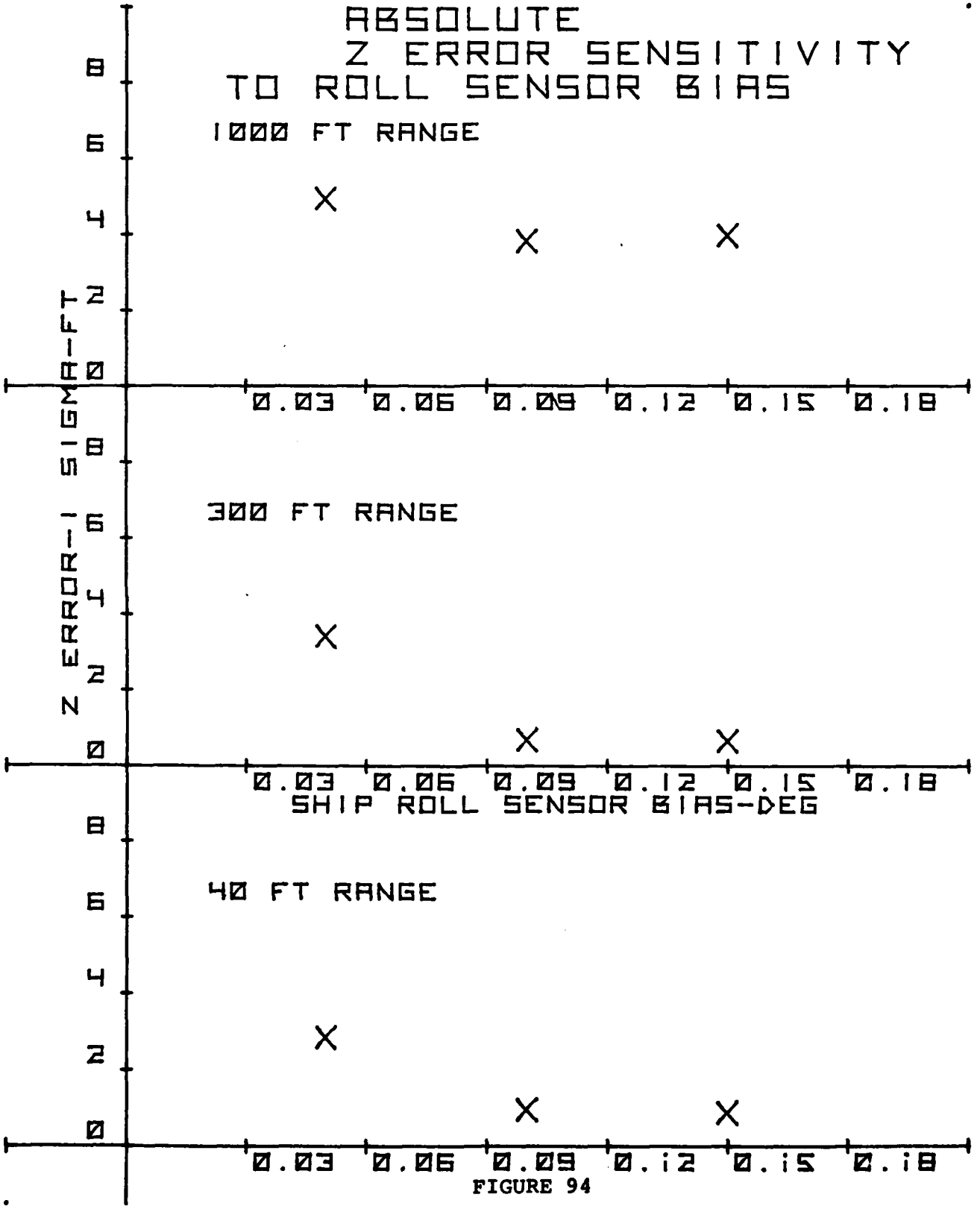
ABSOLUTE
Z ERROR SENSITIVITY
TO ROLL SENSOR BIAS
1000 FT RANGE
300 FT RANGE
40 FT RANGE
Z ERROR-1 SIGMA-FT
0
2
4
6
8
0.03
0.06
0.09
0.12
0.15
0.18
SHIP ROLL SENSOR BIAS-DEG

FIGURE 94

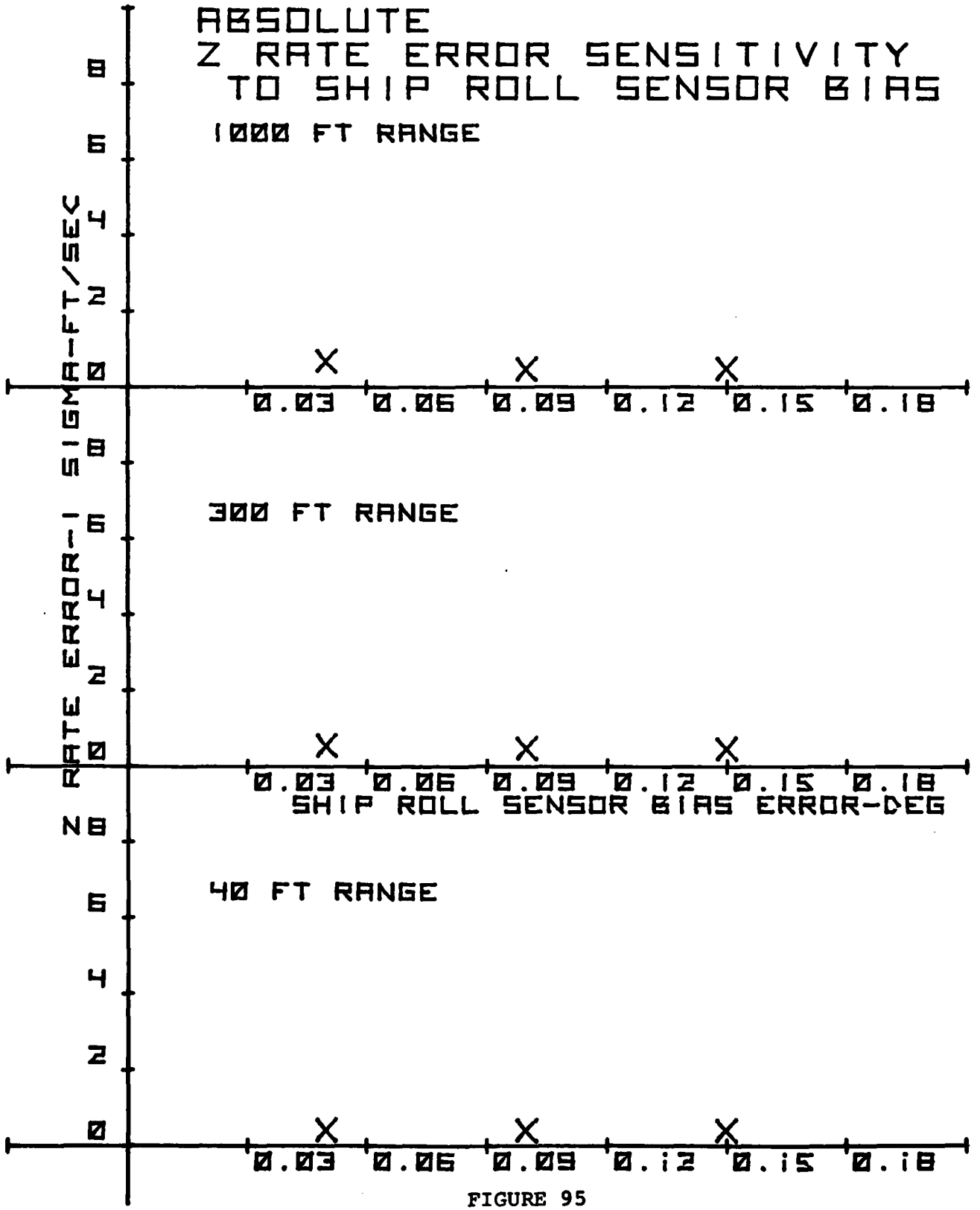
ABSOLUTE
Z RATE ERROR SENSITIVITY
TO SHIP ROLL SENSOR BIAS
1000 FT RANGE
300 FT RANGE
40 FT RANGE
Z RATE ERROR-1 SIGMA-FT/SEC
0
2
4
6
8
0.03
0.06
0.09
0.12
0.15
0.18
SHIP ROLL SENSOR BIAS ERROR-DEG

FIGURE 95

C. SENSITIVITY TO SHIP VERTICAL ACCELEROMETER BIAS ERROR

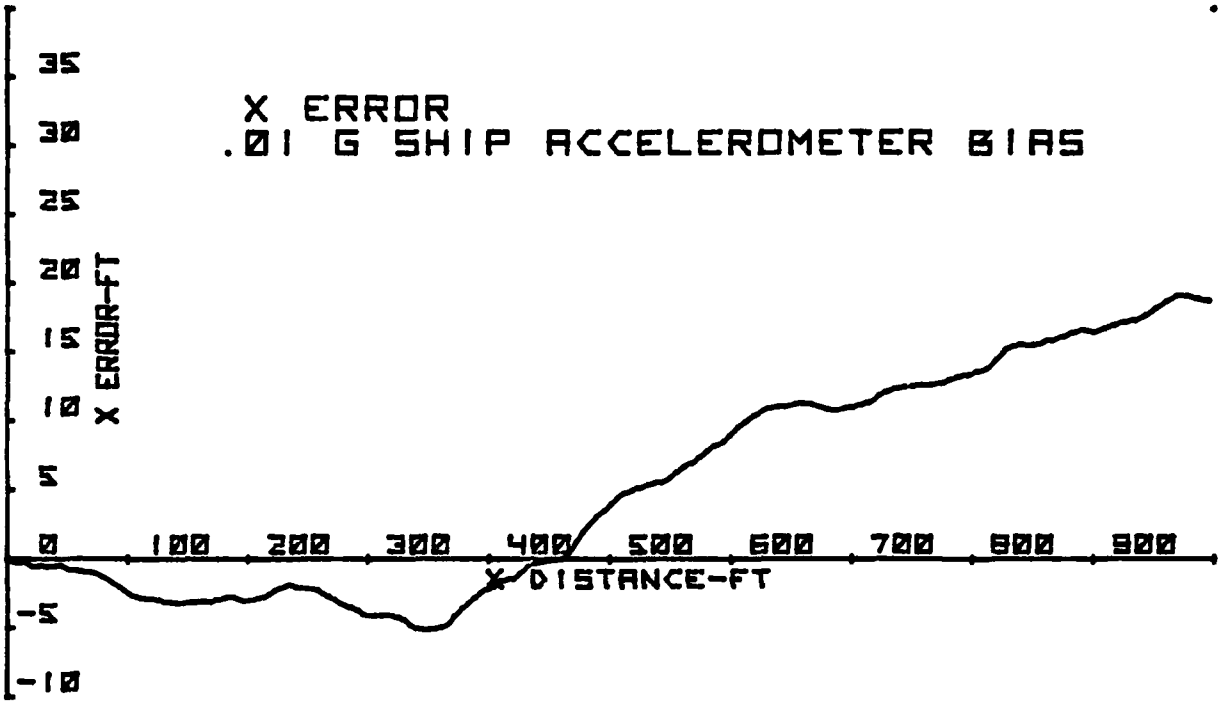
X ERROR
.01 G SHIP ACCELEROMETER BIAS
X ERROR-FT
35
30
25
20
15
10
5
0
-5
-10
100
200
300
400
500
600
700
800
900
X DISTANCE-FT

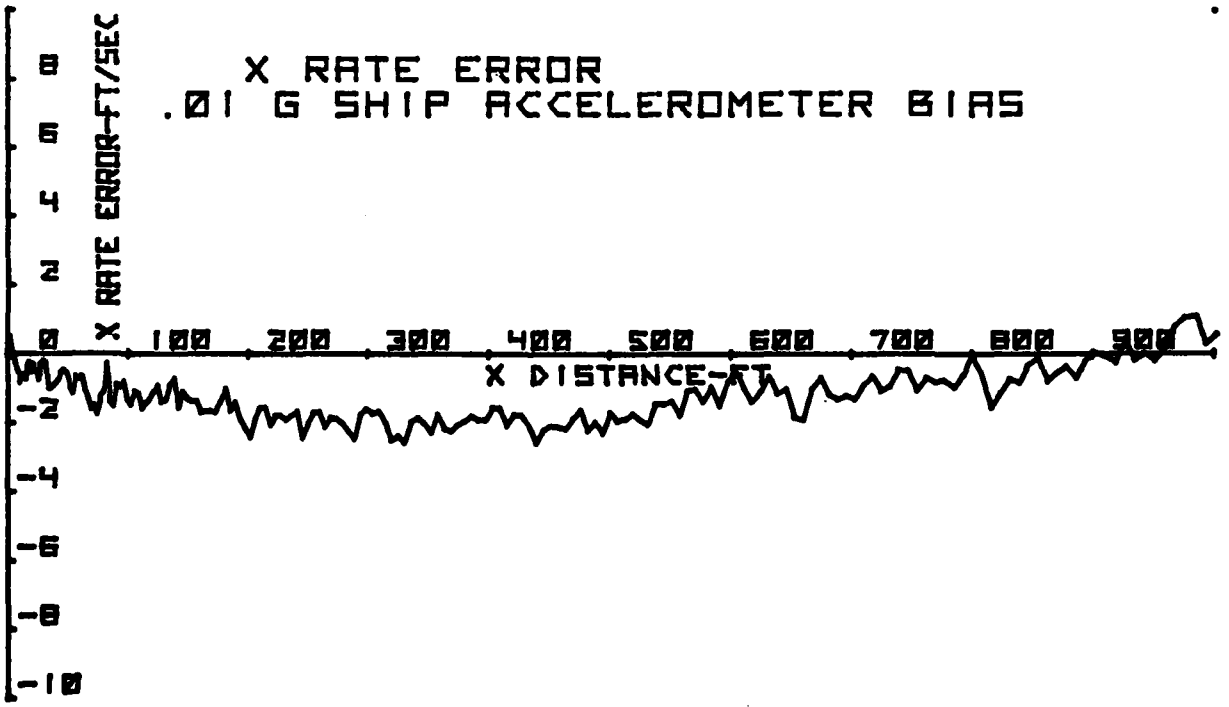
X RATE ERROR
.01 G SHIP ACCELEROMETER BIAS
X RATE ERROR-FT/SEC
8
6
4
2
0
-2
-4
-6
-8
-10
100
200
300
400
500
600
700
800
900
X DISTANCE-FT

FIGURE 96

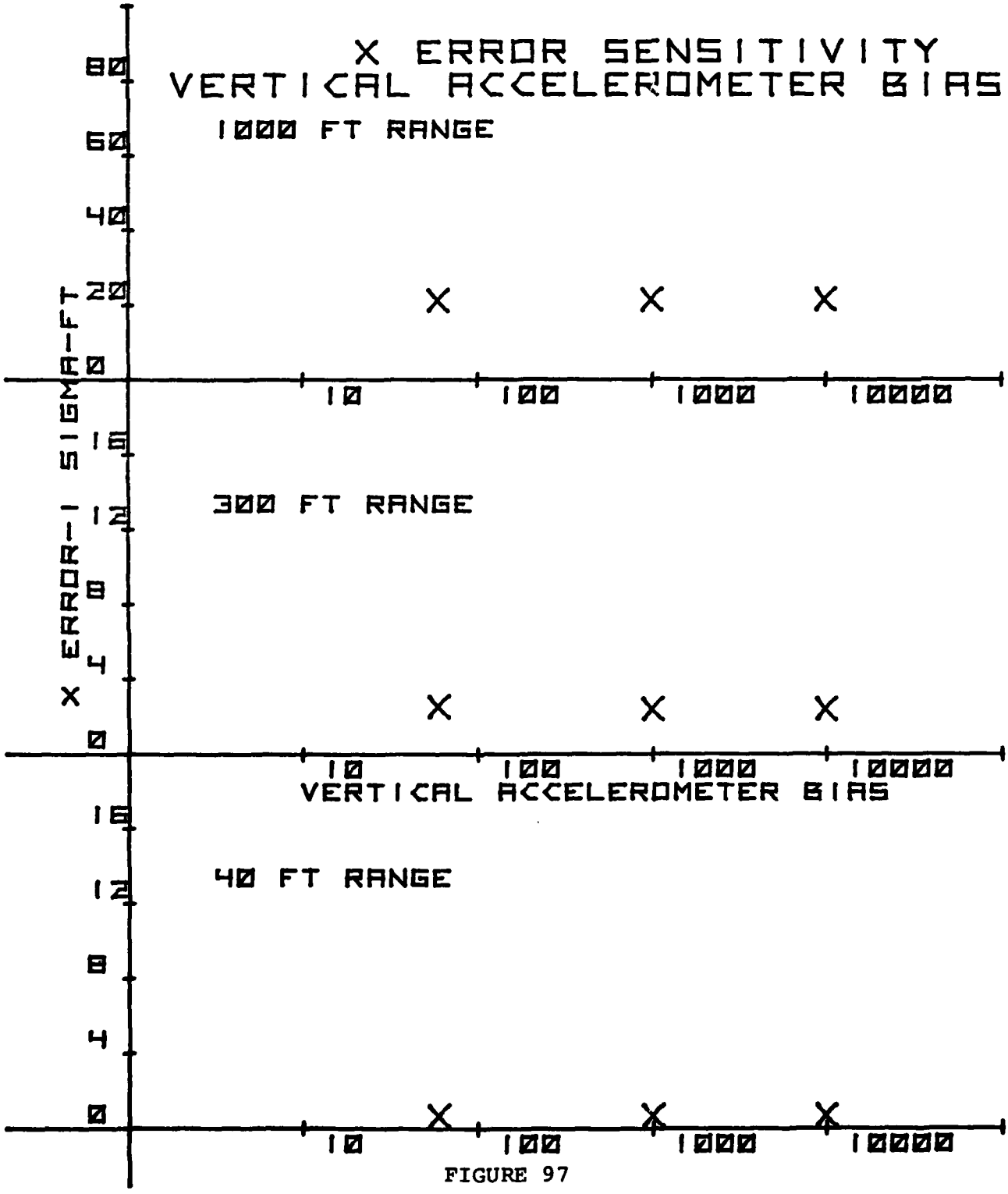
X ERROR SENSITIVITY
VERTICAL ACCELEROMETER BIAS
1000 FT RANGE
300 FT RANGE
40 FT RANGE
X ERROR-1 SIGMA-FT
VERTICAL ACCELEROMETER BIAS
80
60
40
20
0
16
12
8
4
0
10
100
1000
10000

FIGURE 97

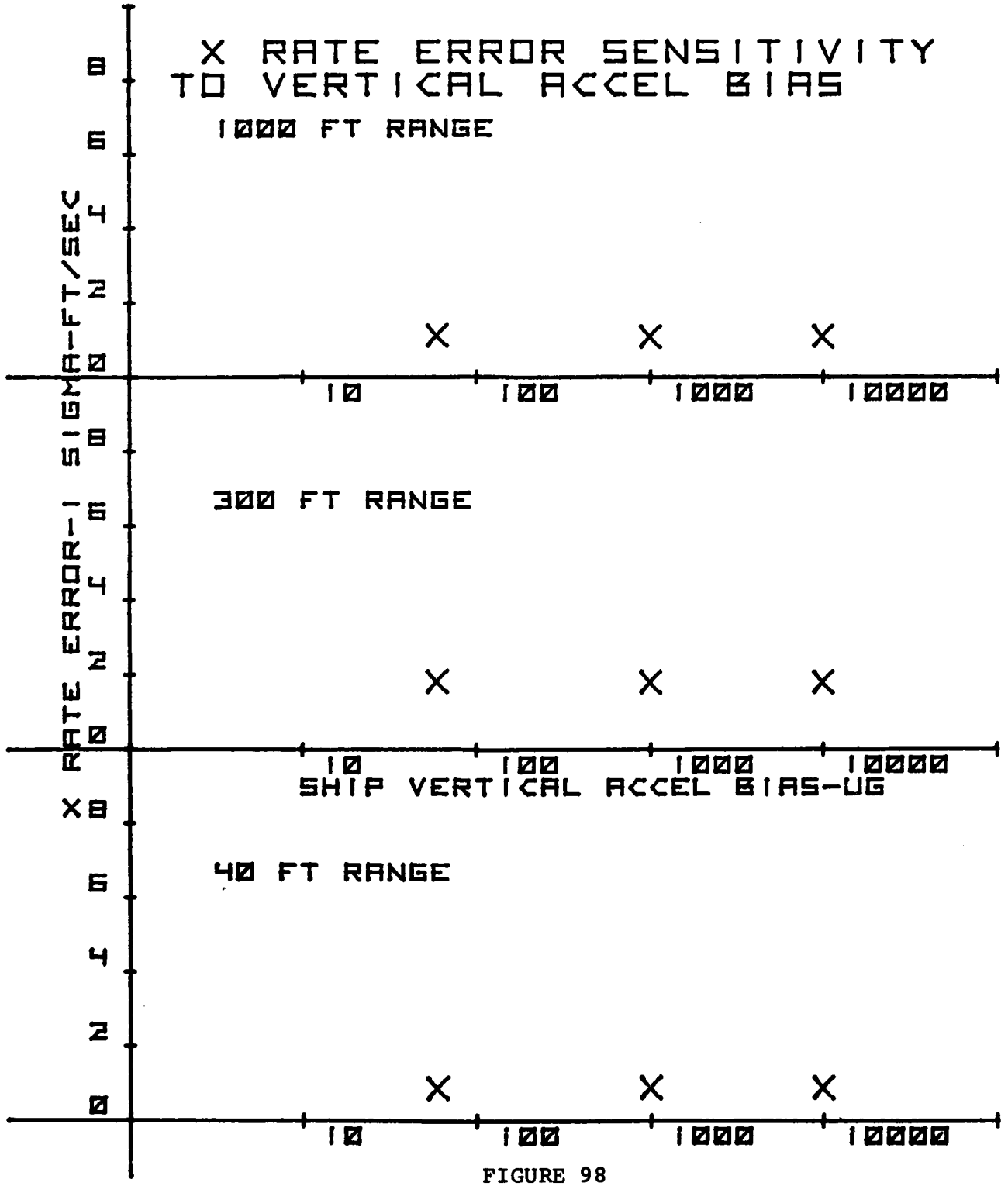
X RATE ERROR SENSITIVITY
TO VERTICAL ACCEL BIAS
1000 FT RANGE
300 FT RANGE
40 FT RANGE
X RATE ERROR-1 SIGMA-FT/SEC
0
2
4
6
8
10
100
1000
10000
SHIP VERTICAL ACCEL BIAS-UG

FIGURE 98

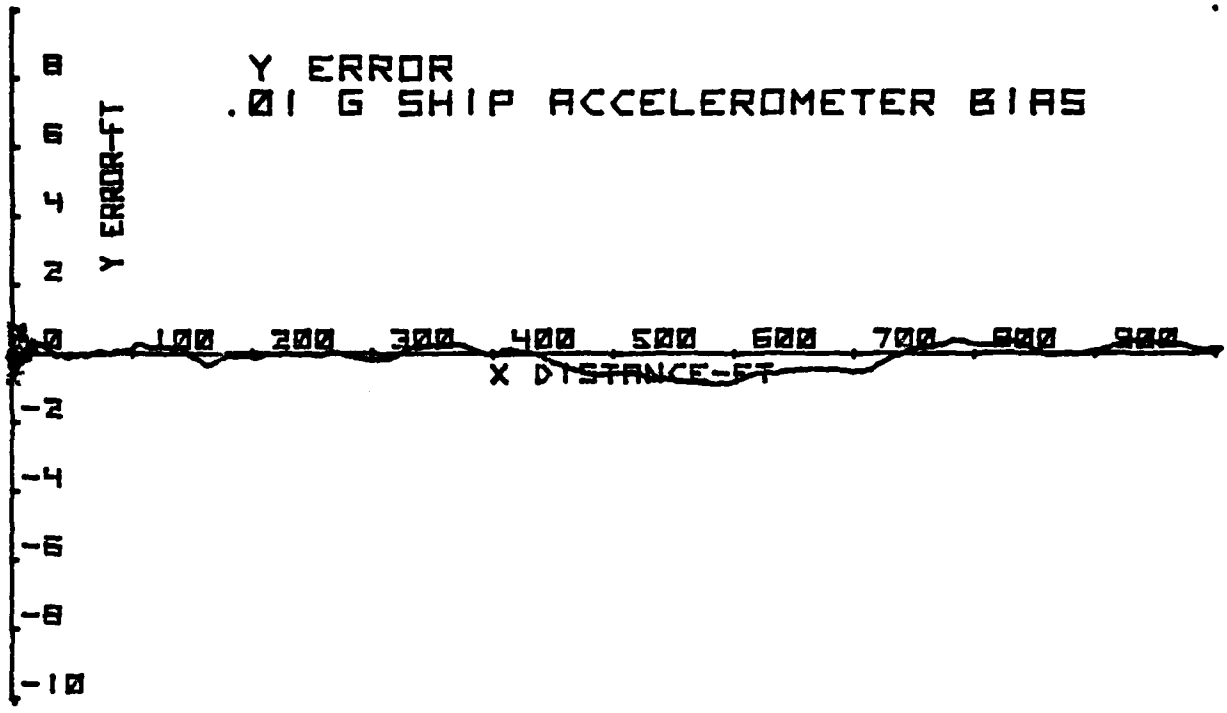
Y ERROR
.01 G SHIP ACCELEROMETER BIAS
Y ERROR-FT
8
6
4
2
0
-2
-4
-6
-8
-10
100
200
300
400
500
600
700
800
900
X DISTANCE-FT

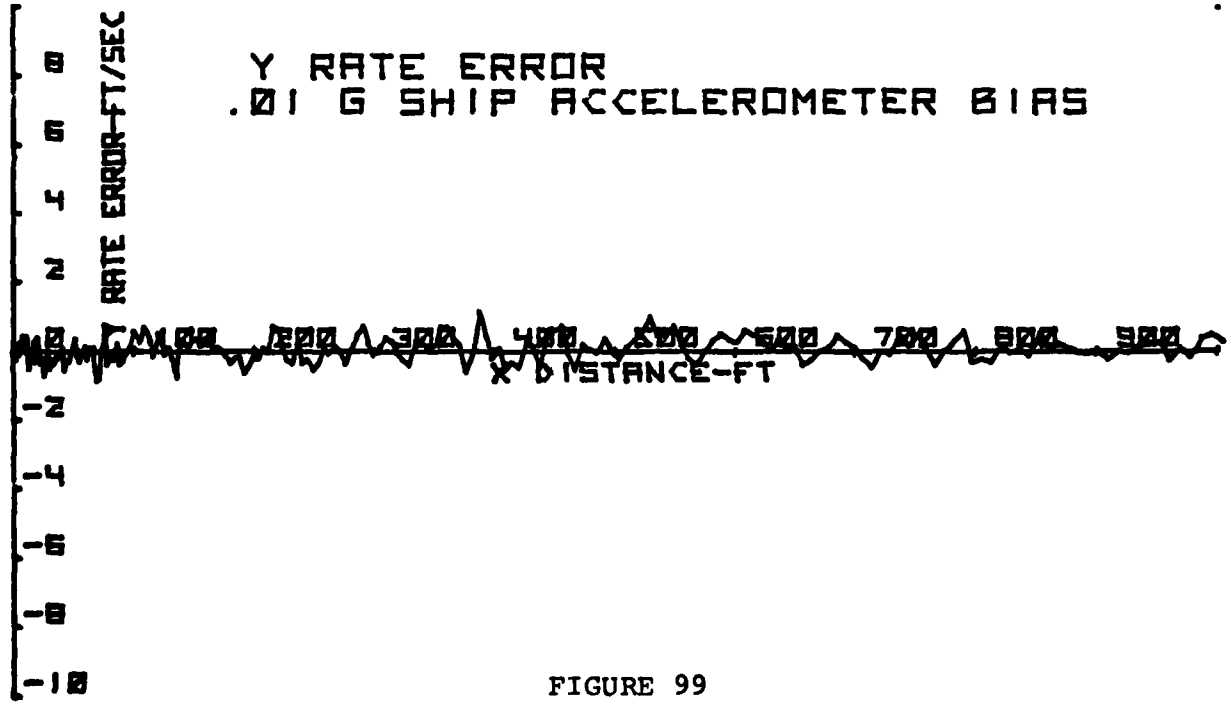
Y RATE ERROR
.01 G SHIP ACCELEROMETER BIAS
Y RATE ERROR-FT/SEC
8
6
4
2
0
-2
-4
-6
-8
-10
100
200
300
400
500
600
700
800
900
X DISTANCE-FT

FIGURE 99

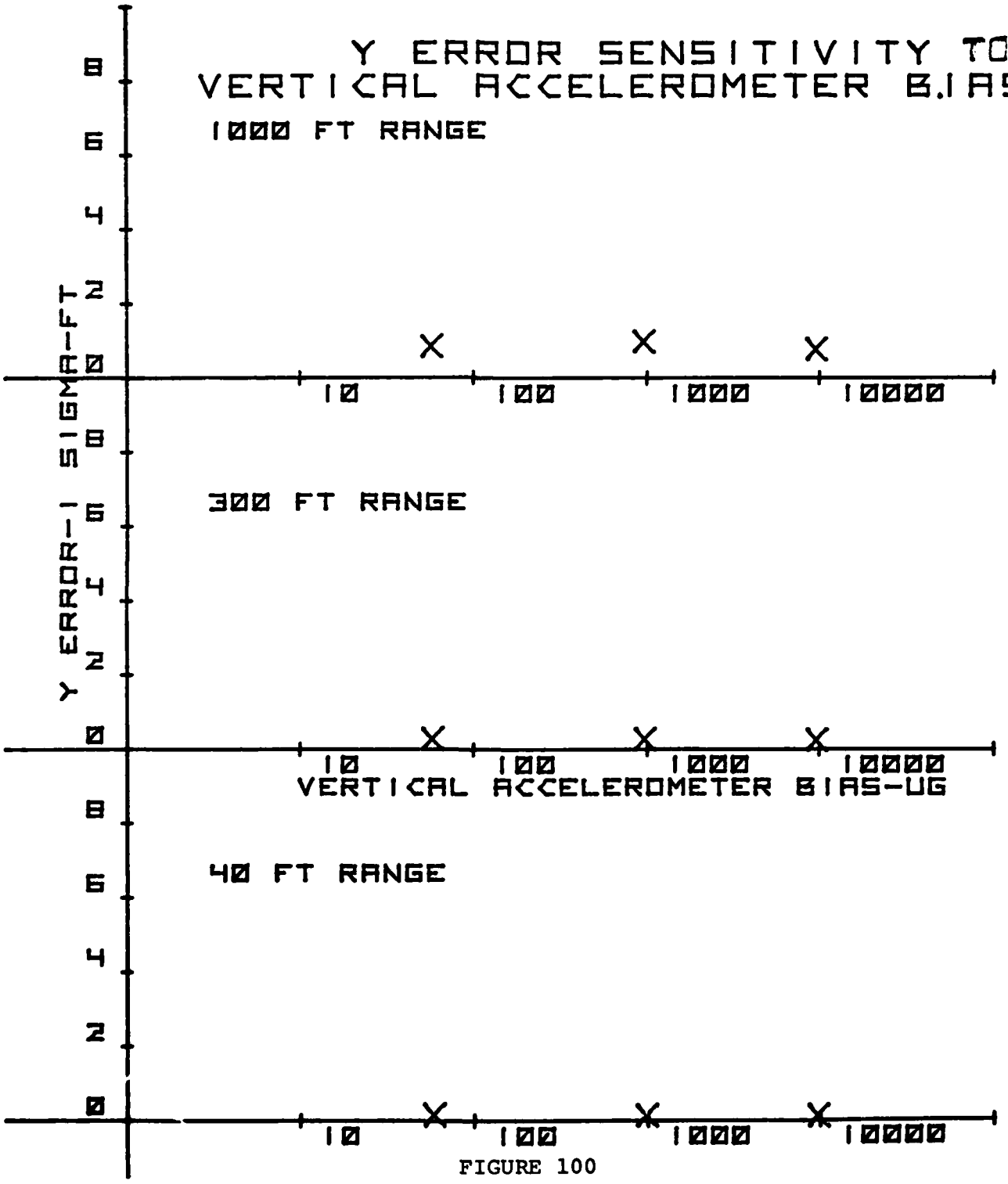
Y ERROR SENSITIVITY TO
VERTICAL ACCELEROMETER BIAS
1000 FT RANGE
300 FT RANGE
40 FT RANGE
Y ERROR-1 SIGMA-FT
VERTICAL ACCELEROMETER BIAS-UG
0
2
4
6
8
10
100
1000
10000

FIGURE 100

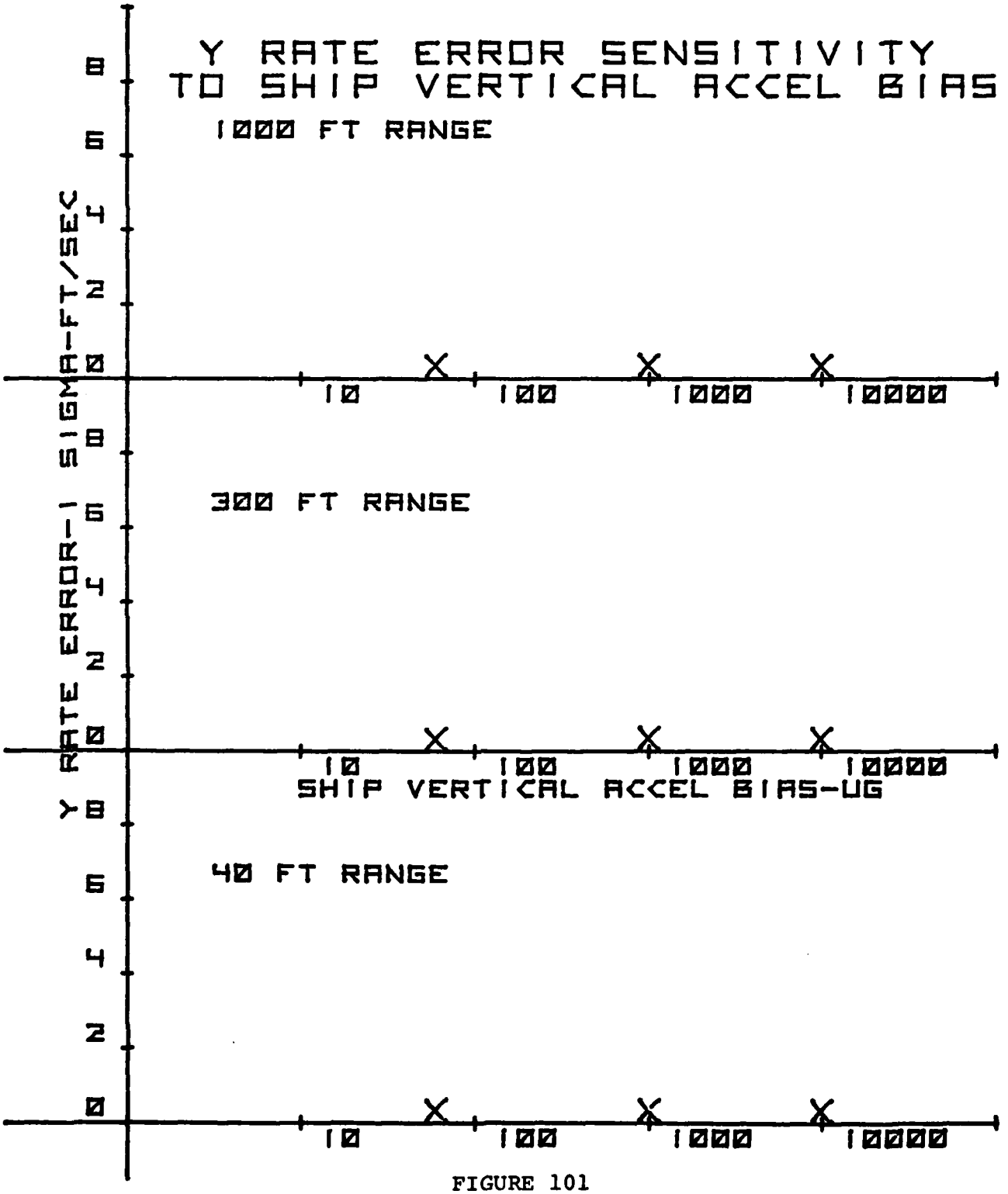
Y RATE ERROR SENSITIVITY
TO SHIP VERTICAL ACCEL BIAS
1000 FT RANGE
300 FT RANGE
40 FT RANGE
Y RATE ERROR-1 SIGMA-FT/SEC
0
2
4
6
8
10
100
1000
10000
SHIP VERTICAL ACCEL BIAS-UG

FIGURE 101

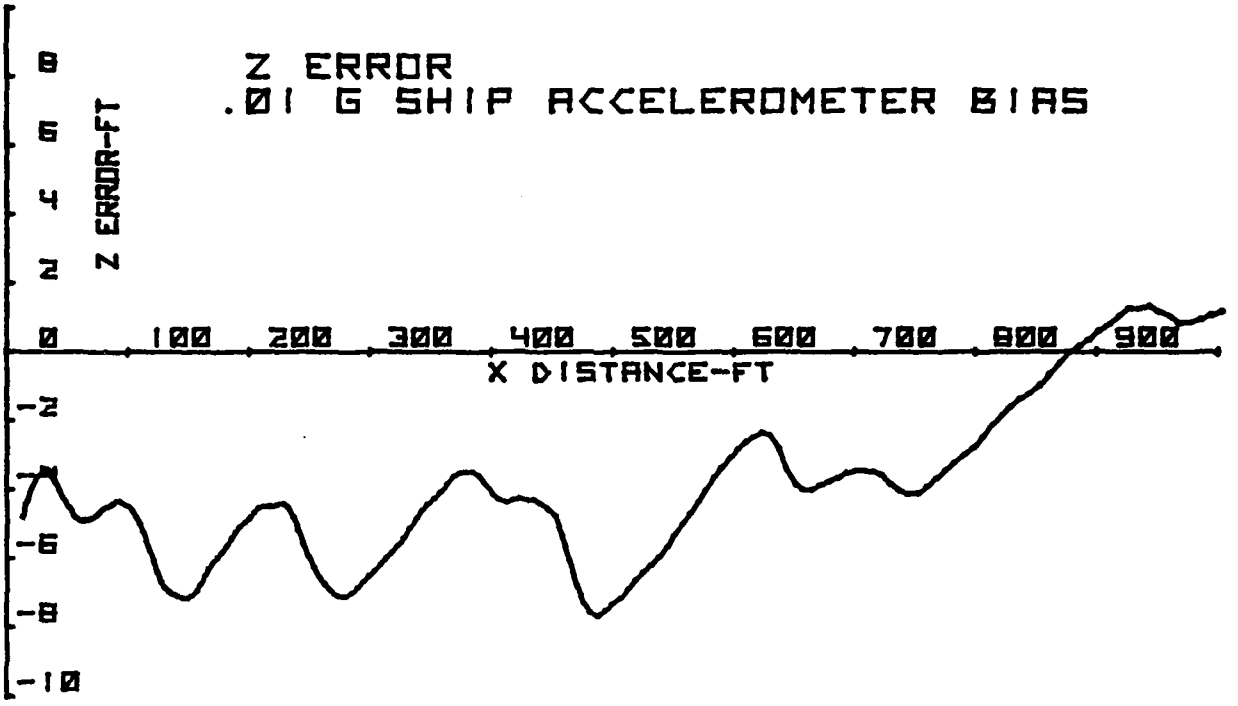

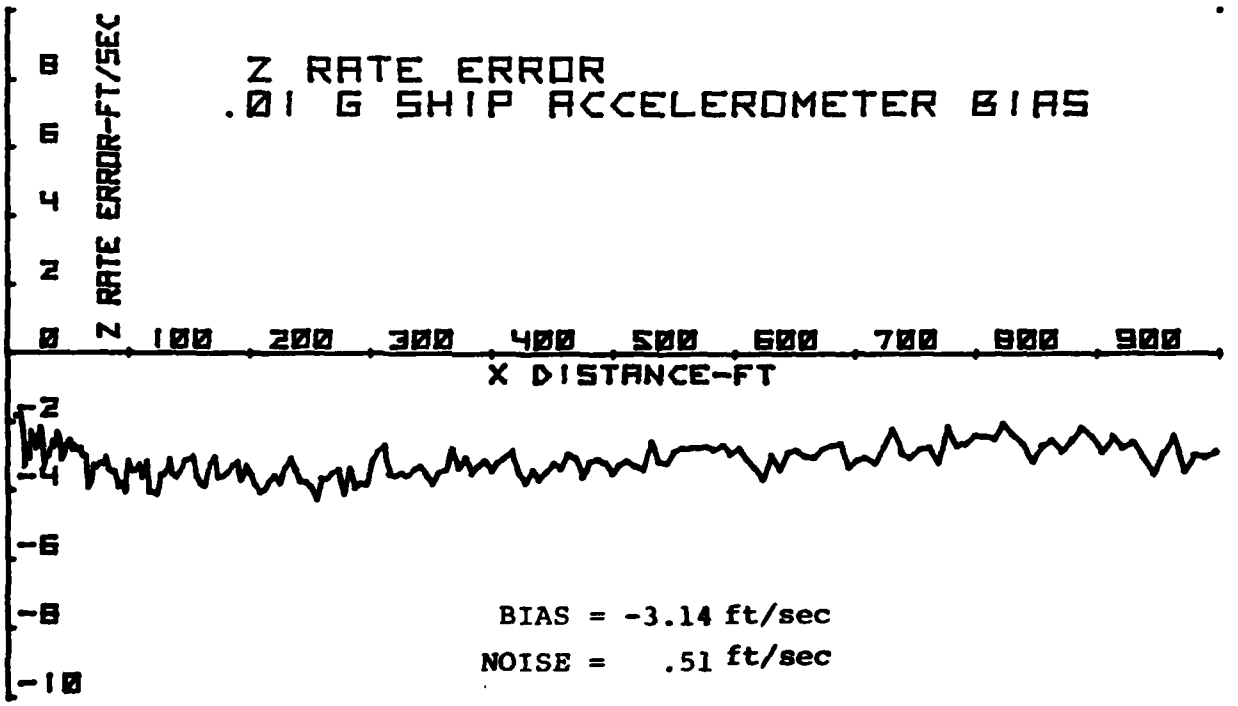

BIAS = -3.14 ft/sec

NOISE = .51 ft/sec

FIGURE 102

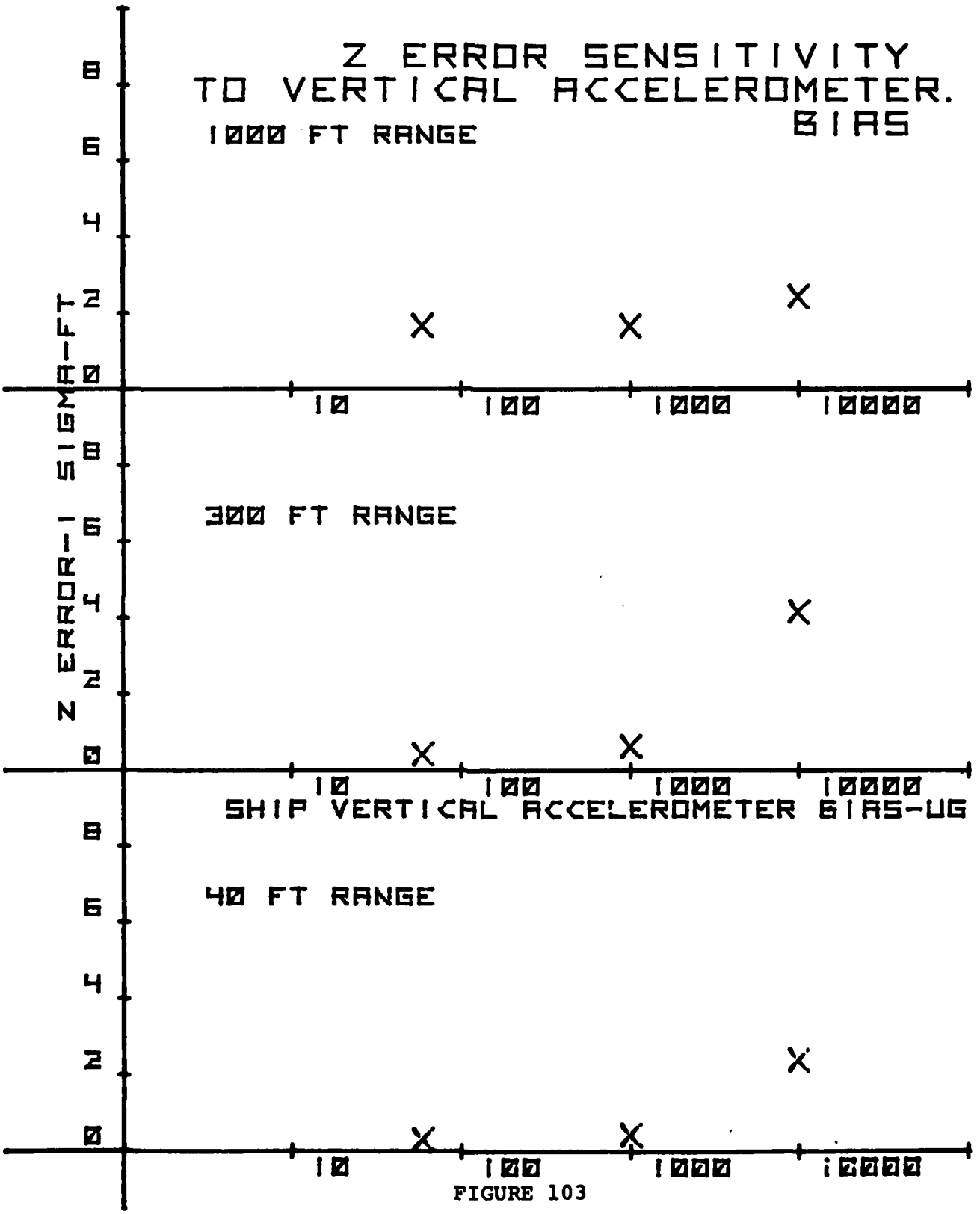
Z ERROR SENSITIVITY
TO VERTICAL ACCELEROMETER.
BIAS
1000 FT RANGE
300 FT RANGE
40 FT RANGE
Z ERROR-1 SIGMA-FT
0
2
4
6
8
10
100
1000
10000
SHIP VERTICAL ACCELEROMETER BIAS-UG

FIGURE 103

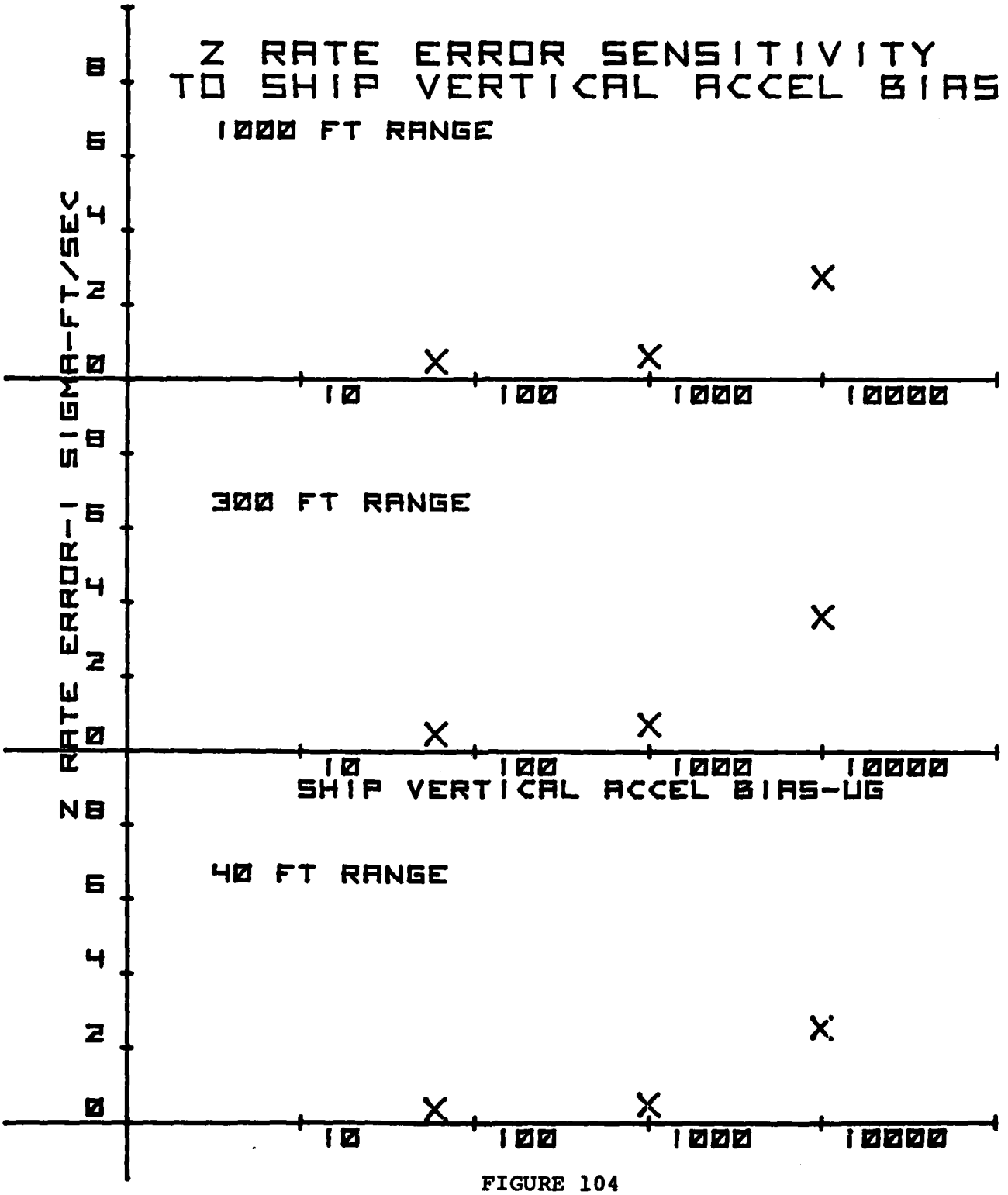
Z RATE ERROR SENSITIVITY
TO SHIP VERTICAL ACCEL BIAS
1000 FT RANGE
300 FT RANGE
40 FT RANGE
Z RATE ERROR-1 SIGMA-FT/SEC
SHIP VERTICAL ACCEL BIAS-UG
10
100
1000
10000

FIGURE 104

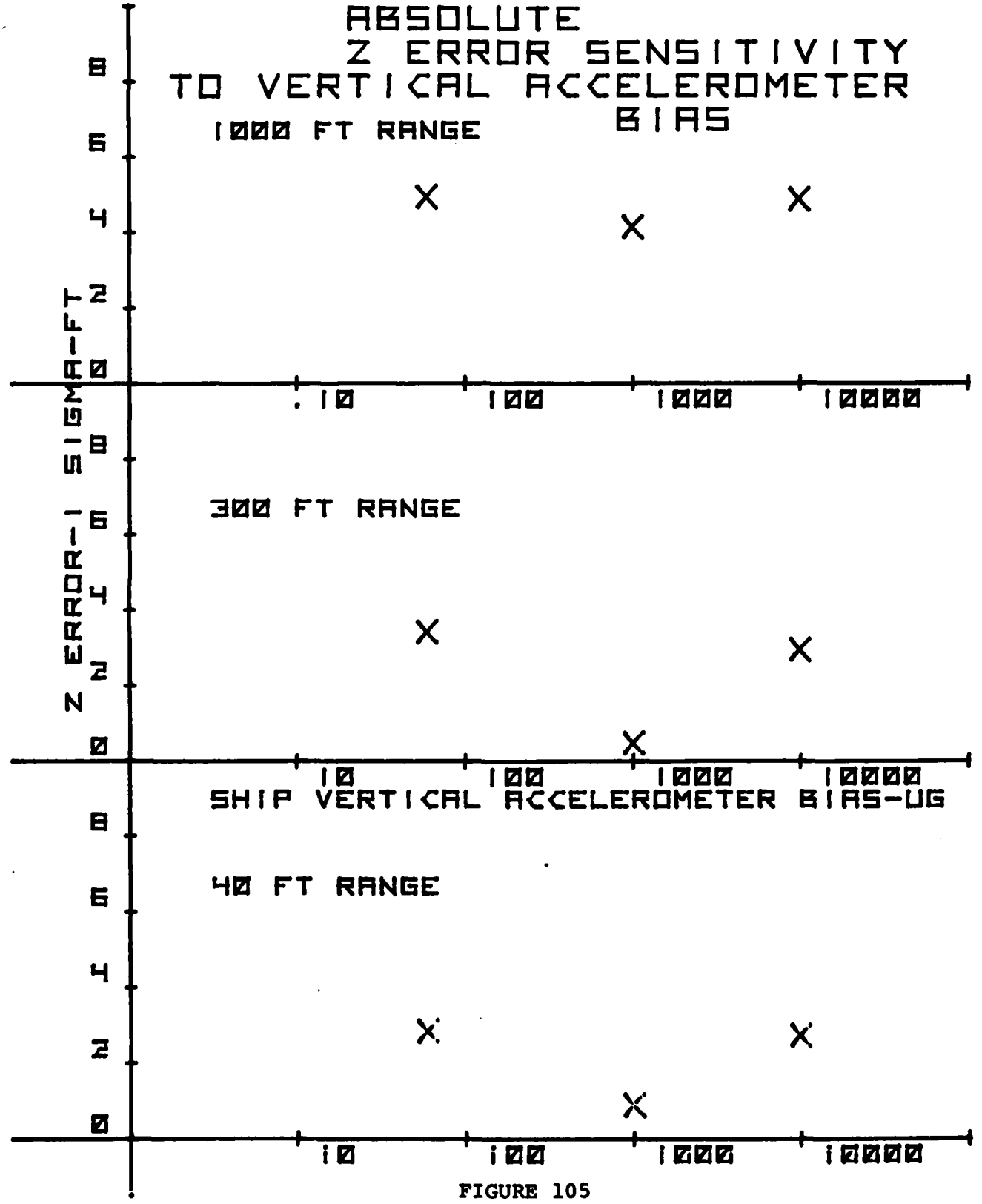
ABSOLUTE
Z ERROR SENSITIVITY
TO VERTICAL ACCELEROMETER
BIAS
1000 FT RANGE
300 FT RANGE
40 FT RANGE
Z ERROR-1 SIGMA-FT
SHIP VERTICAL ACCELEROMETER BIAS-UG
0
2
4
6
8
10
100
1000
10000

FIGURE 105

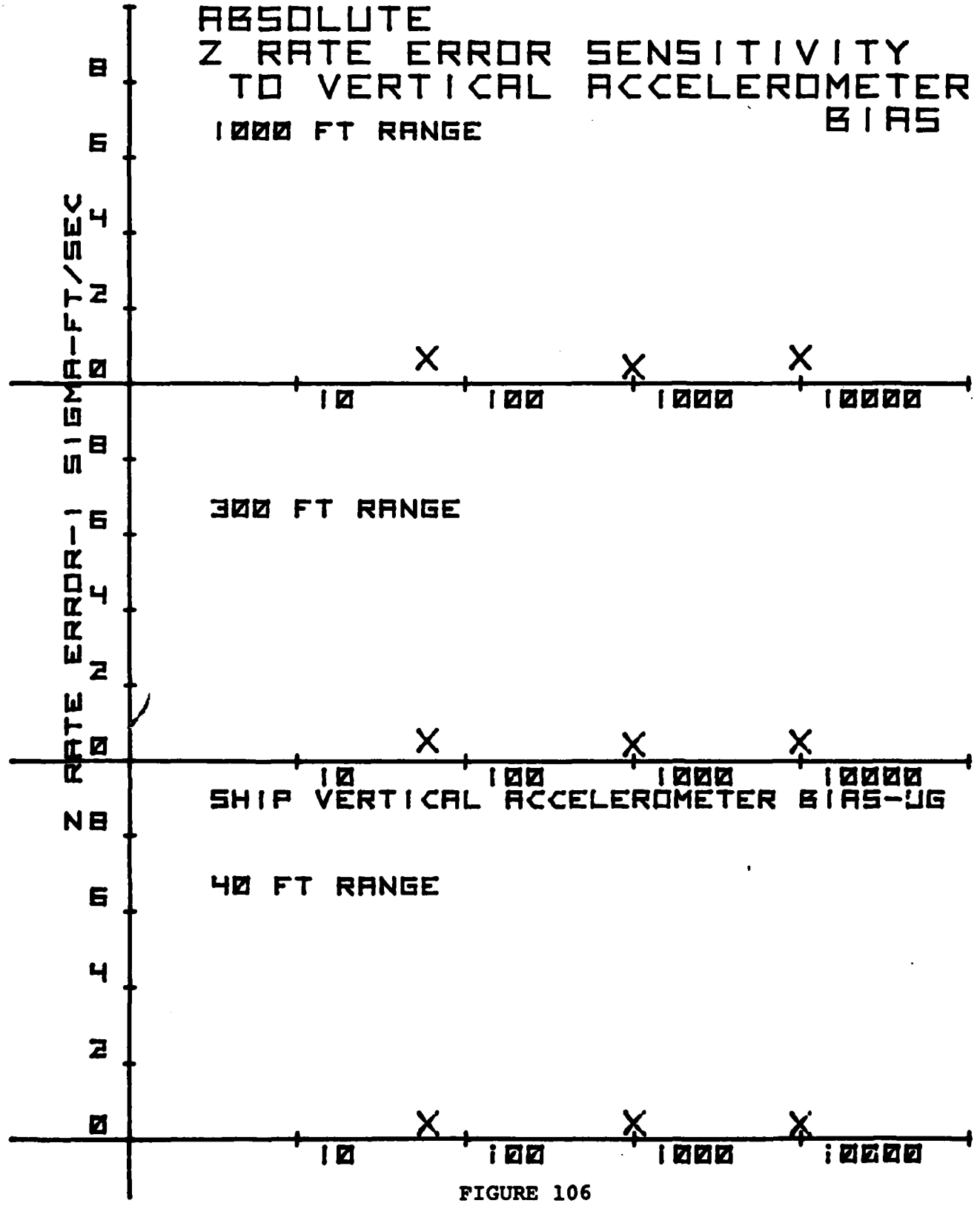
ABSOLUTE
Z RATE ERROR SENSITIVITY
TO VERTICAL ACCELEROMETER
BIAS
1000 FT RANGE
300 FT RANGE
40 FT RANGE
Z RATE ERROR-1 SIGMA-FT/SEC
SHIP VERTICAL ACCELEROMETER BIAS-UG
10
100
1000
10000
0
2
4
6
8

FIGURE 106